COMMUNICATIONS QUARTERLY

THE JOURNAL OF COMMUNICATIONS TECHNOLOGY

Spring 1998 $9.95

An Inexpensive Approach to GOES Satellite Reception

- Tame Your End-Fed Antenna
- The Elusive Conjugate Match
- Improve Frequency Calibration of LC Oscillators with the Modular Dial
- Signal Ducting on the 160-Meter Band
- Elevated Radial Wire Systems Part 2—Phased Arrays
- Science in the News: Gradium Glass™ and Rare Earth Doped Semiconductors
- Tech Notes: An Enlightening Look at the Half-Square Antenna
- The Care and Feeding of the 4CX1600B—Notes on Specifications and Usage

U.S. $9.95

0 73361 64880 8 81>

COMMUNICATIONS QUARTERLY

THE JOURNAL OF COMMUNICATIONS TECHNOLOGY

CONTENTS

Volume 8, Number 2 Spring 1998

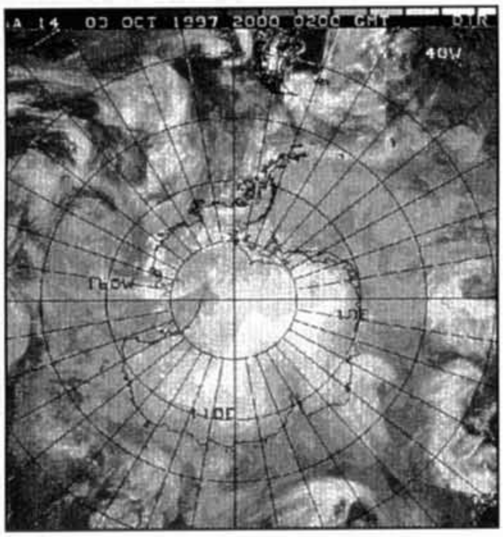

page 9

page 91

On the Cover: Weathermen on the TV news pull in great weather satellite pictures. If you want to capture them for yourself read "GOES Satellite Reception" by Eugene Ruperto, W3KH, on page 9. Cover artist: Bryan Bergeron, NU1N.

EDITORIAL

Rabble rousing: risky business or technical challenge?

The story of the conjugate match first appeared in *Communications Quarterly* in the fall of 1997; but the controversy had already been a part of amateur radio for over 20 years. Since the early '70s, the two major players involved in this debate—Walter Maxwell, W2DU, and Warren Bruene, W5OLY—have been vocal about their conflicting views on the subject.

Last fall, *CommQuart* stirred the pot by printing an article by Walt, John (Jack) Belrose, VE2CV, and Charles (Tom) Rauch, W8JI, called "Source Impedance of HF Tuned Power Amplifiers and the Conjugate Match." We received a lot of letters following the publication—both pro and con—and felt it was important to print Bruene's point of view. W5OLY's "The Elusive Conjugate Match" begins on page 23, and I'm sure it'll bring another big response.

Concurrent with the conjugate match discussion has been a debate over elevated radial systems. Dick Weber, K5IU's, "Optimal Elevated Radial Vertical Antennas" ran in the Summer 1997 issue. After reading Weber's piece, VE2CV wrote his own article. It appeared in the Winter 1998 issue. In one of Belrose's appendices, he modeled and gave his opinions of K5IU's antenna. You'll find this article, "Elevated Radial Wire Systems for Vertically Polarized Ground-Plane Antennas, Part 1: Monopoles" in Winter 1998. Part 2 starts on page 45 of this issue.

Dick warned me his topic was bound to be controversial and it has proved to be so. Besides three articles, we've received letters from readers and K5IU himself, which you'll find in "Technical Conversations" in the Summer and Fall 1997 issues, as well as here. These types of articles, the correspondence, and the additional articles they generate is, perhaps, the major reason why it's important for us to print pieces that other amateur radio publications shy away from. Unresolved issues remain unresolved only when free communication is stifled. A little rabble rousing can stimulate readers and get them thinking technically. This, in turn, may lead to a clearer understanding of knotty technical issues or perhaps resolution.

As I look back through eight years of *CommQuarts*, I see we've chosen the challenging path more than once. Remember the series on baluns by Jerry Sevick, W2FMI? That series came with its own debate between the proponents of current, choke, voltage baluns, and transformer-type balun supporters. Next, we presented a series of articles on fractal antennas by Chip Cohen, N1IR. Many readers were fascinated by the subject; others scoffed. Still, despite the "daring" nature of the work, we felt it was important to give people the opportunity to try something new.

And then there are those stories that we think will bring no comment at all. We were pleasantly surprised when Rick Littlefield, K1BQT's "Tech Note: Build the Nor'easter 6-meter AM Transceiver" caused a little flurry. We figured 6 meters was so dead that no one would respond except to razz us for running such a piece; but we were wrong. A few guys let us know they would be building Rick's little radio, while W1OLP, who flies radio-controlled planes, expressed concern that a renewed interest in the 6-meter band would wreak havoc on RC flyers.

The all-time letter-writing campaign was spawned by readers challenged by Jay Jeffrey, WV8R's "Kirchhoff's Laws: the Classic Cube Problem" (Fall 1997). We received letters about students' first encounters with the cube problem and many offering different solutions. One such letter appears in this issue and there are more to come.

Controversial and interesting ideas beget other ideas, which beget experimentation, which beget letters, which beget articles. And that's what keeps us going. Is it risky to run some of these things? You bet it is! Does it provoke people to speak up? You bet it does! It's what keeps *Communications Quarterly* at the forefront of all that's technical in ham radio. If we took the cautious path, we'd never find out about new technologies. If we didn't find out about new technologies, we wouldn't have anything to talk about. And if we didn't have anything to talk about, where would we be?

Terry Littlefield, KA1STC
Editor

EDITORIAL STAFF

Editor
Terry Littlefield, KA1STC
Consulting Technical Editor
Robert Wilson, WA1TKH
Senior Technical Editor
Peter Bertini, K1ZJH
Managing Editor
Edith Lennon, N2ZRW

EDITORIAL REVIEW BOARD
L.B. Cebik, W4RNL
Forrest Gehrke, K2BT
Michael Gruchalla, P.E.
Hunter Harris, W1SI
Bob Lewis, W2EBS
John Marion, W1QM
Walter Maxwell, W2DU
Jim McCulley, P.E.
William Orr, W6SAI

BUSINESS STAFF
Publisher
Richard Ross, K2MGA
Advertising Manager
Donald R. Allen, W9CW
Sales Assistant
Nicole Tramuta
Accounting Department
Sal Del Grosso
Ann Marie DeMeo
Circulation Manager
Catherine Ross
Operations Manager
Melissa Kehrwieder
Data Processing
Jean Sawchuk
Customer Service
Denise Pyne

PRODUCTION STAFF
Art Director
Elizabeth Ryan
Associate Art Director
Barbara McGowan
Electronic Composition Manager
Edmond Pesonen
Production Manager
Dorothy Kehrwieder
Production
Nicole Tramuta
Electronic Composition
Pat Le Blanc

A publication of
CQ Communications, Inc.
25 Newbridge Road
Hicksville, NY 11801-USA

Editorial Offices: P.O. Box 465, Barrington, NH 03825. Telephone/FAX: (603) 664-2515. **Business Offices:** 25 Newbridge Road, Hicksville, NY 11801. Telephone: (516) 681-2922. FAX: (516) 681-2926.

Communications Quarterly is published four times a year (quarterly) by *CQ Communications, Inc. Communications Quarterly* is the philosophical successor of *Ham Radio Magazine* founded by T.H. "Skip" Tenney, Jr., W1NLB and James R. Fisk, W1HR. Subscription prices (all in U.S. Dollars): Domestic—one year $33.00; two years $62.00. Canada/Mexico—one year $39.00; two years $74.00. Foreign Air Post—one year $46.00; two years $88.00.

Periodical postage paid at Hicksville, NY and additional mailing offices.

Postmaster: Please send change of address to Communications Quarterly, CQ Communications, Inc., 25 Newbridge Road, Hicksville, NY 11801. ISSN 1053-9344.

Printed in U.S.A.

TECHNICAL CONVERSATIONS

Six meters and Radio Controlled Planes

Dear Editor:

The winter edition of *CommQuart* sent chills through me—a 6-meter radio controlled (RC) model airplane flyer.

In Wilson Anderson's article on sunspot cycle 23, he predicts that "6 meters will become the best DX band in 2000 and 2001." And, in Peter Bertini's introduction to Rick Littlefield's article on the "Nor'easter 6-meter AM Transmitter," he suggests that Polycomms, Lafayettes, and Gooney Boxes are being resurrected. Coupled with the amateur free spirits that abound and the general lack of knowledge about the ARRL 6-meter band plan hidden in the *Repeater Handbook*, 6-meter RC activity is in jeopardy. Radio control operation normally takes place between 50.800 and 50.980 MHz (10 channels) and 53.1, 53.2–53.8 MHz (eight channels). The impending propagation changes and influx of activity pose the dangers of lost models, property damage to others, and bodily injury to RC flyers and observers.

The RC flyer has used 53.3 MHz since the 1960s with no interference problem. Currently, there appear to be no interference problems on any of the RC channels with the exception of 6-meter repeaters in some parts of the country. These pose no real problem since they are easily identified and avoided. Apparently, the low-level RC transmitter signals are strong enough at the model's visual range to overcome the occasional daytime DX signal.

Incidentally, my position of New England Area Frequency Coordinator for the Academy of Model Aeronautics gives me continuous input concerning interference on 6 meters and our 27 and 72-MHz RC frequencies.

Que sera sera; thanks for the warning.

George Wilson, W1OLP
juno.com

TECHNICAL CONVERSATIONS

I Don't Agree

Dear Editor:

The following is in regard to the article authored by Rauch, et al, in the last issue of *Communications Quarterly.*

I was acknowledged by authors ("thanks to Fred Telewski, WA7TZY"), which would normally be appreciated and quite appropriate, since I did have several conversations with two of the authors in the '93/'94 time frame. The conversations were of a Devil's advocate nature and did not imply concurrence with the conclusions presented in the article.

I was not given an opportunity to review the work before publication, nor were my reservations regarding certain properties of the measurement technique adequately addressed in the body of the article. I do not want your readers to assume that, because I was acknowledged, I agree with the conclusions presented by the authors when I do not.

Fred Telewski, WA7TZY
Woodinville, Washington

Comments on Elevated Radials

Dear Editor:

This letter is in response to the article, "Elevated Radial Wire Systems for Vertically Polarized Ground-Plane Type Antennas," by Jack Belrose, VE2CV.

Articles which investigate the vagaries of antenna design are of *great* interest, of course, to the ham "community." So are methods that promise great performance at a virtually insignificant cost, either monetary or in effort. The "elevated radial systems" types of articles are of this genre. An old maxim says, "If it appears to be too good to be true," it usually *is* "too good to be true." We seldom get something for nothing. Nowhere is this maxim more true than it is in the field of engineering. (Remember the splash that "cold fusion" made?) At the time, I remember remarking to my wife, "I don't see any mention of residual neutrons, or of transmuted by-products." I told her then, "No neutrons, no fusion." Of course, they did *not* produce "cold fusion." Anybody who was involved with fusion research knows that. But the newspapers and other print media picked up on it. It made a big splash.

Let's review some basics. A thin quarter-wave element with a cosine current distribution on it possesses a radiation resistance of 36 ohms when excited at one end. If one erects it over a lossless ground system, it actually will exhibit a measured as well as a theoretical resistance of 36 ohms.

Putting down a ground-radial system requires both large effort and money. It is very tempting to "sucker in" to the raised counterpoise. Good technical articles *are* appropriate. *They place a great responsibility on the shoulders of the authors, however.* The entire spectrum of hams is in the readership. Many of them need to be "led by the hand" through some designs. (This is not meant to be derogatory; only a small percentage of hams really understand.) The article does a poor job of "leading."

Some discussion of the "Scientific Method" is in order. (Theorize, or Hypothesize, and then PROVE IT.) The proof of the performance of any of the several raised-counterpoise antennas is missing. What we have is a reference to another theoretical raised counterpoise, neither of which can be compared to "real life." One does not use a calculated (but as yet unproved) antenna as a reference. That means nothing. Unfortunately, the ONLY valid reference is a radiator (say a quarter-wave long) erected over a large buried radial system; and *measured* so as to prove the system lossless. Inject a measured amount of power and then measure the far field-strength. NOW you have a yardstick that means something! I'm not espousing anything new; *that's how a "pro" would do it (some permissible FCC guidelines not withstanding).* One does not use another "calculated" system as a reference. Even if one could erect a ground plane several wavelengths above earth ground, he still could not use it as a reference. In high ground-planes, the radial system is part of the radiating system, thus it cannot be used as a reference for comparison of two vertical elements.

There is a proclivity among some to exercise a phenomenon, "GIGO" when using computer programs. It means "Garbage In, Garbage Out." It occurs often, mostly by misapplying a program. (*It's calculated by computer, so it must be right!*) So far as I understand, Roy's programs do NOT calculate the inducted current in the lossy ground under the raised radials. And it certainly exists! Unless the characteristics are compared to a "real" system, ALL the calculations are suspect. There were NO measurements—and there should have been.

W.J. Byron, W7DHD
Sedona, Arizona

Dear Editor:

I would like to make some comments about Mr. John Belrose's (VE2CV) article "Elevated Radial Wire Systems for Vertically Polarized Ground-Plane Type Antennas" that was published in the Winter 1998 issue of *Communications Quarterly.*

In his article, Belrose states, "Resonant quarter-wavelength radials (electrical length at a quarter wavelength) can be used with practical elevated ground-plane type antennas and to simulate 'connection' to ground for numerical modeling programs such as NEC2, which does not allow a wire to touch a lossy ground."[1] I would like to state that radial lengths near or at an exact length of 90 electrical degrees (electrical quarter wavelength) should not be used for practical elevated radial verticals when an omnidirectional pattern or the optimal production of vertically polarized energy is desired. Further, I would like to state that 90-degree long radials (resonant radials by Belrose's terminology) are the wrong choice as a means to simulate a "connection" to ground for numerical modeling programs which do not allow a wire to touch a lossy ground. I will discuss the reasons for my views.

The reason 90-degree elevated radials should not be used is based on the strong likelihood that individual radials which make up the elevated radial system will have different currents. If the currents are not equal, horizontally polarized energy will be radiated. There is a fundamental reason why elevated radials will have unequal currents. With a 90-degree radial, the "open" at the tip is reflected to the feed point connection end as a "short," or as an impedance of 0.0 + j0.0 ohms. When the radial is not exactly 90 degrees, the reflected impedance is not 0.0 + 0.0j ohms, but a non-zero value. This is illustrated in **Figure 1**, which is a plot of a single radial's impedance at 3.75 MHz 10 feet over average ground.[2] **Figure 1** shows that for a very small electrical length difference there are several ohms of differences in impedance. For example, a radial 0.2 degrees longer than 90 degrees has an impedance of 0.0 + j1.8 ohms. Herein lies the problem.

To illustrate this, let's suppose we have an elevated radial vertical antenna with four radials. For the best omnidirectional performance and the maximum generation of vertically polarized energy, the radial currents should be equal. If not, horizontally polarized energy will be radiated by the radial system. This means the current in each of the four radials must be the same. For this to happen, the radials must all have the same impedance. If 90-degree radials are used, all must have an impedance of 0.0 + j0.0 ohms. This is impossible. No two, much less four, things can be identical. In the case of radials, a minor electrical length difference of 0.2 degrees would change a radial's reactance from 0.0 to 1.8 ohms. With only very minor differences in electrical lengths, the displacement currents flowing back to the feedpoint via the radials will not be equal. Does this happen in the real world? Yes, it does, as shown by the following data.

Figures 2, **3**, and **4** provide measured radial currents from 160-meter verticals using elevated radials cut to a quarter wavelength that are in the clear and are not near any other towers or tower-like structures. **Figure 2** shows the measured radial currents at W7XU.[3] **Figure 2A** shows the currents measured before it was discovered the quarter-wavelength radials were not all the same length, but differed by 2 to 3 feet. After the radials were all made 127 feet

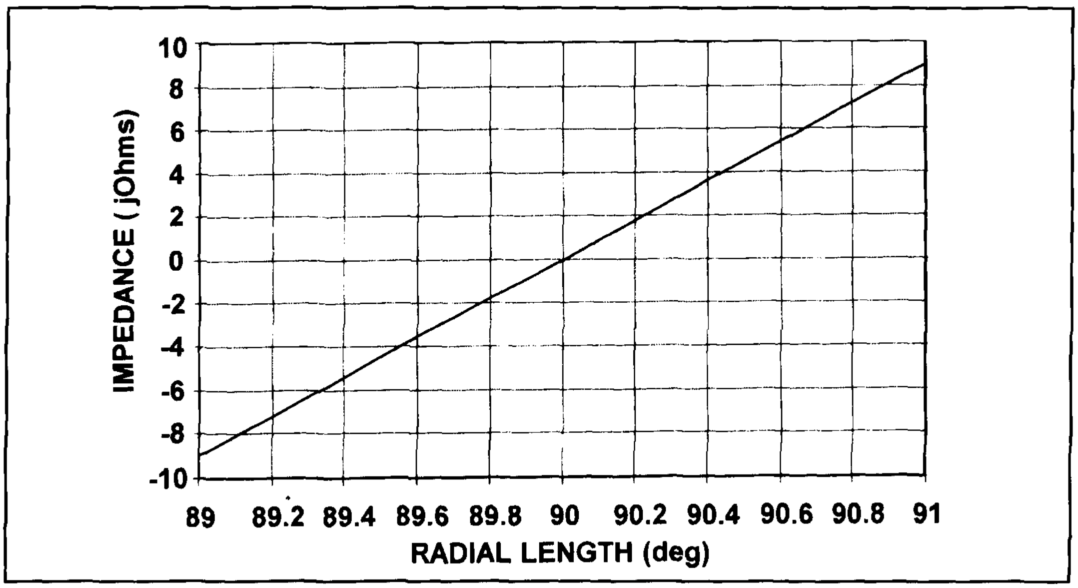

Figure 1. Radial impedance 10 feet above average ground at 3.74 MHz

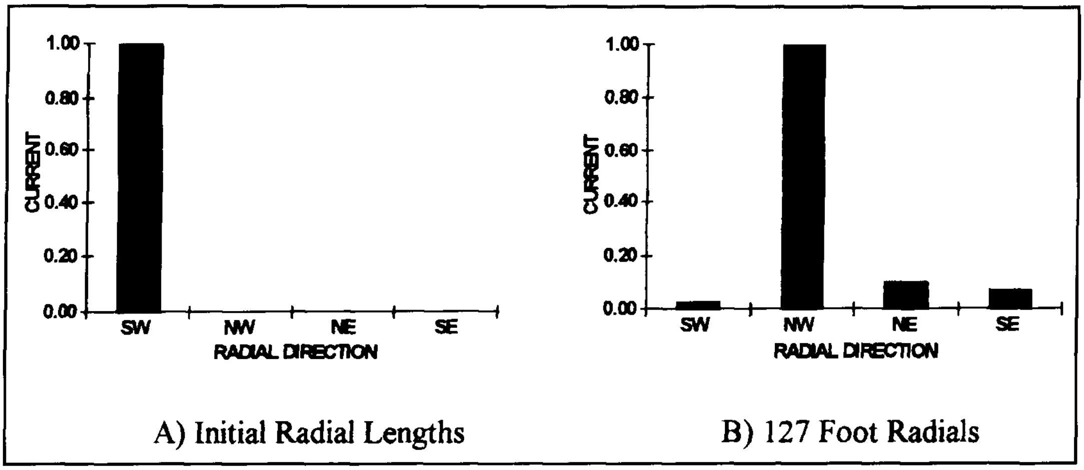

Figure 2. W7XU's radial currents at 1.805 MHz.

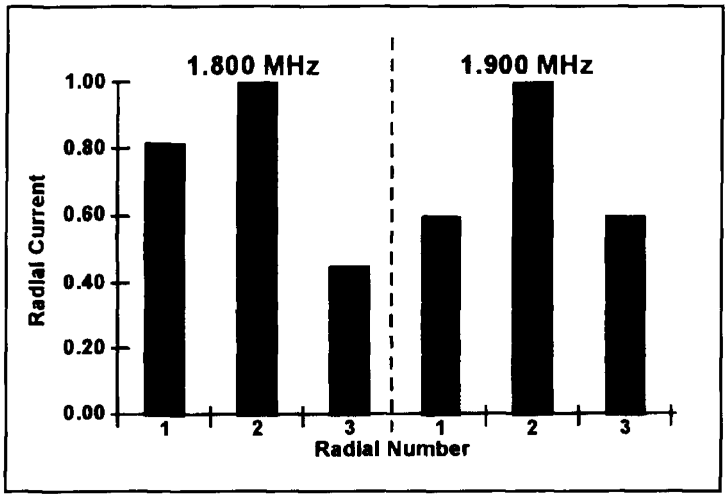

Figure 3. KE7BT's radial currents with 130-foot long elevated radials.

long, the currents were measured again. These are given in **Figure 2B**. Clearly this antenna is not working as originally intended. **Figure 3** shows the currents in the three elevated radials at KE7BT.[4] This figure shows the measured current at two frequencies. Similarly, **Figure 4** illustrates the measured currents in the four 133-foot elevated radials at KA2CDJ.[5] It must be pointed out again that these verticals are in the clear.

Figures 5 and **6** show the measured radial currents in verticals that are not entirely in the clear. **Figure 5** shows the radial currents in the two elevated radial verticals at WXØB.[6] Each antenna has two radials. These two antennas have two towers about 40 to 60 feet away. Clearly these antennas are not working as intended either. **Figure 6** gives the measured radial currents in my 80-meter elevated radial vertical, which is 35 feet from a 140-foot rotating tower.[7] It also has unequal radial currents. From this real world data, I believe it is safe to conclude that radial lengths near or at an exact length of 90 electrical degrees are to be avoided. They do not have the ability to produce near equal radial currents. Ninety-degree radials are too sensitive to minor variations in radial impedances. Influences such as variations in

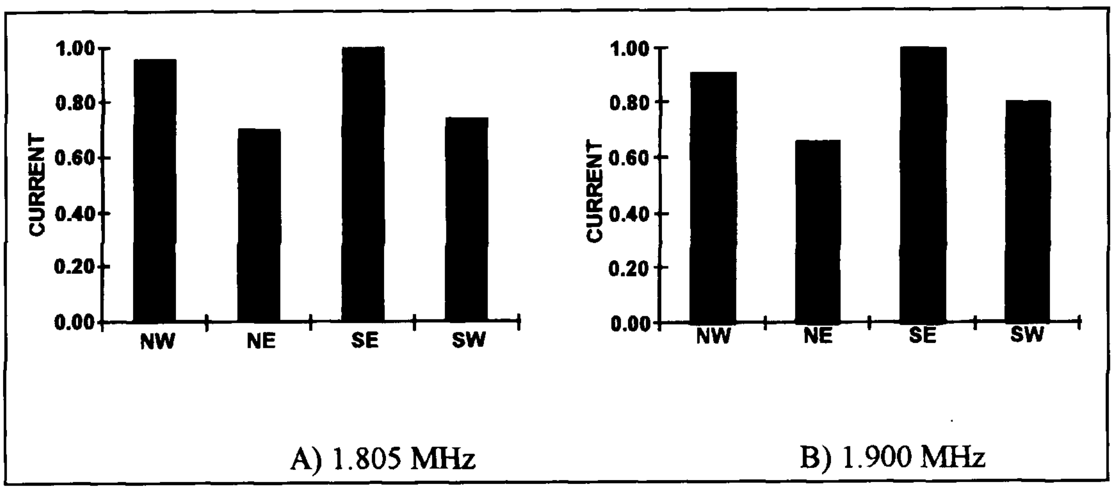

Figure 4. KA2CDJ's radial currents with 133-foot long elevated radials.

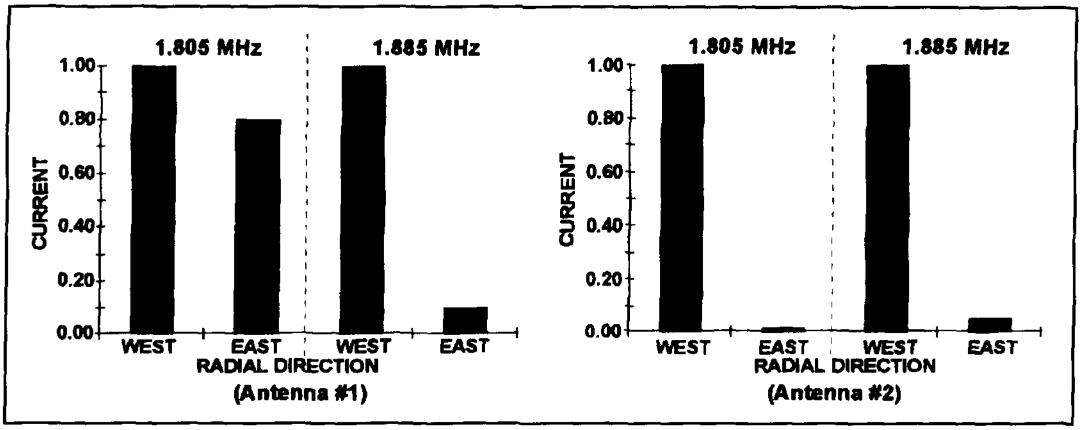

Figure 5. WXØB's radial currents.

soil conductivity, differences in length, and proximity to other towers or other obstacles, such as fences, can result in each radial having a different impedance.

In an article I authored which appeared in the Spring 1997 issue of *Communications Quarterly*, "Optimal Elevated Radial Vertical Antennas," I discussed these issues in detail.[8] In this article, I also stated that radials longer or shorter than 90 degrees will produce more near equal radial currents than radial lengths near or at an exact length of 90 degrees electrical. This is because when radial lengths sufficiently longer or shorter than 90 degrees are used, minor differences in each radial's impedance will not appreciably affect current partitioning. For example, 45-degree radials will each have an approximate impedance of 0.0-j530 ohms when 10 feet over average ground at 3.75 MHz, as shown in **Figure 7**.[2] If all radial impedances were identical, equal current would flow in each. If radial impedances differed by 5 to 10 ohms or so, the currents flowing in each radial would be essentially equal. This is not true with 90-degree radials. Here, several ohms of radial impedance variation can cause one radial's impedance to be many times higher than another because the nominal, or target, impedance is 0.0 + j0.0 ohms. For 90-degree radials, this is like having 0, 0.5, 1.0, and 2-ohm resistors in parallel and expecting equal currents to flow in each resistor. For radials in the vicinity of 45 degrees, it is like having 530, 535, 540, and 525-ohm resistors in parallel. Radials longer than 90 degrees have the same ability to produce near equal radial currents when there are minor differences in each radial's impedance.[9]

To have near equal radial currents requires using radials that are sufficiently longer or shorter than 90 degrees, so minor impedance variations are small compared to the radial's nominal impedance. Has this been verified through testing? Yes. In my article, five graphs of measured radial currents show this.[8] As an

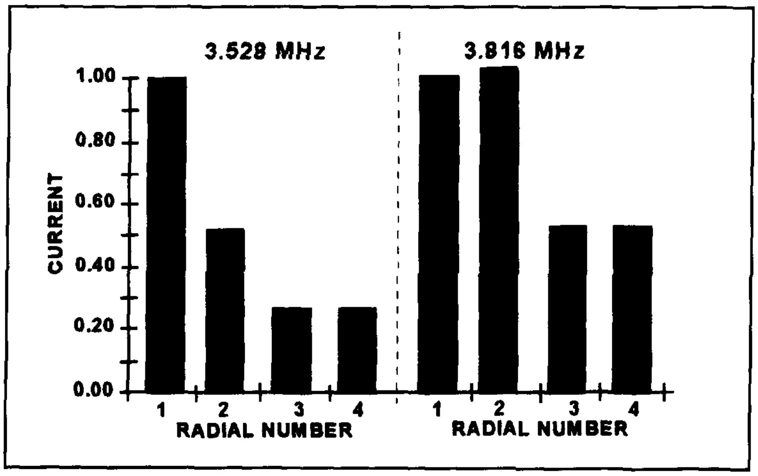

Figure 6. K5IU's 80-meter radial currents.

additional example, KE7BT recently changed from 130-foot radials to 154-foot radials. His new measured radial currents are shown in **Figure 8**.[4] The currents are essentially equal, as compared to those shown in **Figure 3**. When I changed the radials on my 80-meter system, as shown in my article, to lengths of approximately 45 degrees, the radial currents went from those shown in **Figure 6** to those shown in **Figure 9**.[10] After WXØB modified his Antenna #1 to use radials approximately 45 degrees long, radial current measurements showed improved partitioning as illustrated in **Figure 10** as compared to **Figure 5**.[3]

Belrose mentioned that the electrical length of a radial is affected by its height above ground.[11] This well-known effect is shown in **Figures 11** and **12**. These figures show the relationship between the physical length that produces a 90-degree electrical length and the radial's height above average ground using #12 copper wire for the radials. **Figure 11** is for 1.85 MHz and **Figure 12** is for 3.75 MHz. These plots are extremely useful when designing an elevated radial vertical. These are the radial lengths to

(Continued on page 98)

Eugene F. Ruperto, *W3KH*
1035 McGuffey Road
West Alexander, Pennsylvania 15376

GOES SATELLITE RECEPTION

An inexpensive approach

Did you ever wonder where the evening news folks get all those nice weather satellite pictures? If you have a basic low-frequency weather station that covers the low earth orbiting (LEO) weather satellites at 137 MHz, you, too, can capture them by building a simple downconverter. The block diagram and schematic are shown in **Figures 1** and **2**, respectively.

The geostationary satellites transmit on 1691.0 MHz, and are in orbit above the equator at an altitude of roughly 36,000 kilometers. Because the orbital period is 24 hours at this altitude, an eastbound satellite in orbit at the equator appears stationary from the viewpoint of a station on the Earth. Although at least two geostationary orbiting environmental satellites (GOES) can be seen from North America, the one I currently use is GOES-8 (**Photo A**).

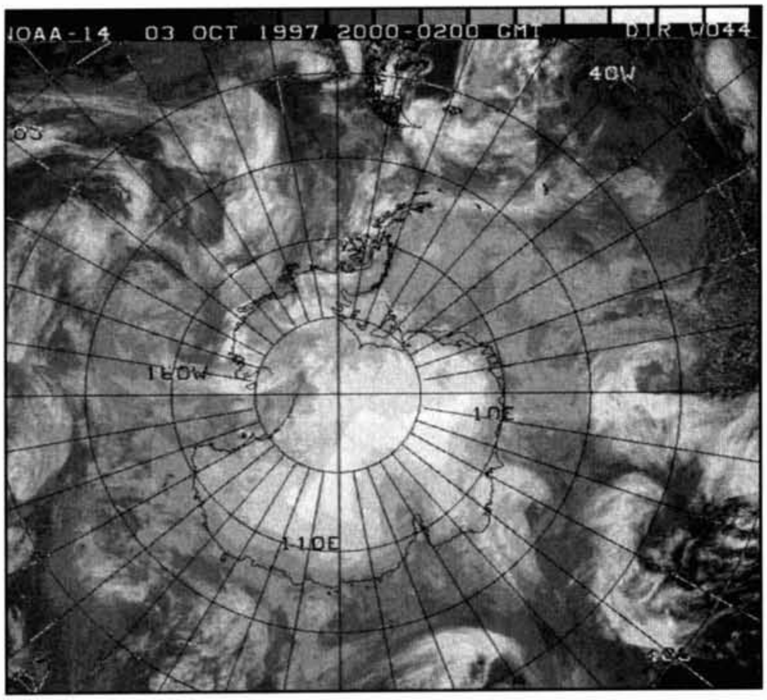

Photo A. A picture of the South Pole area relayed by NOAA14 and retransmitted by GOES-8.

GOES-8 is positioned at roughly 75 degrees west longitude with a satellite subpoint located several hundred miles east of Quito, Ecuador. At this altitude, the acquisition circle for a ground station extends from West Africa to well into the Pacific Ocean. Due to several astrodynamic factors, the satellites describe a small figure-eight pattern with excursions above and below the equator. However, the satellite subpoint varies by only a slight amount, on the order of a fraction of a degree, well within the 3-dB beamwidth of small parabolic dish antennas.

Background

The downconverter shown in **Photos B** and **C** is a modified version of my original,[1] built in 1978 to accommodate the change from the low-frequency geostationary satellites to microwave frequencies. The geostationary workhorse at that time was the Applications Technology Satellite ATS-3, which provided APT and WEFAX products on 135.6 MHz. NOAA made a commitment to move these products to 1691.0 MHz and maintain the same characteristics. As a result, the modulation system and picture characteristics would remain the same and only the frequency would change.

Prior to the launch of the first microwave APT/WEFAX geostationary satellite, NOAA published figures on the expected signal strength of -134 dBm in a technical memorandum.[2] This led me to consider an active mixer

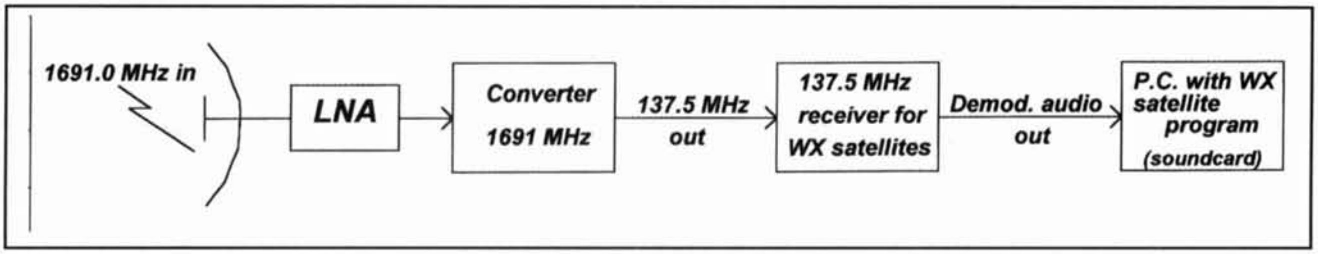

Figure 1. Block diagram of the W3KH system for GOES reception.

(**Figure 3**) using a low-noise transistor rather than the usual lossy diode mixer. The use of an active mixer would actually provide some gain rather than insertion loss experienced with the use of a passive mixer. At this time, the low-noise high-gain devices we now take for granted didn't exist, or at best were hard for the average amateur to find. The best device I could come up with at that time was the Motorola MRF901, which performed well for this application. It boasted a gain of 10 dB and a noise figure of 2.0 dB at 1000 MHz. It may be interesting to note that, in the technical memorandum, NOAA recommended a state-of-the-art preamplifier with a gain of 20 dB and 4.5 dB noise figure at 1691.0. This was located at the prime focus of the recommended 12-foot dish. Today, I alternate between a 3- or 6-foot homemade dish and some quiet bipolar transistors in a preamp to accomplish the same task. A GaAsFET device at the feedhorn makes it even easier to copy full-quieting pictures.

Converter description

The converter makes use of old but proven technology. There are no printed circuit boards to etch, although ample use is made of double-sided pc board material for the cavity construction. The unit basically consists of two half-wavelength lines, center tuned in cavities. One cavity is the signal cavity and the other the multiplier cavity. The center partition separating the cavities is notched to accept the input circuit of the active device, in this case a Motorola MRF901 bipolar transistor. This may be replaced with the newer MRF951 because of its lower noise and better gain characteristics, but that requires some circuit modification because it is basically a 10-volt instead of a 12-volt device.

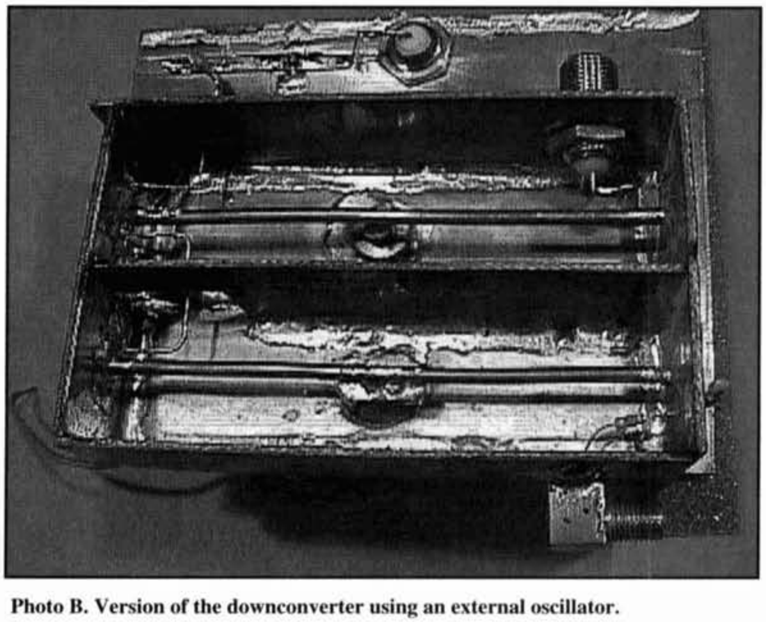

Photo B. Version of the downconverter using an external oscillator.

The oscillator chain in **Figure 4**, designed by W3BQG, has as its first stage a low-frequency third overtone oscillator with a series load crystal in an HC18 holder having a tolerance of 0.001 percent. The oscillator transistor is a 2N3904 or similar audio transistor. This stage is followed by an untuned buffer amplifier, also a 2N3904, followed by a tuned circuit using a 2N5179 to drive a multiplier diode in the multiplier cavity. The multiplication scheme requires a crystal of 38.837500 MHz, which is multiplied by 40 to give a final injection frequency of 1553.5 MHz. The difference between the downlink frequency of 1691.0 MHz and the injection frequency gives us an IF of 137.5 MHz, which is one of the NOAA APT VHF frequencies. Similarly, a different oscillator crystal may be selected to provide an IF output on any of the other common frequencies normally encountered on the weathersat frequencies. The output circuit at 137.xx MHz is a tuned circuit with an emitter follower circuit using a 2N5179 transistor (**Figure 5**).

Construction

The cavities (see **Figure 6**) are constructed on a groundplane of double-sided epoxy pc board. I chose a piece of 4 x 6 inch board. The cavities are made of 1-inch-high strips of pc board. The base or groundplane should be marked with the inside dimension of the cavities and scribed or marked with the layout of the center partition and the location of the half-wavelength lines. Then, the proposed location of the middle of the lines should be marked to indicate where to drill the holes for the tuning screws, which in this case are 10/32 thread, 0.75-inch brass roundhead screws. The outline of the cavity should be about 55 mm x 82 mm. This allows the half-wavelength lines to be about 15 to 20 percent shorter than a free-space half wavelength because they can be pulled lower in frequency with the tuning screws.

Next, cut five 1-inch-wide strips for building the box to be mounted on the groundplane. Before all the inside seams of the cavity box are soldered, there are several holes to be drilled on the strips. The two long sides must be drilled to accept the input connector and the LO injection connection, if used. A small hole should also be drilled and relieved on both sides for the multiplier diode. The shorter two pieces are marked to center the ends of the tuning lines, mark the position of the center partition, and show where to drill a hole for the active device. A small exit hole should also be drilled for the lead of the multiplier diode. The center partition should be notched with a hacksaw or tin-snips. To mount the tuning screws, I use a drill, tap, and die to thread the two holes marked for the screws. Thread them in about halfway, and mount a brass nut to the cavity side of the groundplane.

To ensure good solder connections, make sure the groundplane copper is clean and free of grease. I generally scrub the surface with Brasso™ and give it a warm soap and water rinse followed by an alcohol rinse. I used a 200-watt iron to anchor the nuts. Once the screws and nuts are in place, solder the walls to the groundplane to complete the box. The tuning lines now can be attached and soldered on both sides of the pc board walls. The electronic components are all mounted to the groundplane "dead bug" style.

Tuneup

Of course, the best way to tune up the unit is with a good spectrum analyzer and some high-powered test equipment, including a signal generator. Lacking all of the above, I drew on the expertise of my friends and their ingenuity and performed most of my tuneup with some meters, a handheld counter, and a handheld radio. The satellite itself provided me with the signal source for fine tuning.

The oscillator circuit consists of only one tuned circuit. This is found on the collector side of Q3, the last transistor of the oscillator chain (**Figure 3**). I used a 0–10 mA meter connected in series with the multiplier diode to ground to monitor the diode current. An alternative method is to mount a small-value resistor, say 100 to 200 ohms, to the output side of the diode, outside the cavity, and measure the voltage drop across the resistor. Be sure to bypass the lead as it comes out of the cavity, otherwise readings may be erratic. The oscillator circuit and multiplier diode give a current reading of about 3 to 4 mA of current. This is approximately 1 to 3 mW or slightly more than 0 dBm of injection. After optimizing the tuning, the diode may be directly grounded to the pc board.

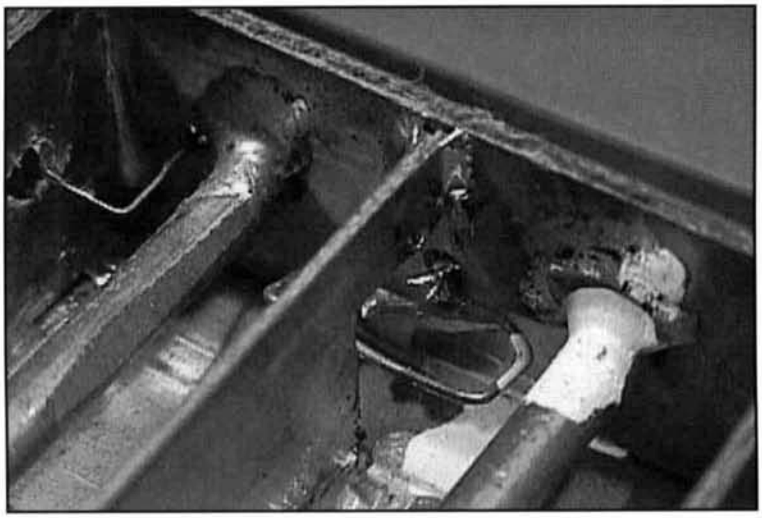

Photo C. Version of the downconverter with an onboard oscillator.

My IF was 137.5, so I tuned the final stage of the oscillator to select 258.917 MHz. This frequency, when multiplied by six, provides an injection frequency of 1553.5 MHz to the multiplier cavity. I tuned the oscillator tank circuit for 258.917 MHz using a handheld counter with a maximum frequency range of 1300 MHz. I monitored the signal on my Yaesu FT50R and tuned C2 for maximum output by watching the LCD signal strength bar on the handheld. The signal from the oscillator was evident on the handheld receiver at a distance of at least 20 feet or better.

If a signal generator is available, tune to 1691 MHz or a subharmonic that will provide this frequency, and tune the cavity screws for maximum signal. Start by having both screws mostly out of the cavity. If more capacitance is needed in the multiplier cavity, a small tab soldered to the tuning line directly above the tuning screw may be necessary, otherwise the screw tip may end up almost touching the line. Once all this is accomplished, attach the low noise amplifier (LNA), the parabolic dish, and retune the cavity screws for the best signal.

Some additional thoughts and caveats

Although the converter seems simple, I wouldn't classify it as a beginner's project. If

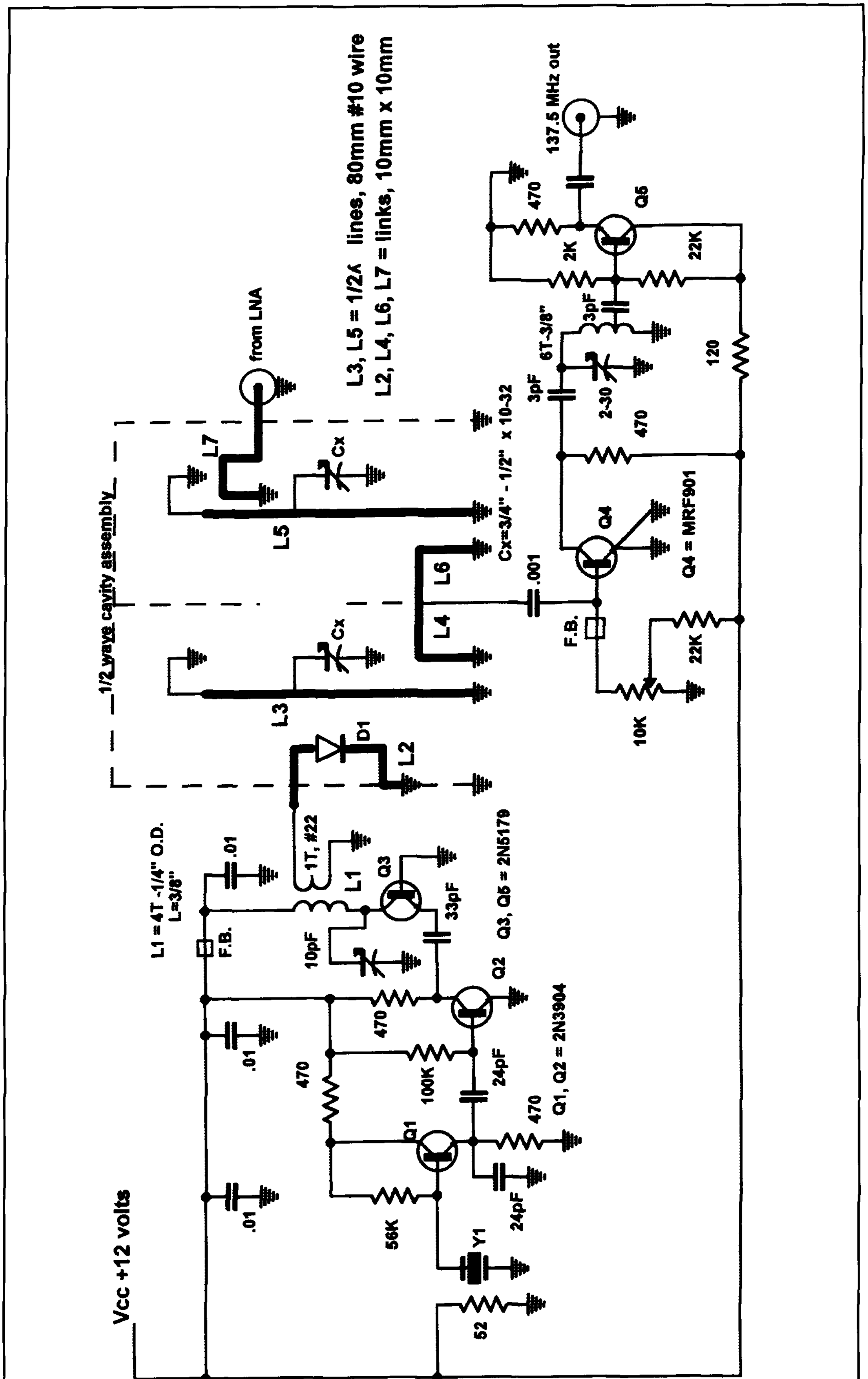

Figure 2. Schematic of the W3KH system.

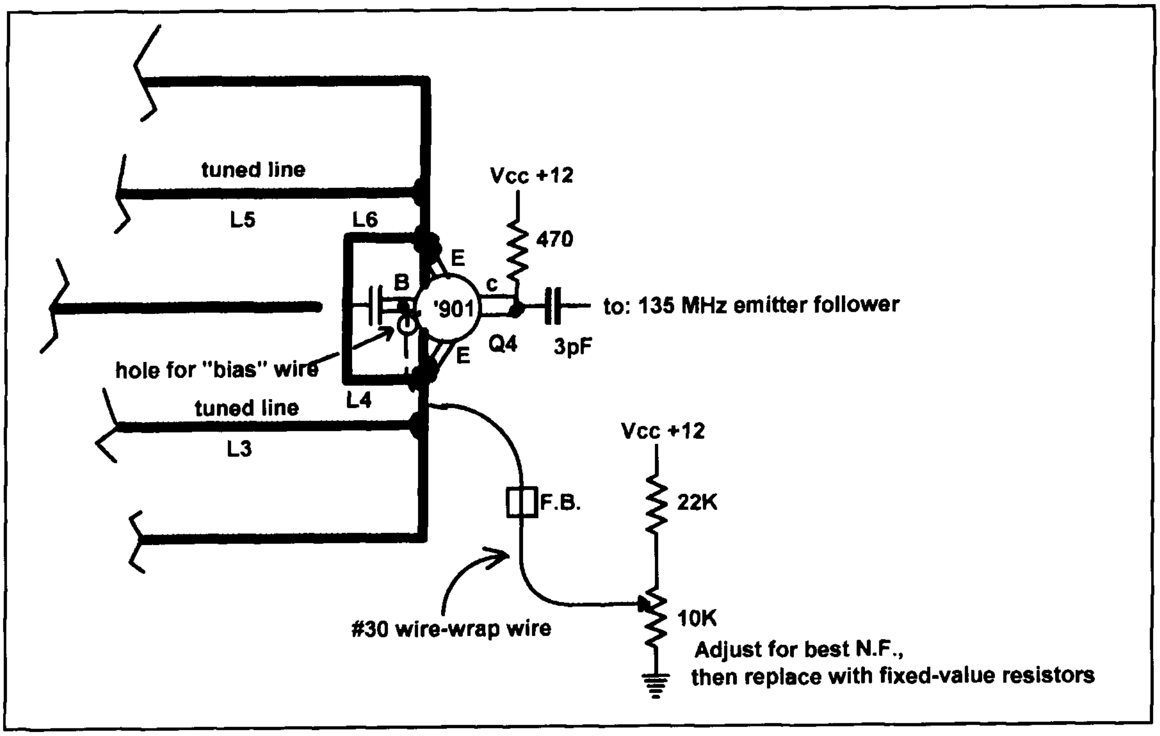

Figure 3. Bias circuit for the active mixer.

you don't have experience building gear that operates in the microwave region, it may be prudent to seek help from someone who does. Depending on the size of the dish and run of coax, I'd recommend a fairly good low noise amplifier at the feed—something in the neighborhood of 23 to 50 dB. My converter is indoors, but it would be more efficient situated at the feed and weatherproofed. The oscillator may not be textbook, but it isn't intimidating, and there are other ways to build it.

The multiplier diode may be replaced with an active device. My last converter used an MRF951 transistor in place of the multiplier

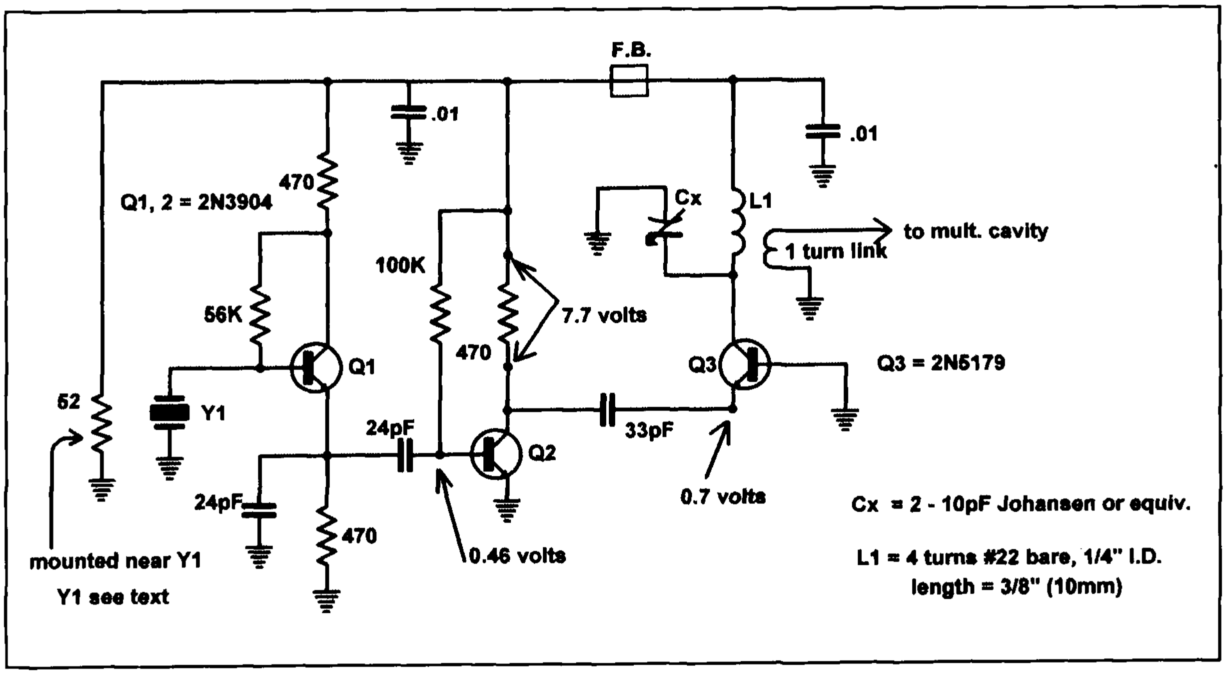

Figure 4. Oscillator chain for the 1691.0-MHz converter.

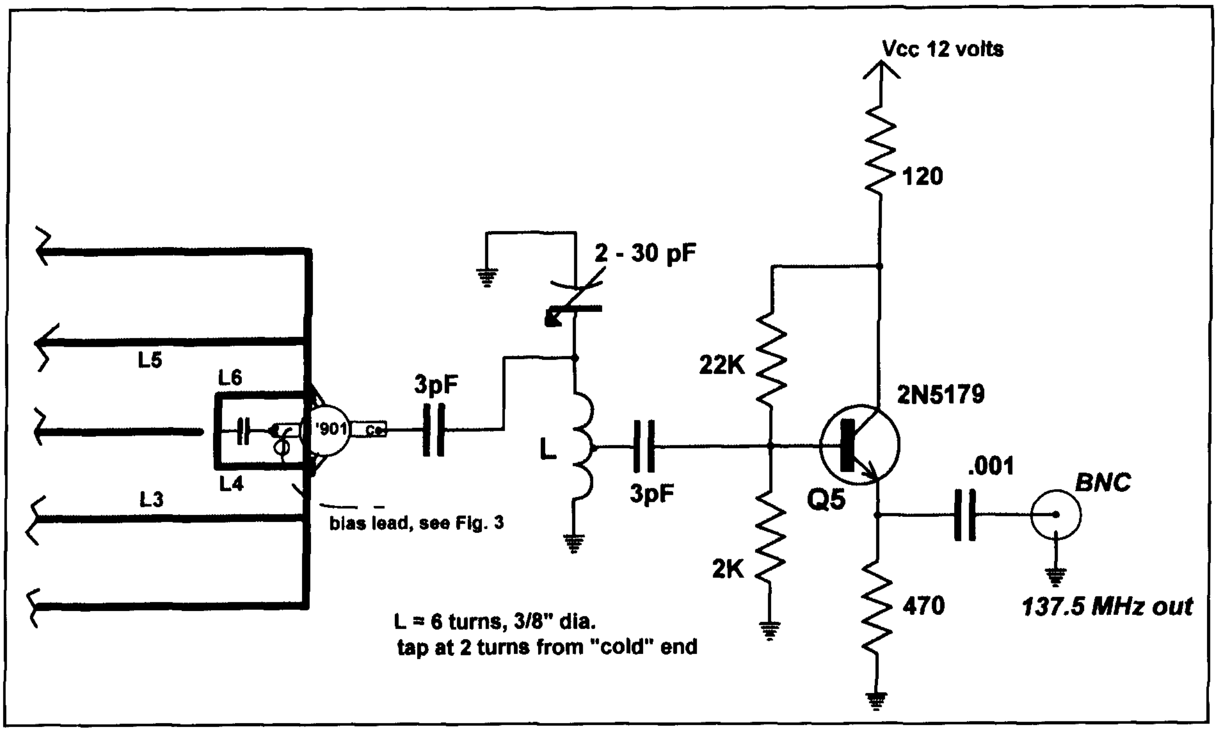

Figure 5. Emitter follower circuit for the 137.5-MHz output.

diode. The groundplane is much larger than necessary. All you really need is about a 1-inch margin to build the oscillator chain. The half-wavelength lines aren't necessary because the same scheme can be accomplished using quarter-wavelength lines and smaller cavities. Dick Bour, W3BQG, built a downconverter using this method.

I've replaced my cylindrical feed with a quadrifilar helix antenna. It minimizes feed blockage and performs as well as the cylindrical feed, although the satellite is linearly polar-

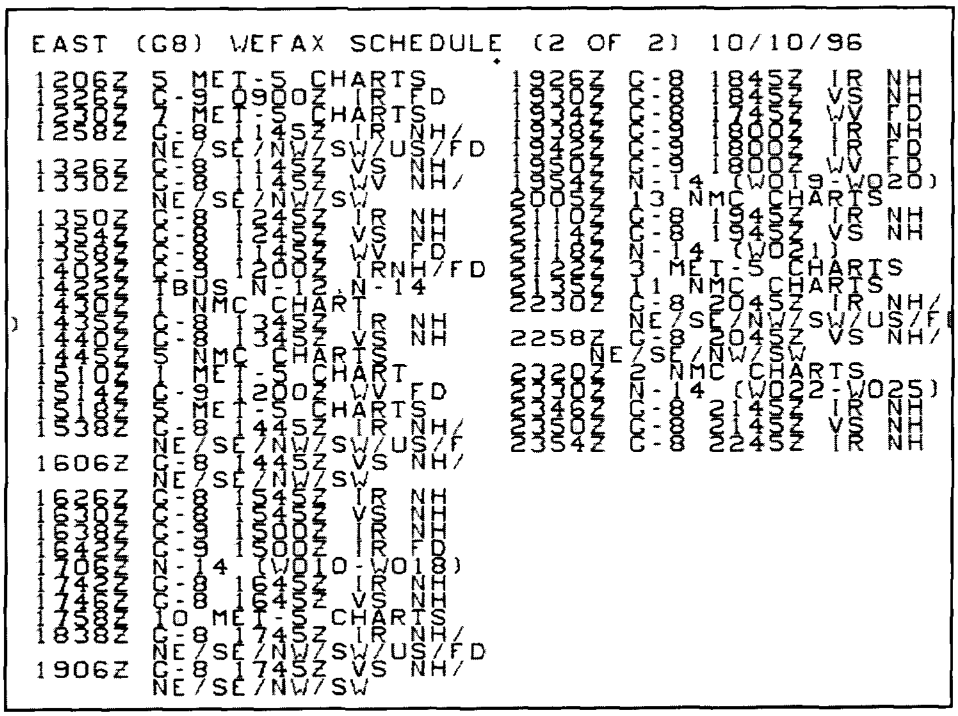

```
EAST (G8) WEFAX SCHEDULE (2 OF 2) 10/10/96
1206Z 5 MET-5 CHARTS
1226Z G-9 0900Z IR FD
1230Z 7 MET-5 CHARTS
1258Z G-8 1145Z IR NH/
      NE/SE/NW/SW/US/FD
1326Z G-8 1145Z VS NH
1330Z G-8 1145Z WV NH/
      NE/SE/NW/SW
1350Z G-8 1245Z IR NH
1354Z G-8 1245Z VS NH
1358Z G-8 1145Z WV FD
1402Z G-9 1200Z IRNH/FD
1422Z TBUS N-12,N-14
1430Z 1 NMC CHART
1435Z G-8 1345Z IR NH
1440Z G-8 1345Z VS NH
1445Z 5 NMC CHARTS
1510Z 1 MET-5 CHART
1514Z G-9 1200Z WV FD
1518Z 5 MET-5 CHARTS
1538Z G-8 1445Z IR NH/
      NE/SE/NW/SW/US/F
1606Z G-8 1445Z VS NH/
      NE/SE/NW/SW
1626Z G-8 1545Z IR NH
1630Z G-8 1545Z VS NH
1638Z G-9 1500Z IR NH
1642Z G-9 1500Z IR FD
1706Z N-14 (W010-W018)
1742Z G-8 1645Z IR NH
1746Z G-8 1645Z VS NH
1758Z 10 MET-5 CHARTS
1838Z G-8 1745Z IR NH/
      NE/SE/NW/SW/US/FD
1906Z G-8 1745Z VS NH/
      NE/SE/NW/SW
1926Z G-8 1845Z IR NH
1930Z G-8 1845Z VS NH
1934Z G-8 1745Z WV FD
1938Z G-9 1800Z IR NH
1942Z G-9 1800Z IR FD
1950Z G-9 1800Z WV FD
1954Z N-14 (W019-W020)
2005Z 13 NMC CHARTS
2110Z G-8 1945Z IR NH
2114Z G-8 1945Z VS NH
2118Z N-14 (W021)
2122Z 3 MET-5 CHARTS
2135Z 11 NMC CHARTS
2230Z G-8 2045Z IR NH/
      NE/SE/NW/SW/US/F
2258Z G-8 2045Z VS NH/
      NE/SE/NW/SW
2320Z 2 NMC CHARTS
2330Z N-14 (W022-W025)
2346Z G-8 2145Z IR NH
2350Z G-8 2145Z VS NH
2354Z G-8 2245Z IR NH
```

Photo D. The GOES-8 schedule sent as alphanumeric characters.

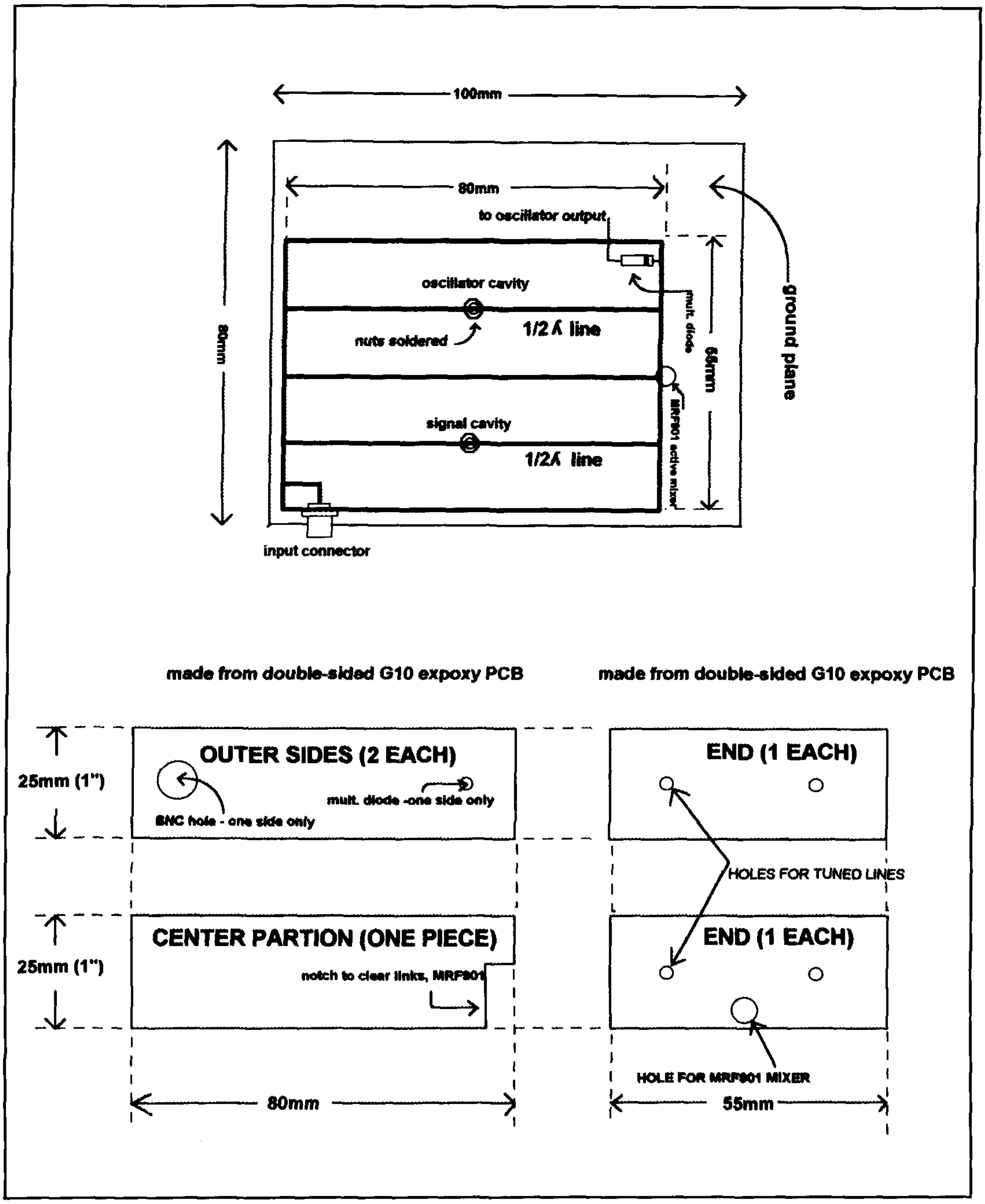

Figure 6. Construction details of the W3KH GOES downconverter.

ized and the QHA is wound for left-hand circular polarization. R1 is a 5-watt, 52-ohm resistor to heat the groundplane. This keeps the temperature constant and the crystal relatively stable. If the crystal is slightly off frequency, it can be pulled a small amount by the addition of a series capacitor or inductor, or a combination of both.

In my opinion, the scheme of multiplying by six from the final stage isn't the best way to get maximum power to the multiplier diode. My prototype downconverter used a commercially built oscillator with an output at 517.833 MHz and was multiplied in the cavity by three to 1553.5 MHz. This provided an IF output at 137.50 MHz. At +10 dBm, the 517.833-MHz signal could be heard anywhere in the house on the handheld.

I'm now using "F" connectors on all connections because they seem to work well enough at this frequency and simplify construction. My feedline is 50 feet of 75 ohm RG-6/U. I've also added a MAR6 device to the mixer input for some extra gain.

The GOES-8 satellite also transmits an EMWIN (Emergency Managers Weather

Information Network) signal, 400 kHz below the main carrier of 1691.0 MHz. Presently, transmitting data on GOES 8 and 9 is in Bell 202 modem format at 1200 baud. National Weather Service is changing over to 9600 baud—275 kHz below the 1691.0-MHz carrier. It requires a separate demodulator to extract the data, and these are available from several vendors, two of which are listed in the **Notes**. A schematic for an EMWIN demodulator can be found at: <http://www.nws.noaa.gov/oso/oso1/oso12document/zerx96a.gif>.

Other countries use similar GOES satellites, operating on or near the same frequency. They include Fen yung (divine wind), Peoples' Republic of China (250 kHz BW); GMS, Japan (BW 250 kHz); GOMS, Russia; and GMS-5 European Consortium. The GOES series of satellites will provide the experimenter with hours of data. These satellites transmit almost constantly and even provide an alphanumeric time schedule of transmitted frames (see **Photo D**). This gives you something to do between polar orbiting satellite passes. A final plus is the availability of a weak test signal for optimizing feeds and antennas. ■

REFERENCES

1. Eugene F. Ruperto, W3KH, "The Microwave Midget: an active mixer for GOES WEFAX," *73*, December 1980.
2. John J. Nagle, "A method of converting the SMS/GOES WEFAX frequency (1691 MHz) to the existing APT/WEFAX frequency (137 MHz)," *NOAA Technical Memorandum NESS 54*, April 1974.

NOTES

1. Zephyrus Electronics, Ltd., 171 S. 122 E. Avenue, Tulsa, Oklahoma 74128-2405, <www.big-z.com>.
2. Maryland Radio Center, Inc., 3394 Fort Meade Road, Laurel, Maryland, 20724, <www.weathernode.com>.

PRODUCT INFORMATION

New Hamtronics® Catalog

Hamtronics, Inc. has a new 1998 catalog, which contains 40 pages of kits and wired units for amateur radio, two-way shops, scientific and industrial users, and OEMs. Several new frequency synthesized transmitter and receiver products have been added to the usual lineup of high-quality VHF & UHF products.

The new T301 Exciter and R301 Receiver provide NBFM and FSK operation. Models are available for 144-148 MHz (and 148-174 MHz) and 220-225 MHz (and 216-220 MHz for export and government services). Features include dip switch frequency selection, low noise synthesizer for repeater service, commercial grade TCXO for tight frequency accuracy in a wide range of environmental conditions.

The T301 Exciter has modulation for voice and subaudible tones. It uses direct FM modulation, which allows FSK transmission of data up to 9600 baud. Power output is 2-3 W and it is rated for continuous duty.

Hamtronics is now able to stock 2-meter and 220-MHz repeaters for next day shipment, since there is no delay waiting for channel crystals.

Three new products are added to the selection of VHF and UHF FM transmitters, receivers, power amplifiers, transmit and receive converters, preamps, repeaters, DTMF controllers, autopatches, and digital radio modems which Hamtronics, Inc. has manufactured for 36 years.

For your copy of the catalog: write to Hamtronics, Inc., 65-F Moul Rd., Hilton NY 14468-9535, call (716) 392-9430, fax: (716) 392-9420, or e-mail <jv@hamtronics.com>. While you are at it, ask for a complete catalog, which also includes all their VHF/UHF transmitters, receivers, repeaters, converters, preamps, and accessories. Please tell them where you saw this announcement. You can also view the entire catalog at their web site <http://www.hamtronics.com>.

YGO Freeware Available

Phadean Engineering Co., Inc., is making a freeware version of YGO, the Yagi Genetic Optimizer, available to anyone interested in ham radio or antennas. YGO is a state-of-the-art genetic algorithm that designs Yagi-Uda arrays using NEC-2D (Numerical Electromagnetics Code, Ver. 2), which is included. The freeware version is fully functional for up to 4-element arrays, and may be freely copied and distributed. YGO is a DOS-based program that requires an 80386 with co-processor or better CPU and at least 1 MB RAM. To obtain a copy, please send your e-mail address to: <phadean@ma.ultranet.com>. The freeware version of YGO will be e-mailed back to you (please note that the download file is about 420 KB). You can also contact Phadean at P.O. Box 611, Shrewsbury, MA 01545-8611 USA, phone (508) 889-6077, fax (508) 889-2890.

Alan Chester, *G3CCB* (Silent Key)
Reprinted with permission
from *Radio Communication*
September 1994

TAMING THE END-FED ANTENNA

The single wire antenna directly connected to the transmitter is often discouraged in the amateur radio manuals because of the close proximity of the radiating element to house wiring and domestic equipment. This undesirable feature is aggravated by the fact that wild excursions of feed impedance occur when changing operation from band to band and good matching is sometimes difficult to achieve.

All in all, however, the antenna is simple, cheap, easy to erect, suits many house and garden layouts, and is easily amenable to base or portable operation. It is not surprising that the end-fed wire is often pressed into service by old hands and newcomers alike, who are prepared to work on its more wayward characteristics to produce a thoroughly acceptable multi-band antenna.

This article sets out to show how the length of an end-fed antenna can be optimized to serve a given set of bands, tuned to resonance (minimum feed impedance) on each band and then coupled to the transmitter using a wide-band matching transformer and any required length of coaxial cable to distance the antenna wire from the operating position. Such an antenna can then be operated against real earth (if a suitable terminal is close at hand) or, more likely, a substitute in the form of a radial (or several) or a counterpoise wire.

Background

The end-fed antenna has traditionally been designed to resonate on one lower band in the HF spectrum, say a quarter wavelength on 80 meters where the current feed will meet an impedance of around 50 ohms. At a half wavelength on 40 meters, the input impedance will rise to a high value presenting a voltage feed to the source. The next band, 30 meters, will fall in the vicinity of current feed again at three quarters of a wavelength and present a fairly low impedance. The next move to 20 meters will meet a high impedance again and then through an off-tune 17 meters to another high at 15 meters. The sequence continues with some extra complication in that odd multiples of wavelength will show generally increasing impedance with frequency whereas even multiples of wavelength (the half-wave points) will show decreasing impedance as the band is ascended.

To achieve a moderate feed impedance on all bands, some means must be found of selecting

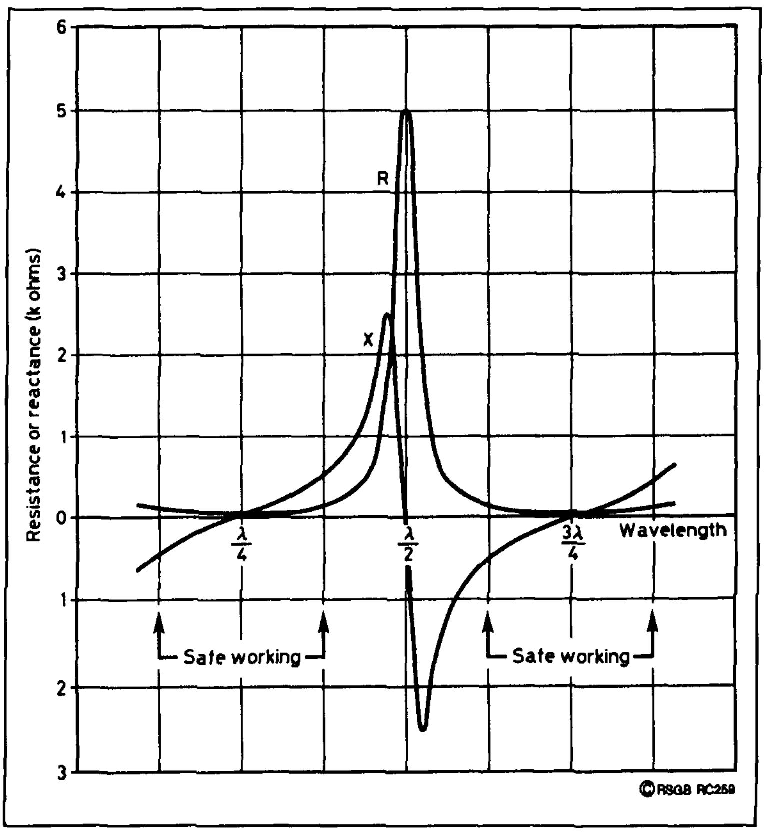

Figure 1. End-fed impedance characteristics of wire from λ/4 to 3λ/4.

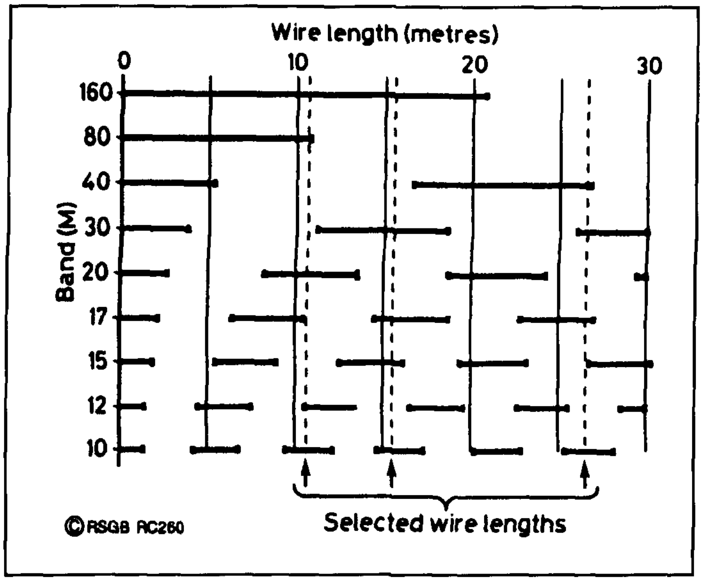

Figure 2. Antenna wire lengths showing "no-go" lengths for various bands.

a wire length that steers well clear of the half-wave points. **Figure 1** illustrates resistance and reactance plotted against electrical length from below a quarter wavelength to three quarters of a wavelength and beyond. It can be seen that dramatic changes begin to occur as the half wave resonant point is approached. These dramatic changes are repeated at multiples of $\lambda/2$ and these regions must be avoided if the impedances of a multiband antenna are to be kept reasonably low and uncomplicated on all bands of operation.

In general, the magnitude of the half wave multiple resistive and reactive excursions decrease as the electrical length of the antenna is increased.

To make a start, it was decided that the sector within $\pm \lambda/8$ from the $\lambda/4$ point represented fairly "safe" working conditions within which the wire could be tuned by adding the appropriate sign of reactance at the feed end.

In other words, wires on the low side of the $\lambda 4$ point (too short) would be tuned by inserting inductive reactance in series with the wire, while lengths on the high side of the $\lambda/4$ point (too long) would be tuned by inserting capacitive reactance in series. It follows that entry into the "danger" areas within $\pm\lambda 8$ from the $\lambda/2$ resonance peak should be undertaken with care. The same principle applies for subsequent quarter and half wavelength regions on longer wires.

In **Figure 2**, wire length is shown against each of the nine HF bands (including 160 meters) with "no-go" portions indicated by the heavy lines. To avoid unnecessary complication, wavelengths were calculated from the lower band edge frequency in each case and no corrections were made for the "end effect" on a real antenna.

To use the chart, a perpendicular straightedge is dropped from the horizontal axis and moved along until a clear way through the gaps between the no-go sectors is found. Thus, for a wire length of 10.5 meters, the straightedge just clips the end of the 80-meter no-go line, then goes through the middle of the 40-meter safe sector and on through the 30-meter gap. At 20 meters, the straightedge is blocked, but there are clear openings at 17, 15, and 12 meters.

The next opportunity presents itself at a wire length of 15.5 meters where openings appear at 80, 40, and 20 meters and, if some tolerance is permitted, at 17 and 15 meters, and then through the clearance at 12 meters. The very next choice of the bands becomes available at a wire length of 26.5 meters which gives all eight bands including 160 meters but not, unfortunately, 10 meters where special arrangements have to be made. The wire lengths quoted here may need some small adjustment when the practical system is built.

Tuning and matching

It can be seen, from **Figure 2**, that there is at least one band for each wire length where the straightedge goes through the center (or very nearly) of a safe working region. At this point, the feed impedance will be fairly low. For other bands, where the straightedge lies to the left or right of the gap center, the impedance will be higher in value and capacitively or inductively reactive. The reactive component is tuned out by inserting an inductor or capacitor of the appropriate value close to the feedpoint leaving a non-reactive antenna feed of moderate value to be matched very easily to the transmitter.

Some general points need to be made here to assist in the selection and adjustment of tuning and matching components. Near the center of the safe working regions, relatively small values of reactance will be required to bring the antenna to resonance; at the extremities, larger values will necessary. The outer limits of these regions may be extended by a small amount as practical examples given in the section "The Practical System" will show. Because the antenna is pre-tuned on each band and designed to offer only a moderate range of resistive input impedances, it only remains to add a simple wideband transformer to match the antenna to the transmitter via 50-ohm cable. Such a transformer is described in **Reference 1**.

Earth plane

Using the principles described in the selection of wire length and tuning, it is now neces-

Tuning and Matching Data

Band (meters)	Tune	Match (ohms)	Notes
25.60-meter wire			
160	32–10 µH	50	Various ground planes
80	150 pF	112	
40	6 µH	112	
30	50 pF	200	
20	>100 pF	112	Near series resonance
17	2 µH	200	
15	25 pF	450	
12	>50 pF	112	Near series resonance
10	1 µH/25 pF	800	Parallel resonance (see text)
15-meter wire			
80	14–10 µH	25–50	
40	100 pF	50	
20	>50 pF	112	Near series resonance
17	25 pF	450	
15	4 µH	450	
12	>50 pF	450	Near series resonance
10	1 µH/25 pF	800	Parallel resonance (see text)
10-meter wire			
80	20–14 µH	25–50	
40	>100 pF	50	Near series resonance
30	50 pF	200	
17	2 µH	112	
15	>50 pF	200	Near series resonance
12	25 pF	450	
10	1 µH/25 pF	800	Parallel resonance (see text)

Table 1. Tuning and matching guidance data for each band against three lengths of antenna wire (elevated or grounded).

sary to consider the earth plane, real or substitute, against which the antenna will operate.

In general, a good earth connection is hard to find and only practicable from a ground floor room. Unless the earth can be reached within a very short distance, the "earth substitute" (radial or counterpoise) comprising a single quarter wavelength wire from the aerial feedpoint is hard to beat and the technique will also ensure minimum RF voltage at this point. The earth stake version, although often less efficient, is convenient for portable operation and avoids the chore of erecting more wires.

The practical system

The full range of tuning component values and feed impedances for each HF band against wires of three lengths is shown in **Table 1**. Any one length of wire can be operated either elevated well above ground using substitute earths or very near ground using a real earth connection via a short lead. The longest wire (26.50 meters) will provide full coverage on all nine bands while the shorter wires (15 and 10 meters) will cover seven bands each with some overlapping. It can be seen from **Table 1** that two wires, used selectively, will provide full coverage without the complication of inductor tuning.

The main wire is measured to the dimensions given in **Table 1** and, after marking, it may be prudent to allow a little extra for fine adjustment during installation; this is accomplished on the 20-meter band for the 26.50- and 15-meter wires and on the 40-meter band for the 10-meter wire where natural resonance occurs in each case. Although it is physically possible to tune the wire to any part of the band as required by the cut-and-try method and avoid the need for the tuning capacitor altogether, it is generally preferable to place the natural resonance a little below the lower band edge frequency and use the variable capacitor (at relatively high value) to move the resonance point up into the band.

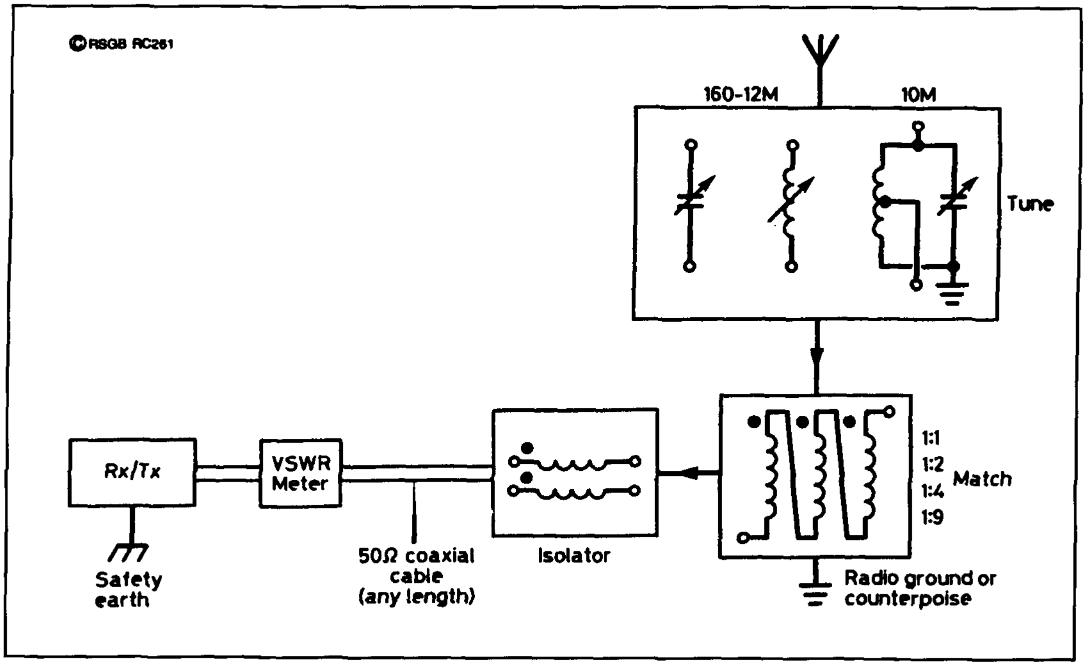

Figure 3. Layout of antenna to transmitter interface.

The quarter wavelength substitute earth wire for the elevated antenna can be cut for the required frequency within each band less 5 percent for end effect. The measurements are not critical and no difficulty will be found in practice because any fine adjustment required will be taken up automatically when the main antenna wire is tuned. The lead length to the earth stake for the grounded version was fixed at 1 meter to maintain some degree of uniformity between the two versions and to ensure reproducibility of the design. The stake used was about 1.5 meters in length and the short connecting wire was adequate for portable operation from car, tent, or even garden shed but, if required, the lead may be extended by a small amount provided an equivalent reduction is made to the main wire. The grounded end-fed wire cannot match the performance of the elevated version unless a very good earthing system is employed. Nevertheless, the simple stake has been shown to provide a useful and convenient earth when operating from a temporary location.

The simplest way to provide the tuning function at any power level is by using one variable capacitor of adequate vane spacing and one variable inductor (roller coaster) connected in circuit as required. The units were calibrated and showed maximum values of 750 pF and 32 μH, respectively, although extra inductance was sometimes required at 160 meters. This was the arrangement used when compiling the data given in **Table 1**. Values given are "broad brush" based on many measurements taken during trials. A range of values is given where the band is particularly wide.

10-meter operation

An examination of **Figure 2** will show that, for the three preferred wire lengths, the vertical straightedge will go through the center (or very nearly) of one of the no-go sectors on 10 meters. Because this point coincides with one of the $\lambda/2$ positions on the wire, a relatively high impedance was expected, which by measurement turned out to be a fairly moderate 800 ohms. Even so, a parallel tuned circuit was called for at the feedpoint and good performance was obtained with a center-tapped inductor providing a convenient input of 200 ohms from the matching transformer. This is included in **Figure 3**. The inductor comprised 2+2 turns of 18 SWG wound on T130-6 powdered iron toroidal core and tuned with 25 pF.

Layout of antenna-to-transmitter interface

It was stated earlier that end feeding a wire antenna may not be in the best interests of avoiding RF breakthrough. Whatever else might be done to assist in this direction, the physical separation of antenna wire from in-house receivers and mains wiring, not to mention the amateur's own equipment, must be regarded as a major step forward. Physical separation of units will depend on local circumstances. At G3CCB the tuner, matching transformer, and isolator are located closed together at the antenna wire entry point and a long coaxial cable is used from this point to the operating position on the other side of the house. Portable operation may not call for the same degree of separation, and a short coaxial cable to the transmitter will then be all that is required.

All antenna wires are measured to the matching transformer terminals and the isolating transformer ensures that tuning is not affected by the way in which the equipment is connected up; e.g., whether or not the equipment is connected to mains earth. Portable or QRP rigs may not be earthed at all or might share this function with the antenna ground in which case the isolator can be safely left out.

A general layout of interface connections is given in **Figure 3**. The VSWR meter is shown connected at the transmitter end of the long coaxial cable where it can serve as a general monitor of the system from the operating position. During initial setting up, it will be beneficial to site the VSWR meter at the antenna terminal unit where the coaxial cable meets the isolator and matching transformer. Details of the isolator and matching transformer are given in **Reference 1**.

Alternative inductor tuning

The arrangements described above for varying the inductor might be considered to be quite appropriate for QRO use.

Where moderate power levels are used, especially down to genuine QRP, the roller coaster may be regarded as an unnecessarily complicated and expensive item. A technique to simulate variable inductance by employing a fixed inductor in combination with a variable capacitor will provide a satisfactory solution.[2] This has been employed on the elevated 26.50-meter wire where variable inductance is required on the 160-, 40-, and 17-meter bands and a version has been scaled down to suit QRP rigs. A brief note on the principle of simulated variable inductance is given in the **Appendix**.

Conclusion

The exercise has produced a set of three end-fed wires to provide coverage of all the amateur bands that can be operated from an elevated or grounded position and which can be very easily tuned and matched to 500 ohms. The opportunity has been taken to try out several interesting techniques which may be regarded as being unconventional, namely the wideband ferrite antenna matching transformer, the isolating transformer of similar construction, and the simulated variable inductor to avoid mechanical methods of adjustment. All these devices have contributed in their way to the simplification of tuning and matching and will assist in the development of remote control of these functions should this be required.

The longest of the three wires (26.50 meters) is undoubtedly the most useful in taking in the whole HF spectrum, but there may be further

Appendix

The effective inductance of a fixed coil may be reduced to a limited extent by adding a variable capacitor in series.

For a series combination of L and C, the net reactance X' is equal to $X_L - X_C$ and will be inductive when $X_L > X_C$. X' can be regarded as the reactance of a reduced inductance $L' = X_L'/2\pi f$. The reduced inductance will, unfortunately, exhibit a correspondingly reduced circuit Q because the loss resistance of the coil will remain unaltered while the inductance is lowered ($Q = 2\pi fL/r$). This fact puts a constraint on the amount by which the inductance may be reduced. Fortunately, most amateur bands are relatively small in width and the inevitable reduction in Q can be kept within reasonable limits. The 160-meter band is a possible exception and it may be desirable to divide the band into two segments for tuning purposes.

For compactness, coils are wound on T130-2 powdered iron cores and tuned with a variable capacitor to the appropriate value shown in **Table 2**. The highest value of capacitance should be sought consistent with the tuning range required.

Tuning Components Lower Frequency Bands

Band	**160**	**40**	**17**	
Coil	40	7	2.5	µH
Former	T130-2	T130-2	T130-6	
Turns	60	25	16	
SWG	22	20	18	
Tuning	<750	>150	>50	pF

Table 2. Components required for tuning the lower frequency bands.

opportunities using longer antennas. For example, extrapolation of the data given in **Figure 2** shows a clear way through the bands from 160 to 10 meters at around a wire length of 55 meters. The longer wire would certainly produce a better antenna on 160 meters (near $5\lambda/8$), which could be tuned by a variable capacitor within this band but might result in generally higher impedances appearing throughout the remainder.

All antennas worked well showing a VSWR at the transmitter generally no worse that 1.5, but the on-air performance of the elevated counterpoise versions outshone the grounded wire by a significant margin. This is undoubtedly due to the modest stake in use for the earth connection, but it should also be appreciated that a grounded end-fed antenna cannot acquire much height—especially for the shorter wires. Perhaps kite flying and very long wires is the answer for portable operation on 160 meters! ■

REFERENCES
1. Alan Chester, G3CCB, "Two useful non-baluns," *RadCom*, October 1993.
2. Pat Hawker, G3VA, "The transmitter antenna interface," *Technical Topics*, December 1984.

PRODUCT INFORMATION

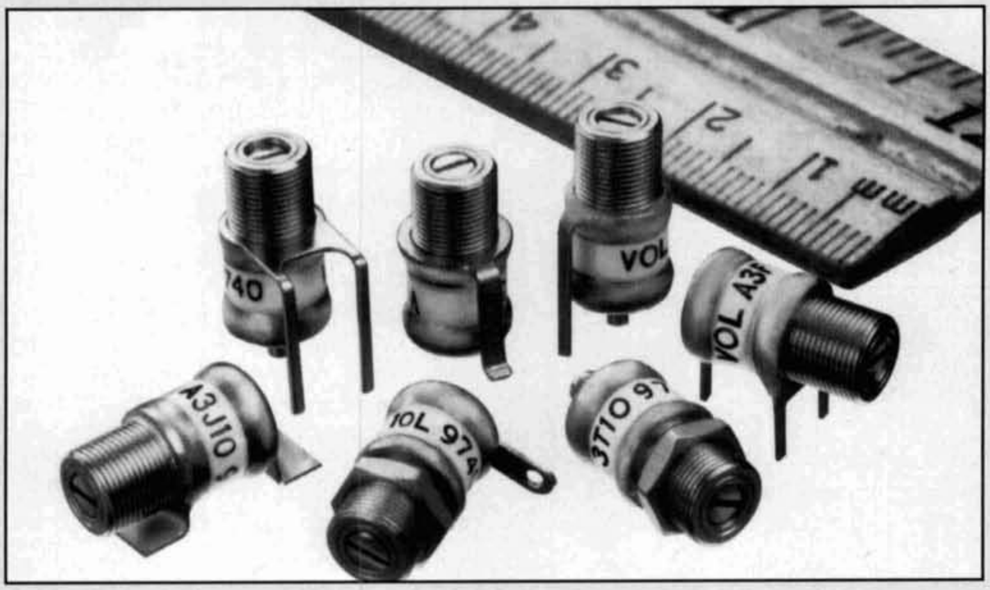

Voltronics New 10pF Solid Dielectric Trimmer capacitor

Voltronics Corporation introduced its new 10pF multi-turn precision trimmer capacitor, the A3 series, which 0.5 inch long, 0.312 inch in diameter. Capacitance range is 1.0 to 10.0 pF, DC working voltage is 250 and DC withstanding voltage is 500. Temperature coefficient is 0 ± 50 ppm° C from -65° C to 125° C. Q is over 2000 at 100 MHz and self-resonant frequency is 2.3 GHz at 10pF.

Tuning is linear over 10 full turns and there are positive stops at minimum and maximum capacitance. Vertical and horizontal PC mount and surface mount are standard along with two-panel mount versions.

A high-voltage option has 1000 working volts DC and 2000 withstanding volts DC.

The price is $1.84 for 100K. Delivery is one week for samples and four weeks for up to 1,000 pieces.

For further information call: Nicholas J. Perrella, Vice President, Sales; Phone: (973) 586-8585; Fax: (973) 586-3404; e-mail: <info@voltronicscorp.com>.

U-Ruler Aids Hardware Installation and Design

The General Devices' U-ruler is an aid for designers and assemblers who need to calculate equipment locations in 19-inch electronic cabinetry. The ruler serves as a guide to the Electronic Industries Association's RS-310 hold configuration. Made of magnetized metal, it comes in a six-U length, with each U separated into a pattern series of 0.25, 0.625, 0.625, 0.25 and matching RS-310 hold configuration.

The U-rule is currently available at no charge. For more information about the U-ruler, contact General Devices Company, Inc., 1410 S. Post Road, P.O. Box 39100, Indianapolis, Indiana 46239-0100; Phone: (317) 897-7000; Fax: (317) 898-2917.

Warren B. Bruene, *W5OLY*
7805 Chattington Drive
Dallas, Texas 75248-5307

THE ELUSIVE CONJUGATE MATCH

In HF tuned power amplifiers

Ever since I became a transmitter design engineer at Collins, I knew that a "conjugate match" did not exist at the plate of a tuned HF power amplifier. But the author of a series of articles published in *QST* in 1973, 1976,[1] and later writings claimed otherwise. I did not challenge him until I noticed this material in an amateur handbook and learned he was the author. In personal correspondence in 1989, I thought I had changed his mind, but I have found that is not the case.

Eventually, I conceived a way to measure R_s of a tube when it was delivering up to full power. My test method and measurements on four different amplifiers were published in *QST*[2,3] in November 1991 and April 1992. I also published an article in *QST* in August 1993 on the theory of grounded-grid operation, where I showed how one could estimate R_s from tube characteristic curves.

In 1996, Tom Rauch, W8JI, duplicated my test method, but claimed that he could tune for a conjugate match. He, Walter Maxwell, W2DU, and John Belrose, VE2CV, then published an article on their findings, and challenging my work, in the fall 1997 issue of *Communications Quarterly*.[5]

In this article, I will first show how to compute tube operating parameters from a set of constant-current curves. Second, I will define tube plate resistance, R_p, and show how the value of R_s can be computer from R_p. I will also show that Rauch, co-author of the article "Source Impedance of Tuned Power Amplifiers and the Conjugate Match,"[5] obtained his conjugate match by driving the linear amplifier will up into the SSB flat-topping region, where one should never operate due to the generation of SSB splatter. Finally, in a sidebar to this article, I will discuss many of the areas in which I dispute the assumptions and circuit analysis stated in **Reference 5**.

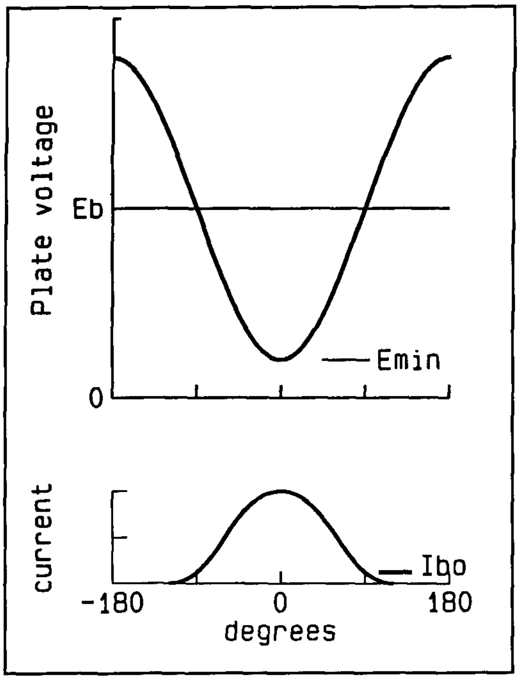

Figure 1. Plate voltage and current waveforms.

Chaffee Analysis

The Chaffee Analysis was popularized by Sarbachr[6] in 1946. It was adopted by many transmitter designers and also by Eimac.[7] The method assumes that the RF grid and plate voltages are sine waves and 180 degrees out of phase for grid-driven amplifiers as illustrated in **Figure 1**. The instantaneous points of operation lie along a straight load-line plotted on a set of

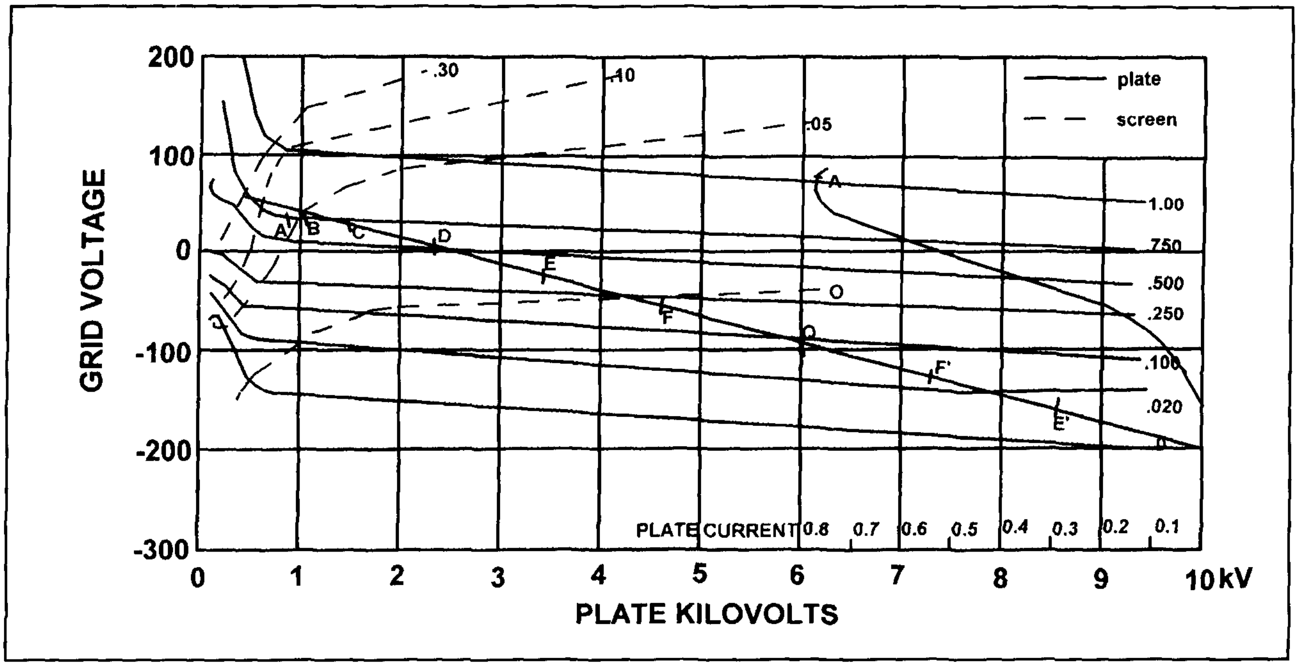

Figure 2. Load line on constant current curves.

constant-current curves of the tube, as illustrated in **Figure 2**. (A separate set of curves is required for each different screen voltage for tetrode tubes.) Also, it is assumed that the harmonic components of plate current are "bypassed" to the cathode with a very low capacitive reactance (the input capacitor of the tank circuit or output network).

Point Q on the load line is located at the intersection of the DC plate and DC grid voltages. The end point, A, of the load line is located at the bottom of the plate voltage swing $e_{MIN} = (e_b - e_P)$ and at a plate current value that will produce the desired DC plate current and RF power output. For linear amplifiers, e_{MIN} is located where the plate current curves start to

Table 1. Condition for Maximum Linear PEP

Computer output

Data	A	B	C	D	E	F	Q
Plate	0.75	0.74	0.688	0.5	0.38	0.2	0.1
Screen	0.06	0.04	0.03	0.01	0.005	0	–
Grid	0.045	0.04	0.03	0.02	0.01	0	0
R_P	5555	12500	20000	25000	25000	25000	25000

4PR65A Pulse tube

DC plate voltage	6000	Vdc
DC screen voltage	500	Vdc
DC grid voltage	-90	Vdc
DC plate current	280	mAdc
DC grid current	9	mAdc
DC screen current	12	mAdc
RF plate voltage	5150	Vpk
RF grid voltage	155	Vpk
Grid driving power	1.3	W
Plate input power	1678	W
Plate output power	978	W
Plate dissipation	701	W
Plate efficiency	58.2	%
Plate load resistance	13566	ohms
Screen dissipation	6	W
Output resistance	225550	ohms

curve up significantly. The following equations can be used to eliminate tube operating parameters from the location of point A.

$I_b = I_A/\pi$ ma.	DC plate current
$P_O = (\pi/4)e_P I_A$	Watts RF power output
$P_{IN} = I_b E_b$	Watts DC plate input
$P_d = P_O - P_{IN}$	Watts plate dissipation
$eff = 100(P_O/P_{IN})$	Percent plate efficiency

where I_A is the plate current at the selected point A.

Make a few trial calculations to establish the best location for point A. Then draw a load line from point A through point Q and on to the point of plate current cutoff.

Next, plot the instantaneous plate current versus grid voltage on the right side of the chart. Use the same scale with zero at (or near) the edge of the chart. **Figure 2** illustrates such a representative plot of plate current. Using a straight edge, extend the straightest part of the plate current curve down to the zero current axis. Next project up (from the right side of the chart) to the plate current curve. This is the value of zero-signal plate current for minimum SSB intermodulation distortion. Usually, a lower value of current must be used instead to keep zero-signal plate dissipation down to a reasonable value—somewhere between 1/2 and 2/3 of rated plate dissipation. The value of zero-signal plate dissipation has little effect upon the plate dissipation at maximum single-tone power output level. The curvature at the top end of the plate current curve in **Figure 2** indicates how much we are entering the peak envelope flattening distortion area.

Now we are ready to perform the Chaffee Analysis. Basically, this is just a simple method of performing a Fourier analysis of the plate current pulses to determine the DC and fundamental components of plate current. (This method can also determine the second and third harmonics, but these are not important for the subject at hand.)

Next, we need to establish the points along the load line for 15-degree steps along the RF plate voltage wave, points A, B, C, etc. The distances from point Q to point B, etc. are:

QB = QAcos15
QC = QAcos30
QD = QAcos45
QE = QAcos60
QF = QAcos75
QF' = QAcos105
QE' = QAcos120

Where QA, QB, etc. represent line lengths. Determinations are not needed beyond plate cutoff, of course.

A good method of determining the plate voltage for each of these points spaced at 15-degree intervals is to program a computer to calculate

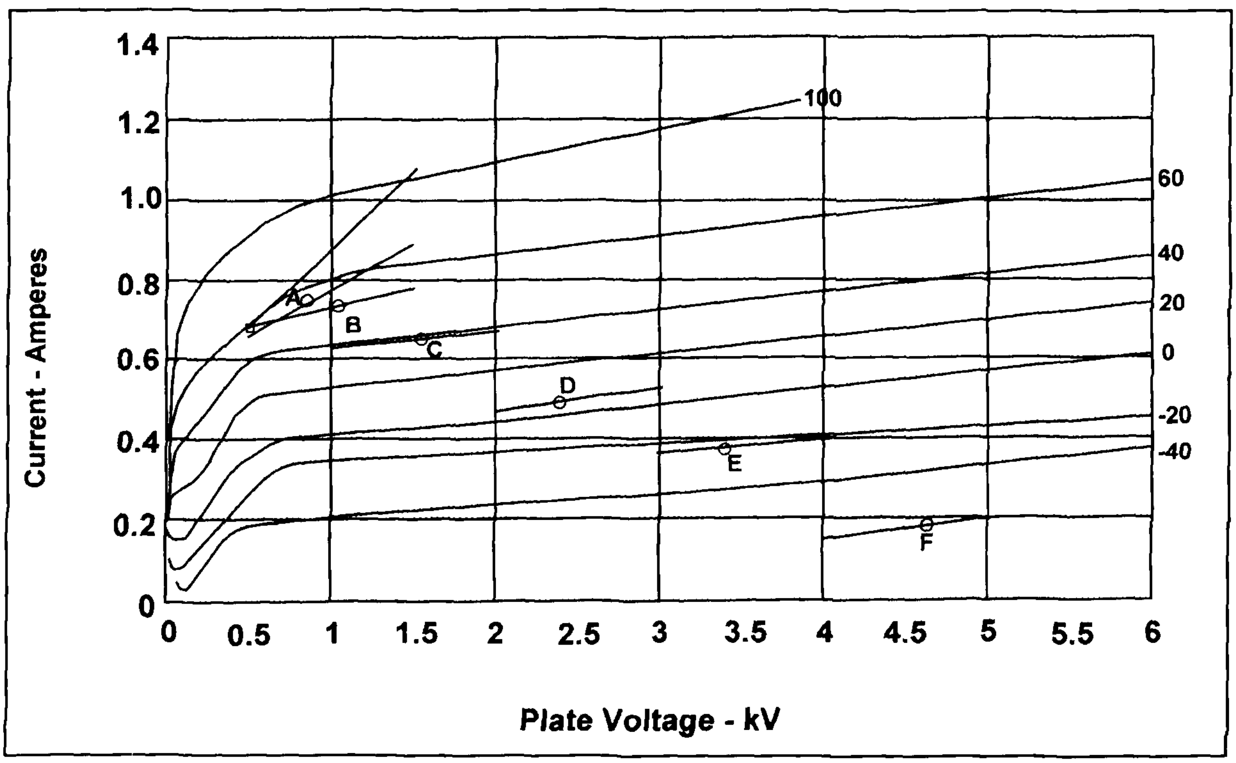

Figure 3. Slope of curves in a measure of R_P.

Table 2. Operating Conditions Just Beyond a Conjugate Match

Input Data	A	B	C	D	E	F	Q
Plate	0.7	0.75	0.7	0.59	0.45	0.23	0.1
Screen	0.2	0.1	0.04	0.01	0.002	0	-
Grid	0.05	0.049	0.035	0.02	0	-	0
R_P	3571	3571	20000	25000	25000	25000	

4PR65A pulse tube		
DC plate voltage	6000	Vdc
DC screen voltage	500	Vdc
DC grid voltage	-90	Vdc
DC plate current	293	mAdc
DC grid current	11	mAdc
DC screen current	29	mAdc
RF plate voltage	5500	Vpk
RF grid voltage	165	Vpk
Grid driving power	1.6	W
Plate input power	1759	W
Plate output power	1090	W
Plate dissipation	669	W
Plate efficiency62	%	
Plate load resistance	13871	ohms
Screen dissipation	14.7	W
Output resistance	12726	ohms

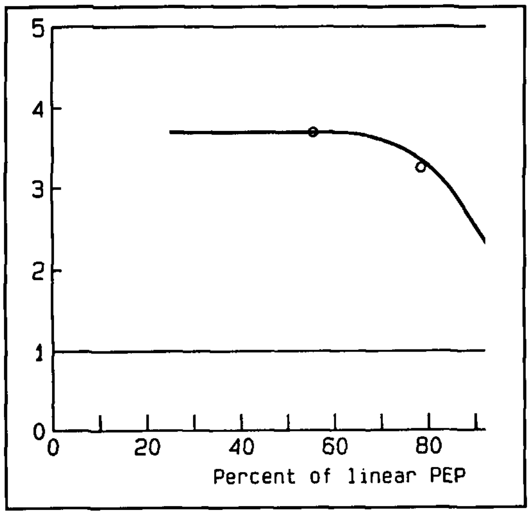

Figure 4. Variation of RS/RL versus percent of PEP in example amplifier.

the plate voltage E at each of the points using the following equation:

$E = E_b - (e_P \cos\theta)$ with θ in 15-degree steps

Then find these plate voltage points along the load line. Read the plate current at each of these points interpolating as accurately as possible. The curve plotted on **Figure 2** may help with this interpolation. Enter these values (labeled simply as A, B, C, etc.) in the following equations for the average plate current and for the fundamental component of plate current.

$$I_{AV} = (1/12)(0.5A + B + C + D + E + F + Q + F' + E'...)$$

$$I_1 = (1/12)(A + 1.93B + 1.73C + 1.41D + (E - E') + 0.52(F - F'))$$

Compute the plate parameters using the following equations:

$P_O = e_P I_{1/2}$	Watts RF power output
$P_{IN} = E_b I_{AV}$	Watts DC power input
$P_d = P_{IN} - P_O$	Watts plate dissipation
$R_L = e_P/I_1$	Ohms plate load resistance

Normally, the designer performs similar calculations for grid current (if operating Class AB^2) to determine DC grid current and RF drive power. The DC screen current is calculated for tetrodes to determine screen dissipation.

Output (source) resistance, R_S

R_S is a function of the plate resistance, R_P, which is a property of the tube. The definition of R_P given by Terman[6] is:

$R_P = (\Delta E_P/\Delta I_P)$ with E_g constant

Definitions of Terms

The following definitions are from the *IEEE Standard Dictionary of Electrical and Electronics Terms, Fifth Edition*.

impedance, output (1. device, transducer, or network). The impedance presented by the output terminals to a load. Note: (A) Output impedance is sometimes incorrectly used to designate load impedance.

impedance, source. The impedance presented by a source of energy to the input terminals of a device or network.

impedance, conjugate. An impedance the value of which is the complex conjugate of a given impedance. Note: For an impedance associated with an electric network, the complex conjugate is an impedance with the same resistance component and a reactance component which is the negative of the original.

matched impedances. Two impedances are matched when they are equal. Note: Two impedances associated with an electric network are matched when their resistance components are equal and when their reactance components are equal.

matched transmission line (data transmission). A transmission line is said to be matched at any transverse section if there is no wave reflection at that section.

matching impedance. See: load matching.

load matching (2. circuits and systems). The technique of either adjusting the load-circuit impedance or inserting a network between the two parts of a system to produce the desired power transfer or signal transmission.

Discussion of these definitions

I have been criticized me for using the term "output (source) resistance." Note that the above definitions of "output impedance" and "source impedance" are essentially the same, but that output is often mistaken for load impedance. I simply combined the terms to make my meaning crystal clear.

Also observe that "impedance matching" does **not** require adjusting for **equal** source and load impedances nor **conjugate** source and load impedances.

Finally, observe that a transmission line is matched when its load impedance is equal to the characteristic impedance of the transmission line. The source resistance at the line input has nothing to do with the matched condition.

In other words, it is the slope at any point on a *constant grid voltage* plot of the tube plate characteristics as shown in **Figure 3**. This kind of plot is used for class B audio modulator calculations and for pulse generators because, in these cases, the load line is a straight line on this kind of plot. When tuned grid and plate circuits are used, constant current curves must be used for a straight load line.

(Note: I am using the obsolete 4PR65A pulse tube for an example because its data sheet provides both kinds of plate characteristic curves. The tube can only be operated in short pulses—at these voltage and current levels—to avoid excessive dissipation, but it makes it possible to prove my point.)

Observe that the slope of the lines in **Figure 3** are nearly constant for all plate voltages above 1000 volts. The curves turn down steeply at lower plate voltages, which means that R_P becomes much lower. In fact, near the left edge where the grid voltage lines merge into a nearly vertical line, R_P is extremely low compared to that in the normal operating range.

This provides a clue as to the reason why a conjugate match condition can be found when driving the tube into the high distortion region.

The value of R_S can be calculated by first determining the R_P at points A, B, C, etc. along the load line shown in **Figure 3**. These values are then inserted into the following equation, which includes the correct weighting for each point (like the Chaffee Analysis equation for I_1).

The R_P at points A, B, C, etc. are found by locating the same points on the other curves (same plate voltage and same plate current). Using a straight edge, draw a line tangent to the grid voltage curve at that point. Interpolate as necessary. Assume that R_P is nearly constant for points D, E, and F. Theoretically, the values of R_P at points F', E', and D' must be combined with their counterparts F, E, and D, respective-

Discussion of Disputed Assumptions and Statements

The following are quotations from the article, "Source Impedance of Tuned Power Amplifiers and the Conjugate Match," followed by their location in the article, and, finally, by my comments.

"Clearly, plate resistance R_P of the active element (tube, transistor, etc.) is a dissipative ***RESISTANCE*** *that converts electrical energy into heat."* (bottom of column 2, page 25) I have shown in the above discussion that this statement is false.

"And, since the instantaneous values of V/I at every instant of time correspond to instantaneous values of an impedance, the average dynamic output impedance of the source, Z_S, must equal the load impedance R_L, for all practical purposes." (near bottom of column 2, page 26) This statement is proven false because R_S and R_L are rarely equal for normal tube operating conditions as explained above.

"One effective approach to use the definition of conjugate match as one that provides for maximum power transfer (The Maximum Power Transfer Theory)." (bottom of column 2, page 26) This is true for the theoretical case of Thevenin's theorem where the system is linear with no limits on current or voltage. It does not represent the case when a HF power amplifier is being tuned for "maximum available power" with a given grid drive voltage. The end of the load line for this condition is at the intersection of the peak grid voltage and some value of plate current down in the nonlinear plate saturation condition. Moving point A down (by retuning and reloading) reduces plate current and hence power output. Moving point A to the right along the peak grid voltage line reduces e_P and hence power output. Plate current will increase some, but power output goes down. The maximum power output is clearly determined by nonlinear tube conditions and **not by a conjugate match.**

"Simply stated, when the matching network presents a load that provides for a maximum transfer of available design power from the active device, the device is conjugately matched." (near top of column 1, page 27). Again, this is false for reasons given above.

"A constant plate current flows in Class A amplifiers, even in the absence of a signal on the grid. The output source impedance, a resistance, is therefore easy to identify and measure. The generator may be considered a current generator that is impedance matched when the load resistance is equal to the dynamic output resistance of the source." (near center of column 1, page 27) They then reference Sabin, who is wrong on this subject also.

The "plate current" referred to in the first line must be designated as the "DC plate current" because if there were no variation in plate current there could be no output! A current generator has infinite output source resistance, by definition, therefore, a conjugate match would require an infinite resistance load resistance. How on this earth, where we are limited by finite voltages, can you get any power at all into an infinite load resistance? For example, in IF stages of old tube receivers, the tubes had a very high value of R_P (and R_S) compared to the IF load which the IF transformer places on them. **There is no conjugate match.**

"From a practical standpoint, the output impedance of an RF power amplifier is almost entirely established by the characteristics of the tank circuit." (bottom of column 2, page 27.) This is false. The tank circuit presents the desired load impedance, R_L, to the tube at the fundamental frequency and bypasses the harmonic components of plate current to the cathode. It has nothing to do with R_S.

"In fact, in all but Class A amplifiers, the power generated and transferred from the power supply to the output terminals isn't even transported through the active device." (7th line, column 1, page 28) Perhaps the authors should analyze a series-fed circuit instead of parallel DC feed. On the downward RF plate voltage swing, the tube draws current through the tank circuit storing enough energy to last for the rest of the RF cycle.

"The optimum load impedance..." (second paragraph of column 1, page 28.) The authors frequently use the term "optimum" without really making clear what they mean by "optimum." In other places, they indicate that it is the load that provides a "conjugate match" or "maximum available power output." Either of these definitions would be wrong for reasons given earlier.

"However, current and voltage define an impedance, therefore, the effective dynamic output impedance of the tube is:

$$Z_S = (E_P - E_{MIN})/I_1 \quad .$$

This is exactly what our technical literature has been calling R_L." (bottom of column 1, page 28.) The authors couldn't be more wrong because I_1 is negative (because the current is flowing "out" of the tube resistance and not "into" it, which makes Z_S **NEGATIVE**! A negative resistance is a **source** of power. The equation is for Z_L, not Z_S, as explained earlier.

The example given near the bottom of column 2 on page 28 for the resistances at the voltage and current nodes on a transmission line would require a 40-ohm transmission line characteristic impedance. Unless otherwise stated, the reader usually assumes that you're referring to 50-ohm line.

Near the top of column 1 on page 29 we find the equation:

$$Z_S = V/I = (E_P - E_{MIN})I_1$$

This example is for Z_L, not Z_S, as explained before.

***"In addition, comparing the above expression with Equation 2** provides further evidence that $Z_S = R_L$, the condition for delivery of all the available power in accordance with the Maximum Power Transfer and Conjugate Match Theorems."* (end of paragraph 2, column 1, page 29) This conclusion is wrong because the authors made an incorrect assumption, as I explained earlier.

"Yet, from the outside, it appears that the amplifier behaves as if its effective internal dynamic output impedance were equal to its optimum load impedance, as this is the condition for maximum power output for a given amount of drive power." (bottom of column 1, page 29) False again, for the same reasons.

"When correctly tuned to provide maximum power for a given operating condition, operating into the design optimum load impedance (RL), the plate voltage and voltage and current vary over the RF cycle in such a way that the amplifier appears to have an average impedance ZS equal to the design load impedance RL, referenced to the plate of the tube." (bottom of column 1 and top of column 2 on page 29) Again, this false statement is based on the same false logic.

"The dynamic output impedance also changes as the drive level is changed." (middle of paragraph 2, column 2, page 29) This is what happens when you drive a linear up into the nonlinear, high-distortion region. It stays fairly constant over much of the linear operating range.

"However, the correct, or optimum load impedance, where $R_L = Z_S$, is obtained when the loading is adjusted to deliver the maximum available power with the given plate voltage and drive power." (middle of column 1, page 30, also see the last sentence in the paragraph) Again, this condition exist only fleetingly in SSB operation when excessively overdriven.

"The pi-network now transforms this new complex output load impedance to $Z_L = R_L + jX$ at the input of the pi-network, which presents a 3:1 mismatch to the source impedance Z_S." (near the bottom of column 1, page 30.) Wrong, the 3:1 mismatch is with reference to R_L.

"PA dynamic plate resistance, R_P." (heading column 2, page 30) This entire section is incorrect because it describes a resistance that is not the resistance defined by Terman. It doesn't have a name that I know of. It's related to plate dissipation and has nothing to do with R_P.

"Experiments that measure load impedance, output impedance, and provide support for the concept of a conjugate match." (heading in middle of column 1, page 31) I will accept that Rauch's measurements are correct and that he did find a tune condition that produced a conjugate match. Again, the operating point is undoubtedly outside the range of acceptable SSB linear amplifier operation. Obtaining a conjugate match in this way serves no useful purpose in ham radio.

Now I'll skip to another subject starting under the heading on page 32: *"Measuring/Calculating complex conjugate impedances."* Here, Belrose tunes the (ASTU) in the coax going to an antenna (which as an input impedance other than 50 ohms) to achieve a 1:1 SWR in the coax at the input of the (ASTU). Then he **assumes** that the RF power amplifier has an output (source) impedance of 50 + j0, at the amplifier output coax terminal, so he replaces the power amplifier with a 50-ohm dummy load. Now he finds a conjugate match everywhere he opens the circuit anywhere between the 50-ohm dummy load and the antenna. He does because he made the same bad assumption that is made consistently throughout the article; but all that he is proving is that the dummy load resistance is 50 ohms! He is not measuring the RF power amplifier because it is disconnected.

The measurements in the section *"Measuring mismatch loss,"* which begins on page 34 are flawed because they do not recognize the existence of the phase delay between the tube plate and the coax output terminal of the output network. A pi-network typically has on the order of 150 degrees phase delay on the lower bands, and perhaps up to 165 degrees or so on the higher bands. For a worst case example, let us assume that the phase delay is 145 degrees and that the desired R_L of 2000 ohms is obtained when tuned for a 50 + j0 load. Now change the load to 100 + j0 without retuning. The input impedance Z_L to the pi network at the tube plate will be 1600 - j1200. Change the load to 25 + j0 and Z_L becomes 1600 - j1200. The two values of Z_L will **not** be 4000 + j0 and 1000 + j0, as the authors infer. However, Z_L has an SWR of 2:1 in all cases. Check it out on a Smith Chart.

Under *"Direct measurements of output impedance"* found in column 2 on page 35, Sabin's method is flawed for the same reason. He didn't account for the phase delay in the amplifier output network.

The test set up in **Figure 5** is also flawed with regard to determining whether the injection signal is at a current or voltage node at the tube plate because Rauch doesn't account for the phase delay in the pi-network.

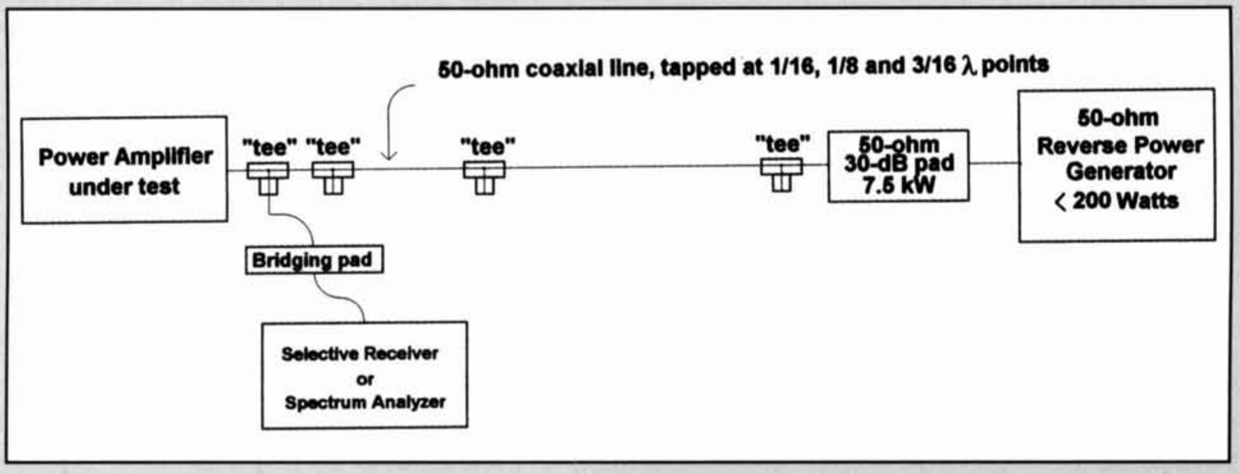

Figure 5. Test setup used by Belrose et al to measure output impedance (Figure 5 from "Source Impedance of HF Tuned Power Amplifiers and the Conjugate Match," ***Communications Quarterly*****, Fall 1997).**

Finally, let's look at the *"Discussion"* beginning in column 2 on page 38. This section is nearly all incorrect because it's based on all the incorrect assumptions already covered. An exception is the last paragraph about VLF/LF transmitter systems. I can say this with certainty because I designed the output network/antenna coupling system for a solid-state power amplifier, which used the fact that a conjugate match did not exist to enhance antenna bandwidth. These transmitters are rated for 250 kW and up, and are in current operation.

ly. The combined values will be approximately the same. Good data is hard to obtain in this region. Accuracy isn't very important because the weighting factors reduce the significance of these points. Thus, we can simplify the equation with little error using only the R_P values determined for points A, B, and C.

$$R_S = 6(1/(0.5R_A + 0.933/R_B + 0.75/R_C + 0.50/R_C + 0.25/R_C + 0.067/R_C))$$

Table 1 gives the operating parameters for the load line in **Figure 2** ending at point A. Note the values of R_L and R_S. The ratio R_S/R_L is approximate. This signal level is the maximum to which the tube should be driven for single sideband with acceptable low intermodulation distortion.

Table 2 gives the operating parameters when the amplifier is overdriven into the nonlinear range. Point A is moved along the load line to an end point where e_{MIN} is 500 volts. Observe that R_S and R_L are now approximately equal.

This explains why Rauch can tune for a conjugate match. He simply drives the amplifier far too hard for linear SSB use. Also, the conjugate match exists at just one drive level for a given R_L. Alternatively, it exists at just one value of R_L for a given grid signal level. **Figure 4** illustrates approximately how the ratio R_S/R_L varies with RF power output. Note that this curve is very similar to the curve for a linear amplifier shown in my *QST* article.[2] I just plotted the data we measured without explanation. I suspect that we operated the linear a little too lightly loaded, because it should have delivered 1 kW before being very far down on the curve.

R_S is a nondissipative resistance. It is also approximately constant in value over much of the normal signal level range of a linear amplifier. Typical values of R_S are on the order of 5 times that of R_L for most tubes used for SSB. The value is less than this in the example because the tube is operated at twice the plate voltage that could be used for SSB. Operating at 3000 volts DC plate voltage would reduce R_L by approximately half, while R_S would remain nearly the same.

RF voltage feedback around the final amplifier can be used to lower R_S to equal R_L in which case a conjugate match would exist. It only takes 4.5 dB or so. RF voltage feedback has been used to keep the power output more nearly constant with variations of antenna impedance with a sweeping or frequency hopping signal, for example. The tube must be operated within its linear range for all values of Z_L to realize this benefit.

Conclusion

I hope that this discussion finally puts to rest the myth that a conjugate match normally exists in tuned HF power amplifiers.

My thanks to Forrest Cummings, W5LQU, a transmitter designer who retired from Collins/Rockwell. ■

REFERENCES

1. Walter Maxwell, W2DU, series of articles in *QST* in the 1970s entitled "Another Look at Reflections" and his sections in the *ARRL Handbook* and *ARRL Antenna Book*, "The Conjugate Match and the Z_0 Match" and "The Conjugate Match and the Pi-Network Tank" from 1986 to 1994. This material has been deleted from the most recent editions.
2. Warren B. Bruene, W5OLY, "RF Power Amplifiers and the Conjugate Match," *QST*, November 1991.
3. Warren B. Bruene, W5OLY, "Technical Correspondence," *QST*, April 1992.
4. Warren B. Bruene, W5OLY, "Inside the Grounded-Grid Linear Amplifier," *QST*, October 1993.
5. John S. Belrose, Walter Maxwell, Charles T. Rauch, "Source Impedance of HF Tuned Power Amplifiers and the Conjugate Match," *Communications Quarterly*, Fall 1997.
6. R.I. Sarbacher, "Graphical Determination of Power Amplifier Performance," *Electronics*, December 1942, pages 52–58.
7. "Tube Performance Computer," *Application Bulletin 5*, Eitel-McCullough, Inc., San Carlos, California, 1952. Also described in more recent editions of "The Care and Feeding of Power Grid Tubes."
8. Warren B. Bruene has described the "Chaffee Analysis" in three books: *Radio Engineering Handbook, Fifth Edition*, Chapter 18, "Radio Transmitters" edited by Henney, McGraw Hill, 1959; *Single Sideband Principles and Circuits*, Chapter 9, "Linear RF Amplifier Operating Conditions," Pappenfus, Bruene, Schoenike, McGraw Hill, 1964; and *Single-Sideband Systems and Circuits*, Chapter 14, "High-Power Linear Amplifiers," Sabin, Schoenike, McGraw Hill, 1987.

Appendix

The equation for R_S is also based on the Chaffee Analysis principle. The difference is that the power delivered during each 15-degree time period requires coefficient of $\cos^2\theta$ instead of just $\cos\theta$ used for computing current values. The coefficient for "A" is 0.5 because there's only one "A" time period per pulse while there are two of each of the others. Sarbacher multiplied all coefficients by 2 and divided the entire sum by 12, whereas I just divided by 6 instead.

PRODUCT INFORMATION

Alinco Introduces Family Radio Service DJ-S46

Alinco announces the DJ-S46 Handheld Transceiver (HT) designed to operate on the Family Radio Service (FRS) band. The new HT, about the size of a paging "beeper" has been type accepted by the FCC.

The unit features all 14 FRS channels and, using AA batteries, transmits with an output power of 340 milliwatts.

The DJ-S46 has a pivoting "swing up" antenna. The flexible design allows the radio to remain compact in pocket or purse without detaching the antenna. It also does away with the risk of misplacing a detached antenna.

Features include rechargeable NiCd battery and the option to use AA cells in place of the NiCd, large illuminated display, pager "alert" alarm, hi/low transmit power setting, programmable auto power off feature and more. The radio comes with a belt clip and carry strap.

For details, write Alinco at 438 Amapola Ave., Suite 130, Torrance, CA 90501.

Joseph J. Carr, *K4IPV*
P.O. Box 1099
Falls Church, Virginia 22041
E-mail: <carrjj@aol.com>

Facts, Opinions, Theories, Hypotheses, and Laws: Part 2

Exploring the differences

Some people reduce theory to the status of uninformed opinion, of which all possible variations are equally acceptable or disdained. The exception, of course, is one's favorite theory, which may look like a rock-solid fact. Other people look on theory as something that stands on a foundation of sand and has no merit in their "practical" world. Still others elevate theory, especially scientific theory, to the exalted status of unassailable immutable law of the universe. This is especially true of those theories they personally favor.

Too often we hear, "it's just a theory," in regard to a specific line of thinking. Part of the problem is that lay people and scientists use the word *theory* to mean opposite things. To the layperson, a theory is a weak statement based on little or no evidence. For example, according to a news story, the state of Alabama places an insert in high school biology textbooks warning that the theory of evolution is "just a theory...not a fact," implying that the student shouldn't take it too seriously. Similarly, a radio talk show guest recently claimed that "...AIDS being caused by the HIV virus is *just a theory*," and then went on to amplify his own ideas of the origin of the disease.

Although scientists are usually outraged by such statements, they should actually nod their heads, smile knowingly, and agree wholeheartedly. Why? Because to a scientist, a theory is not a fact. Rather it is an *explanation of how things work*, consistent with all known relevant data. In other words, while the layperson sees a theory as a bit wobbly or lacking support, the scientist sees it as well supported by all the known evidence and not refuted thus far.

Defining the word theory

According to several dictionaries, among them *Webster's New Collegiate Dictionary*[1] a theory is defined as:

1. The analysis of a set of facts in their relationship to one another;
2. A belief, policy, or procedure proposed or followed as the basis for action ("On the theory that...");
3. An ideal or hypothetical set of facts, principles, or circumstances—often used in the phrase "in theory";
4. The general or abstract principles of a body of fact, a science, or an art (for example, music theory);
5. A plausible or scientifically acceptable general principle or body of principles offered to explain phenomena (for example, the wave theory of light);
6. A hypothesis assumed for the sake of argument or investigation;
7. An unproven conjecture or assumption;
8. A body of theorems presenting a concise systematic view of a subject;
9. Abstract thought or speculation

According to Selltiz et al,[2] a theory is "...a set of concepts plus the interrelationships that are assumed [or shown] to exist among these concepts. A theory also includes consequences that we assume logically to follow from the relationships proposed in the theory. These consequences are called *hypotheses*."

Any statement of a theory must include as complete a statement as possible of the underlying assumptions (which could prove critical later on), the consequences, and the predictions of observations that could be logically assumed to follow from the theory.

A theory is not a scientific discovery (only facts can be discovered), but rather an intellectual construct derived from human ingenuity in the mind of the scientist. Theories are used to explain discoveries, but are not in and of themselves scientific discoveries. They can be, and often are, proven wrong either on initial examination or later (sometimes centuries later).

What is a "good" theory?

In order for a theory to be considered "good," certain factors must be present. Thomas Kuhn, in his book *The Structure of Scientific Revolutions* (1970), proposed a five-fold test of a good theory.[3]

First, the theory should be *accurate*. In other words, the statement of the theory and its practical consequences should accurately reflect the experimental results. All observations should be accounted for, and no aspect of theory should be without some experimental support.

Second, the theory should be *consistent* both within itself (contain no inherent contradictions) and with the known laws of science. If there is any logical inconsistency within the theory, it will fall to criticism. And, if there is any disagreement with the known laws of nature, then either those laws or the theory must be scrapped or revised to accommodate the difference.

Third, the theory should be *broad* enough to reach beyond the specific set of circumstances it describes. In other words, the theory should define more than the specific experiments from which it resulted. "The greater the specificity, the worse the theory" is a good rule of thumb.

Fourth, the theory should be *simple*. The Principle of Ockham's Razor requires that we prefer the theory that fully describes the observations in the simplest terms possible. If a theory requires a major rewrite of science, or a miracle to have occurred, then it is suspect and should be abandoned unless there is a substantial amount of evidence to support such a massive change.

Fifth, the theory should be *fruitful*; that is, it should predict or disclose new phenomena, previously unnoticed relationships, or provide some indication of a means for reliably testing the theory.

Whether the theory lies in science, or some other systematic search for knowledge, these five attributes of a high-quality theory should be present. To the extent that one or more of these attributes are either present or missing, the theory can be judged either good or bad.

Observations, theories, and laws

The relationship between observations, theories, and laws are seen in our development of knowledge of the solar system, of which Earth is a part. Prior to the 16th century, most Europeans believed that the Earth was at the center of the universe—a view put forth in ancient times by the Greek ruler of Egypt, Ptolemy. Nicholas Copernicus, a Polish monk (ca. 1543) published the results of more than three decades of research which showed that the motions of the Ptolemaic system were best described by placing the Sun at the center of our solar system (the *heliocentric* view). Because of opposition from the Church, Copernicus withheld his speculations until he was on his deathbed. This, unfortunately, was a precaution that his disciple Galileo failed to take, to his ultimate regret.

The Danish astronomer Tycho Brahe (1546–1609) spent a lifetime making observations of the positions of the stars and planets. Brahe's work differed from earlier studies because of the accuracy and precision of his measurements. Tycho Brahe, however, never did work up a viable theory or model concerning the data he spent a lifetime gathering. That job was left to his disciple, Johan Kepler (1571–1630), a mathematical physicist. Kepler discovered that the theories of Copernicus were not exactly correct because they disagreed with the observed data. By replacing Copernicus' circular orbits with ellipses, however, Kepler's model was able to explain the data and predict future positions of the planets. Kepler's statements of how the data behaved are collectively known, appropriately enough, as *Kepler's Laws*.

Isaac Newton stood on the shoulders of Kepler, Brahe, Galileo, and Copernicus and derived his own laws of motion. These laws are still discussed as part of elementary physics classes today (even though later in the same course the relativity and quantum exceptions are also discussed).

The theoretical process

One may start out by making some observations, either in conjunction with a formal experimental research protocol or by serendipity. These observations are then analyzed and a model of how they work (or what they mean) is created. A tentative theory (as described above) is then developed from the model. From the theory, predictions and hypotheses are derived, and these form the basis for an ordered observation or experiment that makes additional observations. The process continues around and around the loop until the theories and laws derived are refined. But even then, the loop doesn't really stop; it only drops into very low gear, for there's always the possibility of a novel observation coming along and restarting the process.

Sometimes, a tentative theory branches off onto a different course because some of the predictions are truly profound. Einstein performed one of these tricks using Max Planck's theory of energy quanta (1900) and won the Nobel Prize in Physics for his descriptions of the photoelectric effect.

Junk science: meet the skeptic

In my final installment of this series on junk science, I will discuss the process of skeptical discourse—the process that celebrates reason as the basis for development of facts and ideas into knowledge, their refinement, and their communication to others. ■

REFERENCES

1. *Webster's New Collegiate Dictionary*; G.& C. Merriam Company; Springfield, Massachusetts; 1979.
2. Claire Selltiz, Lawrence S. Wrightsman, and Stuart W. Cook, *Research Methods in Social Relations*, 3rd Edition, Holt, Rinehart and Winston, New York, 1976.
3. Thomas Kuhn, *The Structure of Scientific Revolutions*, University of Chicago Press, Chicago, 1962.

BIBLIOGRAPHY

1. John L. Casti, *Paradigms Lost: Images of Man in the Mirror of Science*, William Morrow & Co., Inc., New York, 1989.
2. Hy Ruchlis, *Clear Thinking: A Practical Introduction*, Prometheus Books, New York, 1990.

PRODUCT INFORMATION

Belden Offers New Brilliance® Analog Audio Cable

Belden Wire & Cable Company announces another addition to its Brilliance family of audio and video cables: its Part No. 1883A Analog Audio Cable. This single twisted pair cable is designed for line-level applications in permanent and semi-permanent multichannel professional audio installations. Belden 1883A is ideal in single- or multiple-room pro audio environments where a high-quality cable is needed to run from the punch-down blocks to equipment such as equalizers, limiters, compressor/expanders, harmonizers, or flangers.

Belden 1883A features one pair of 24 AWG stranded (7x32) tinned copper conductors, insulated with polypropylene. Conductors are color-coded black and red. A 24 AWG copper drain wire is included inside the shield. Shielding is Belden's, high-performance 100%-coverage aluminum-polyester Beldfoil®, bonded to the PVC jacket material. Available jacket colors include brown, red, orange, yellow, green, blue, violet, gray, black, and white. This cable is NEC and CEC type CM-rated.

The nominal outside diameter of Belden Line Level Analog Audio Cable is 0.123 inches (3.12 mm). Capacitance between conductors is 31 pF/ft. Between one conductor and the other conductor connected to the shield, nominal capacitance is 58 pF/ft. Maximum working voltage is 300VRMS.

Easy installation is assured since the Beldfoil shield in Belden 1883A is bonded to the PVC jacket. As a result, both can be removed simultaneously. This saves time and reduces installation cost. And because 1883A is available in ten different vivid colors, identifying pairs during-or after-installation is easy.

Belden 1883A Line Level Analog Audio Cable is available in 1,000-foot lengths in Belden's exclusive UnReel® carton. Also, for gray color only, this cable is available in both 500- and 1,000-foot packages, in a choice of standard spool or UnReel® carton.

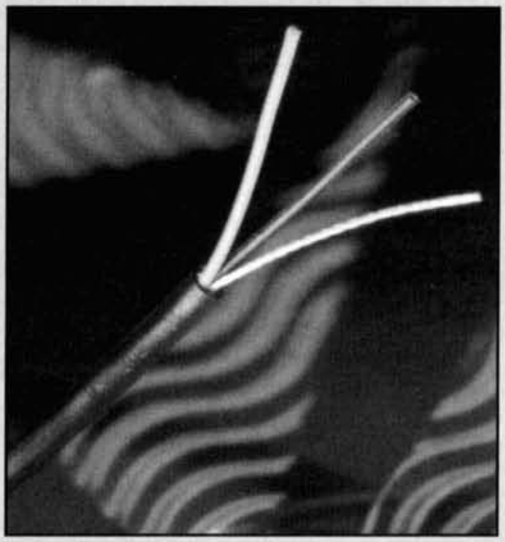

Other members of the Belden Line Level Analog Audio Cable family offer 16, 18, 22, or 24 AWG conductors, in single- and multi-pair configurations. Plenum-rated versions are also available.

For more information, contact Belden Wire & Cable Company, P.O. Box 1980, Richmond, IN 47375, or call 1-800-BELDEN-4. Home Page: <www.belden.com>.

William Carver, *W7AAZ*
690 Mahard Drive
Twin Falls, Idaho 83301

THE MODULAR DIAL

Improve the frequency calibration of LC oscillators

An LC oscillator is a good way to tune a homebrew receiver or transceiver. It has a spurious-free output whose harmonics can be easily filtered. With mechanical tuning, its phase noise is lower than ordinary mixers require. It has virtually infinite tuning resolution with an ARC-5 transmitter tuning capacitor and can be temperature compensated to have little drift. Klass Spaargaren, PAØKSB, described frequency locking of oscillators,[1] and Richey's "Cyclemaster"[2] and this modular dial use a PIC microcomputer to lock the oscillator to a specific frequency.

Dials

Over the years, the frequency calibration of my homebrew LC oscillators has ranged from fair to horrible! A digital counter offered a potential solution to the problem; but except for a direct-conversion SSB rig, an ordinary counter won't show the received frequency. Counter dials that permit entry of an offset are available, but none had the frequency resolution or bright LED display I wanted, so I designed my own.

The Modular Dial

This modular dial is a computing counter with two signal inputs: F1 and F2. F1 is the local oscillator (LO), F2 is the transmit carrier oscillator. F2 is counted *once* when first turned on, briefly displayed as a diagnostic tool, then saved—a process requiring about two seconds. Thereafter, the dial counts F1 five times per second, either adds or subtracts F1 and F2, and displays the computed result to the nearest 10 Hz on seven LEDs.

The counter hardware is rated to 50 MHz. The three units I made counted beyond 75 MHz. The math to add, subtract, and convert counts to decimal numbers for display stops

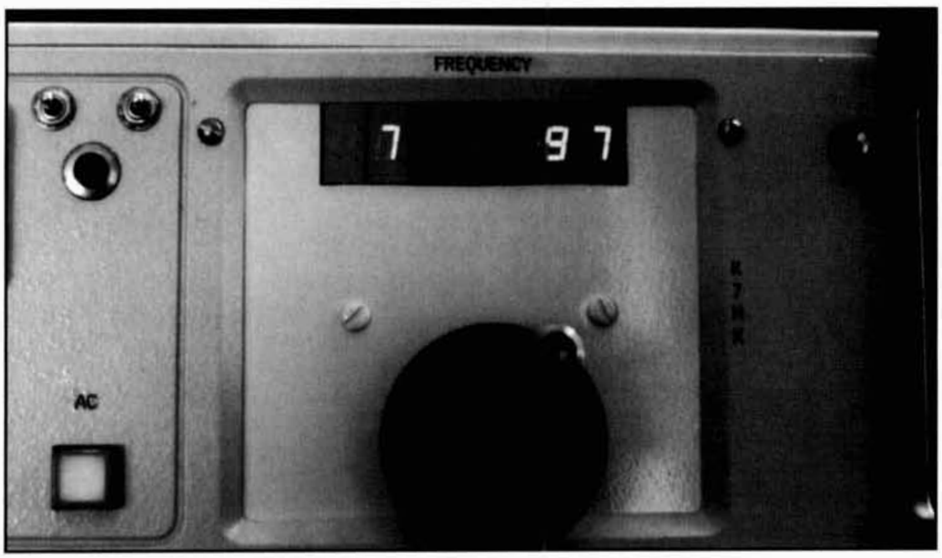

The Modular Digital Dial.

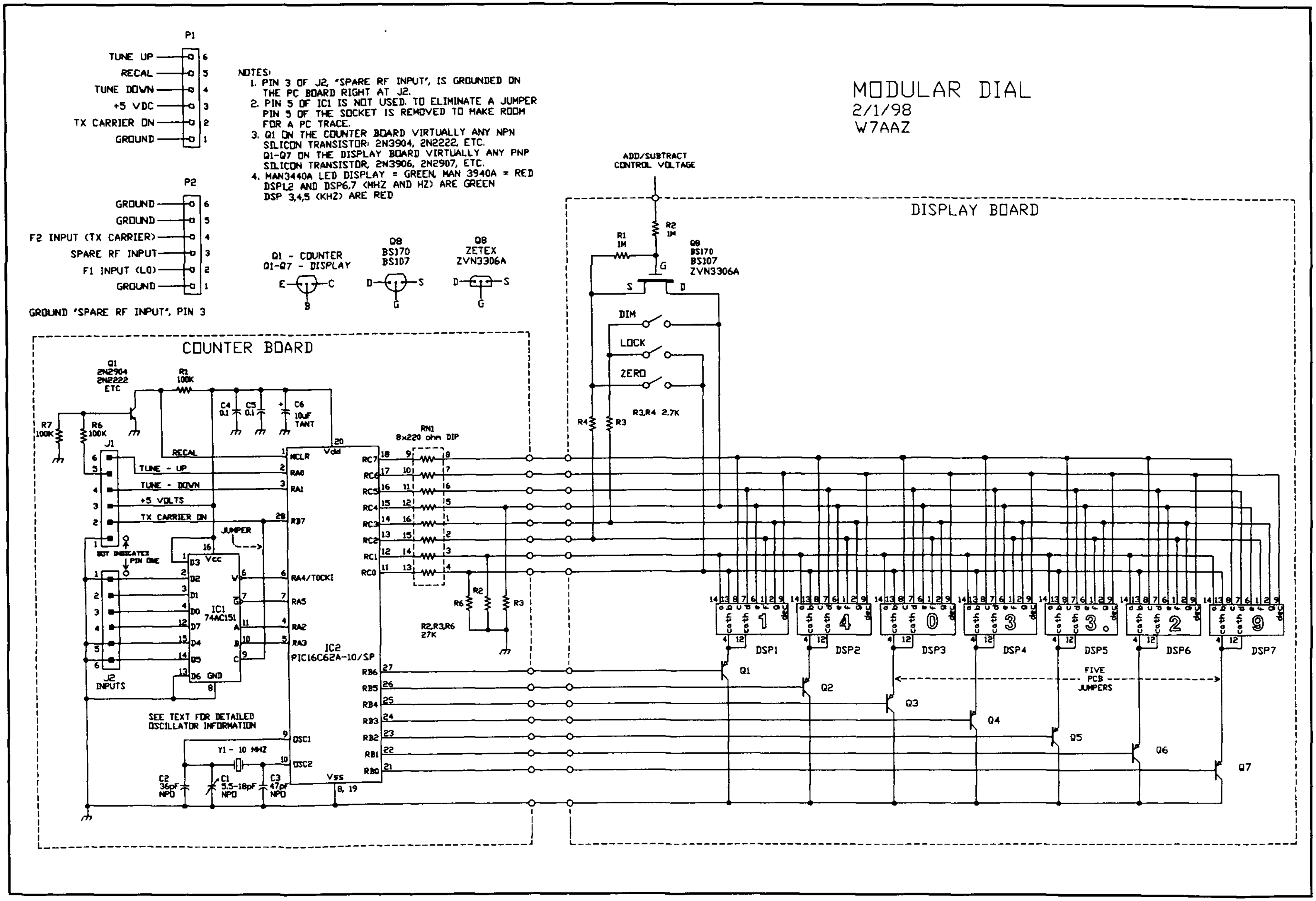

Figure 1. Schematic for the counter/display board pair.

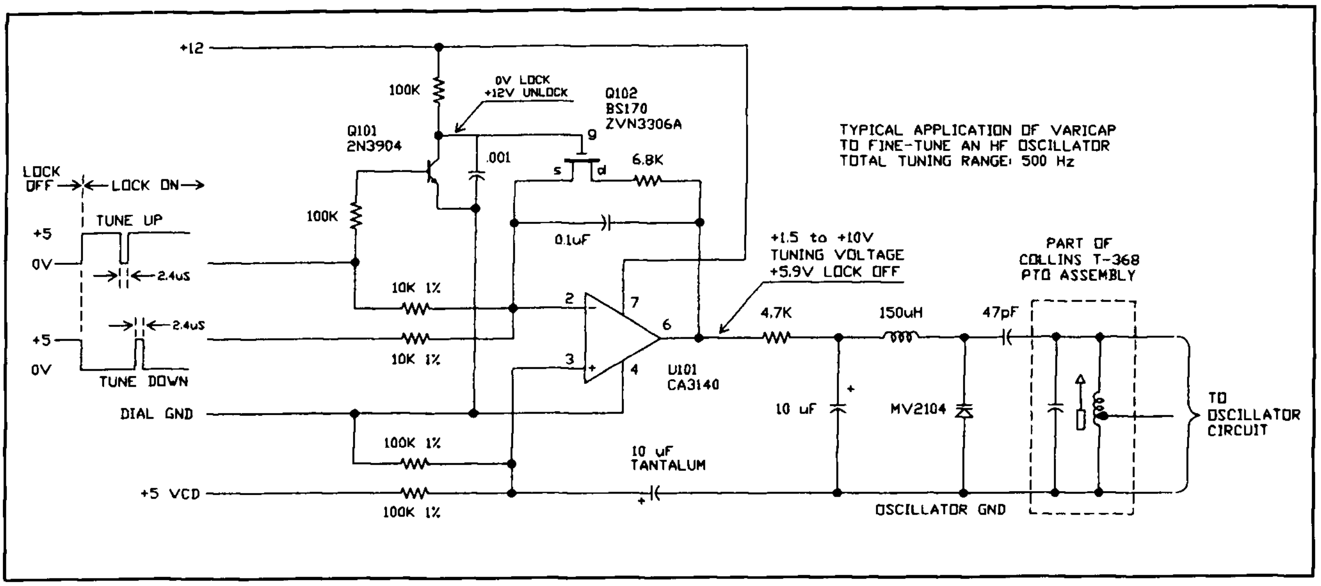

Figure 2. The F1 and F2 squaring circuits, the circuit for turning the carrier oscillator on (both functions are accomplished in the same circuit for F2), and the long coax driver.

working at 83.886 MHz. Neither hardware nor software is provides a serious limitation for an HF transceiver.

Transmit carrier oscillator F2 is set to the center of the filter passband for CW and 85 Hz lower than center for RTTY and AMTOR. When power is applied, the dial momentarily generates a +5 volt signal on pin 2 of J1 to turn the carrier oscillator on for measurement. See **Figure 1** for circuits to use this control signal. If the receive beat frequency oscillator (BFO) is used for F2, the dial will read the zero beat frequency. That's fine for SSB where the BFO and transmit carrier oscillator are the same frequency.

When the ADD/SUBTRACT pin is unconnected or grounded, F1 and F2 are added. For example, when tuning 20 meters with a 5 to 5.5-MHz LO and 9-MHz IF, the two frequencies will be added when the ADD/SUBTRACT pin is left open. For 75/80-meter operation with the same frequencies, applying +12 volts to the ADD/SUBTRACT pin will display the F2-F1 difference. F1 can be larger or smaller than F2; the dial computes F1-F2 and F2-F1 and displays the positive difference.

As another example, a 4434-kHz IF tuning 7.000 MHz can use a 11,434 (high side) or 2566 (low side) local oscillator. For low-side injection, F1 and F2 are added by grounding or leaving the ADD/SUBTRACT pin unconnected. For high-side injection, subtraction is invoked by connecting the ADD/SUBTRACT pin to +12 volts. In either case, the dial reads 7000.00 kHz.

Leading zero suppression

The dial suppresses leading zeros. For example, on 40 meters the display will show "7040.00" rather than "07040.00." If you know

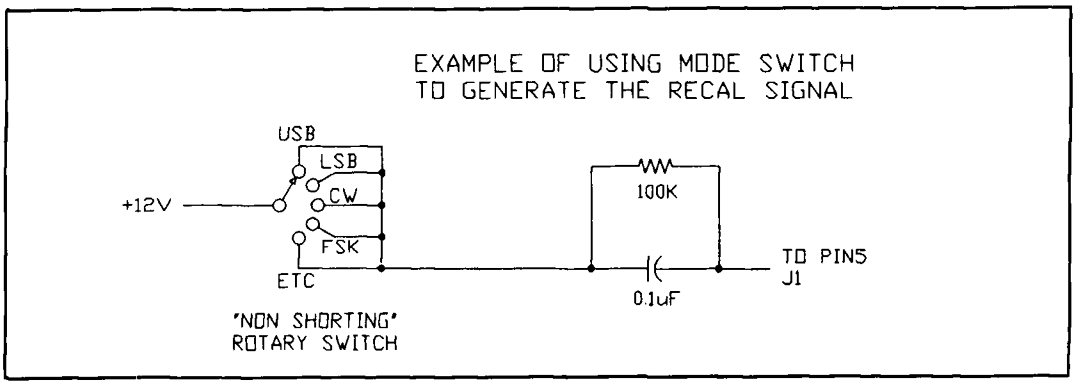

Figure 3. The AGC tank circuit.

what band you're on and want to save a few dollars, you can just leave the 10 and 1-MHz digits off. Similarly, if 10-Hz resolution makes your VFO look bad, the 10 Hz and even the 100 Hz digits can be left off, too. Obviously, my personal preference was to see all the digits; previous five and six-digit versions were scrapped. But we homebrewers have the advantage of being able to customize our own gear!

Zero function

When the ZERO pushbutton is pressed, the next count is stored. Subsequent counts, either positive or negative, are displayed relative to the stored count. This is extremely useful for net operation and DXing, but it's also nice for casual operating. Pushing the ZERO button again restores the absolute frequency display.

Frequency locking

References 1 and **2** list recent amateur articles; but counters have been used for many years to provide correction for oscillator drift in both amateur and professional equipment. This function is virtually free in a microcomputer-based counter.

The oscillator should be as good as possible *before* locking. The dial can correct the drift of even an VHF oscillator. But this is not phase locking and it will not reduce oscillator phase noise or the reciprocal mixing that results from having phase noise. On the other hand, neither will frequency locking transfer the spurious signals of a DDS-based phase reference onto the oscillator.

I modify surplus Collins PTOs, replacing the tubes with transistors. Drift rarely exceeds 10 cycles per hour, so drift correction is not a critical need. Correction is kept small and very slow. But it is comforting to know that, barring power failure, I can leave home for a week and find the 30-meter AMTOR receiver still *exactly* on frequency when I return.

Refer to **Figure 2**. Initially locking is off. The TUNE UP pin will be at ground and the TUNE DOWN pin will be at +5 volts. Trans-istor Q101 is off, its collector at about +12 volts. MOSFET Q102 will be on, connecting the 6.8-k resistor at pin 6 of the CA3140 op amp to its input, and disabling the integrator. The tuning voltage will be fixed at about +5.9 volts.

When the LOCK button is pressed, all decimal points of the dial go on, the TUNE UP pin is raised to +5 volts, and TUNE DOWN goes to ground. Q101 turns on, MOSFET Q102 goes off, allowing the output of U2 to integrate pulses on TUNE UP and TUNE DOWN to correct the oscillator frequency. The DC output voltage doesn't change until pulses are generated on the TUNE UP or TUNE DOWN lines. Another press of the LOCK button disables locking.

As Q101 turns on, MOSFET Q102 goes off, allowing the output of U2 to integrate pulses on TUNE UP and TUNE DOWN to correct the oscillator frequency. The DC output voltage does not change until pulses are generated on the TUNE UP or TUNE DOWN lines. Another press of the LOCK button disables locking.

When LOCK is enabled, the next counter number is stored. Subsequent counts are compared to the stored count. If they are the same, the dial produces no tuning pulses, and the CA3140 output voltage is unchanged. A lower count causes a 2.4-microsecond pulse to ground on the TUNE UP pin, slightly increasing the output voltage of the CA3140. A higher count causes a 2.4-microsecond pulse to +5 volts on the TUNE DOWN pin, slightly decreasing the output voltage of the CA3140. The CA3140 output is connected to a varactor diode and retunes the oscillator until the stored count is obtained. This is a feedback system and the loop can reach a "limit cycle" with frequency continuously cycling up and down like "huffen-puff." By pressing LOCK, then ZERO, you can watch the tuning up/down decisions being made on the frequency display.

The CA3140 circuitry should be part of, or located very close to the oscillator. TUNE UP, TUNE DOWN, power, and a DC ground are wired back to the dial to eliminate a ground loop. The one grounding exception is the 10-µF bypass capacitor whose negative end is connected to oscillator ground, another noise-reduction precaution.

Figure 2 includes the modified Collins PTO currently on the bench with the dial. This is an adaptation of the K7HFD oscillator.[3] The 47-µF tantalum integrating capacitor from output to input of the CA3140 op amp corrects drift very slowly, which suited my need. The size of the integration capacitor could be different in your situation because of a different tuning rate. For further guidance on locking refer to Spaargaren's *QEX* article.

DIM

The brightness and power consumption of the LEDs can be cycled through four levels with the DIM switch. Initial brightness is high. Pressing the DIM button reduces the brightness, with four presses bringing it back to the starting high brightness.

Power consumption depends on what is displayed as well as brightness. An "8" uses more than double the power of a "7" and the leading digit is only on above 10 MHz. Counter power consumption increases at higher frequencies. Counting an 11-MHz LO with medium bright-

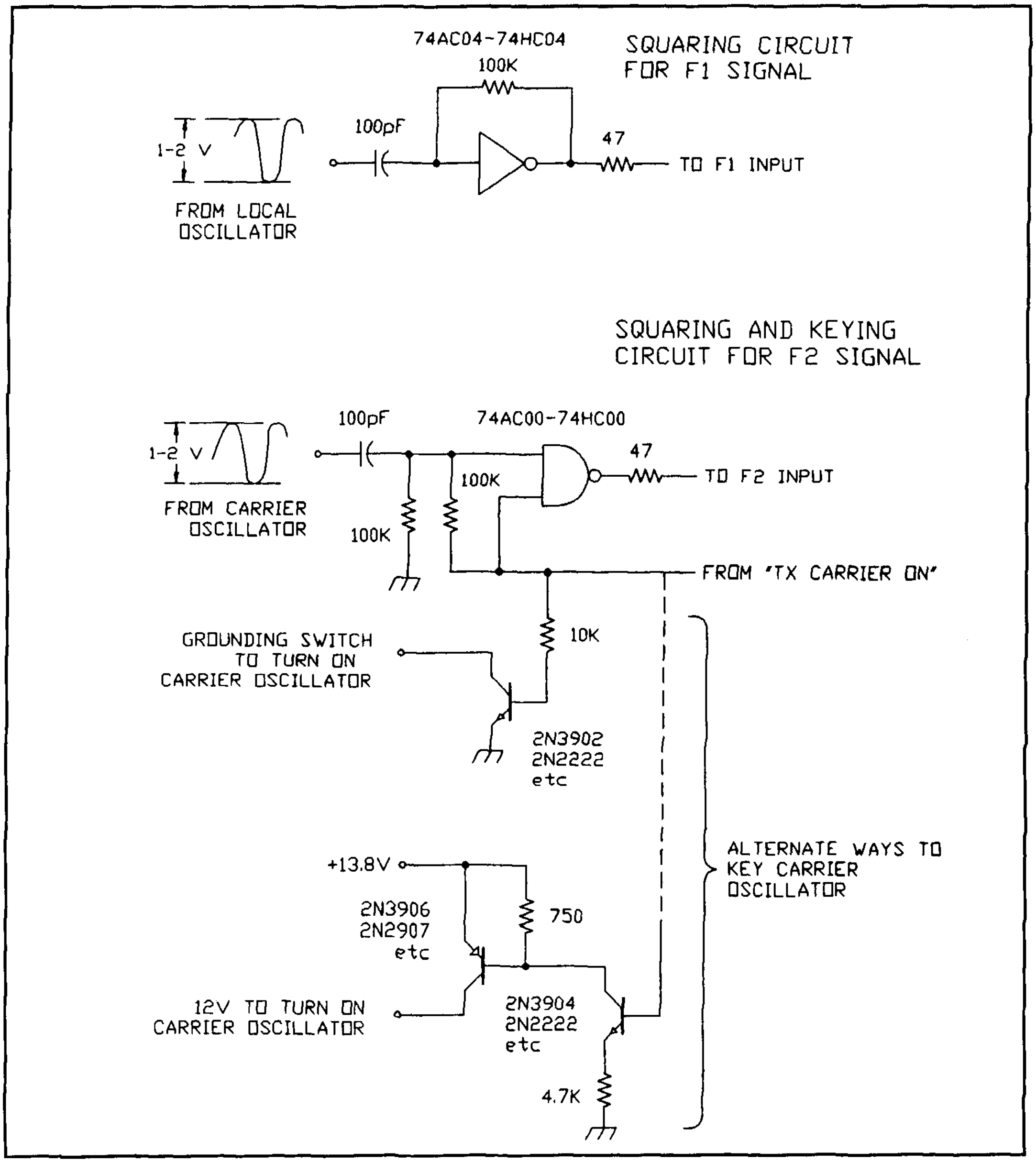

Figure 4. A 1:1 scale of the counter pc board traces and silkscreen.

ness, the current drain is 30 MA. At 75 MHz, with the brightest display setting, it draws about 100 mA—a power consumption of 500 mW.

With the RECAL switch closed, the counter is disabled, reducing power consumption to less than 10 mA. For battery operation, manual recalibrate and power-saving functions could be combined in one SPDT center-off toggle switch with one side having momentary (spring return) action.

RECAL

If your carrier oscillator does not change during operation, no connection is necessary to "recal" pin 5 of J1. If F2 does change during operation, say due to changing modes, its new frequency can be measured by momentarily connecting +5 volts to pin 5 of J1. A spare section on the mode switch would be most elegant. The dial recalibrates itself in a few seconds.

Figure 3 shows a switch and parallel RC network that will generate that signal as the mode switch is rotated. Contact is made at every switch position, but it must be open circuited between contact positions. This is the most common, "non-shorting" type of switch, with a narrow contact blade for the rotating contact.

PIC microcomputers

The simplest of the Microchips 16C5x-series microcomputers has a prescalar-counter capa-

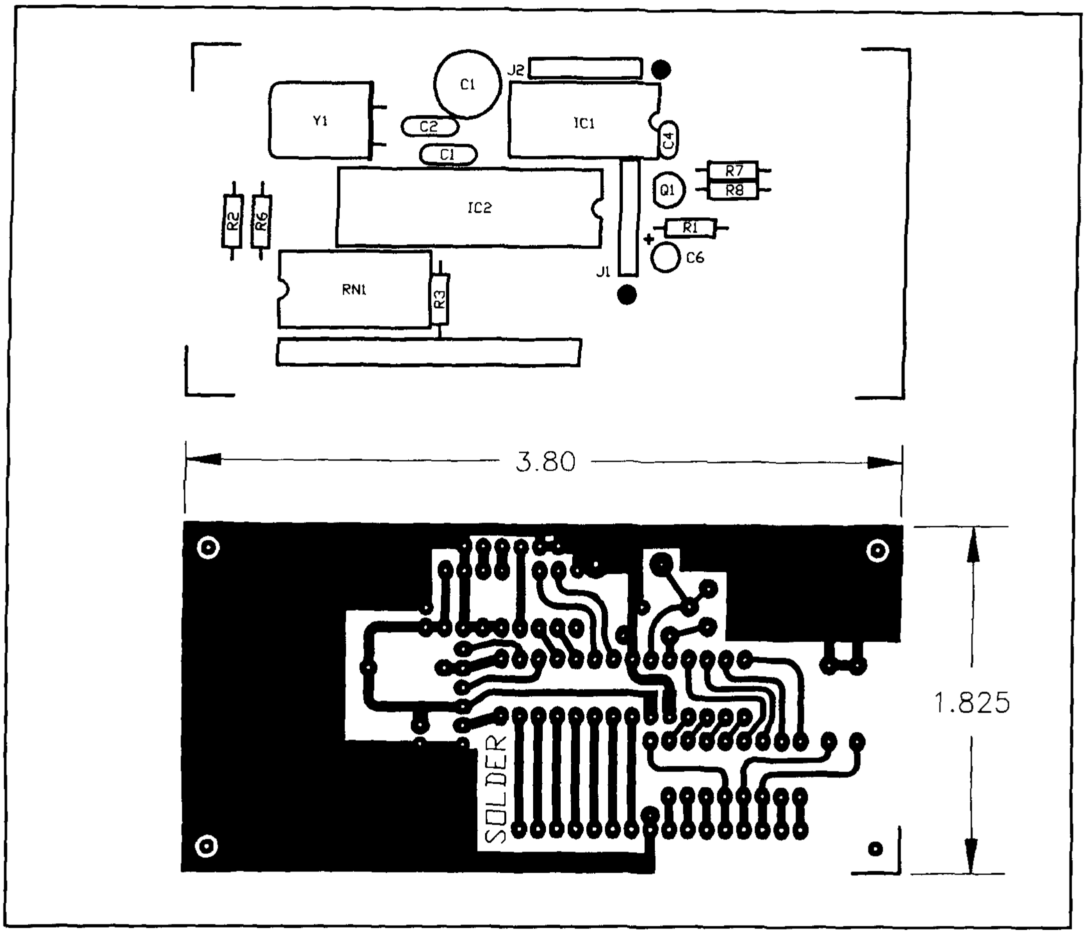

Figure 5. A 1:1 scale of the display pc board traces and silkscreen.

ble of counting a 50-MHz digital signal. Application note AN592, "Frequency counter Using PIC16C5X" explained one way to use this prescalar in a frequency counter, using software-generated delays to determine the counting interval.

I used the PIC16C62A-10/SP. For a few dollars more, it contains three internal timers, permitting a *hardware* gate time and freeing the processor while counting, so a multiplexed LED display can be operated by the software. Only about half the 16C62A program space was used.

The instruction set for this chip "feels" like a circa 1965 PDP-8 minicomputer and programming is clumsier than, say, a Z-80. But if you have programmed other microprocessors, you should be able to adapt and modify the code and add other features if something you want is missing. The extensively commented source for the counter is available for an SASE containing 2 ounces postage from *Communications Quarterly*. The program occupies slightly more than half of the available program space, so there's plenty of room for other features.

Microchips has an Internet Web site.* The DOS assembler (MPASM), DOS simulator (MPSIM), operations manuals for both programs and data sheets for their chips can be downloaded from that site. Printing the chip data and manuals was a huge job, filling four loose-leaf binders with single-sided pages. Printed manuals, available from Digi-Key, make more sense.

The program assembles in a few heartbeats, which is nice for the repeated assemblies necessary while fixing mistakes. The DOS software is a refreshing change from "cute," but slower Windows-based software.

The EPIC programmer and programming software was purchased from microEngineering Labs.** The specified chip can be programmed ONLY ONE TIME. Purchase an erasable version of the chip, the PIC16C62A/JW, if you want to develop your own software. The microEngineering Labs EPIC Plus Pocket PIC Programmer, part number EPICA, and a 40/28 Pin ZIF adapter, part

*The Microchip Web site is http://www.microchip2.com/products/micros/.
**microEngineering Labs, Inc., Box 7532, Colorado Springs, Colorado 80933; Phone: (719)520-5323; Web site: <http://www.melabs.com>; E-mail: <support@melabs.com>.
†Far Circuits, (847)836-9148. $7 for each set of two boards, plus S/H.

number 4028Z. are required to program the PIC16C62A.

Chips programmed with the described functions and compatible with the FAR Circuits pc boards are available for $15 postpaid in the United States. I would prefer to have you *build* this dial, but I know how time consuming getting parts can be. I'm prepared to supply an assembled and tested dial with two-color 0.4 digits for $57 postpaid in the U.S.

Hardware description

The 16C62A chooses between inputs of F1, F2, ground, or +5 volts by changing the control lines of a 74AC151 8-input multiplexer under software control. Four inputs of the 74AC151 are unused.

The seven digits are multiplexed, blinking at a high rate of speed. The processor applies +5 volts on PORTC to the segments needed for a digit, then grounds a pin of PORTB to pull the emitter of a "digit" transistor to 0.7 volts, turning on the segments.

Switches are also multiplexed, checked for closure between each "blink" of a digit. The DIM, LOCK, and ZERO pushbutton switches are mounted along the bottom edge of the display board to eliminate connectors, wiring, and radiation of multiplex signals.

In a multiband rig, add or subtract might be a function of the band; but I did not want to run noise multiplexed wires around a rig. MOSFET Q8 is used as a remote switch. Its gate control signal can be heavily filtered so noise will not be conducted to a bandswitch carrying weak signals. Place a 0.001 to 0.1-µF bypass capaci-

Parts List

IC1	Microchips PIC16C62A-10/SP*	Digi-Key
IC2	74AC151PC	Digi-Key
IC101	CA3140E	Digi-Key
Q1-7, Q101	NPN silicon	2N3904, PN2222, etc.
Q8, Q102	N-channel MOSFET	BS170, Zetex ZNV3306A
DSP1-7	0.3-inch-high RED	Mouser 512-MAN3940A
	0.3-inch-high GREEN	Mouser 512-MAN3440A
DSP1-7	0.4-inch-high RED	QT Optoelectronics** MAN4740A
	0.4-inch-high GREEN	QT Optoelectronics MAN4440A
S1-S3	Panasonic pushbutton switches	Digi-Key P8012S-ND
RN1	eight 220-ohm resistors, 16-pin DIP	Bournes 4116R-1-221
RN2	eight 2.7-k resistors 16-pin DIP	Bournes 4116R-1-272
Y1	10-MHz 30-pF HC49 crystal	Digi-Key CTX-083
C1	5.5-18 pF NPO (Newark Electronics)	Erie Murata DC11PS18A
	16-conductor 0.1-inch flat cable assembly	Digi-Key A9AAT-1602F-ND
	Connectors are nice, but optional	
J1,J2	6-pin connector housing (Molex 50-57-9006)	Digi-Key WM2804-ND
	Molex 16-02-1125 high-pressure contacts (for #24-30 wire)	Digi-Key WM2554-ND

*A programmed IC1 is available from the author for $15.
**QT Optoelectronics were obtained from FAI Electronics (800)767-8139.

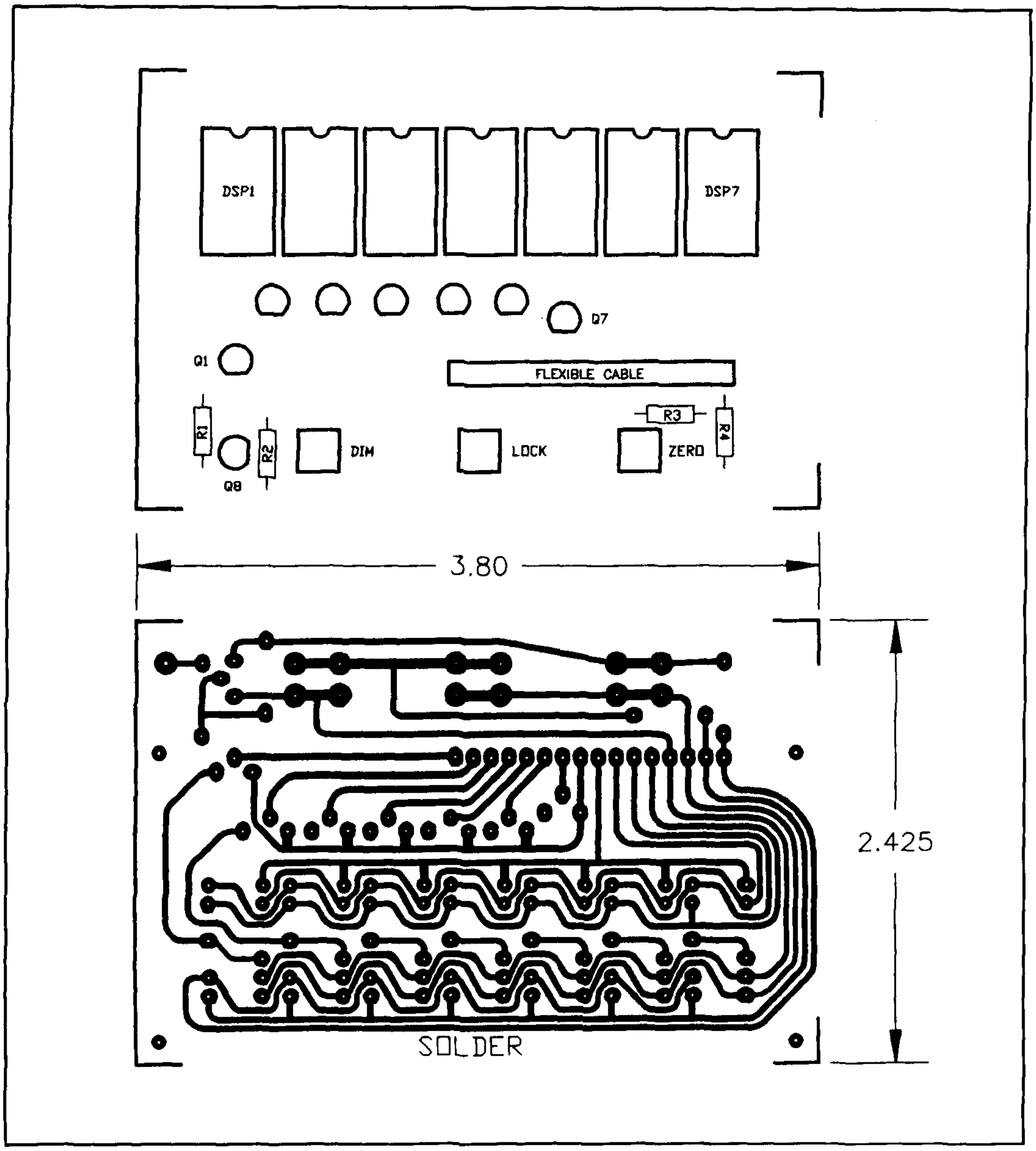

Figure 6. A circuit to generate the "RECAL" signal from a typical rotary MODE switch.

tor to ground on the control voltage where it leaves the dial enclosure.

If your rig needs to always add or always subtract F1 and F2, transistor Q8 and resistors R1 and R2 are not needed. If it always adds, just eliminate them; if it always subtracts, place a wire jumper between the MOSFET source and drain pads.

F1, F2 signal processing details

Because the dial was designed to work in several different projects, I chose to convert oscillators to 5-volt square pulses at their source. **Figure 4** shows squaring circuits for F1 and F2. "AC" logic, like "HC," is biased to 2.5 volts DC, the middle of its input range, with a 1 to 5-volt p-p RF signal. The F2 squaring circuit only has an RF signal during calibration. Midpoint bias must be removed after the F2 calibration interval, or the logic gate will draw excessive DC current.

Despite the fast signal risetimes of AC logic, there were no problems driving the counter through 9 inches of RG-174. Routing the pulses inside a normal-sized rig should not be a problem. For very long distances, **Figure 4** shows how to drive the counter through a pair of back-to-back 4:1 bifilar transformers that experimentally operated the counter over 20 feet of coax from the simple 74AC04 squaring circuit.

Construction and part notes

To conserve panel space, the dial is built on two-sided pc boards (see **Figures 5** and **6**) available from Far Circuits.† The front display board, with the LEDs, digit driving transistors, and pushbutton switches is 2.43 inches high and 3.8 inches wide. The rear board has the counter electronics, and is the same width, but is 1.83 inches high. The FAR Circuits boards are sheared slightly oversized, so be prepared to trim the board edges a bit, or allow for board cutting tolerances by reserving a 2.75 by 4-inch space for the dial.

The two boards were stacked on four 1/2-inch long metal spacers. Signals pass between boards on a 2-inch long AMP 16-conductor flat flex cable. The counter operates with boards folded open, convenient when troubleshooting. The tips of the solder pins at each of the cable were bent 90 degrees to solder the cable parallel to the boards. It was folded in the middle to fit between them when they were bolted together. Longer flex cables are also available.

The display board pads accept Panasonic pushbutton switches available from Digi-Key. There are three different stem lengths, the longest is the Digi-Key P8012S. The stem diameter is 0.134 inch. In most cases, these stems must be extended to protrude a reasonable distance through a panel, but they list no buttons for these switches. A 1/4-inch diameter plastic rod can be drilled to accept the switch stem. If you decide to use other switches off the board, use care and do not route switch wires outside the display if at all possible.

U1 and U2 were socketed. Two end-stacked 14-pin sockets were used for the 16C62; however, a single 28-pin socket will do. Pins 3, 5, 10, and 11 of the LEDs are missing, and the board space is used for PC traces. If sockets are used for the LEDs, these pins must be removed from the sockets.

To have a continuous groundplane, yet still make the counter pc board single-sided, a 0.1 μF bypass is soldered directly between pins 19 and 20 of the PIC16C62 on the solder side of the board. Pads are provided for a 1208 surface mount capacitor, but a leaded capacitor with 0.1-inch spacing will work just as well. One jumper is required on the processor board between pin 9 of U1, the 74AC151, and pin 28 of U2, the 16C62. Pin 5 of IC1 is not used. To eliminate a jumper, pin 5 of the socket is removed to make room for a pc trace.

On the display board, five jumpers connect the emitter of the five-digit driver transistors Q3–Q7 to their digits, DSP3–DSP7, respectively. I used #30 Kynar-insulated wire-wrap wire as heat-resistant, unobtrusive jumpers, but any kind of insulated hookup wires will work.

I liked the bright green 0.3-inch-high characters of the MAN3440A, but my brain couldn't read seven digits quickly. I changed the 3-kHz digits to red MAN3940A LEDs, leaving green MHz and Hz digits on their left and right. Now, I have instant frequency recognition at a glance from across the room. After building several units, I found the red MAN3940A LEDs were temporarily out of stock. The parts list provides parts numbers of alternative displays with 0.4-inch-high digits that are compatible with the pc board.

Trimmer C1 permits adjustment of the microprocessor clock to exactly 10 MHz. The crystal must be cut for a parallel resonant 30-pF load, *not* series, or you won't be able to get it down to 10 MHz. I know because a junkbox *series* resonant crystal wouldn't work.

After building several units, I became frustrated using plastic trimmers for C1; although widely available and inexpensive, they don't adjust smoothly. I finally settled on a Erie/Murata DV11A18A 5.5 to 18-pF NPO ceramic trimmer. A small air trimmer could be substituted. It's possible that this trimmer may not have enough capacitance to always compensate for crystal tolerance: having 16 and 62-pF NPO or silver mica capacitors to substitute for the 36 and 47-pF values makes it possible to use the NPO trimmer and obtain exactly 10 MHz with any reasonably accurate crystal. If your crystal will not adjust to 10 MHz, C3 or C2 could be changed or another crystal tried. This probably won't be necessary: all crystals in a group of 10 were adjustable to exactly 10 MHz in my four units, and the fixed capacitor was always rated at 36 pF. K7HK reported no problem obtaining exactly 10 MHz when he build his dial.

Wires for signal, power, and switch connections can be soldered directly to the board. This is both economical and reliable. To provide more flexibility, I put strips of 0.25-inch pins on the board and use Molex "C-Grid" connector housing and terminals. Their WM2554 crimp terminals have high contact force and provide a secure connection even with the small number of pins. The add/subtract connection on the display board was soldered, although a one-pin connector could be used.

Display noise

The dial generates a modest level of EMI. I expected shielding would be required to keep wideband noise of the multiplexed LED display from being heard in the receiver, but none was detectable at 7 MHz—even with the dial within 1 inch of an unshielded VFO and diode mixer *with background noise from an antenna.*

However, K7HK found that weak spurious signals could be heard in his *very* hot 20-meter receiver. Plan to enclose the dial in a metal box. The add/subtract connection should be filtered with a 0.1-μF capacitor to chassis ground where the wire enters/leaves the box.

Credits and conclusions

A bright, two-color frequency display showing frequency to 10 Hz makes a beautiful first impression in a homebrew rig. It provides crystal-controlled stability to the LO, which makes a *lasting* good impression.

This modular digital dial was duplicated by several other homebrewers while the article was being prepared—two by K7HK alone. Special thanks to Harry for his faith, the photograph of one of his receivers and for his feedback during the dial development. ■

REFERENCES

1. Klass Spaargaren, PAØKSB, "Frequency Stabilization of L-C Oscillators," *QEX*, February 1996.
2. Lee Richey, WA3FIY, "The Cyclemaster," *QST*, September 1997, pages 37–42.
3. Wes Hayward, W7ZOI, *Solid-State Design for the Radio Amateur*, ARRL, Newington, CT, 1989, page 126.

PRODUCT INFORMATION

CEL Adds New 3-GHz, Divide-by-4 Prescaler to Its Line of Ultra Miniature NEC RFICs

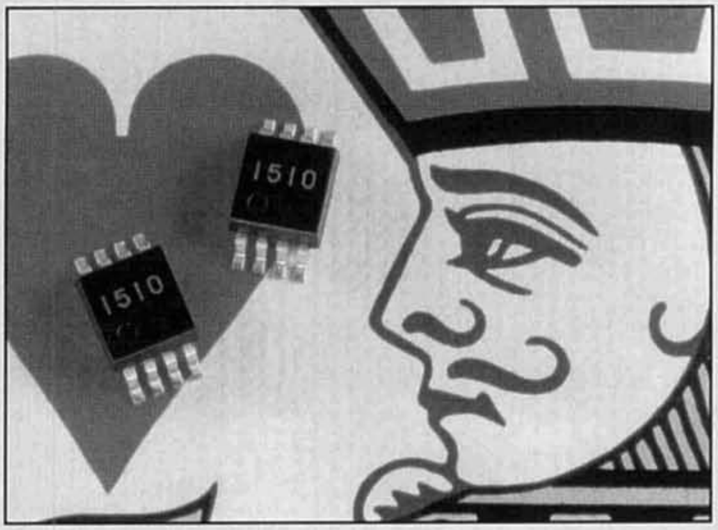

California Eastern Laboratories has announced the availability of another new silicon RFIC prescaler from NBC. The UPB1510GV features 3-GHz frequency response and low current consumption, making it an ideal candidate for PLL synthesizer applications in UHF/VHF TV and DBS receivers. The UPB1510GV features Upper Limit Operating Frequency, 3.0 GHz; Supply Voltage, 5.0 V, Supply Current (typ.), 15 mA.

The UPB1510GV is housed in NEC's miniature eight pin SSOP "GV" package. Less than half the size of NEC's "G"-packaged prescalers, the UPB1510GV can help engineers in the miniaturization of their designs. Priced at 99¢ in 100K quantities, the UPB1510GV is available on tape and reel. For samples and data sheets call CEL at (408) 988-3500.

Philips ECG Microsoft® Windows® Version of Semiconductor and Relay Cross Reference

Philips ECG® introduced its Computerized Semiconductor and Relay Cross Reference for Windows on 1.44M diskettes.

ECG has included its popular Relay cross reference along with the Semiconductors. Over 4,000 ECG semiconductor replacements cross to approximately 300,000 industry part numbers, and 775 ECG relay replacements cross to approximately 60,000 industry part numbers.

The Instant Cross program also displays the full Semiconductor and Relay device description, case style, and a reference to any special or general notes that may apply. Another feature of the software permits the user to select from a number of font sizes for easy viewing.

The Instant Cross program contains the same cross reference database as published in the *ECG Semiconductor Master Replacement Guide* (ET-2762), now in its 17th edition and the *8th Edition Relay Guide* (ET-2700-1). The ECG product line comprising this database includes replacements for transistors, ICs, SCRs, TRAICs, rectifiers, diodes, optoelectronic devices, solid-state relays, general purpose relays, timer relays, optical sensors and many other devices.

To obtain the Windows version of Instant Cross software (ET-2604W), the ECG Semiconductor Master Replacement Guide (ET-2762), the Relay CompuCross® software (ET-2822D), the Relay Guide (ET-2700-1), the DOS Instant Cross software (ECG2604) and the many other ECG products, contact your local distributor. To locate the nearest distributor, call toll-free, 1-800-526-9354.

John S. (Jack) Belrose, *VE2CV*
17 Tadoussac Drive
Aylmer QC J9J 1G1 Canada
<john.belrose@crc.doc.ca>

ELEVATED RADIAL WIRE SYSTEMS FOR VERTICALLY POLARIZED GROUND-PLANE TYPE ANTENNAS

Part 2—Phased Arrays

In Part 1 of this article,[1] I gave an overview of the subject of monopole ground-plane type antennas that use elevated horizontal resonant radials instead of the conventional multi-wire buried radial ground systems. Part 2 is concerned with phased array antenna systems, where each element of the array uses elevated radials. The conclusions reached are based on new information, measured results, and numerical analysis—a more detailed numerical analysis (using NEC-4D rather than NEC-2) then was available at the time I published an earlier paper on the subject. That paper was presented in a forum for radio amateurs.[2]

Introduction

As was noted in Part 1, some MF broadcasters in the United States who have tried elevated radials to resolve site problems swear by them, while others swear at them. Beverage[3] has achieved excellent performance for a 0.17-wavelength MF broadcast tower with six elevated radials, and Carl E. Smith has successfully used elevated radials for a broadcast station in Alaska.[4]

In spite of the agreement between theory and experiment reported in Part 1, there are some experiments not in accord with expectation. For example, Tom Rauch, W8JI's, experiments with elevated radials[5] do not agree at all with predicted outcomes. Rauch's measurements, as the number of radials were changed for an 80-meter wire monopole antenna, showed a trend that is almost identical with what one would expect for a radials-on-the-ground situation. He reports that others have found similar results.

Concerning directional arrays, some broadcast station engineers have reported problems in achieving standard horizontal pattern gains with directional arrays using elevated radials.[6] WVNJ is a four-tower directional array near Oakland, New Jersey, operating on 1160 kHz. The site is in a rocky area where a conventional buried radial wire ground system was considered to be impractical, so elevated radials were tried. The station was installed in 1993 and, with the elevated wire system installed, it never did achieve expected performance.

The site was restricted and some of the radials had to be shortened to approximately 70 percent of the full quarter wavelength. A free-space quarter wavelength for the operating fre-

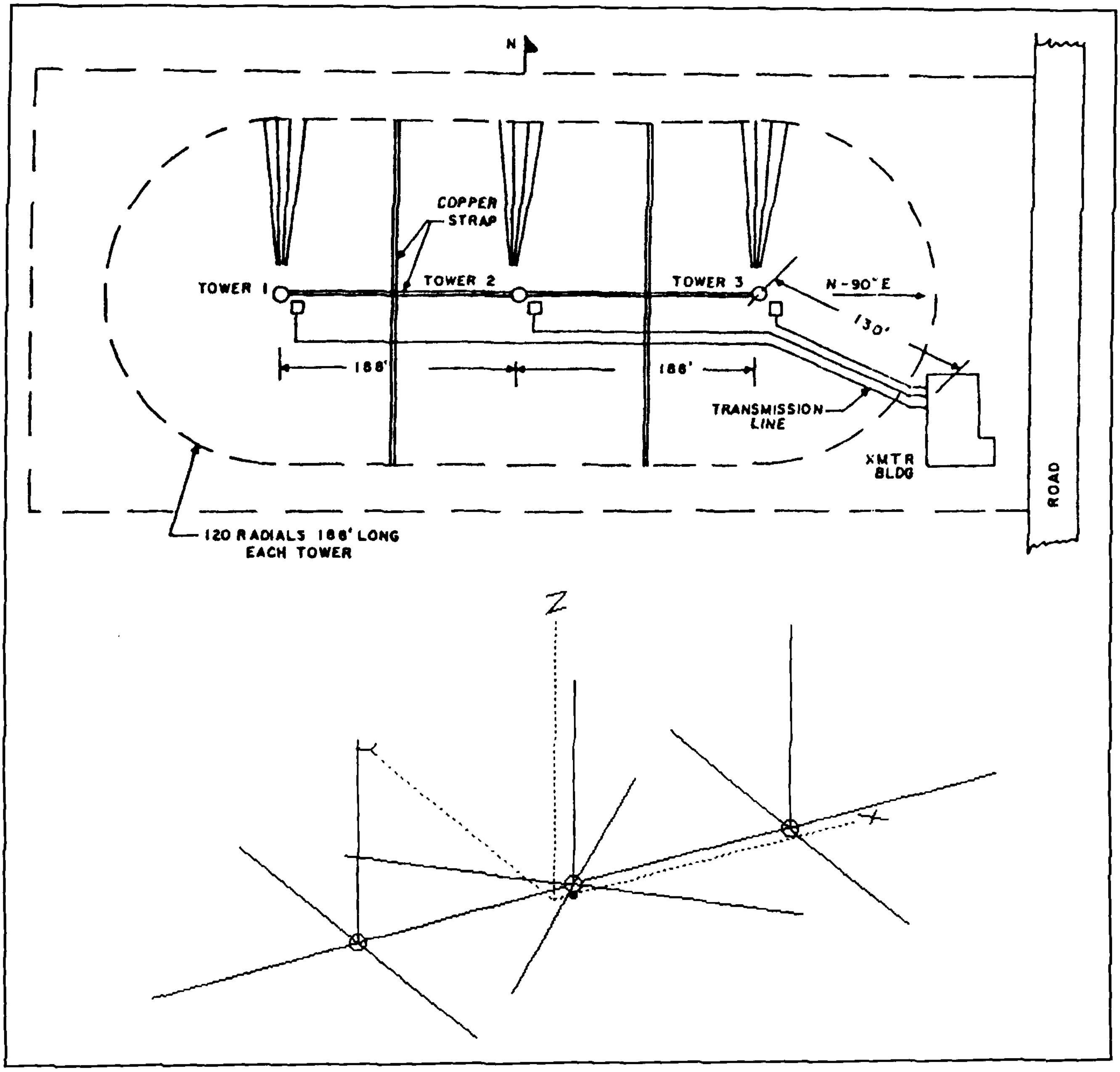

Figure 1. (A) An example of a conventional, three-tower MF broadcast directional array, after Smith;[7] and (B) a proposed antenna system that could be used instead, which has four elevated resonant radials associated with each tower in the array.

quency 1160 kHz is 64.6 meters. A resonant radial length (according to NEC-4D) is 62.15 meters, where the radial height is 6.1 meters over average ground. (The site conductivity, not measured, is probably somewhat worse.) Installed radial lengths varied from 45.3 to 66 meters. Because six elevated radials were installed on each tower, some of the radials ran almost parallel with a radial associated with an adjacent tower, and some were overlapping. This, I believe, was the problem.

Clearly, the subject of elevated radials needs further study. This is particularly true if the elevated radials are used for the elements of a directive array.

Ground systems: buried versus elevated radial wires

You will remember that MF broadcast antennas conventionally use 120 buried radial wires, with each wire 0.25 to 0.4 wavelength long. Radio amateur installations typically use as many radials as possible. The number used depends on one's enthusiasm for burying wire

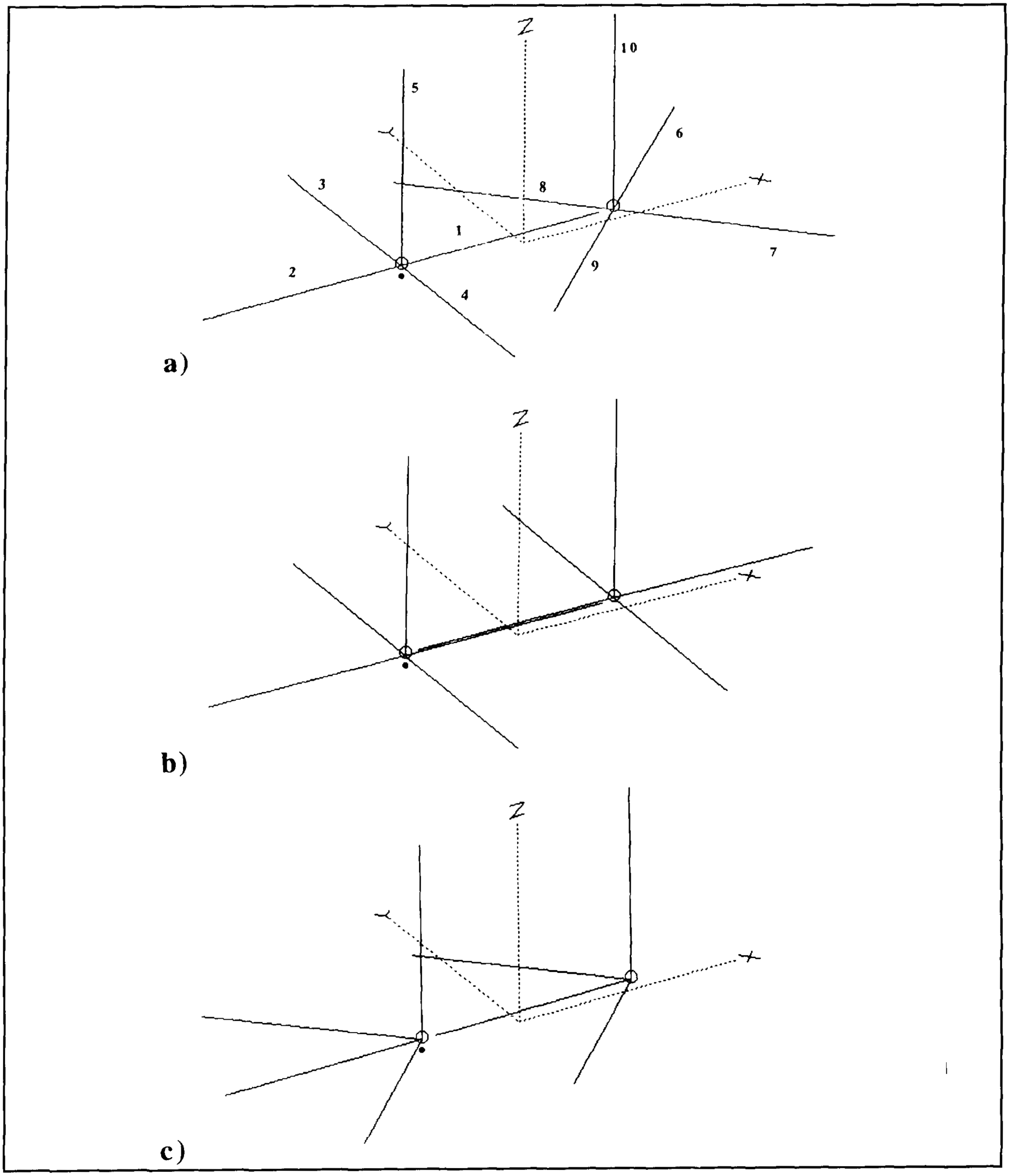

Figure 2. (A) A two-tower array using four elevated resonant radials, where the radials are oriented for maximum symmetrical separation between radials associated with each tower; (B) the radials of the adjacent tower are oriented for a minimum separation; and (C) a suggested arrangement for use with towers fed so the pattern is a cardiod, the "crow's foot" radials point in the direction of maximum gain.

and on practical and perhaps financial considerations. The ground systems for MF broadcast directional arrays use non-overlapping radial wire ground systems, where the radial wires (buried) are terminated and bonded to a copper strap at their junction. **Figure 1A** is a representative MF broadcast station installation for a 1310-kHz directive array antenna system

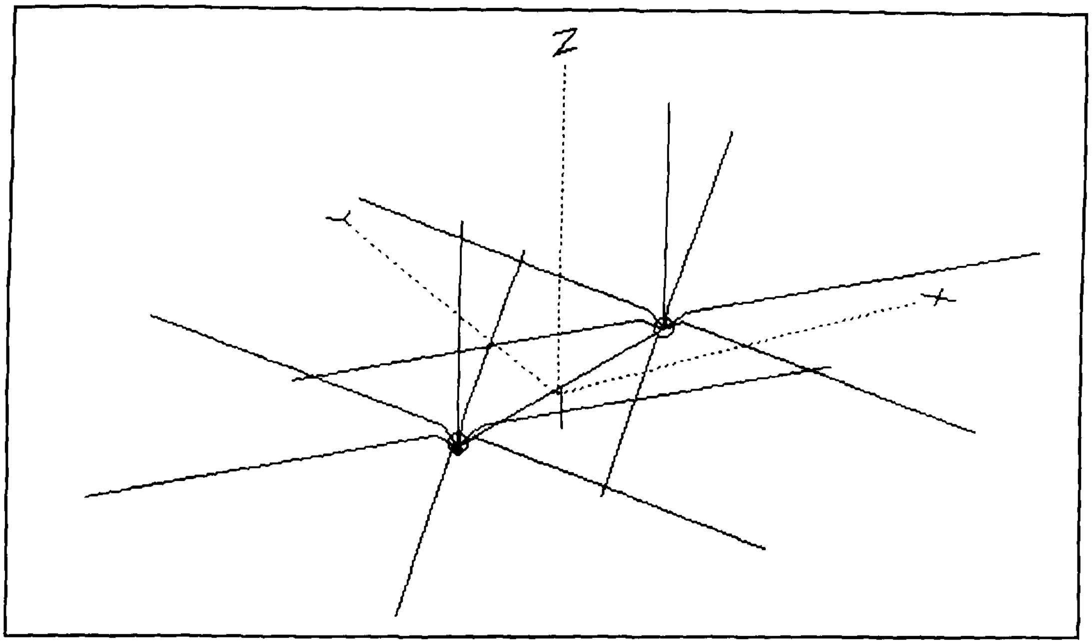

Figure 3. The model used to numerically simulate performance for the MF broadcast station KGGN 890 kHz, Gladstone, Missouri, which uses such an elevated radial system.

described in some detail by Smith.[7] Notice that (comment by the author), perhaps not in accord with the concept that radial wire ground systems are arranged to collect ground current associated with each tower separately, a copper strap between towers and the bonding of the wires to a copper strap at the junction of the ground radials provides connectivity of the ground systems.

Critical antenna systems use additional complexity to stabilize the base impedance. For example, in the case of another directional array given by Smith in the above reference (see also Belrose[8] who has numerically modeled this antenna system using elevated radials), the ground system for an MF (1360 kHz) directional array antenna system using six towers, has 120 radials 15 meters long equally spaced between the 120 radials 67 meters long that are surrounding each tower. Can we expect comparable performance for directional arrays which use only four elevated radials, centered on each tower (**Figure 1B**)? That is the theme of this article.

Phased arrays

Comments on how to configure radial systems

Ground systems for directive arrays have traditionally used non-overlapping multi-wire ground systems. With elevated resonant radials, current flowing on one radial wire can couple with current flowing on an adjacent radial wire associated with another element of the

Wire	Phase difference source currents		
Number	0 degrees	90 degrees	180 degrees
1	0.11 < -32.1	0.31 < -28	0.36 < 23.8
2	0.36 < -9.4	0.33 < 18.4	0.16 < 18.9
3	0.28 < 12.4	0.21 < 6	0.25 < -10
4	0.28 < 12.4	0.21 < 6	0.25 < -10
5	1.0 < 0	1.0 < 0	1.0 < 0
6	0.33 < -4.3	0.23 < 76.2	0.20 < -164.6
7	0.33 < -4.3	0.23 < 76.2	0.20 < -164.6
8	0.18 < 8	0.28 < 100.8	0.31 < 170.4
9	0.18 < -8	0.28 < 100.8	0.31 < 170.4
10	1.0 < 0	1.0 < 90	1.0 < 180

Table 1. Currents on radials for a two-element phased array (see Figure 2A). All elements #10 wire, length 20 meters (λ/4 for the modeling frequency 3.75 MHz). Radial height 1 meter, over pastoral ground.

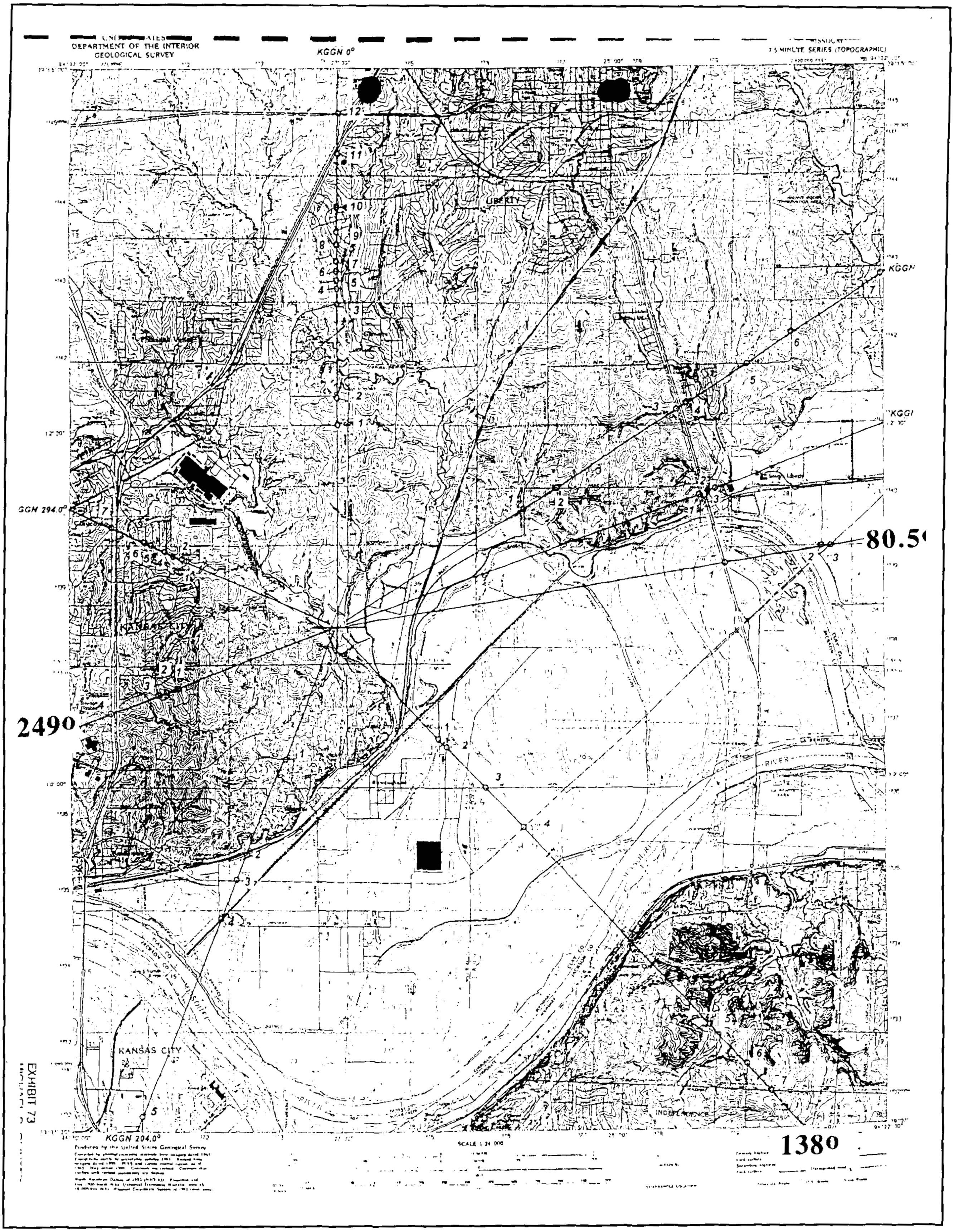

Figure 4. Map showing terrain features surrounding MF broadcast station KGGN, highlighting three azimuthal directions pertinent to our analysis of the measured data.

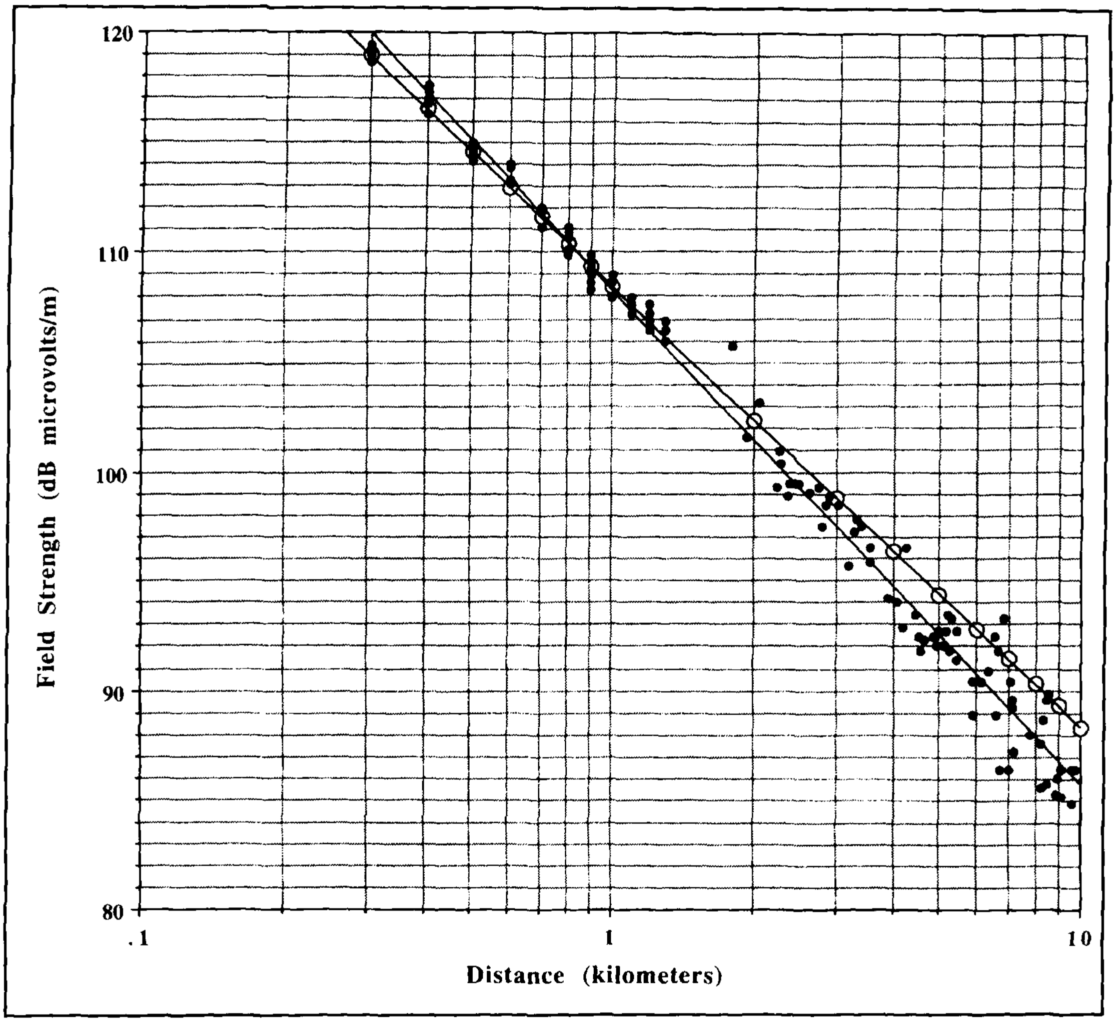

Figure 5. Measured ND field strengths (dB microvolts/m) versus distance for KGGN, for all data measured in eight azimuthal directions. The theoretical field strength is the continuous curve through the open circles; the continuous curve, which lies above and below this curve is the best logarithmic fit curve to the measured data.

array. This is a matter of no concern, or at least it is not considered in the case of buried radial wire systems.

I have redone my initial studies[2,8] using NEC-4—actually EZNEC-4D (a double precision), available from Roy Lewallen.* The initial work concerned a two-tower array with the towers a quarter of a wavelength high spaced a quarter of a wavelength apart. The ground system for each tower consisted of four radial wires, arranged symmetrically to provide minimum coupling between wires associated with the adjacent tower (see **Figure 2A**). Intuitively, I considered this a good arrangement. The length of each radial was the length necessary for the radial to be resonant. The radials were 1 meter above average ground (σ = 5mS/m, ε = 13), frequency 3.75 MHz.

*Available from Roy Lewallen, W7EL, P.O. Box 6658, Beaverton, Oregon (e-mail<w7el@teleport.com>). Note: EZNEC pro is normally supplied with the NEC-2 engine, because NEC-4 is not available unless the user is licensed to use NEC-4.

Certainly, there are unequal currents on radial wires. It is interesting to examine the currents on the radial wires as the phase difference in the feed currents is changed. I have given the radial and radiator wires a number. **Table 1** shows the currents on these wires, the currents on the segments nearest the source, computed using EZNEC-4D-for radiator phase differences of 90 degrees (cardiod pattern), 180 degrees (figure-eight pattern), and 0 degrees (a broadside array). Currents on radials 3 and 4, 6 and 7, and 8 and 9 are equal; but, as might be expected, currents on radials 1 and 2 are different, and the difference is dependent on the phase differences of the source currents. I have not tried to interpret this result. In any case, it makes little difference, as the desired pattern and gain is realized.

I have since examined the situation where the radial wire systems are arranged, so a radial associated with one tower runs parallel to and beside (very close spacing) a radial associated with the adjacent tower (**Figure 2B**), in which case currents on these radials can be reduced to almost zero. A radial carrying zero current is not a very effective radial, so these radial wires might as well not be there!

If a cardiod directional pattern is desired, radials can be arranged in a *crow's foot* pattern directed toward the azimuth of maximum gain, as in **Figure 2C**. This improves the front/back ratio, with only a small effect on forward gain (plus-or-minus a fraction of a dB).

A case study

To illustrate some of the pertinent factors and expectations if elevated radials are used, and to validate NEC-4D, I will consider two-tower array, MF broadcast station KGGN, operating on 890 kHz, near Gladstone, Missouri. I am fortunate to have the detailed proof of performance report for this station.[9]

KGGN uses two vertical radiators of 60 meters height (physical height 64 electrical degrees), 69.3 meters (74 electrical degrees) apart, on a bearing of N 69 degrees E True. The towers are guyed, uniform triangular cross section, face width 0.457 meters. The ground system for each antenna consists of six counterpoise wires arranged at 60-degree intervals for symmetry, 86 meters long.** The radial system is elevated 5 meters above ground until the radials come to a point 5 meters from each tower base. At this point, they slope downward at an approximately 45-degree angle, terminating in insulators attached to the concrete base pier. The base height of the towers is 1 meter above ground. The two counterpoises are not connected to each other (and cannot accidentally touch) except at the base of each tower, where a copper strap runs along the tower line and through the transmitter building. The copper strap is for lightning protection, tying the phasor, transmitter, collection rings of each counterpoise, mains breaker panel, and tele-

**Note: the radials are too long to be resonant. The resonant frequency for the 86-meter long radials configured as above, according to NEC 4-D is 841 kHz.

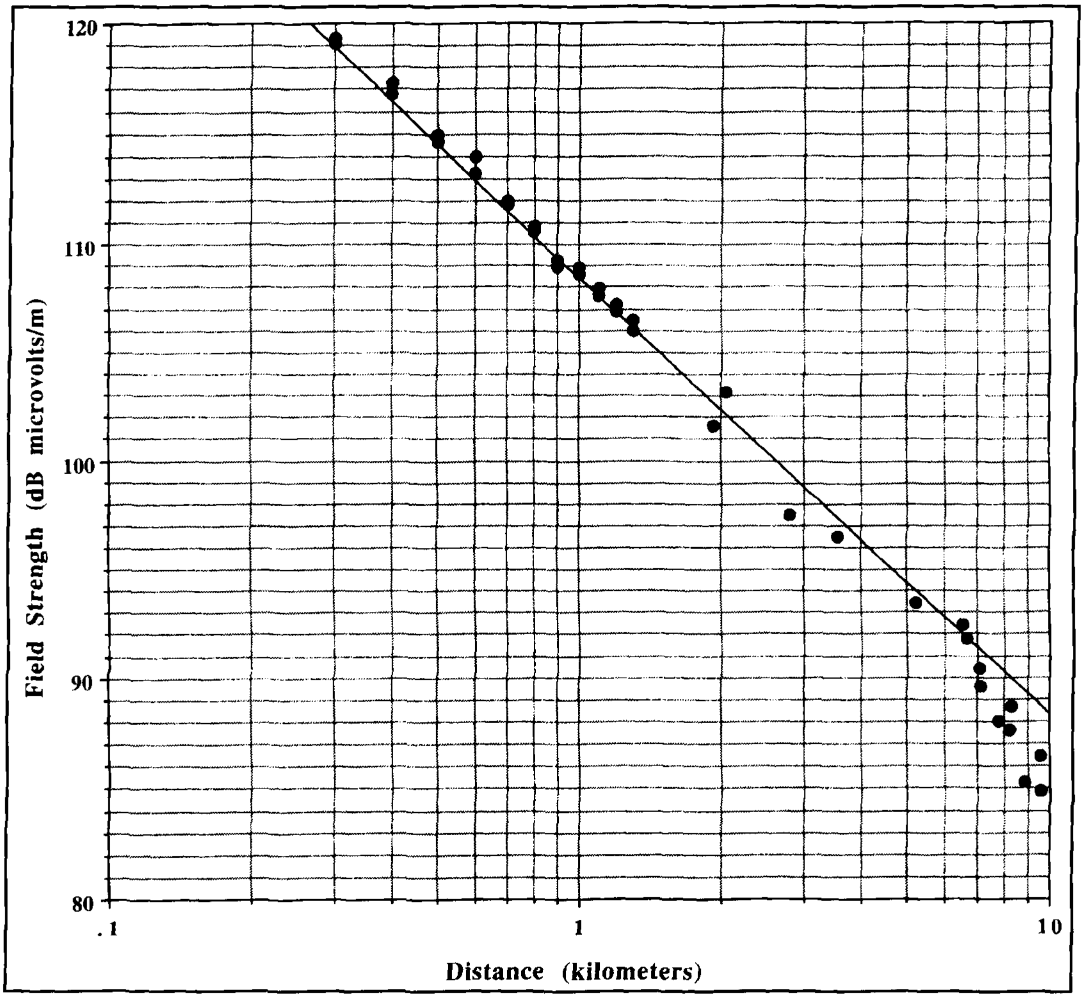

Figure 6. Measured ND field strengths versus distance for KGGN, for the best two azimuthal directions (80.5 degrees T and 138 degrees T)—see map in Figure 4. The continuous curve is the theoretical field strength (the same curve shown in Figure 5).

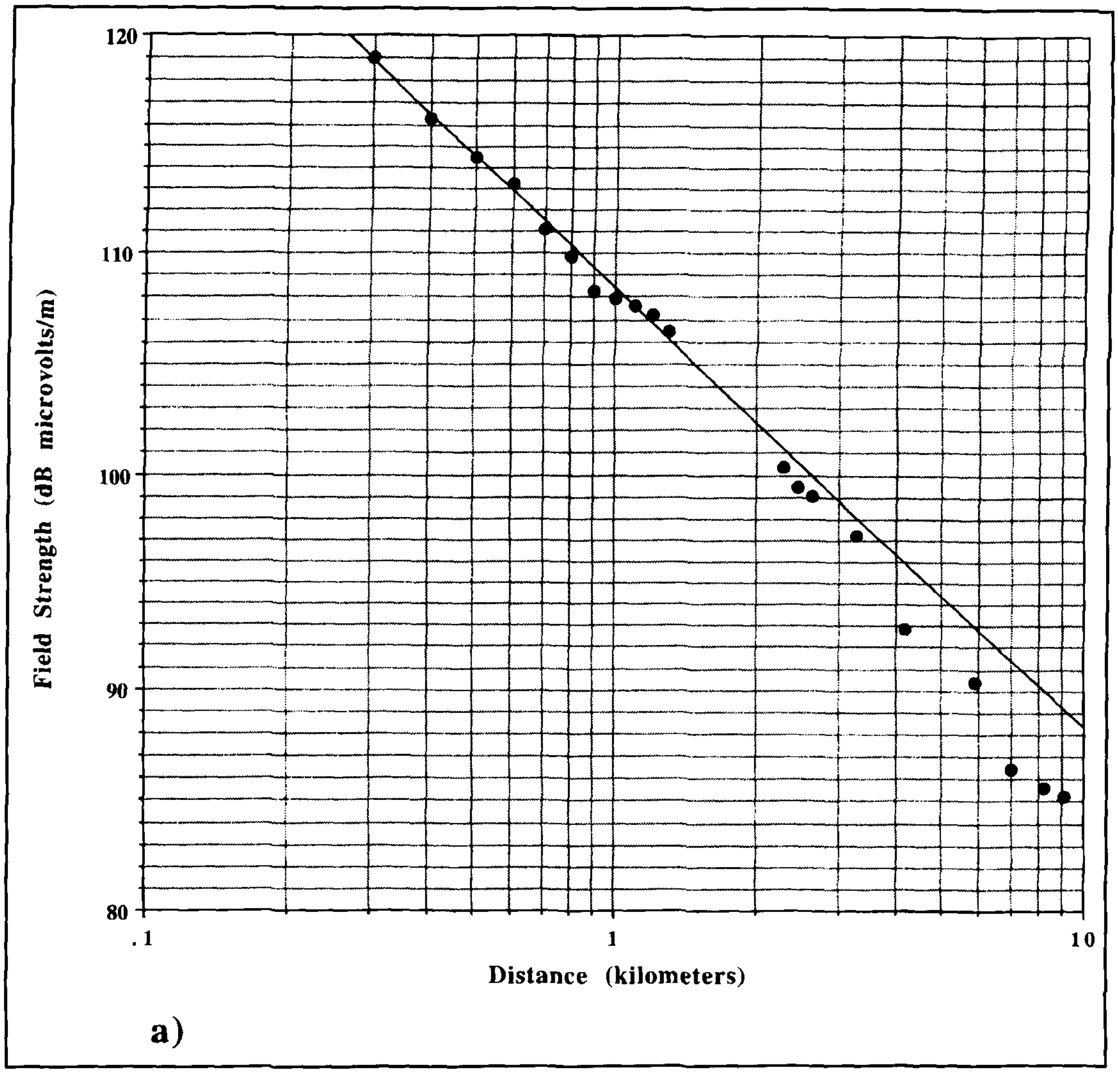

Figure 7A. Measured ND field strengths versus distance for the azimuthal directional array (249 degrees T), and theoretical field strength curve (the continuous line, which is the same curve in Figures 5 and 6).

phone gas protectors to a common earth. For this model, I have assumed that the connection to earth is by means of a 10-meter ground rod—the modeled antenna array is sketched in **Figure 3**. Tower 1, the tower on the left, carries a current Of 1.0<0 degree amperes; Tower 2's current is 0.92<107.5 degree amperes.

The station's proof of performance documents: 1. field strengths, first for the case of single nondirectional (ND) tower; 2. measurements made at many locations in eight azimuthal directions, in the distance range 0.3 to 40 kilometers; and 3. field strengths for the directional array measured in the same azimuthal directions, and at the same locations, in the distance range 3 to 40 kilometers.

Gladstone is NNE of Kansas City, Missouri, and all azimuthal directions, except 80.5 degrees T and 138 degrees T, are initially over rough terrain (see **Figure 4**). Some of these radial paths pass through residential and urban areas. This results in a scatter in the field strengths measured. In **Figure 5**, I show the measured ND tower field strengths in the distance range 0.3 to 10 kilometers in all eight azimuthal directions (the data points on the graph), and the best logarithmic fit curve to these data. The computed field strengths, according to EZNEC/4D (see first **Footnote**), are represented by the curve through the open circles. The reference transmitter power is 1000 watts. The best fit curve to the measured data lies above and below the theoretical curve. Clearly, there is a considerable scatter in the measured data (filled in circles), and there is a consistent departure with increase in distance between the best fit measured and calculated curves.

Figure 6 shows a similar plot, but here the data points are for only two azimuthal direc-

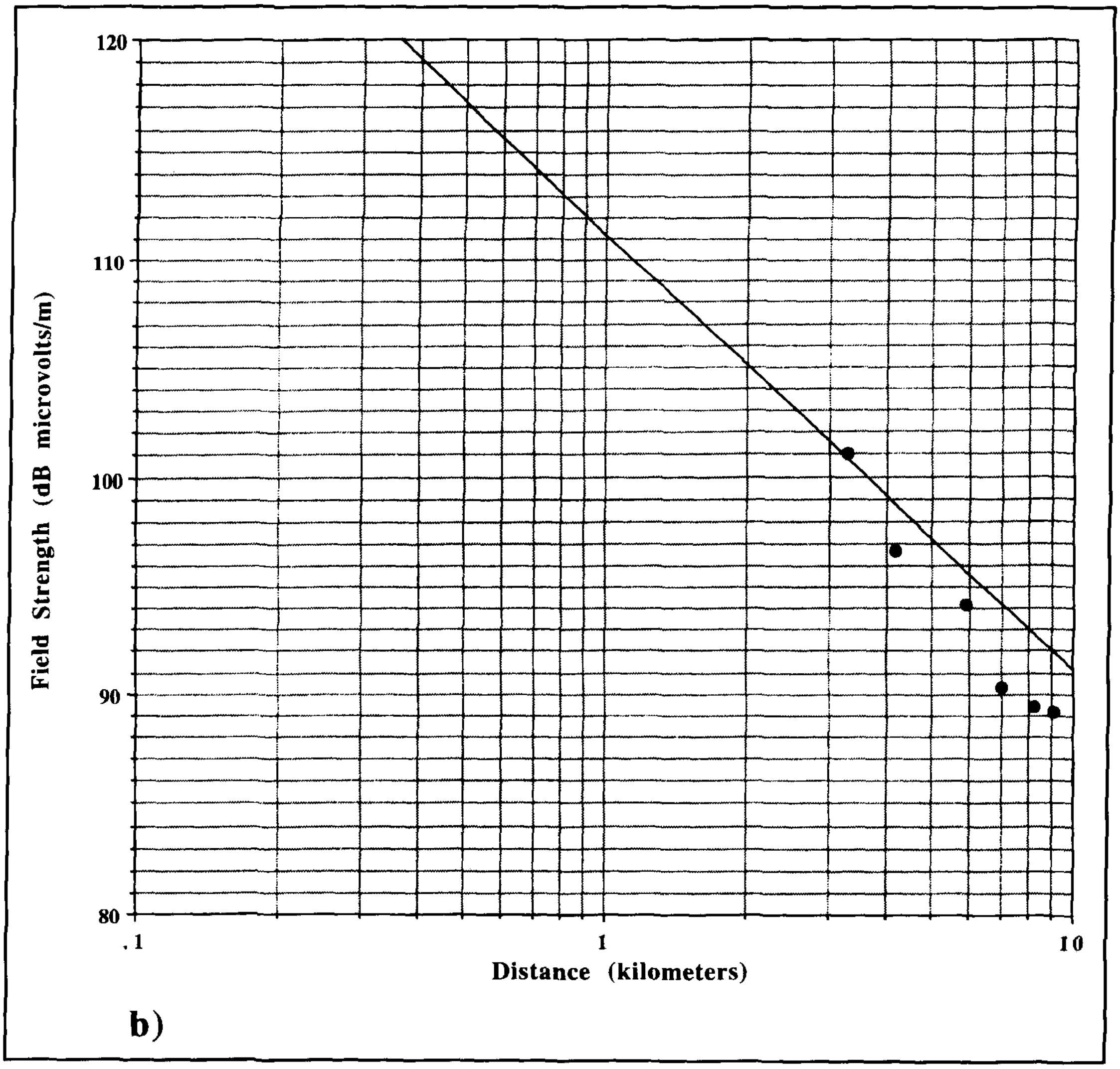

Figure 7B. Measured directional gain field strengths versus distance and theoretical curve (the continuous line) for the array (Figure 3's antenna) for this same azimuth.

tions, 80.5 degrees T and 138 degrees T—the only two paths that lie over rural fairly open and level land (see **Figure 4**). The computed curve (the continuous line) has been calculated for average land ($\sigma = 5$ mS/m, $\varepsilon = 13$), a conductivity that is consistent with the measurements. I have not fitted a curve to the measured data. Notice that the measured data points cluster quite well about the theoretical curve. I conclude that indeed NEC-4D accurately predicts the ground wave field strength.

Now look at measured field strengths in the azimuthal direction corresponding to that of the main beam (249 degrees T) for the directional array. **Figure 7A** gives the results for the ND tower in this direction. Again, the continuous curve is the theoretical curve, and the filled-in circles are the measured data. Notice the sudden break in agreement between measured and predicted field strengths in the distance range of 4 to 10 kilometers. This is considered to be due to the rough terrain over which the wave passes to reach the various measurement locations.

In **Figure 7B**, I compare the theoretical field strength curve for the directional pattern (the continuous line) with the measured data (the filled in circle data points). Again notice that the data points in the range 4 to 10 kilometers lie below the theoretical curve. In fact, the only data point that lies on the theoretical curve is that measured at 3.3 kilometers, which fortunately is a location where the field strength for the ND tower is very close to the theoretical curve (see **Figure 7A**).

You may not consider this a very satisfactory agreement between measurement and numerical modeling. But you can compare measurement with theory in another way. The array gain, gain over the ND tower, can be quite accurately determined from the ratio of mea-

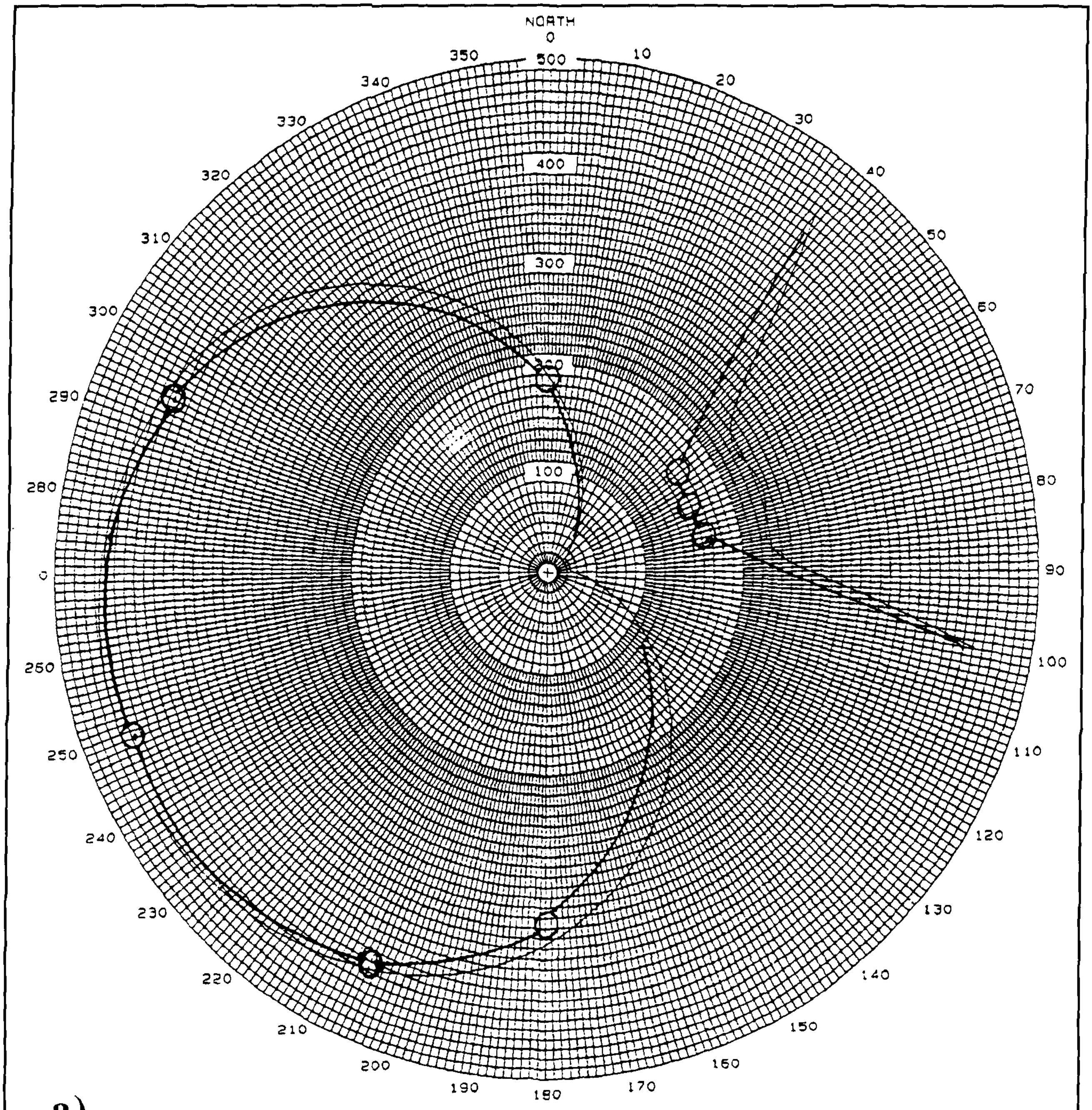

a)

Figure 8A. Measured and predicted horizontal plane patterns (standard pattern based on a simple analysis, which also assumes a PEC perfectly electrical conducting ground) for KGGN, after Glinter.[9] *The scale is mV/m referenced to the unattenuated ground wave field strength at 1 kilometer for a transmitter power of 960 watts.* Detail in the null direction is plotted on a x10 scale.

sured field strengths (since ND and directional field strengths were measured at the same locations) in the distance range 3 to 12 kilometers (nine values). The median value for the measured array gain is 3.83 dB. The predicted array gain, ratio of unattenuated field strengths at 1 kilometer (array versus ND tower), is 3.71 dB (difference -0.12 dB). You can also compare the front/back, predicted versus measured (**Figure 8**), 28.9 dB compared with 28.8 dB.

In conclusion, the measurements show the difficulty in determining accurate field strengths for comparison with numerical modeling (modeling assumes a flat smooth earth). Fortunately sufficient detail was given in the station's proof of performance to sort the data and establish that indeed there is very good agreement between measured and predicted field strengths.

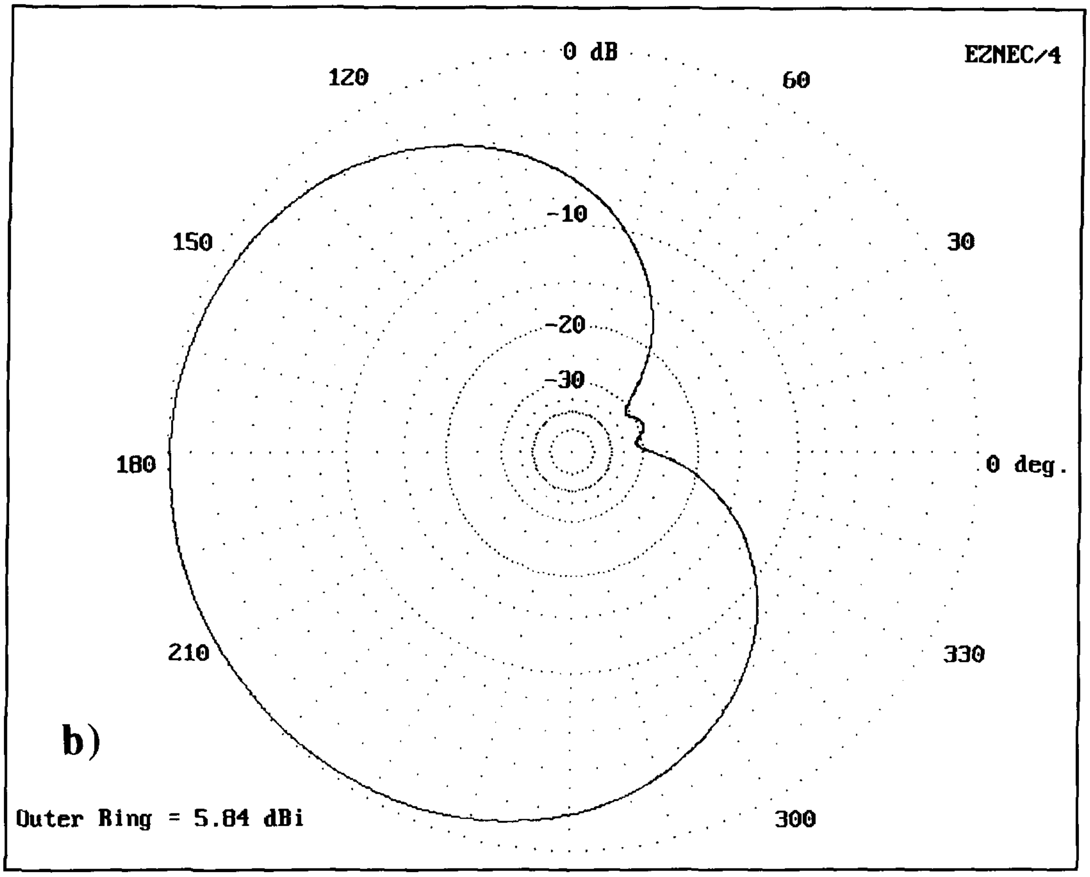

Figure 8B. Ground wave pattern (dBi) according to NEC-4D for qualitative comparison (distance 1 kilometer, height 1.5 meters).

A consideration of elements for directive arrays

I will now discuss antenna systems that might have a more practical interest for the radio amateur. In our discussion thus far, I have considered monopole GP-type antennas with four elevated horizontal resonant radials (excepting for the case study above), as shown in **Figure 9A**. But for the radio amateur, a monopole with drooping radials (**Figure 9B**) or a GP-type half-diamond loop (**Figure 9C**) could be used as an element for a directive array. Because I am concerned here with phased arrays to provide directivity in a particular direction, it would be useful if the elements of the array themselves had an intrinsic self-directivity in the desired direction. This can be realized if only one radial is used, pointing in the desired direction. Refer to the antenna arrangements shown in **Figures 9D**, **E**, and **F**.

Figure 10 shows the (spacewave) elevation patterns for each of the antennas shown in **Figure 9D**, E, and **F**. For this comparison, the antenna is resonant, the frequency is 3.75 MHz, and the radials are resonant at a height of 2.5 meters (a practical height because the radials are above head height). For the monopole with the drooping radial, the end height is more practically 1 meter. Average ground is assumed. As past experience indicates, the GP-type half-diamond loop is the antenna having the greatest gain. This is followed closely by the monopole with one drooping radial (this element is derived from a monopole with four drooping radials, in which case it behaves somewhat like a $\lambda/2$ radiator), and the $\lambda/4$ monopole with one horizontal radial has the least gain. But all antennas have a similar directive pattern.

All of these antennas, when dimensioned for the 80-meter band, are somewhat impractical for most amateurs; I am concerned here with the fundamentals of antenna performance. The $\lambda/4$ monopole with one horizontal radial is the most practical because it can be shortened (keeping the radial resonant), as is commonly the case for monopole elements used in MF broadcast arrays. A disadvantage when a shortened radiator is used is that the elements in the phased array have to be tuned and matched, as well as phased and power combined. But even when one uses antennas which are self-reso-

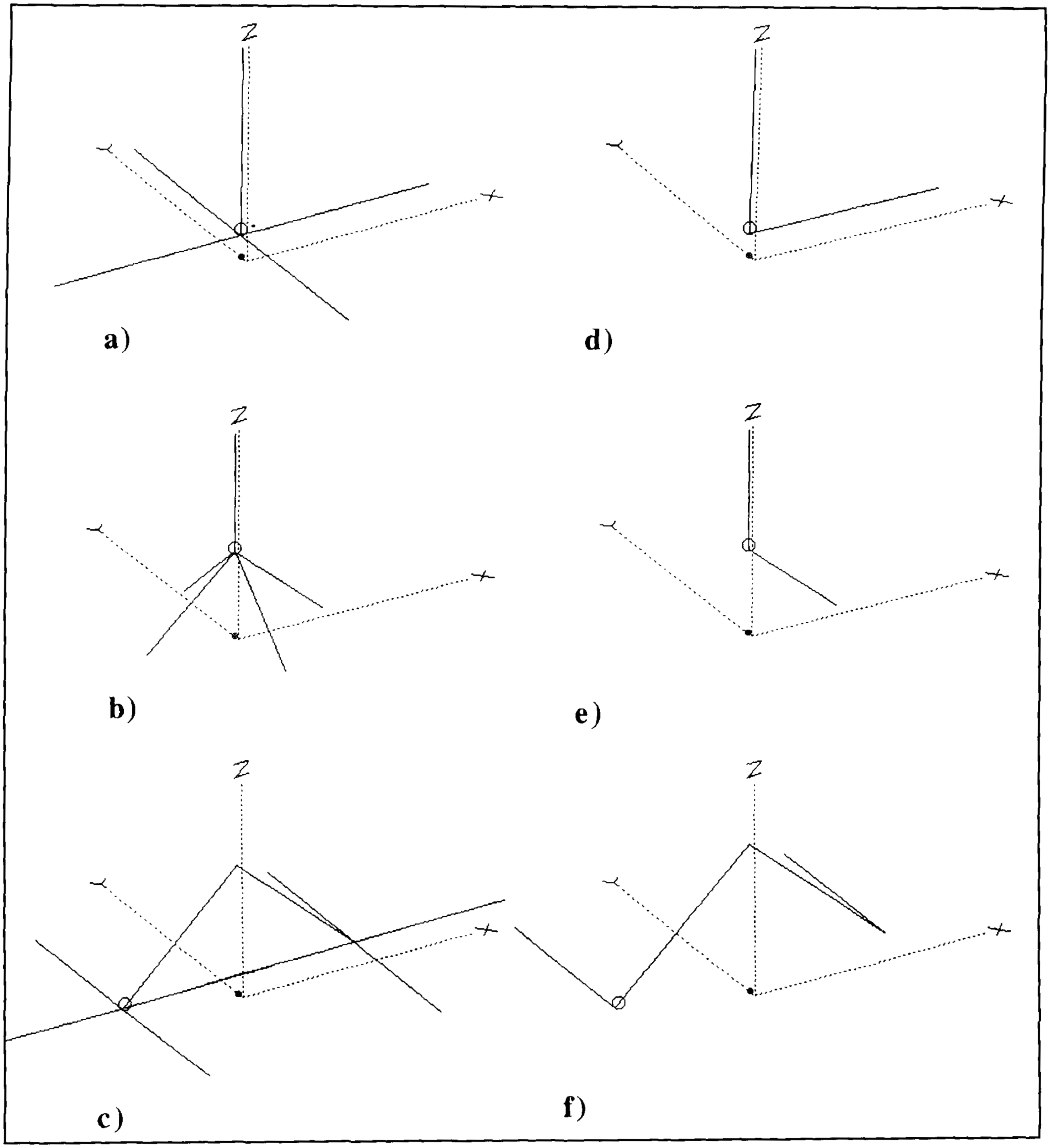

Figure 9. (A) A monopole with for elevated horizontal radials; (B) monopole with four drooping radials; (C) GP-type half-diamond-loop with three elevated radials (and as well as a wire which joins the fed end of the loop to the far end); (D) monopole with one horizontal radial (E) monopole with one drooping radial; and (F) GP-type half-diamond-loop with two horizontal radials.

nant, the elements of the array must be tuned, matched, and phased—at least for MF broadcast applications.

Some example directive systems

Next, I will describe three types of directional antenna arrays: two using monopoles and one using GP-type half-diamond loops. Although these antennas do not represent any particular installation that I put up and used operationally, they are technically correct and could be implemented by the interested reader. A two-element half-delta loop array has been experimentally modeled,[10] and my colleagues and I have successfully used a version of it

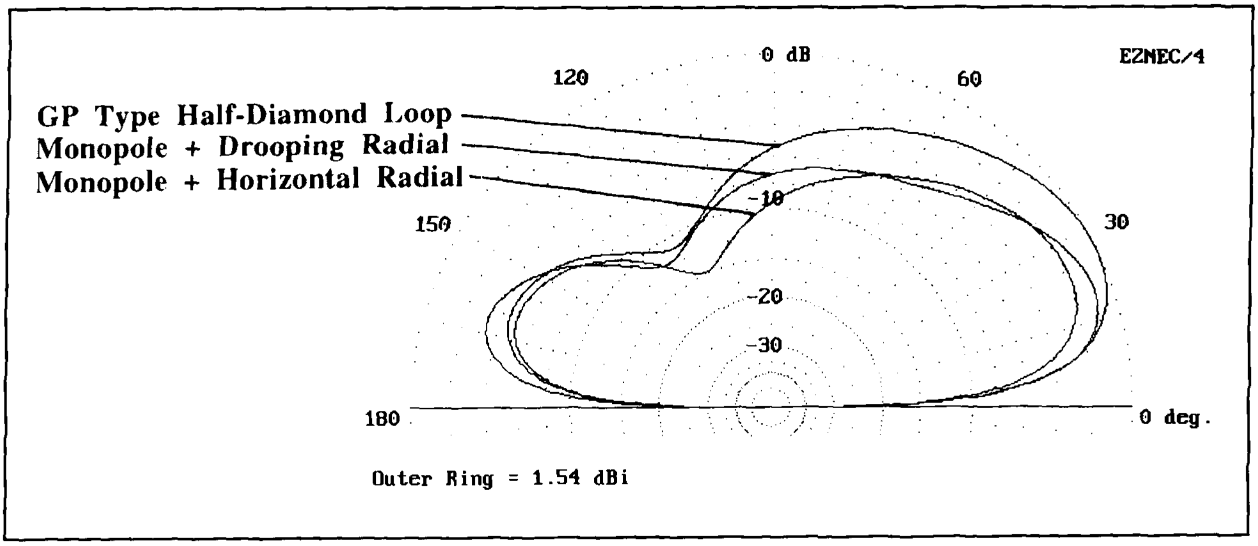

Figure 10. Elevation patterns (spacewave) for the antennas shown in Figures 9D, E, and F.

dimensioned for the 40-meter band for field day. This antenna system is very practical for this band.

Cardiod pattern directional arrays

A cardiod pattern is realized by using two or three in-line antennas, where the phase of the currents feeding adjacent elements or antennas differ by 90 degrees. **Figure 11A** is a sketch for a three-element directional array. The monopole elements are $\lambda/4$ resonant, and the radial length for a frequency of 3.75 MHz, radial height 2.5 meters over average ground is 19.2 meters. Note: the antenna elements do not touch—the monopoles are spaced 20 meters apart, and the length of the radials is 19.2 meters. Numbering the antenna elements 1, 2, and 3, from left to right, the currents for the three-element array are: 0.5<90 degrees amperes, 1.0<0 degree amperes, and 0.5<-90 degree amperes, respectively. Changing the amplitude and phase of the currents in antennas 1 and 3 changes the detail in the null of the pattern. For the two-element array, both antennas are fed with equal amplitude currents, but the phases differ by 90 degrees (1.0<90 degree amperes for the example here).

The principle plane patterns for the one, two, and three-element antenna arrays are shown in **Figures 11B** and **C**.

Unidirectional broadside monopole arrays

A unidirectional broadside antenna array is realized by using two or three in-line antennas—monopoles with one horizontal radial, where the phase and amplitude of the currents feeding adjacent elements are identical. **Figure 12A** is a sketch for a three-element unidirectional array. The monopole elements are $\lambda/4$ resonant, and the radial length for a frequency of 3.75 MHz, radial height 2.5 meters over average ground is 19.2 meters.

The principle patterns for the one, two, and three-element antenna arrays are shown in **Figures 12B** and **C**.

This antenna system would be much easier to adjust than the one described above. It makes a neat bidirectional antenna system because, to reverse the direction of the maximum gain, one would simply switch by relays to radials pointing in the opposite direction. There would be no change in matching or phasing.

Unidirectional broadside GP-type half-diamond loop array

I am a GP-type half-loop enthusiast.[11] They are much quieter (background noise levels are usually lower) compared with vertical monopoles, they are not subject to precipitation static, and wire loops are easy to set up and adjust. A unidirectional broadside antenna array is realized by using two in-line loops, where the phase and amplitude of the currents feeding adjacent elements are identical. In fact this is easily achieved since both loops are fed at a common point.

In **Figure 13A**, I show a sketch for a two-loop directional array. For a frequency of 3.75 MHz, the side length for the loops according to NEC-4D is 21.23 meters, the radial lengths for a height 2.5 meters over average ground is 19.2 meters. The input impedance for a single two-loop array (for loops having this same dimension) is 60 - j17 ohms.

The principle plane patterns for the single-loop and the two-loop array are shown in **Figures 13B** and **C**.

This antenna system is the easiest of the three

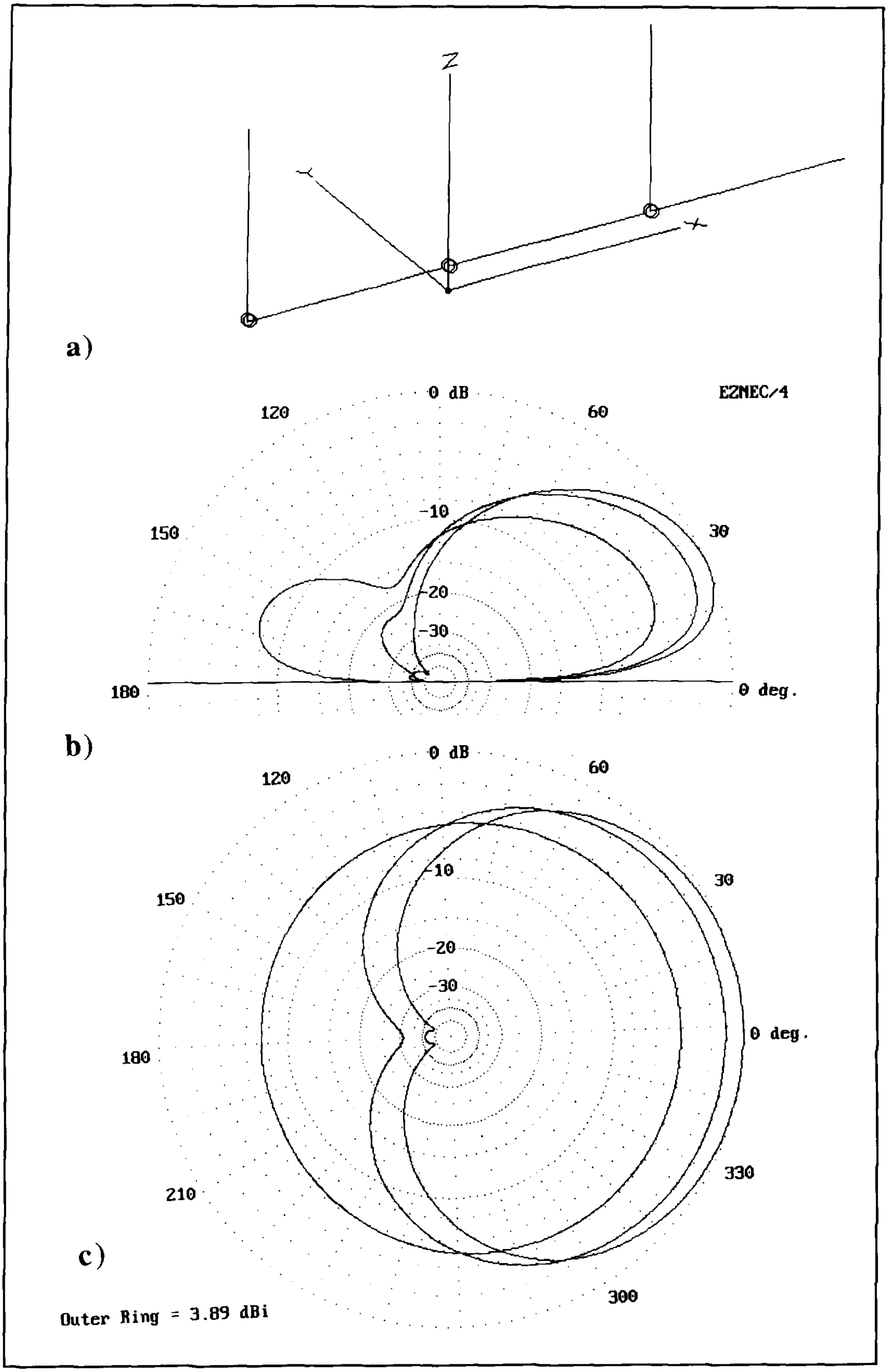

Figure 11. *(A) Sketch for a three-element directional array, where the monopole elements are fed to realize a cardiod pattern (see text); and, the principle plane elevation (B) and azimuthal (C) patterns for a one, two, and three-element array.*

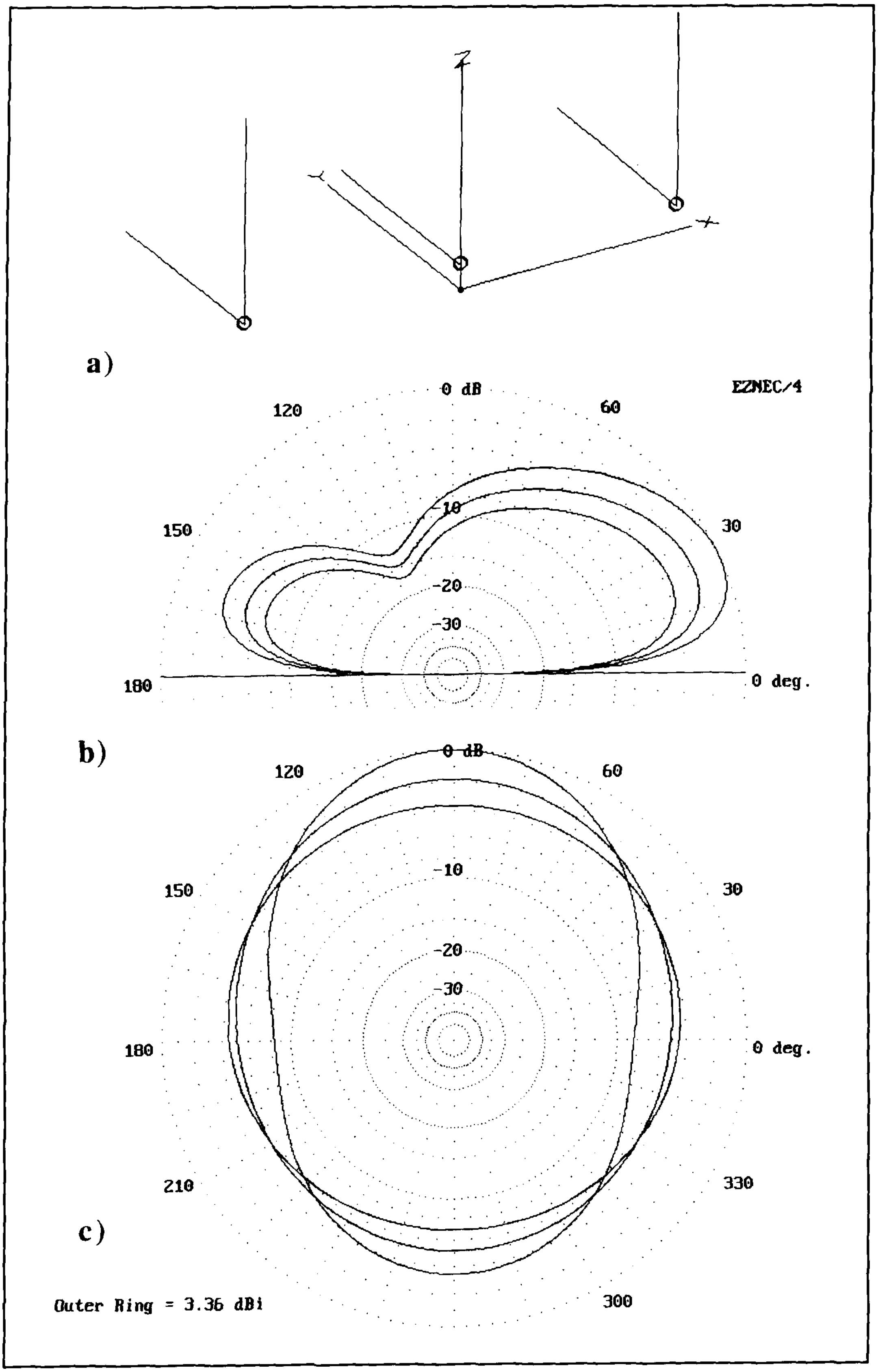

Figure 12. Sketch for a three-element directional array, where the monopole elements are fed to realize a unidirectional broadside pattern (see text); and the principle plane elevation (B) and azimuthal (C) patterns for a one, two, and three-element.

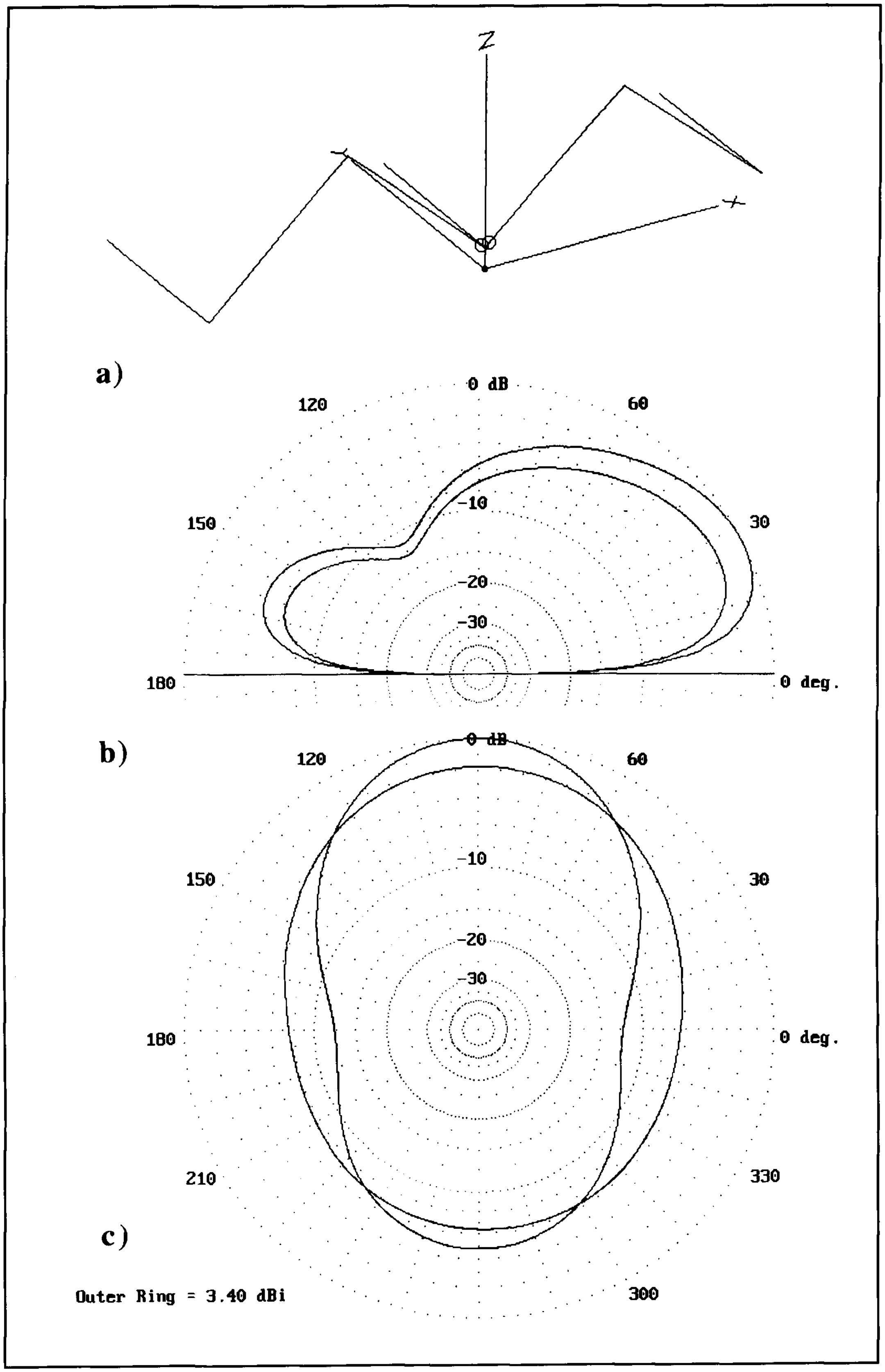

Figure 13. (A) Sketch for a two-element directional array, where the half-diamond-loop elements are fed to realize a unidirectional broadside array (see text); and the principle plane elevation (B) and azimuthal (C) patterns for a one and two-element array.

described to set up and adjust. Both loops are fed at a common point. It makes a good bidirectional antenna system because, to reverse the direction for the maximum gain, one would simply switch by relays to radials pointing in the opposite direction.

Concluding remarks

Phased arrays are, in general, not simple antennas to accurately set up and use. This is particularly true if one wants to reverse the azimuthal direction of maximum gain. They also present difficulties for amateur deployment because antenna systems are used for a band of frequencies. Most amateurs who use phased directive arrays pay no attention to tuning and matching the individual elements in the array. They simply use coaxial cables of differing lengths to provide a phase shift. The ideal patterns shown here would, therefore, seldom be realized in practice. I have not given details on antenna impedance for the monopole antenna arrays since towers or wires (tree-supported) could be used for the monopole elements and typically the monopoles would not be resonant. But the radials need to be resonant. Dimensions for the loop antenna array are given, since loops are wire antennas.

The purpose of this article is to convince the reader that elevated radials are very practical, whether the antenna is a single element, or the element is a part of a phased array. And, the gains realized in practice can be almost the same as those achievable by using extensive multi-wire buried radial wire ground systems.

A disadvantage is that the field strengths between the radial wires can be rather large, particularly in the vicinity of the ends of the radials, when high powers are used (amateur stations use powers up to 1000 watts, but MF broadcasters use powers up to 50,000 watts). EZNEC pro (whether one uses the NEC-2 or NEC-4 engine) can be used to estimate these fields. But this is a subject for a paper in itself concerned with near fields. A paper discussing the whole subject of elevated radials, giving new results of experiments yet to be done, is planned for publication in the *IEEE Antennas and Propagation Magazine*.

Acknowledgment

I am currently a radioscientist with the Radio Science Branch of the Communications Research Centre, Ottawa, ON K2H 8S2, and have access to their facilities. These facilities have sophisticated electronic instrumentation, computers, and plotters. I also have well-established channels for interaction with engineers in industry and the academic world, not normally available to the amateur in radio. ■

REFERENCES

1. J.S. Belrose, "Elevated Radial Wire Systems for Vertically Polarized Ground-Plane Type Antennas, Part 1: Monopoles," *Communications Quarterly*, Winter 1988, pages 29–40.
2. J.S. Belrose, "Ground-Plane Type Antennas with Elevated Radial Systems," *Conference Proceedings* for 12th Annual Review of Progress in Applied Computational Electromagnetics, Monterey, California, March 1996, pages 2–11 (paper presented in a special session for amateurs in radio).
3. C.M. Beverage, "New AM Broadcast Antenna Designs Having Field Validated Performance," paper presented at 49th Annual Broadcast Engineering Conference of the National Association of Broadcasters, Las Vegas, Nevada, April 13, 1995.
4. C.E. Smith, personal communications, 1996.
5. C.T. Rauch, personal communications, 1995.
6. C.T. Rauch; personal communications; 1996, 1997.
7. C.E. Smith, "Design and Operation of Directional Antennas," Smith Electronics, Inc., Cleveland, Ohio, 1969, pages 2.12-2.16.
8. J.S. Belrose, "Vertical Monopoles with Elevated Radials: An Update," IEEE Tenth International Conference on Antennas and Propagation, April 14–17, 1997, Conference Publication No. 436, pages 190–195.
9. M. Glinter, "Directional Antenna Proof of Performance," KGGN, Gladstone, Missouri, August 8, 1996 (a copy of the this report was sent to the author by C.M. Beverage, December 1997).
10. J.S. Belrose, "A Half Twin-Delta Loop Array," *QST* ("Technical Correspondence"), April 1983, pages 39–40.
11. J.S. Belrose, "Loops for 80-Meter DX," *QEX*, August 1996, pages 3–16.

PRODUCT INFORMATION

HP 1998 Test & Measurement Catalog Now Available

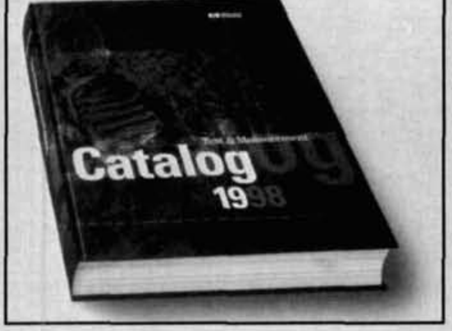

Hewlett-Packard Company has introduced the 1998 edition of its *Test & Measurement Catalog*. The publication includes descriptions of more than 1,400 HP test and measurement products, systems and services. The 640-page catalog is available free of charge by calling (800) 452-4844, ext. 5766, or can be ordered via the Internet at: <http://www.hp.com/go/tmc98>.

Douglas Page
608 Esplanade-7
Redondo Beach, California 90277-4174
<dougpage@ix.netcom.com>

SCIENCE IN THE NEWS

Gradium Glass and a solution to an old LED problem

Now Playing at the Multiplex Odeum: Communication at Light Speed, Starring WDM, Gradium Glass, and Soliton Propagation

The explosive growth of computer internetworking and the demands of multimedia, high-speed LANs, telemedicine, supercomputer-to-supercomputer interconnections, digital libraries, and virtual reality applications are driving data transfer requirements beyond the realm of Megabit/sec into the Gigabit/sec range and beyond.

Traditional networking techniques can't handle the traffic demands of emerging broadband communications. Over the past decade, multiwave optical networks have become the new backbone of the communications infrastructure. Using time division multiplexing (TDM) technology, carriers now routinely transfer data at 2.4 Gb/s (gigabits per second) on a single fiber. Some carriers deploy equipment that quadruples that rate to 10 Gb/s.

But even this technology, widely recognized for its capacity and flexibility, has struggled to keep pace with a demand that doubles every five weeks, according to WorldCom CEO John Sidgmore. Sidgmore predicts that by the year 2000 half the bandwidth use will be for the Internet, while half will be for voice calls. By 2003 or 2004, he says, the Internet will account for 99 percent of all bandwidth usage.

Vint Cerf, senior vice president of Internet technology at MCI and co-inventor of the TCP/IP—the language of Internet communication—says his fiber optic network is growing 400 percent a year. Cerf expects to need 80 to 160 Gb/s capability by the year 2000. He thinks major carriers like MCI could have 700 Gb/s technology three years after that, and Terabit/sec (one trillion bits per second) technology by about 2010.

Researchers are trying all sorts of things to gain more bandwidth, from increasing the data rate to wavelength division multiplexing (WDM). (It should be noted that capacity and bandwidth aren't the same thing. WDM technologies provide greater capacity by creating more "wires," not higher bandwidth by making faster ones.)

Wavelength Division Multiplexing

Wavelength Division Multiplexing technology is generally considered a key to satisfying the escalating bandwidth requirements of the Information Age. WDM devices serve as traffic cops, allowing a wide range of data, at varying speeds, to move simultaneously through an optical fiber network. An enormous amount of unused bandwidth (approximately 24 x 1012 Hz) exists in the low-attenuation communications bands (the 1.3- and 1.5-millimeter optical transmission bands) of a optical fiber. One fiber thread is capable of carrying more than 2,000 times as much information as all the current radio and microwave frequencies.

WDM allows the large bandwidth of the optical fiber to be more fully exploited. With WDM, optical fiber becomes more than a simple one-to-one replacement for copper wires. WDM divides the optical transmission spectrum into non-overlapping wavelength bands, or channels, where each channel may operate at

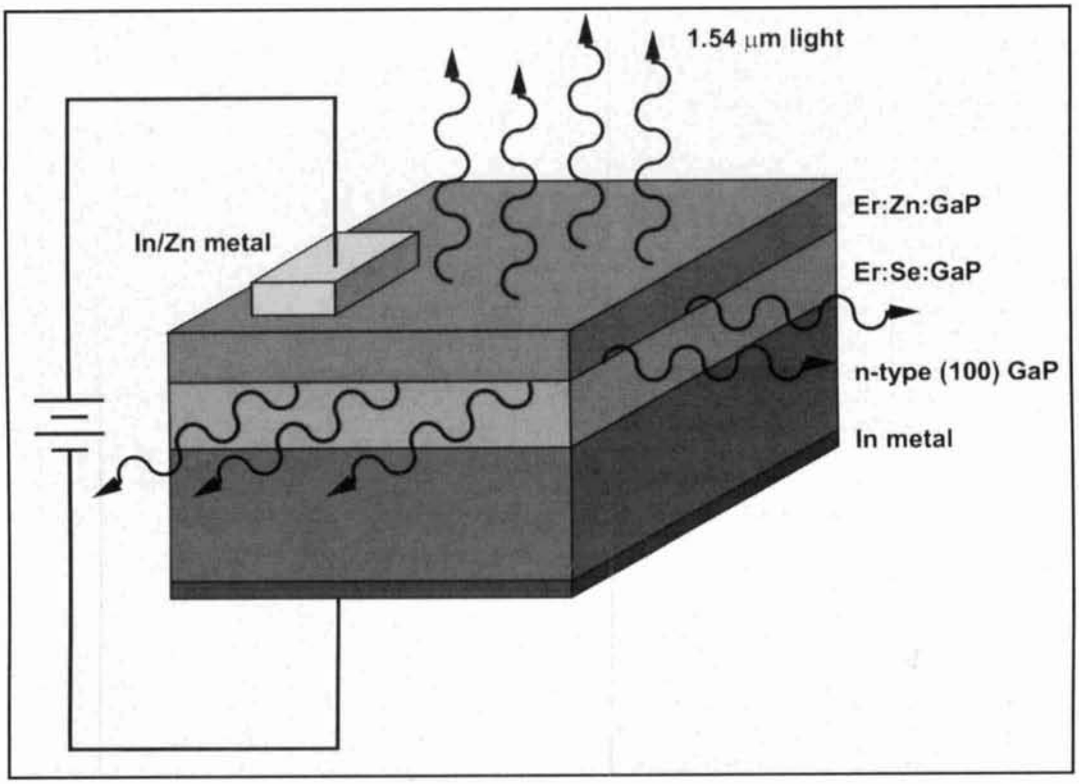

Figure 1. Diagram of the new light source developed at Northwestern University using the rare earth element erbium doped on gallium phosphide semiconductors, combining properties of gas lasers and semiconductor lasers on a single solid-state device. Note that light is emitted from both the top and sides of the device. The technology is expected to permit fabrication of cheaper, longer-lasting, more powerful LEDs. (Courtesy of Northwestern University.)

peak speed, allowing multi-Gb/s data rates. One example of an emerging WDM technology, called Dense Wavelength Division Multiplexing, multiplies the capacity of a single fiber sixteen fold, to a throughput of 40 Gb/s.

Once the electrical "bottleneck" is overcome (by removing electronics from the network the requirement for a complex central switch is eliminated), optically multiplexed WDM data travels at light speed over the fiber optic cable, supporting multi-Gb/s or even Tb/s data transfer.

Transmission capacity of signals via fiber optic links is virtually unlimited and can be achieved over huge distances. Optical erbium fiber amplifiers replace electronic switches by regenerating and amplifying the optical signal without conversion into electrical signals, then feeding the signal back into the fiber cable. In contrast to optoelectronic signal processing, which is less flexible and more complex and expensive, the new technology allows network operators to make more economical use of their fiber links. Still, many carriers are worried about where all the bandwidth will come from in next few years.

Gradium Glass

One new development from LightPath Technologies that may help is Gradium™ Glass, a high performance glass said to be capable of the work of multiple pieces of glass by virtue of its precise, internal light-bending characteristics. Fiber optic products rely on lens systems to harness light's various properties. According to physics, the perfect path for light to travel in most contemporary applications is curved, not straight. Science has sought for years for a means to produce optical conduits that have light bending power within the material. According to LightPath, Gradium Glass technology integrates more and more functions within a single lens element or optical component. It's so powerful a paradigm shift, the company believes the technology will have the same impact on the optics, optoelectronics, and photonics industries as the invention of the integrated circuit had on the electronics and computing industries.

Soliton propagation

In addition to high-speed lightwave systems, the concept of using optical nonlinear solitons as a transmission scheme is emerging as a solution to data communications concerns. Soliton propagation is a phenomenon observed in nonlinear systems whereby energy is propagated by solitary waves called solitons rather than by a continuous wave train. The effect can be used for efficient pulse transmission in optical fiber networks. According to Carolyn Davenport, a network engineer at Los Alamos National Laboratory's Computing, Information and Communications Division, solitons are very short time-division optical pulses that are not easily destroyed by small propagation inhomogeneities in fibers. Since pulse distortion due to dispersion does not occur, the time duration of a bit can be very short (100 to 200 fsec), so it's possible to achieve a very high transmission rate.

Revolutionary experiments at Bell Labs by L.F. Mollenauer and his group have demonstrated soliton WDM transmission at 80 Gb/s over transoceanic distances.

New Light Shed on Old LED Puzzle

Science has known for 30 years that a new light source should be possible by combining the properties of gas lasers and semiconductor lasers into a single solid-state device, using the advantages of both.

In 1963, Ronald Bell theorized that this could be done by combining rare earth elements into semiconductors. Exactly which rare earths was the tricky part. For decades, efforts have been made to find the right combination of rare earth element, semiconductor material, and manufacturing method to fabricate the stable, efficient light-emitting devices first proposed by Bell.

Researchers find formula

Researchers at Northwestern University found the formula. The Northwestern recipe calls for using the rare earth element erbium incorporated into gallium phosphide semiconductors and manufactured with metalorganic vapor phase epoxy. The product of this union is the first LED that works at room temperature.

"This is a new light source for telecommunications," said Bruce Wessels, professor of materials science and engineering at the Robert R. McCormick School of Engineering and Applied Science at Northwestern University. "It is potentially more efficient than the diodes currently in use."

The new diodes are being developed for optical communications, optical computing, and integrated optics. "They should be cheaper to fabricate, longer lasting and more powerful," said Wessels. "They have the potential for becoming very low threshold lasers."

The findings were announced in April 1997 in a paper presented at the annual meeting of the Materials Research Society in San Francisco by Northwestern graduate student Gregory Ford, Wessels' research assistant.

High color purity at precise energy levels

Because the light is generated only by the isolated erbium atoms incorporated into the semiconductor, the devices emit light of high color purity at a very precise energy level. They can be electrically excited, as in semiconductor lasers, but the extremely well-defined energies of the light make it possible to transmit information far more efficiently than with conventional semiconductors, according to the research team.

The advantage of gas lasers is the high spectral power of the laser light with a single energy. The advantage of semiconductor lasers is that they can be electrically pumped. The new device combines both of these advantages into a single unit.

Current research is now focusing on the possibility of low threshold lasers, improving the efficiency of the devices, and integrating them with silicon to make integrated optical circuits. "We would like to see if these devices can lase," said Wessels. "The low absorption of emitted photons by a rare earth doped semiconductor implies that the theoretical threshold for lasing could be quite low: orders of magnitude lower than commercial semiconductor lasers used today. A low threshold laser would have broad applications because of its potential low power requirements."

Rare earth doped semiconductors

Since Bell first proposed a DC pumped rare earth laser (in a 1963 issue of Physical Review Letters), there has been interest in rare earth doped semiconductors for use as LEDs, optical amplifiers, lasers, and other electro-optical devices. "Rare earth ions are exceptional because electron transitions between their unfilled 4f-shell states provide luminescence that is independent of temperature and host material. The hope was to unite these light emitting properties with the electronic pumping capabilities of the semiconductor," Wessels explained. The latest interest in the study of erbium doped semiconductors has been spurred on in part by the growth of the telecommunications market and the subsequent demand for cheaper lasers that can be monolithically incorporated into the processing chip design.

"Although there has been much success in using the rare earth neodymium in insulators to make laser devices, the dopant of choice for semiconductor doping has been erbium. The energy transition from the first excited 4f-shell state to the ground state is about 1.54 um, conveniently the low loss wavelength for silica optical fibers," Wessels said. ■

Robert R. Brown, *NM7M*
504 Channel View Drive
Anacortes, Washington 98221

SIGNAL DUCTING ON THE 160-METER BAND

Features of top-band propagation at times of high sunspot count and the summer solstice

Communication on the 160-meter band is largely controlled by ionospheric absorption. As a result, most long-distance contacts in the Northern Hemisphere are attempted during the winter months when paths of interest, perhaps across the polar cap to Europe from the West Coast or the Orient from the East Coast, are completely dark. But those efforts may be hampered by solar activity—the solar wind giving rise to auroral disturbances that disrupt propagation by increasing ionospheric absorption of signals. In addition, the ionization created by energetic electrons during auroral activity reaches *E*-region altitudes and

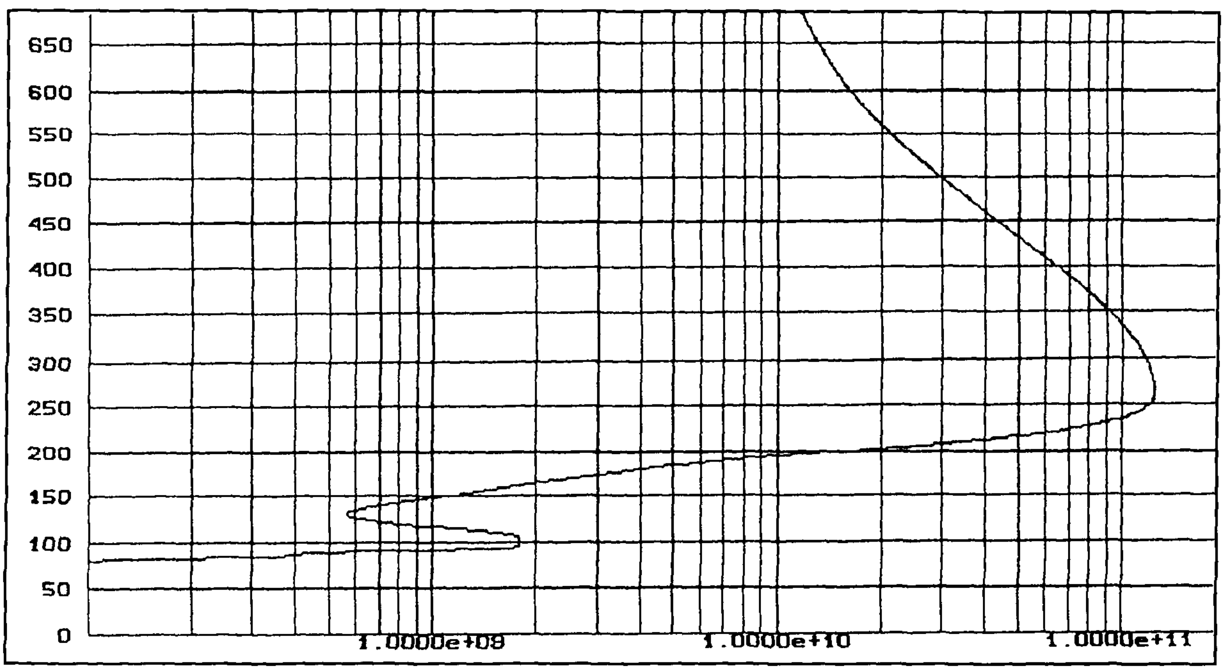

Figure 1. Example of the electron density valley above the nighttime *E*-region. Heights are in kilometers and electron densities in electrons per meter.

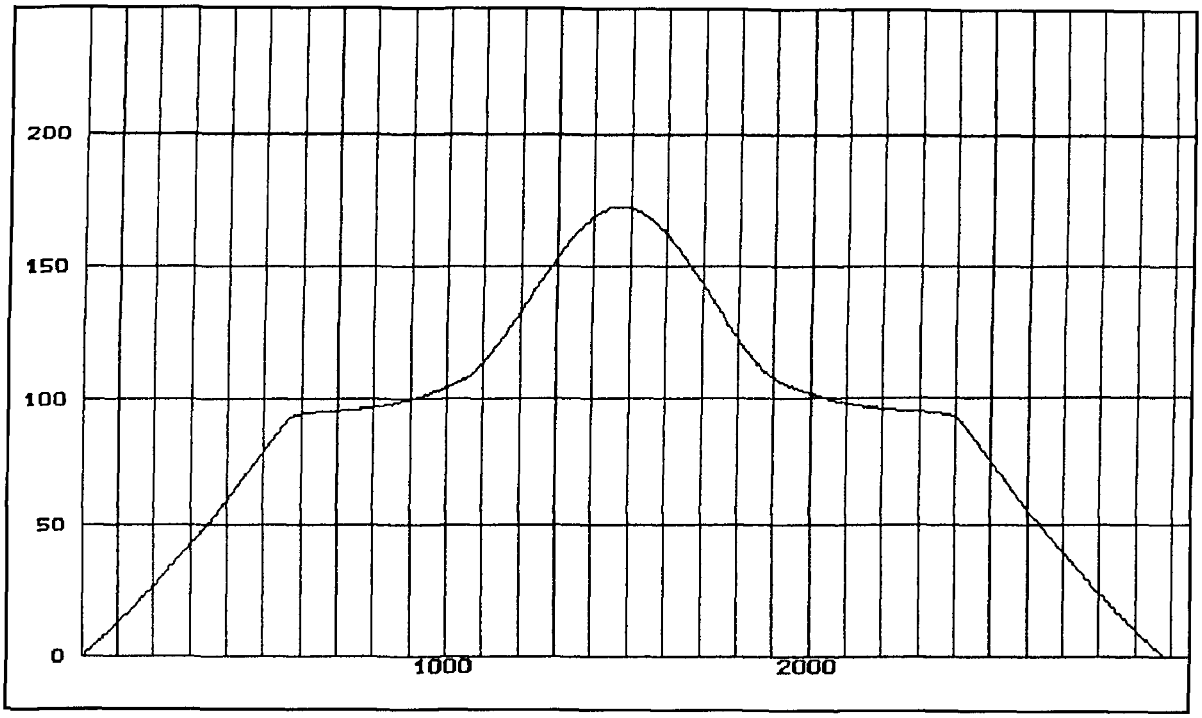

Figure 2. Long *EF* hop just before sunset on a path directed toward Heard Island from Boston. Heights and horizontal distances are in kilometers.

will increase signal absorption as well as skew signal paths in unpredictable ways. Thus, 160-meter communication across high latitudes is best attempted during winter at times of low solar and geomagnetic activity.

In striking contrast to those circumstances, there is quite a record of 160-meter contacts across low latitudes, particularly during the summer months and at times of high solar activity. Starting in 1990 when the smoothed sunspot number was around 145, the SEANCE (South East Australia North America Communications Exchange) Net was established by VK4YB, with operations from mid-May to mid-August, and it continues to the present. The features of the 160-meter openings between Australia and British Columbia in 1990–1991 have been reported in the literature.[1] They include the almost daily contacts with Australia before dawn and signals often noted for their remarkable strength.

This article examines the features of 160-meter propagation at times of high sunspot count and at the summer solstice, starting with a path like the one from Australia to Western North America. Then, for comparison, it ana-

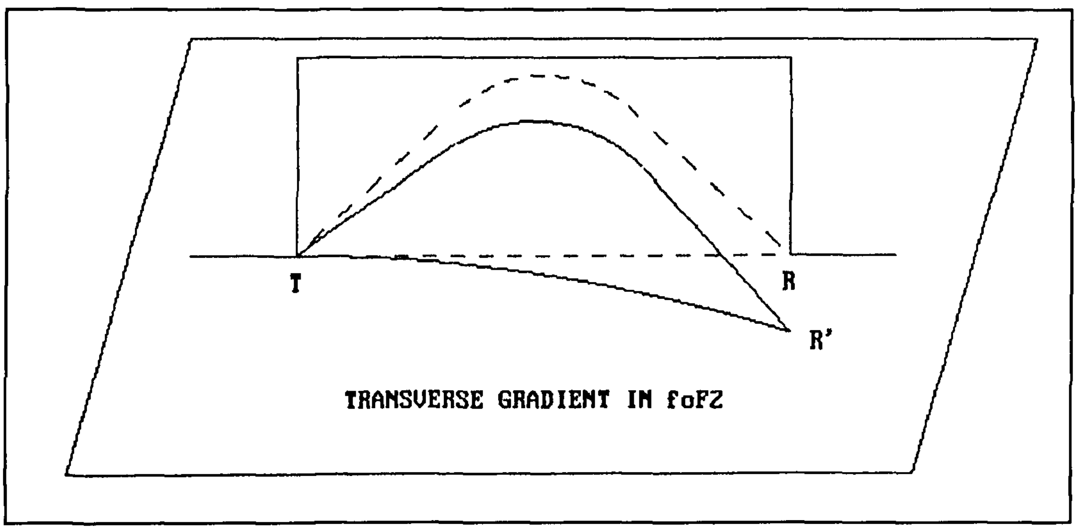

Figure 3. Schematic representation of HF path skewed by a transverse gradient in electron density.

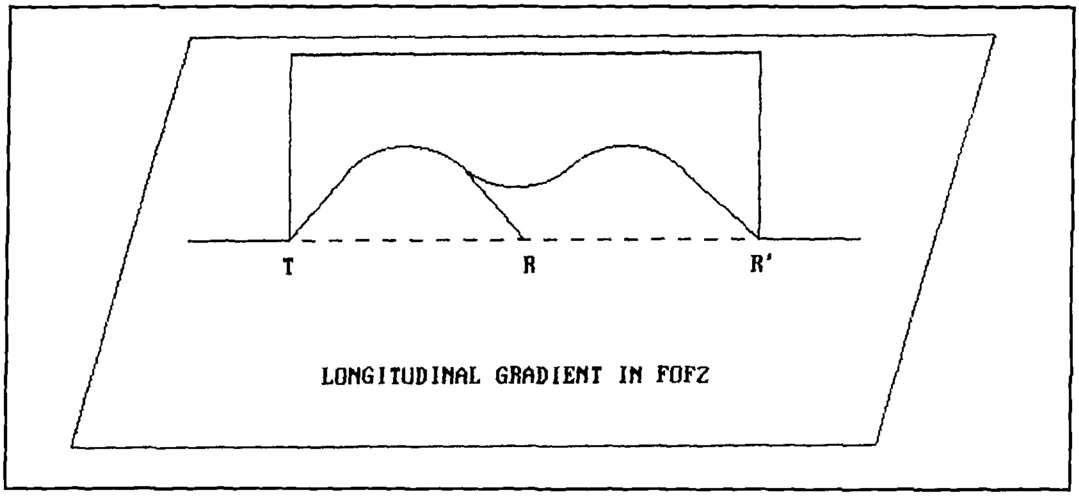

Figure 4. Schematic representation of ducting on an HF path due to a negative, longitudinal gradient in electron density.

lyzes other paths at other times of the year, as well as sunspot counts. In this study, propagation was reviewed particularly for examples of ionospheric ducting—signals which advance along a path while making many vertical excursions or oscillations in altitude but without any intermediate ground reflections.

The ducting type of propagation comes to mind as incoherent scatter radars have found that a deep electron density valley is present above the E-region at night.[2] This is a region where signal ducting may take place via reflections between the upper part of the E-region and the lower part of the F-region. A typical electron density profile showing the nighttime valley is given in **Figure 1**.

In regard to the possibility of the ducting of 160-meter signals, two-dimensional ray traces for nighttime paths showed that signals at low angles of incidence are refracted downward on short E-hops while, at high angles of incidence, the RF would go up into the F-region and then be refracted back to earth. However, from scanning across those angles, it was found[3] that there is a range of angles just above the angle of the Pedersen Ray for the E-region peak, where the E-region can refract signals at small angles to the earth's surface for great distances before they go up to the F-region and then are refracted toward earth. Such a circumstance is shown in **Figure 2**, which is taken from a ray trace for 160-meter signals from Boston which were directed toward Heard Island during the time of the recent DXpedition. In that study, it was suggested that type of refraction could be the basis of signal ducting if signal refraction were weaker or the elevation angle of a downgoing ray were sufficiently reduced by some means, perhaps from the effect of ionospheric tilts along a path.

This article deals with three-dimensional ray-traces of 160-meter signals and reveals other means of ducting from the presence of the earth's magnetic field.

HF propagation

The concept of signal propagation over great distances with contact between ionospheric regions, but without any intermediate ground reflections, is not new. Indeed, it was suggested before World War II as a possible explanation for round-the-world echoes,[4] and after World War II in connection with long-path propagation in amateur radio.[5] In addition, a comprehensive theoretical discussion of long-distance propagation of HF signals, with emphasis on signal ducting and related to the "Woodpecker," a Russian OTH radar, was presented by Gurevich and Tsedilina.[6]

The work of Gurevich and Tsedilina used a "full-wave theory" formulation of Maxwell's Wave Equation, but also related those results to the more familiar formulation of signal propagation—geometrical optics. Their discussion, limited to the HF portion (3 to 30 MHz) of the spectrum, dealt primarily with the effects from horizontal inhomogeneities in electron density and lateral deviations of paths, as well as the ducting of signals. For a given path, inhomogeneities are better described as gradients, transverse or longitudinal, providing measures of the rate of the electron density variation with distance either perpendicular to the path direction or along the path.

The effect of a transverse gradient is illustrated in **Figure 3**, which shows a path displaced from the original great-circle direction. The effect of a longitudinal gradient is shown in **Figure 4**—a single hop being converted to a short duct. In regard to those figures, it is

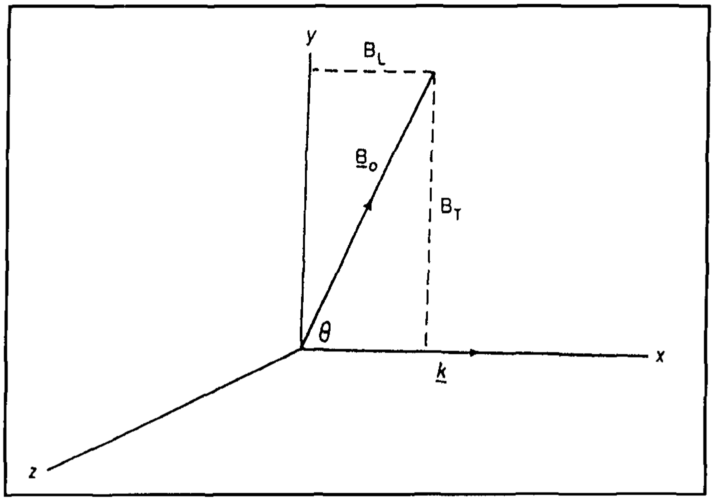

Figure 5. Coordinate system used in discussing magneto-ionic propagation. The x-axis is the direction of signal propagation; the y-axis lies in the plane of the x-axis and the direction of magnetic field B.

important to note that the effects depend on both the magnitude and direction of the gradients. For a non-great circle (NGC) path, the lateral deviation in the HF range is away from regions of higher ionization while longitudinal gradients may increase or decrease refraction, depending on whether the electron density increases or decreases along a path.

For the multi-hop situation in **Figure 4**, the electron density decreases along the path in going to the right of the figure, thus reducing refraction on the down-going leg of the first hop to the point that it never reaches ground. Instead, it continues upward for another refraction. By that token, if the electron density continued to decrease along the path at a comparable rate, some additional refractions of the same type could result, amounting to the ducting of the signal over a greater distance without any ground reflections.

Magneto-ionic considerations

The frequencies used on the 160-meter band, around 1.8 MHz, are close to the gyro-frequency of ionospheric electrons in the earth's field. As a result, the HF approach to signal propagation must be modified to include magneto-ionic effects,[7] which arise from ionospheric electron motions in the earth's magnetic field. Thus, the derivation for the index of refraction of the ionosphere used for HF problems—involving only the wave frequency and the electron density, or plasma frequency—at points in the ionosphere must be expanded to take into account not only the strength of the earth's field, but its direction and the direction of the waves being propagated relative to the field lines. After that is done, the geometrical optics methods for propagation studies may again be used to carry out ray traces through the ionosphere, now embedded in the earth's field. Of particular interest here is the possibility of finding ray traces that show signals ducted in the nighttime electron density valley above the *E*-region.

In that regard, magneto-ionic theory begins with equations describing the motions of ionos-

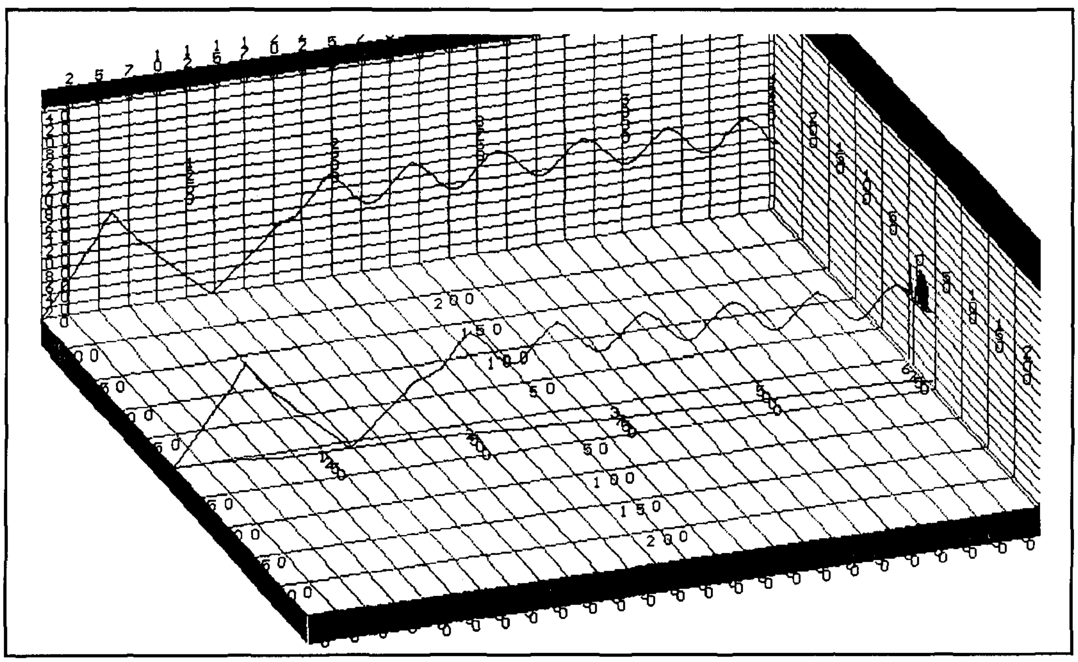

Figure 6. Example of the many ducted signals with radiation angles between 7 and 25 degrees. This 3-D ray trace shows an *F*-hop followed by ducting at 12.2 degrees from midway in the VK-VE7 path toward B.C. The path has been skewed by about 30 kilometers or 0.4 degrees in direction by magneto-ionic effects over 6,250 kilometers.

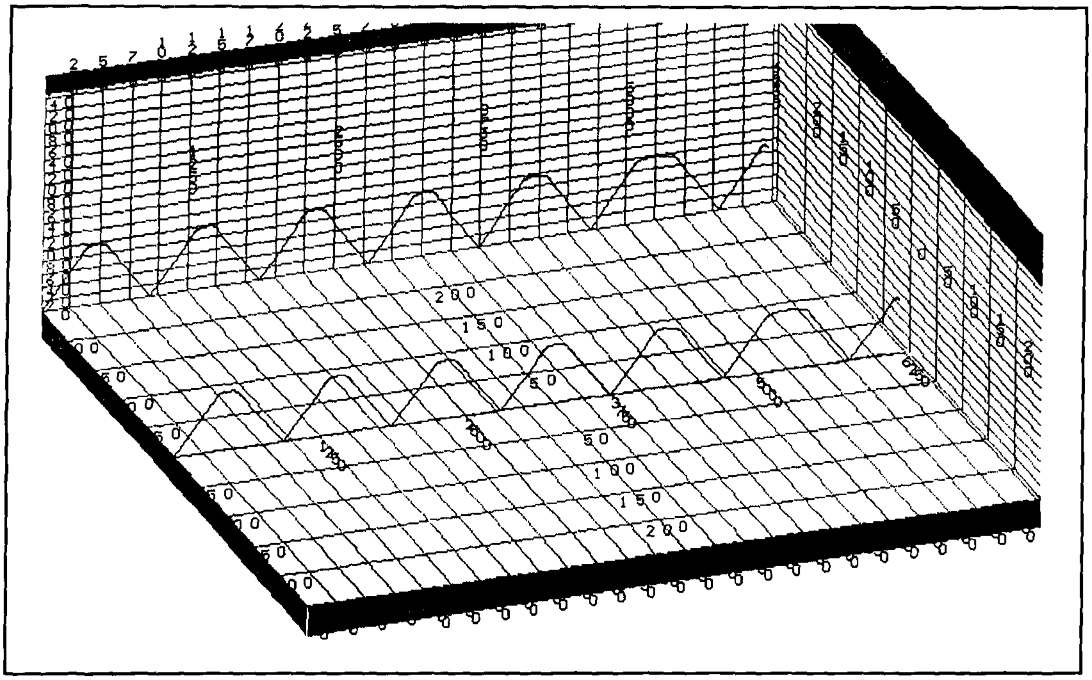

Figure 7. The "no-field" 3-D ray trace for the same circumstances in Figure 6, now showing *E*-hops that peak near the limit for Pedersen Rays. Note the absence of skewing.

pheric electrons exposed to the influence of a passing wave. While both electric and magnetic fields are associated with an electromagnetic wave, ionospheric electrons are influenced primarily by the wave's electric field. That is the case as the force an ionospheric electron experiences from the wave's magnetic field is a factor of (v/c) smaller than the electric force, where v is the electron's mean speed (1E+7 cm/sec) and c is the velocity of light (3E+10 cm/sec). The earth's magnetic field is much larger than that of a passing wave, so it must be included when considering how an electron's motions are affected by the E-field of a wave.

When the equations of motion for ionospheric electrons are solved, using components of the E-field of the incident waves as well as components of the geomagnetic field, it is found there are two characteristic wave motions that are propagated in any region of the magneto-ionic medium—elliptically polarized waves with their major axes inclined 90 degrees to each other and having opposite rotations of their electric field vectors. The two waves are termed "ordinary" and "extraordinary" waves because of their properties when compared to wave behavior in the absence of a magnetic field or when field effects are negligible, say at the top of the HF spectrum.

For the special case where waves are propagated perpendicular to the magnetic field direction, the two elliptically polarized waves go over to linearly polarized waves at right angles to each other. For the other case, when the waves are propagated along the magnetic field direction, circularly polarized waves result and have opposite senses of rotation for the electric field. In that regard, the sense of rotations are easy to describe: if one's thumb points in the direction of the magnetic field, the rotation of ordinary E-field vectors is given by the fingers of the left hand and that of the extraordinary wave is given by the fingers of the right hand. Note that ionospheric electrons, being negatively charged, gyrate around the magnetic field in the same sense as an E-field vector rotates for extraordinary waves.

Details of the wave polarization depend not only on the direction of propagation relative to the magnetic field, but also the field strength B, the electron density, and the collision frequency of electrons with atmospheric constituents. Those same quantities determine how the waves are refracted and the index of refraction of the magneto-ionic medium is different for each of the two characteristic waves. The same is true of the polarization and absorption coefficient for the waves.

In considering wave propagation, the physical quantities which typify the medium are better expressed as frequencies and compared with that of the electromagnetic wave. In doing that, the wave frequency f in MHz is written as an angular frequency:

$$\varpi = 2\pi f \qquad (1)$$

Using that, the variable Y compares the angular frequency of electron gyration about

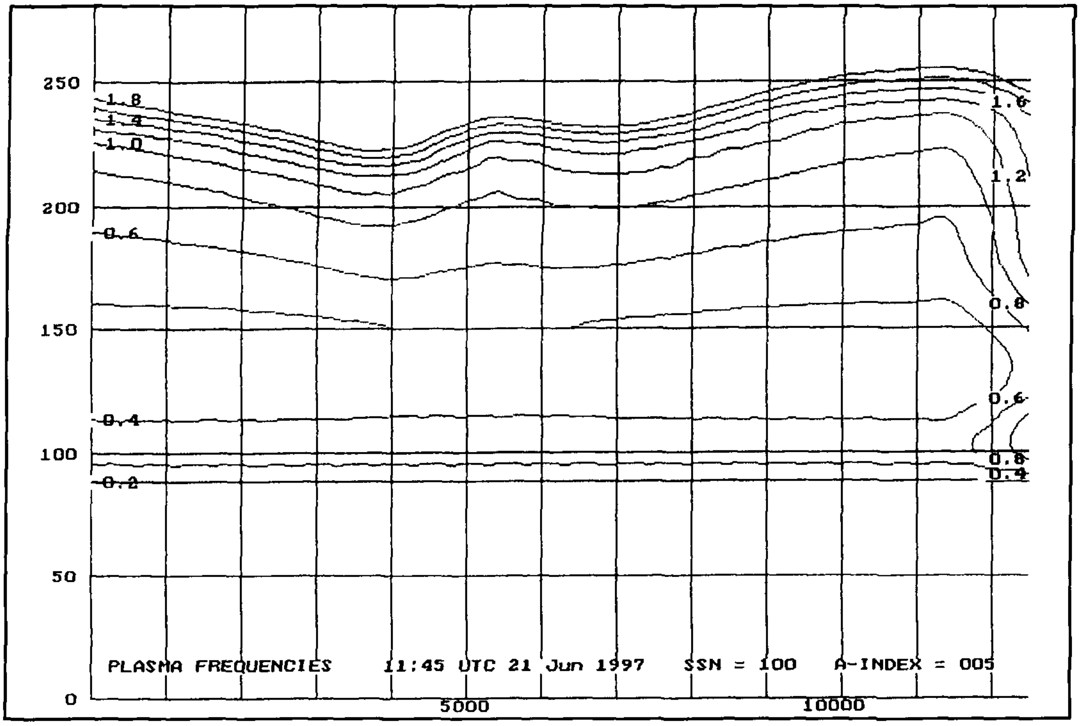

Figure 8. Transverse plasma frequency map for path from Australia (left) to B.C. (right) for 1145 UTC at the summer solstice when the sunspot number is 100. Plasma frequencies are in MHz and contours in 0.2 MHz intervals.

the magnetic field to the angular frequency of the wave:

$$Y = \frac{\varpi_B}{\varpi} \qquad \textbf{(2)}$$

where

$$\varpi_B = e\frac{B}{m} \qquad \textbf{(3)}$$

in radians per second, where e is the electron charge, m its mass, and B the magnetic field, all in M.K.S. units.

The variable X compares the square of the plasma frequency of the ionospheric electrons to the square of the frequency of the wave:

$$X = \left(\frac{f_N}{f}\right)^2 \qquad \textbf{(4)}$$

and variable Z compares the collision frequency of ionospheric electrons with nearby constituents with the angular frequency of the wave:

$$Z = \frac{\upsilon}{\varpi} \qquad (5)$$

The last variable required to discuss propagation is the angle the wave makes with the field direction. For that, a set of coordinate axes are needed, as shown in **Figure 5**, where the x-axis is in the direction of propagation and the coordinate system is oriented so the y-axis lies in the plane determined by the propagation direction and that of the magnetic field. That axis system corresponds to the one used by Davies.[8]

With those variables—X, Y, and Z—as well as the angle θ between the direction of propagation and the field, an expression for the index of refraction[7] can be developed and used to determine how the RF wave is refracted as well as absorbed by the medium. And by using extreme values for X, Y, and Z, various circumstances may be illustrated. Thus, the case when Y=0 corresponds to the absence of a magnetic field, Z<<1 is the case when electron-neutral collisions and losses are quite negligible and, finally, X<<1 is the case for highest frequencies in the RF spectrum.

While magneto-ionic theory is quite complex, there are certain approximations that can be made to simplify matters, essentially indicating when situations can be treated in a manner similar to the two limiting circumstances which were cited above—propagation perpendicular to the magnetic field direction or along it. Thus, when the collision frequency is very small compared to the RF frequency, Z<<1, as in the *E*-region and defining two quantities in terms of Y and θ,

$$Y_t = Y\sin(\theta) \qquad Y_l = Y\cos(\theta) \qquad \textbf{(6)}$$

the quasi-transverse and quasi-longitudinal approximations of the various quantities in magneto-ionic theory, say for the index of refraction and polarization, can be obtained by considering cases when

$$(Y_t)^4 \gg 4(1-X)^2 (Y_l)^2 \qquad [\text{QT}] \qquad \textbf{(7)}$$

and

$$(Y_t)4 \ll (1 - X)^2 (Y_l)^2 \qquad [\text{QL}] \qquad \textbf{(8)}$$

Perhaps for mathematical convenience, Ratcliffe[7] considers that the QT approximation applies if the ratio of the quantity on the left side of those inequalities is greater than the one on right side by a factor of 9 or more, and the QL approximation applies if the ratio is less than 1/9. In that regard, the ratio of the transverse quantity on the left to the longitudinal quantity on the right is termed QT/QL and will be used in the discussion which follows, noting whether QT/QL is greater than 9 or not.

Of course, there are still the two characteristic waves to be considered in each approximation. For the quasi-transverse case, the ellipses for the two polarizations are long and narrow, not too much different from the linearly polarized case. In a similar fashion, the ellipses for the quasi-longitudinal case are short and wide, not too much different from the circularly polarized case.

Those two quantities, Yt and Yl, involve the gyro-frequency of ionospheric electrons and, thus, some sort of model for the earth's field. The simplest model to use is a centered dipole with the magnetic axis tilted about 10.7 degrees with the earth's geographic axis. In that approximation, the magnetic north pole is located at 79.31 degrees N latitude and 71.67 degrees W longitude, and the present strength of the field gives a gyro-frequency of about 0.87 MHz near the equator and 1.4 MHz at midlatitudes in the Northern Hemisphere.

In magneto-ionic theory, the usual expression for ionospheric absorption in dB per kilometer of path[8] must be modified to include the effect of electron gyrations around the field. That means the angular frequency of RF waves in the denominator of the absorption equation is replaced by

$$\varpi \pm \varpi_B \cos(\theta) \qquad \textbf{(9)}$$

where the positive sign applies to the ordinary mode and the negative sign to the extraordinary mode. So, for RF frequencies differing from electron's gyro-magnetic frequency by a few hundred kHz, the extraordinary wave in magneto-ionic theory is regarded as heavily absorbed compared to the ordinary mode and thus will not be considered here. This leaves only the ordinary wave in the discussion of signals on the 160-meter band.

The above paragraphs dealt with the formal, mathematical aspects of magneto-ionic theory. The application of those ideas to propagation begins with waves leaving an antenna and entering the ionosphere. There, the initial wave polarization formed by the antenna, say linearly polarized waves from a vertical antenna, gradually goes over to the characteristic waves which are supported in the ionospheric region, one form or another of elliptical polarization with both ordinary and extraordinary modes.

The waves are then refracted according to their frequency, the local electron density, and magnetic field strength as well as their direction of propagation with the field lines. The two modes will be absorbed to some extent as they advance through the ionosphere, the extraordinary wave suffering more absorption than the ordinary wave. When propagation ends and the waves leave the ionosphere, the final polarization of the waves reaching the receiver will depend on magneto-ionic conditions—X, Y, and Z—at the point where the waves descend toward ground as well as the angle of the down-going rays relative to the magnetic field at the base of the ionosphere. In general, that final polarization will not be exactly the same polarization as the original one from the transmitting antenna and, for that matter, it may not match that of the receiving antenna.

As the preceding discussion suggests, wave polarization is a very complicated subject and polarization will vary as signals are refracted along a path as well from path to path with the same transmitting antenna. Because wave polarization is not exactly part of the common lore of amateur radio, and the amateur antenna systems now in use are not large nor complex enough to identify the different polarizations or any changes, the present discussion will simply limit the use of magneto-ionic theory to matters related to ray refraction and signal strength—particularly the question of ionospheric ducting. That will be done by using a three-dimensional ray-tracing program based on magneto-ionic theory and looking at cases of oblique propagation in terms of the magneto-ionic variables discussed above. Even with that limitation, results of the study are both informative and interesting.

Ray tracing

The PropLab Pro program[9] was used to examine the possibility of signal ducting on the 160-meter band. This program is based on the three-dimensional ray-tracing model developed in the late '60s and early '70s[10,11] in the laboratory of the Environmental Science Services Administration (ESSA) in Boulder, Colorado.

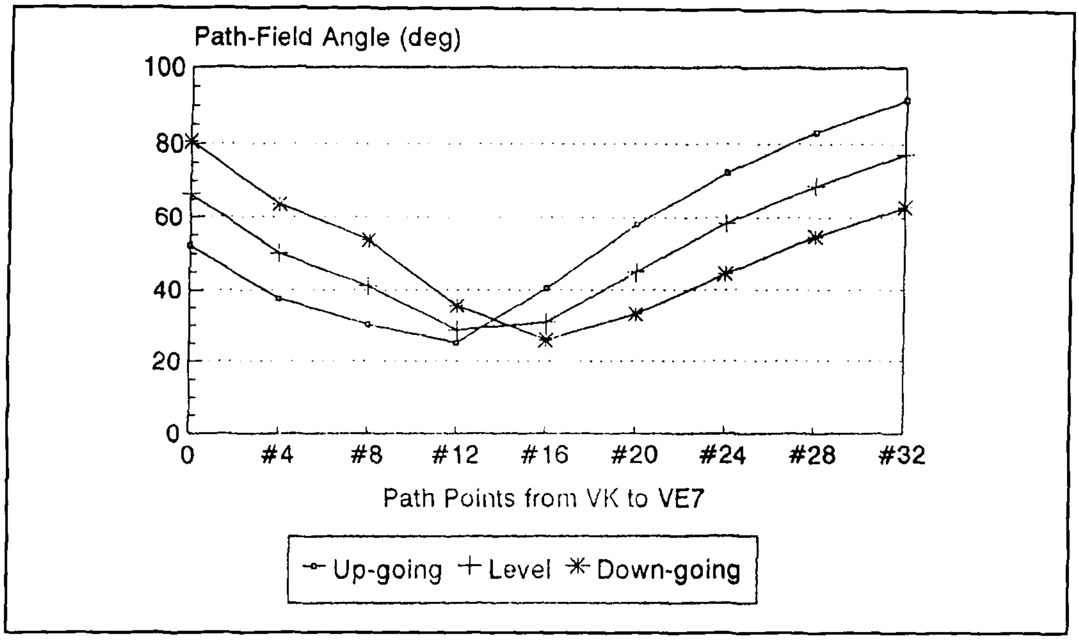

Figure 9. The path-field angle variation for the path in Figure 8.

It makes use of the Appleton-Hartree version of magneto-ionic theory, but contains revisions in source code, validated against the original results, to improve the speed of computations. It has been altered to allow input from the International Reference Ionosphere (IRI),[12] CCIR, and URSI models which apply only to non-auroral latitudes and times without geomagnetic disturbance.

In using those models for 3-D ray tracing, the PropLab Pro program creates electron density profiles along the path, from 3 to 5 degrees to either side in the present calculations, and for the date, time, and sunspot count of interest. Then, paths broken are down into shorter segments, from 1,000 to 1,500 kilometers in length and with a minimum of 10 profiles across each of the segments in the present instances.

That done, the program calculates ray trajectories from the transmitter using the model ionospheres, set up as above, for any range of radiation angles. For the VK-VE7 path related to the SEANCE Net between Australia and Western North America, the path went from 33.9 degrees S latitude, 151.2 degrees E longitude to 49.3 degrees N latitude, 123.1 degrees W longitude, covering a distance of 12,500 kilometers. It should be noted that the geomagnetic coordinates of those endpoints are 41.4 degrees S gm latitude, 228.4 degrees E gm longitude and 55.1 degrees N gm latitude, 296.9 degrees E gm longitude, respectively. The calculations were made using parameters similar to those for the time of the SEANCE Net: the summer solstice, a sunspot number of 100 and 1145 UTC (a half-hour before ground sunrise at the northern end), and radiation angles swept in small steps from 7 to 25 degrees.

With the three-dimensional analysis, it was at once apparent from ray traces going north from Australia toward British Columbia that the earth's magnetic field produces a small skewing of *F*-hops relative to regions of higher ionization. As expected, the hop structure ranged from *E*-hops at low angles to *F*-hops at high radiation angles. But in varying the radiation angle at the southern end of the path in small steps from 7 to 25 degrees, there was little evidence of any ducting of 160-meter signals over long distances, only a number of long *EF* hops, and some rather brief episodes of ducting in the electron density valley which were limited to the Southern Hemisphere.

Next, the same procedure was used on the northern part of the path, directing 1.8-MHz signals northward from the midpoint of the path toward British Columbia. The results obtained were quite different with about one-third of the radiation angles showing large-scale ducting, and signals undergoing vertical excursions from 110 to 160 kilometer altitude for distances ranging from 1,500 to 6,000 kilometers. A typical example of such ducting is shown in **Figure 6**.

Before going on, note that the geomagnetic field is the factor which makes ducting possible, as may be seen by comparing ray traces with and without the earth's field in the calculations. Thus, **Figure 7** shows the "no field" ray trace in three dimensions for the same radiation angle and circumstances in **Figure 6**. That result shows that the effect of the earth's field is to reduce refraction at the *E*-region

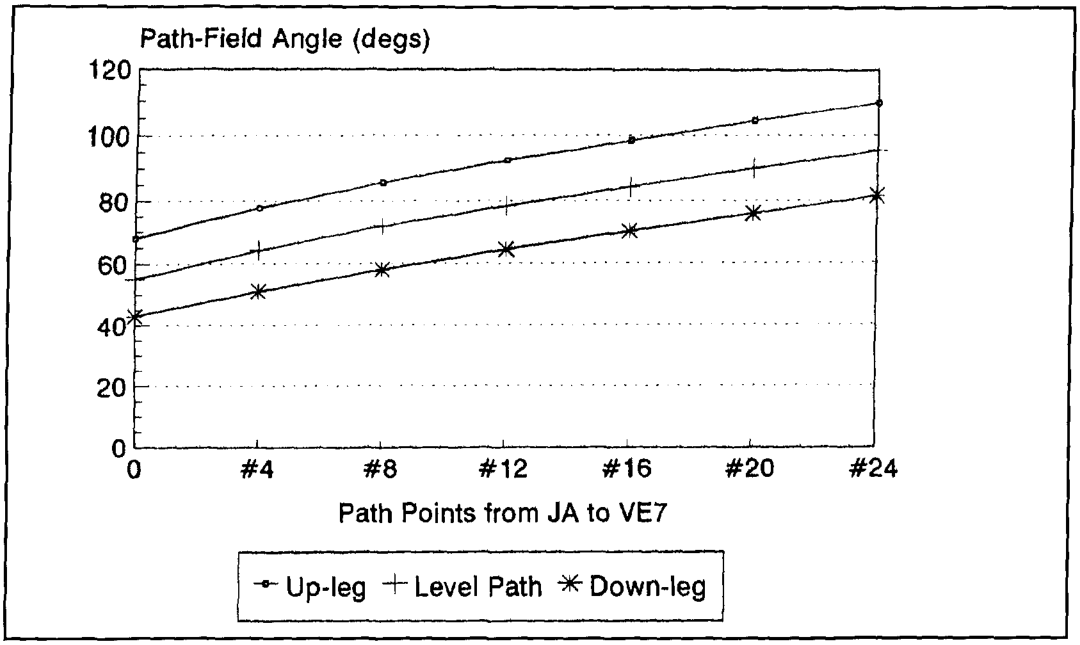

Figure 10. The path-field angle variation for a path from Japan (left) to British Columbia (right).

level to the point where ducting could develop.

With ducting the result of a magneto-ionic effect, the 160-meter case is different than that for HF ducting. Thus, Gurevich and Tselidina[6] suggested that the entry of HF signals into a ducting region was due to scattering of HF waves by ionospheric irregularities. But for the 160-meter signals, the entry of signals into a ducting region occurs quite naturally, requiring nothing in the way of special or unusual ionospheric circumstances as the earth's field is always present.

Now, when signals were directed southward from the northern end of the path toward Australia, signal transmission via ducting proved rather non-reciprocal as ducting of signals from the south and toward a sunrise terminator at the time of a solstice was about 10 times more frequent than away from the terminator and toward the south. In an effort to understand how features of the path relative to the geomagnetic field were related to the ionosphere responsible for those results, the magneto-ionic circumstances were examined.

First, the PropLab Pro program was used to obtain a vertical or transverse map of the plasma frequencies of the ionosphere all along the path. Such a map, with Australia on the left and British Columbia on the right, is given in **Figure 8**. That figure maps the contours of plasma frequencies from 0.2 to 2.0 MHz in 0.2-MHz intervals. The peak of the nighttime *E*-region is close to the lower part of the 0.4-MHz contour and the valley or ducting region extends to the upper part of the 0.4-MHz contour. That map was for 1145 UTC, a half-hour before sunrise, and the presence of weak solar illumination at high altitudes may be seen in the shape of the contours on the right-hand side of the figure. On the other hand, the sun was far below the horizon on the left-hand side of the figure and the main changes in the 0.4-MHz contour were around the geomagnetic equator, near the 5,000-kilometer mark.

Next, because refraction in magneto-ionic theory is sensitive to the angle between signal direction and the geomagnetic field, that angle was calculated for a number of points along the path in intervals of 390 kilometers. In calculating the angles between the path and field direction, the dipole model was used to find the declination, horizontal, and vertical components of the field. Those values were obtained from a geomagnetic utility program[13] from the National Geophysical Data Center and converted to direction cosines relative to a right-handed coordinate system with positive values to the east, north, and upward, respectively. It should be noted that since magnetic field lines come out of the earth in the Southern Hemisphere and go back into the earth in the Northern Hemisphere, vertical field components are positive in the south and negative in the north.

Path directions were taken along the great-circle path from Australia to British Columbia. Three local elevation angles were used, on the horizon as well as 15 degrees above or below the horizon. The level path direction would apply at the peak of any hop or the top and bottom of a ducted signal while the other angles were reasonable estimates of local elevation angles on upward and downward portions of

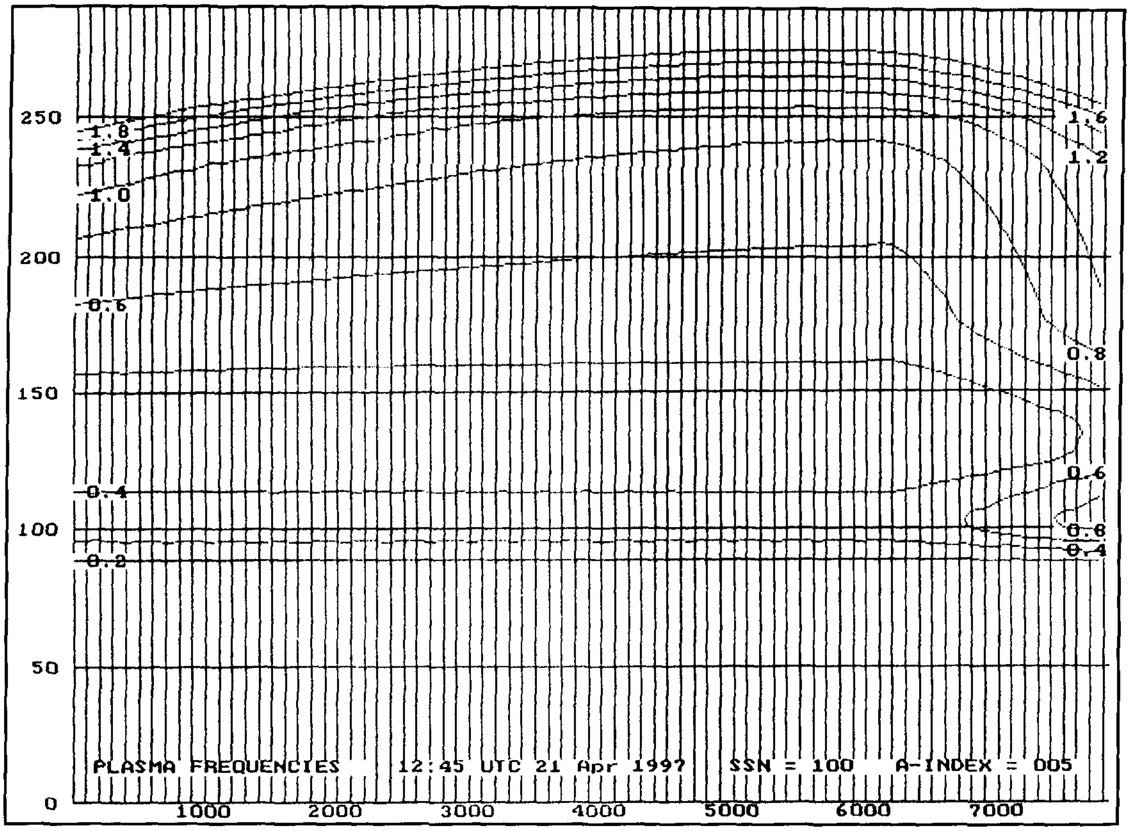

Figure 11. Transverse plasma frequency map for the path in Figure 10, evaluated at 1245 UTC on April 21 and when the sunspot number is 100. Plasma frequencies are in MHz and contours in 0.2-MHz intervals.

the paths at ionospheric heights. After those directions were converted to direction cosines in the same coordinate system, point by point, analytic geometry was used to find the angles between the path and the field vectors, as shown in **Figure 9**.

The path to British Columbia crosses the geomagnetic equator at an angle of 25 degrees between points #12 and #16 in **Figure 9** and the angle between the path and the geomagnetic field is at a minimum there, some 30 degrees. The distance between the geomagnetic equator and the southern terminus of the path is less than the corresponding point for the northern terminus and the same is true for the magnetic latitudes at the termini.

With that information, it is possible to examine other features of the path in terms of magneto-ionic factors. For example, the electron gyro-frequency varies from 1.28 MHz at the southern end of the path to 0.87 MHz around the geomagnetic equator and 1.46 MHz at the northern end. With that information and path-field angles from **Figure 9**, the variation of ionospheric absorption of 160-meter signals can be determined—that for the extraordinary waves relative to the ordinary waves. In this regard, in terms of dB, the X/O absorption ratio rises from 3.2 at the southern end to 5.9 across the equator and drops then to 2.1 at the northern end. The average X/O ratio for the entire path is 5.0, meaning that the loss in dB for extraordinary waves would be 5 times that for ordinary waves, say 100 dB for X-waves when the loss is 20 dB for O-waves, etc.

Another question that can be examined is the extent to which the propagation along the path approaches the quasi-longitudinal or quasi-transverse limits mentioned earlier. In that regard, the necessary data include electron gyro-frequencies, path-field angles, and plasma frequency at the various data points. The path-field angles are given in **Figure 9** and gyro-frequencies are easily obtained from the geomagnetic dipole model. The remaining quantity, plasma frequency in X, may be estimated using the map in **Figure 8** or by going to the ionospheric models and actually averaging the plasma frequency from calculations using the altitude variation of the electron density across the ducting region. When that is done, the propagation on most of the path turns out to be like that for the quasi-longitudinal case, in going away from the equatorial region toward point #4 or point #24. At the northern end, where the path-field angle approaches 80 degrees, the QT/QL ratio reaches 3.2, still far from the factor of 9 to make propagation fit the quasi-transverse case.

Another path

The magneto-ionic description of the VK-VE7 path did not show any clear, separate distinctions to help understand the signal ducting that was shown by ray traces. In an effort to develop the problem further, the path from Japan to British Columbia was explored. That path was shorter (7,800 versus 12,500 kilometers), and involved much less calculation time for ray-trace calculations.

In addition, it also had the advantage that, being in one only hemisphere, its great-circle path resulted in larger path-field angles at the northern end, as shown in **Figure 10**.

With shorter calculation times, two different months were used, April and June, to see if seasonal effects might also be present—specially since the SEANCE Net only operated for about two months either side of the summer solstice. Beyond that, the features of the calculations were the same as before: for a half-hour before sunrise at the northern end of the path and a SSN value of 100, with ray-traces made in small steps in radiation angle between 7 and 25 degrees.

For the JA-VE7 path, ray traces also showed ducting for about one-third of the radiation angles, even starting on the first hop. In addition, there was about the same degree of non-reciprocity for 160-meter signals directed toward Japan from British Columbia. But more important, in comparing ducting between April and June, it was clear that the length of the ducts was greater in April than in June. Thus, the average distance from the start of ducting at *E*-region heights (e.g., at 2,000 kilometers in **Figure 6**) to the end of ducting, or the VE7 terminus, decreased from 5,000 to 3,800 kilometers between April and June.

This result may arise from more of a sun-earth geometry factor than anything else; but before dealing with it, it is necessary to discuss the various magneto-ionic factors for the path. Those were a bit different than on the VK-VE7 path, the electron gyro-frequency increasing from 1.05 MHz at the southern end of the path (25.5 degrees N gm latitude, 205.8 degrees E gm longitude) to 1.46 MHz, as for the VK-VE7 path. From the variation of the electron gyro-frequency, it was found that the X/O absorption ratio falls from 4.0 at the southern end to 1.4 at the northern end. The average X/O ratio for the entire path is 2.0, less than the 5.0 average for the VK-VE7 path, indicating the extraordinary mode may be more significant on this path.

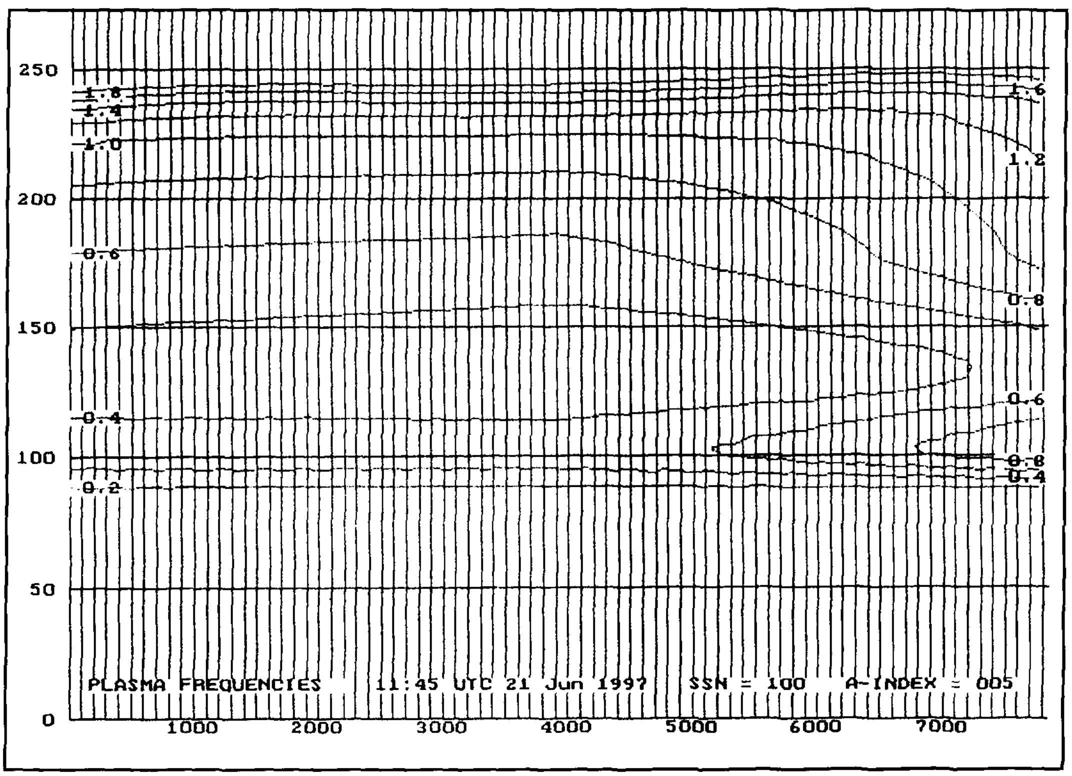

Figure 12. Transverse plasma frequency map for the path in Figure 10, evaluated at 1145 UTC on June 21 and when the sunspot number is 100.

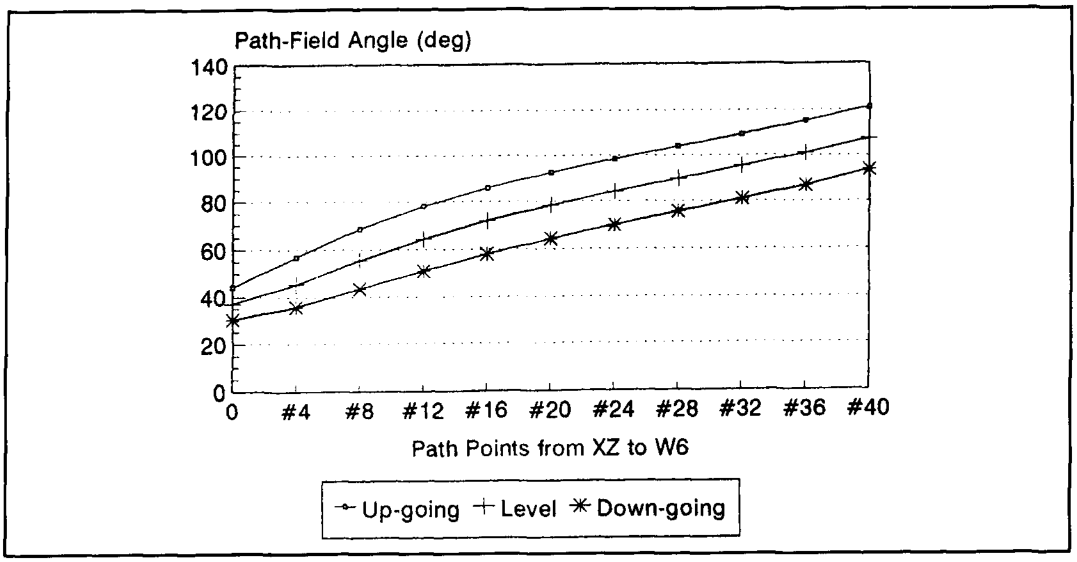

Figure 13. Path-field angle variation for a path from Burma (left) to California (right).

With the path-field angles in **Figure 10** and gyro-frequencies obtained from the geomagnetic dipole model, the last quantities needed for the magneto-ionic description of the JA-VE7 path, the plasma frequencies, were estimated by using a plasma frequency map between Japan, on the left, and British Columbia, on the right, as shown in **Figure 11**. It should be noted that particular map is for two months before the solstice, April 21, and 1245 UTC, a half-hour before ground sunrise on that date.

Turning next to the question of whether the propagation can be considered quasi-longitudinal or quasi-transverse, the angles in **Figure 10** suggest a transition from QL starting around Japan and going over to QT as Canada is approached. In point of fact, with the magneto-ionic variables, the QL/QT ratio goes from 7 by Japan to 1.3 by point #8 in **Figure 10**; then the inverse ratio, QT/QL, rises to more than 18 by point #16 and beyond.

Note that the path-angle information in **Figure 10** depends only on the path direction and the geomagnetic field, and is independent of time or solar conditions. However, the plasma frequency map does change with time and solar conditions, as shown by the map in **Figure 12**, now for 1145 UTC on June 21. As a result, the estimated values from **Figure 12** alter those QT/QL ratios beyond point #12 in **Figure 10**, raising them by about 10 percent at the far end of the path.

A comparison of the plasma maps in **Figures 11** and **12** shows that the penetration of ionization into the path at the sunrise terminator end is lower in April than in June, to about 1,500 kilometers in the first instance and to 4,000 kilometers in the second. Penetration of ionization that deep in June is due to the fact that the northern swing of the signal path comes closer to the northern limit of the region of darkness or, equivalently, that the angle at the far end of the path between the path and the sunrise terminator is less, 21 degrees in June and 40 degrees in April.

Another way of expressing the same idea is in terms of the gradient of ionization across the far end of the path being greater when the path is closer to the northern limit of the region of darkness at the solstice than in April, shortly after the spring equinox. Thus, given that the QT/QL ratio changes by only about 10 percent at the far end of the path, while the ducting distances were about 25 percent shorter in June than in April, it would seem that ducting distances are also affected by the geometry of the path relative to the terminator, being greater when the perpendicular gradient of ionization along the path is the least or the angle is close to 90 degrees.

Another path, another SSN

In an effort to obtain a clearer view of how signal ducting depends on magneto-ionic variables, another path was used with a different sunspot count: from Burma (XZ) to California (W6), now during solar minimum when the SSN is about 15. This choice is relevant as a recent DXpedition to Burma[14] provided some information on the questions considered here, principally problems with non-reciprocity of 160-meter propagation. The XZ-W6 path is longer than the other paths considered earlier, now some 12,800 kilometers. Being in one hemisphere like the JA-VE7 path but with a far terminus at a lower latitude, its great-circle path goes to higher latitudes and gives even greater path-field angles at the northern end, as shown in **Figure 13**. In this case, the coordinates of the end points are 17.8 degrees N latitude, 96.4 degrees E longitude and 37.3 degrees N latitude, 120 degrees W longitude. In terms of magnetic coordinates, the terminii are at 7.3 degrees N gm latitude, 168.5 degree E gm longitude and 43.9 degree N gm latitude, 55.6 degrees W gm longitude.

The electron gyro-frequency along the path increases from 0.51 MHz at the southern end of the path to 1.49 MHz when the path reaches its highest geomagnetic latitude, 56.7 N degrees, at point #28. From the variation of the electron gyro-frequency and path-field angles, it was found that the X/O absorption ratio falls from 5.0 at the western terminus to about 1.0 by point #24, again showing greater absorption of the extraordinary wave, now over 61 percent of the path and the average X/O ratio of absorption in dB is 3.2 for the entire path.

With the path-field angles in **Figure 13** and gyro-frequencies obtained from the geomagnetic dipole model, the QT and QL factors for the XZ-W6 path can be obtained by using the plasma frequencies from the map in **Figure 14**, with Burma on the left and California on the right. It should be noted that this map is for the winter in the Northern Hemisphere, November 20, 1996 and at 1420 UTC, the date of the recent DXpedition and a half-hour before the ground sunrise at the eastern end of the path. A comparison of the plasma map in **Figure 14** with the previous plasma maps shows that the penetration of ionization into the path at the sunrise terminator end was relatively small, due to the fact the angle between the path and the sunrise terminator at the far end of the path was 64 degrees, the greatest of the three cases.

As for the question of whether the propagation can be considered quasi-longitudinal or quasi-transverse, the angles in **Figure 13** again suggest a transition, from QL starting around Burma and then going over to QT around point #24 as the path-field angle rises toward 90 degrees. Calculation shows the QL/QT ratio goes from over 100 by Burma to 1.2 by point #16 in **Figure 13**; the inverse ratio, QT/QL, rises and stays above 17 between #24 to # 36 and then falls rapidly to values for QL propagation for the last part of the path. Thus, from the western end of the path, there was a span of 3,800 kilometers where propagation was quasi-longitudinal and a comparable distance near the far end of the path where the propagation was quasi-transverse in nature. With those clear distinctions, it is interesting to look at the results from making ray traces, starting at one end of the path and then the other.

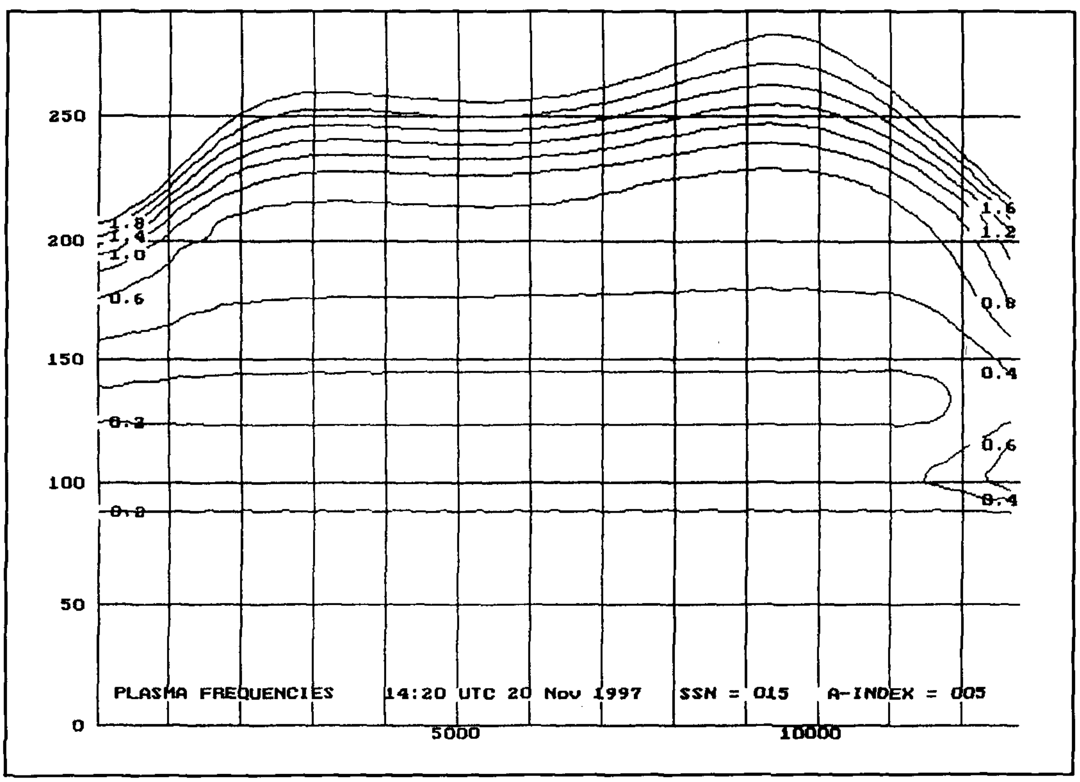

Figure 14. Transverse plasma frequency map for the path in Figure 13, now evaluated at 1420 UTC on November 20 and when the sunspot number is 15.

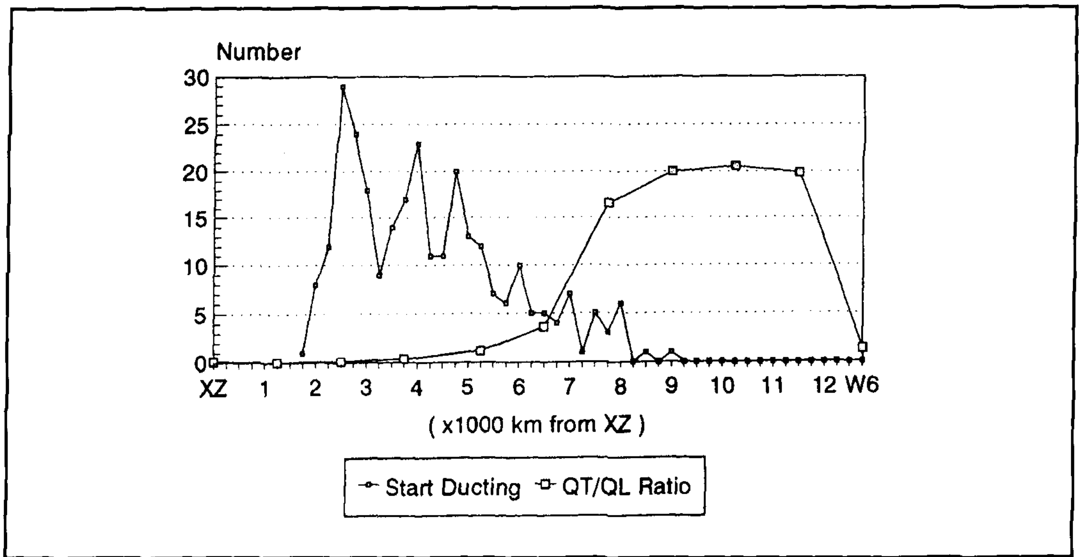

Figure 15. The number-distribution of positions for the start of ducting on the path in Figure 13. The figure shows variation of the QT/QL ratio along the path.

In that regard, the ray tracings on the XZ-W6 path were made over a greater span of time, every 15 minutes from 1250 UTC to 1420 UTC, 30 minutes before sunrise. Ray tracings were evaluated in a different manner, noting for each radiation angle the distance from the transmitter to where the ducting began.

For the direction from Burma toward the West Coast, over 1,000 ray traces were made in small angular steps of radiation angle between 7 and 25 degrees. As for the occurrence of ducting, there was no significant difference in the number of times ducting was noted in each 15-minute interval. That was not an unexpected result as magneto-ionic conditions along the western end of the path, where ducting begins, did not change appreciably in the time between 1250 UTC and 1420 UTC. However, there was a difference in the ends of ducting. The early ducts ran over and beyond the eastern end of the path; but ducts became shorter toward 1420 UTC, with some ray traces going back to ground level when the condition needed to continue ducting was not fulfilled. Presumably, this was due to changes in plasma frequency contours near the sunrise terminator.

For the whole period, 28 percent of the radiation angles that were sampled gave rise to ducting and the majority of the ducts went as far as the eastern terminus, except as noted above. For signals going in the other direction, only about 10 percent of the radiation angles gave rise to ducting and those were quite different: about half started with the very first hop and the ducts seldom went beyond a distance of 5,000 kilometers from the starting point. Thus, propagation via signal ducting in the electron density valley was not fully reciprocal in number or signal strength for the paths, the E->W ducts being both fewer in number and much less efficient because of their shorter lengths.

A matter of interest related to the previous points is the distribution of locations where ducting begins and the variation of the QT/QL ratio along the path, given in **Figure 15**. That figure shows that ducting from the western end of the XZ-W6 path begins after a distance of about 2,000 kilometers when the first hop is completed, just as shown earlier in **Figure 6**. Beyond the first peak in the distribution for ducts starting after the first hop, the other peaks in the distribution around 4,000 kilometers, 5,000 kilometers, and 6,000 kilometers are due to ducts starting after 2, 3, and 4 *F*-hops, etc.

In regard to the QT/QL ratio, it should be noted that the functions of the path-field angle and other quantities in its definition are all raised to even algebraic powers. This means the QT/QL ratio does not change sign when signal directions are reversed, making the ratio at a point the same for both directions.

Inspection of **Figure 15** shows that only a small fraction of the signals going eastward formed ducts beyond 7,000 kilometers distance, the position on the path where propagation began to change from quasi-longitudinal to quasi-transverse. Also, in that connection, only a few of the ducts formed by signals going to the west ever went beyond that same location along the path.

Discussion

The present study was directed toward exploring whether ducting of 160-meter signals occurs or not, particularly since the electron density valley above the nighttime *E*-region is a likely site for such propagation. The method was to use 3-D ray tracing to look for ducted signals along paths of significant interest or use by 160-meter operators. It should be noted the three-dimensional ray tracing technique has been available in scientific circles for more than 20 years, but only recently did it become available to radio amateurs. In the same regard, the electron density valley above the *E*-region has been known for more than 25 years but seems not to have been noticed in amateur radio or SWL circles.

The operating frequencies in the 160-meter band (1.8 MHz) are close to the gyration frequency of ionospheric electrons around geomagnetic field lines. As a result, it is not correct to just consider 160-meter propagation to be an extension of what is known to apply at HF frequencies. Instead, the concepts of magneto-ionic theory must be considered as well as applied, as was done in the developing the ray-tracing program.[11] That results in an approach to signal propagation where the direction of ray paths relative to magnetic field lines becomes very important.

Historically, the first results of magneto-ionic theory were in connection with signals along and perpendicular to field lines and the theory indicated there were significant differences for the two cases. But with questions of interpretation of ionograms from vertical ionospheric soundings at mid-latitudes, the theory was extended by means of approximations so as to apply at oblique angles of propagation relative to the geomagnetic field lines.

In that connection, it should be noted that considering only great-circle paths and magnetic dip angles is not sufficient in determining path directions relative to field lines for use in the approximations; those only provide a qualitative evaluation about path-field angles for regions along a path when more detail is required. For the necessary detail, a geomagnetic model and the methods of elementary vector analysis or analytic geometry in three dimensions are needed to obtain actual path-field angles.

But to find the range of angles where those approximations may be used to simplify the discussion, some additional information is necessary—specifically, the electron densities or plasma frequencies along the path. That requires ionospheric profiles such as in CCIR or URSI models in the International Reference Ionosphere.[12] With these profiles, the other aspects of magneto-ionic theory may then be dealt with, largely with regard to refraction and signal polarization.

The present study makes use of those approximations and methods to identify where quasi-longitudinal and quasi-transverse propagation conditions prevail. No calculations are made as to the wave polarizations that go with them. Thus, the main use of magneto-ionic theory is to identify those aspects that could be related to signal ducting. While polarization is interesting in its own right, it is secondary to the present discussion and the reader may turn to treatises[7] on magneto-ionic theory to gain further insight on the subject.

An earlier part of the discussion[3] suggested that long *EF* hops could be the basis of ducting if the refraction on down-legs from the *F*-region were less due to the effects of ionospheric tilts. Another possibility was that the critical frequency fo*E* of the *E*-region might be raised, perhaps due to effects from acoustic/gravity waves[15] changing the neutral particle density at the peak of the *E*-region, thus trapping signals in the electron density valley.

Those considerations were based on two-dimensional ray traces; but early in the present study, the three-dimensional ray traces based on magneto-ionic theory showed that the earth's field skewed signals slightly—a fraction of a degree in heading. In addition, it was evident that the geomagnetic field essentially weakened ionospheric refraction to the point that signals destined for *E*-hops would be refracted less, making them more likely to approach the *E*-region with the characteristics of Pedersen rays and then be ducted. Thus, long *EF* hops would not require ionospheric tilts to begin ducting, thanks to magneto-ionic effects.

Turning to the present analysis, almost 2,000 ray traces were made in connection with the study. The greatest number were for the propagation path from Burma to California—one where there is a clear separation between quasi-longitudinal and quasi-transverse propagation conditions. While all three paths showed ducting, the ducting from west to east (W->E) on the Burma path was more probable than in the other direction, with about 30 percent of those radiation angles showing W->E ducting while only about 10 percent of the angles showed E->W ducting.

The W->E ducts were generally long, essentially over-flying the receiver to the East, while the E->W ducts were considerably shorter and the signals returned to ground several thousand kilometers before reaching the receiver. As a result, while all three paths used in this study showed the presence of ducting, the results for the Burma path suggest that ducting is more probable for conditions of quasi-longitudinal propagation than those for quasi-transverse propagation.

One fine distinction of interest is whether ducting began with the first hop or not. The ducting data in **Figure 15** shows a complete absence of ducting on the first hop for the XZ->W6 path, but first-hop ducting was quite

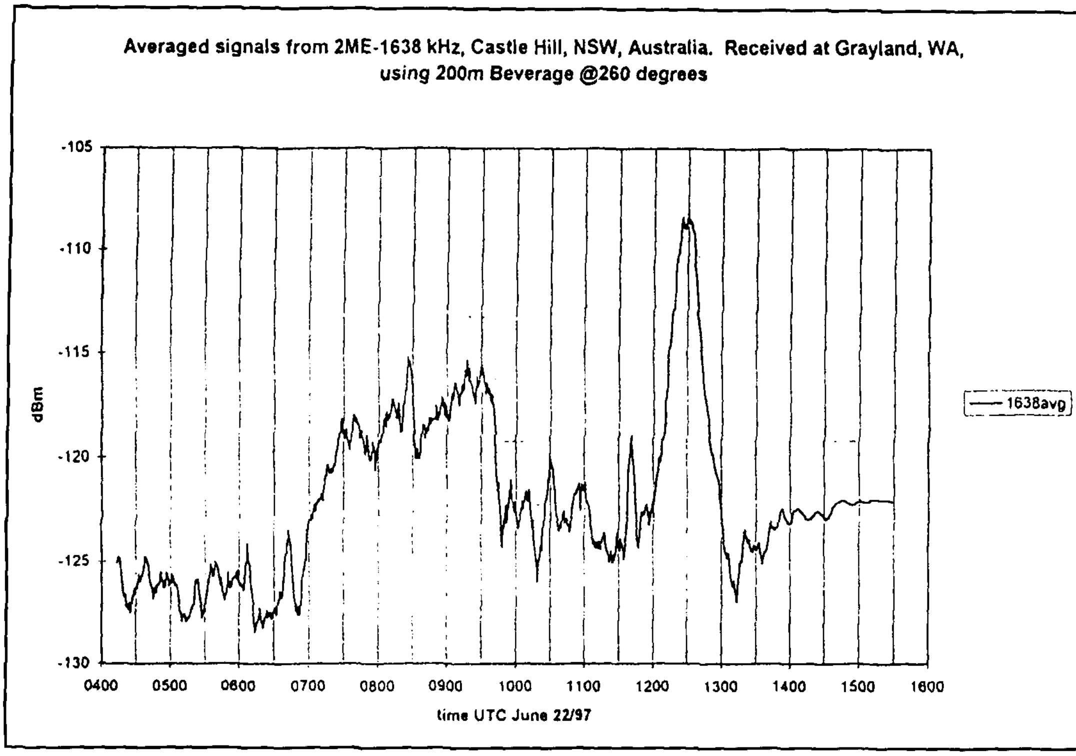

Figure 16. An intensity-time plot for 1.638-MHz signals from Sydney, Australia to Grayland, WA, on June 22, 1997. Signals were sampled once every 20 seconds; the plot shows the running average of signal strength over seven-minute intervals. Sydney sunset was at 0649 UTC, Grayland sunrise at 1226 UTC.

common for the JA-VE7 path. That difference appears to be related to the strength of the magnetic field, as the field along the path around Japan is greater than that close to Burma by a factor of 1.22. This is due to its greater geomagnetic latitude (25.5 degrees N versus 7.3 degrees N). Support for that idea is found in a calculation of field strength at 2,000 kilometers along the XZ->W6 path, showing that the field has increased to the level at the start of the JA->VE7 path.

The discussion above has dealt largely with the overall aspects of the matter, including the presence or absence of ducting on the various paths, but not the details of the physical processes that go into ducting. The observation that ducting happens because of the presence of the field is of major importance, showing that ducting is a regular feature of propagation on the 160-meter band and will occur day in and day out. And, ducting was noted at high and low levels of solar activity: an SSN of 100 for the JA path and 15 for the XZ path. But the results from the differences in length of ducts on the JA-VE7 path between April and June show that the extent of ducting varies as the intrusion of solar ionization changes the shape and depth of the valley and increases the electron density along the valley region.

The change in length of ducted paths bears on another matter: the stability of ducting in the nighttime electron density valley above the *E*-region. The long ducted paths suggest there is a stabilizing process in effect, so that once ducting starts, it serves to keep signals within the duct. However, ducts that end prematurely before reaching the far end of the path at times close to sunrise, or short ducts, as with the JA-VE7 path at the solstice, show the stabilizing factor can be over-ridden by additional ionization in the duct.

The simplest explanation of this is in terms of *F*-region tilts. Thus, changes in the slope of the constant electron density contours, as in the transverse plasma frequency maps toward the sunrise end of the path, would alter the local refraction angles in the duct. When that gets to the point that signals are refracted downward toward the ground from the top of the duct or upward into the *F*-region from the bottom of the duct, signal ducting would end and *F*-hops with ground reflections would ensue.

Such changes in electron density serve to increase the variable X (and decrease 1-X) used in evaluating the QT/QL ratio. As a result, the QT/QL ratio would increase and have an effect on propagation, mainly decreasing even further the small fraction of E->W signal ducting through QT regions. Normally, such changes take place slowly as seasons advance, but if electron density mapping, as in **Figure 14**, is not available, the angle between a path and the dawn terminator would serve as a surrogate to evaluate how the range of the intrusion of ionization changes, being least at a given terminus when the angle is as large as possible.

The paths of interest in the present discussion were all across regions of darkness. Of the three, the JA->VE7 path at the summer solstice came the closest to the terminator—the dividing line between sunlit and dark regions. For that case, a deep electron density valley extended over half of the path, but beyond that the valley began to narrow and become shallower. In that regard, paths very close to the terminator, the familiar gray line situation, would not have any appreciable valley region associated with them and thus there would be no question of signal ducting. Instead, propagation of signals would be entirely by *F*-hops, but with a differential absorption between the X and O waves that would depend on path-field angles along the path.

It was suggested earlier that tilts in the *F*-region could play a role in ducting and that tilts along a path, like the irregularities in the HF case, could contribute to signal leakage along a path. At the end of a path, however, turbulent *F* region tilts driven by solar heating around sunrise could serve as a means of getting signals out of the duct. Consequently, the dawn enhancement of 160-meter signals is well known but only in a qualitative sense, at least until recently.

Now, however, signal recordings, as shown in **Figure 16**, are becoming available[16] to provide quantitative data, intensity versus time, for dawn enhancements on comparable frequencies and for paths similar to the those of interest here. Such data would seem to provide strong quantitative support for the idea that solar-excited tilting releases the ducted signals. That being the case, the ducting of 160-meter signals would be more frequent than that of HF signals as the earth's field as well as sunrise are both there, day in and day out, and hardly represent any special circumstance.

Before the time of dawn enhancement, the present discussion suggests the propagation of signals would be largely via *F*-hops in both directions. In that regard, it should be noted that ducting would still be in progress. Rays advancing without ever returning to ground level would divert some RF energy from the *F*-hops heading in the direction of the receiver, reducing the amount of energy propagated at low altitudes. Thus, ducting would have a negative effect on the received signal strength, at least until sunrise tilts and the dawn enhancement bring the signals down from the duct. But there would be a net signal gain then as the ducted signals would not have suffered the same losses as they would have if they were propagated by earth-ionosphere hops.

In connection with the dawn enhancement, recent observations[17] provide examples where signals from stations on Kermadec and Norfolk Islands were heard an hour or more after ground sunrise in the Midwest. In that regard, signals which spill out of a high-altitude duct in connection with the dawn enhancement provide a ready explanation for late signal reception, at a time when *D*-region absorption would have normally exacted a very heavy toll on signals propagated by earth-ionosphere hops. Thus, late signals, well after sunrise, also argue for the presence of ducting in 160-meter propagation.

The effect of ionospheric tilts, spilling signals out of a duct, may also apply to signal leakage along a duct and have some connection with the "searchlight" aspect often reported by 160-meter operators, where signals are heard in small regions to the exclusion of others. Thus, there is the question of the day-to-day "meteorology" of ionospheric tilts. It has been suggested they play an important role around sunrise and sunset. The question is what role they play when it comes to the departures of 160-meter propagation from average conditions.

Ionospheric tilts and traveling ionospheric disturbances (TID) are known to result from acoustic/gravity waves and atmospheric heating associated with auroral events.[18] While those events are not recorded to the same extent as magnetic variations and the other solar-terrestrial variables, a promising line of approach is the continuous monitoring of signals in the high part of the broadcast band, as seen in **Figure 16**. With the new solar cycle about to start, signal records of intensity versus time during the cycle, particularly at sunrise and times of geomagnetic activity, would be most helpful in understanding more about propagation on the 160-meter band.

Summary

The present study, using 3-D ray tracing based on magneto-ionic theory and current models of the ionosphere, indicates that 1.8-MHz signals may be ducted in the electron density valley that develops above the *E*-region at night. For the paths used in the study, ducting showed a non-reciprocal character with signals ducted more often and further in the west-to-east direction than in the opposite direction.

With the aid of data on the direction of propagation relative to the magnetic field lines and electron densities in the valley regions, it was discovered that ducting occurs more often in ionospheric regions where propagation paths in the geomagnetic field satisfy the quasi-longitudinal approximation than the quasi-transverse approximation.

From the well-known dawn enhancement of 160-meter signals and recordings of signal strengths on a path similar to that used in the study, it is suggested that the dawn enhancement represents signals being spilled out of a duct by turbulent tilts in the *F*-region which result from solar heating at dawn. At other times, such tilts along ducted paths may contribute to signal leakage and a promising line of research would be the monitoring of signal strengths of broadcast stations at sunrise and looking for signal enhancements with geomagnetic activity of Cycle 23. In any event, the magnitude of the dawn enhancement probably provides a measure of the importance of signal ducting at the time.

Acknowledgments

I am indebted to Robert Eldridge, VE7BS, for many stimulating discussions about top-band propagation. I want to thank Dr. John Bryant for calling my attention to the work of Nick Hall-Patch, VE7DXR, and to Nick Hall-Patch for copies of his recordings of signal strength of Australian broadcast stations. In addition, I want to thank William Hohnstein, KØHA, for information about late signals from Kermadec and Norfolk Islands.

Finally, I am indebted to Cary Oler of the Solar/Terrestrial Dispatch for his contributions in making the ray-tracing technique available to the amateur radio community. ■

REFERENCES

1. R.C. Eldridge, "Summer 1991 on 160 Meters," *The Canadian Amateur*, March 1992.
2. Michael C. Kelley, *The Earth's Ionosphere*, "Chapter 5: The Mid-Latitude Ionosphere," Academic Press, 1989, pages 217–222.
3. R.R. Brown and R.C. Eldridge, "On Long EF-Hops and Top Band Propagation, (unpublished), June 1997.
4. H.A. Hess, "Investigations of High-Frequency Echoes," *Proceedings of the I.R.E., Vol. 36*, 1949, pages 981–992.
5. H.J. Albrecht, "Investigations on Great Circle Propagation Between Eastern Australia and Western Europe," *Geofisica Pura e Applicata, Vol. 38*, 1957, pages 169–180.
6. A.V. Gurevich and E. Tsedilina, *Long Distance Propagation of HF Radio Waves*, Springer-Verlag, 1985.
7. J.A. Ratcliffe, *The Magneto-Ionic Theory and Its Applications to the Ionosphere*, Cambridge University Press, 1959.
8. K. Davies, *Ionospheric Radio*, Peter Peregrinus Ltd., London, U.K., 1989.
9. Cary Oler, "PropLab Pro-A High Frequency Radio Propagation Laboratory," Solar Terrestrial Dispatch, 1994.
10. R.M. Jones, "A Three-dimensional Ray-Tracing Program," *Digest of ESSA Technical Reports*, ITSA No. 17, *Radio Science*, 3, 1968.
11. R.M. Jones and J.J. Stephenson, "A Versatile Three-dimensional Ray-Tracing Computer Program for Radio Waves in the Ionosphere," *OT Report* 75–76, U.S. Government Printing Office, Washington, D.C., 1975.
12. *International Reference Ionosphere (IRI 90)*, D. Bilitiza, National Space Science Data Center, Greenbelt, Maryland.
13. *NGDC, Utility Programs for Geomagnetic Fields*, National Geophysical Data Center, Boulder Colorado, 1996.
14. W.E. Hill, "The Reopening of the Door to Amateur Radio in the Union of Myanmar," *CQ*, August 1997.
15. R.D. Hunsucker, "The Sources of Gravity Waves," *Nature*, Vol. 238, Nr. 6127, July 1987, Page 204.
16. Hall-Patch, private communications.
17. Hohnstein, private communications.
18. L. Hajkowicz and R.D. Hunsucker, "A Simultaneous Observation of Large-scale TIDS in Both Hemispheres Following An Onset of Auroral Disturbances," *Planet*, Space Science, 35, 1987, page 785.

PRODUCT INFORMATION

"Credit Card" Transceivers

Alinco has two new "micro" transceivers designed to operate on the popular 2-meter and 70-centimeter (420~450 MHz) bands. The DJ-C1T and DJ-C4T are only slightly larger than a credit card, are powered by a large capacity (500 mAh) Lithium-ion battery that can run for up to 100 hours between charges, and recharge in approximately two hours.

Both radios feature 21 non-volatile memories, CTCSS encoder, and an offset capability up to plus or minus 99.995 MHz (within operating range). The units have both a telescoping antenna and a flexible "clip on" wire antenna for receiving when the telescoping antenna is retracted. Accessories include a variety of speaker mic and earphone mic units, a mobile charging cable, and a cable to allow the use of Alinco and compatible speaker mics.

The DJ-C1T and DJ-C4T have been type approved by the FCC. Both radios are available through authorized Alinco dealers. For more information, photos, and specifications, contact <http://www.alinco.com>.

Edited by Peter Bertini, K1ZJH
Senior Technical Editor

Our "Tech Note" for this issue comes from Hannes Coetzee, ZS6BZP, of South Africa. He comments: "The performance of this low-band DX antenna is evaluated by on-the-air texts and computer simulations against the claims of spectacular performance by numerous authors. The results are quite enlightening."

Thanks, Hannes, for an interesting article—our first submission from your country.

—de K1ZJH

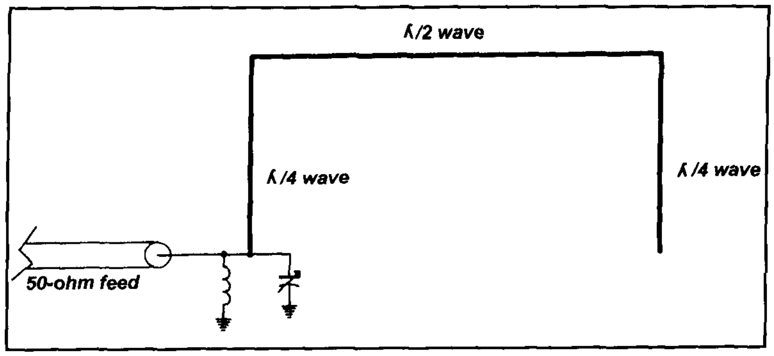

Figure 1. Half-Square antenna. (Voltage feed.)

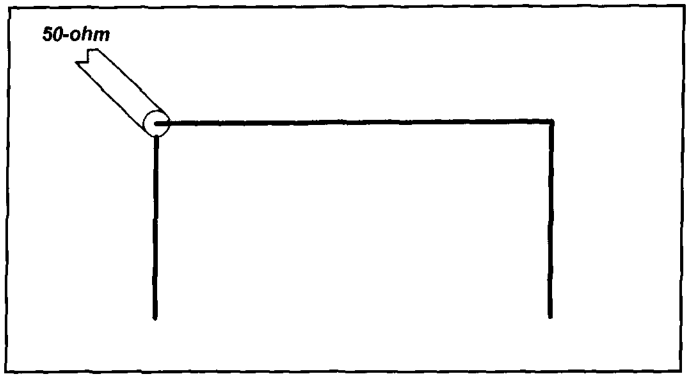

Figure 2. Current-fed Half-Square antenna.

A Visit to the Half-Square Antenna

Experiments provide interesting information.

Hannes Coetzee, ZS6BZP

Back in 1985, when I was still a student at the University of Pretoria, I read an article by Jerrold A. Swank, W8HXR[1] on rotating the Half-Square antenna. (It is also referred to as the Bobtail.)

What really impressed me from the article was that the author, when working into Antarctica "could get a 5/9 report barefoot and break into a pileup any time" when using this antenna. From my limited experience, I considered this to be no mean feat and filed the article for use the moment I had settled down and had invested in the necessary infrastructure to also put up one or more of these antennas. In the meantime, I also collected any other applicable literature.

That day partially arrived during the first quarter of 1997, and it was with great enthusiasm that my first 20-meter effort was put up on two 6-meter masts. I felt that this would reflect the capabilities of the 40-meter version planned for two masts, each 12 meters high, as the "main course" at my QTH.

Basic Half-Square Antenna

The basic form of the antenna is two quarter-wave verticals spaced a half-wavelength apart (**Figure 1**). They are connected at the top by a single wire. Use can be made of either voltage feed at the base of one of the verticals, or current feed between one of the verticals and the horizontal line.

According to previous articles, the half-wavelength spacing between the vertical elements combined with the half-wavelength horizontal line produces a bidirectional, broadsided, vertically polarized radiation pattern. There is supposed to be very little radiation from the horizontal line.

First Antenna

It was convenient to use a current feed for my first 20-meter version as the shack was on the first floor of the house (**Figure 2**). The feedline could then run horizontally, at right angles from the antenna to the transmitter. This would guarantee minimal interaction between the feedline and the antenna for the first round of experiments.

When I was trying to match the antenna cut to the formulas presented by GW2DDX,[2] the first signs of a snake in the grass became apparent. The antenna did not resonate properly! I trimmed the various dimensions until an acceptable match was found. Somehow this didn't seem quite right. It became obvious that I would need to put some thought into the

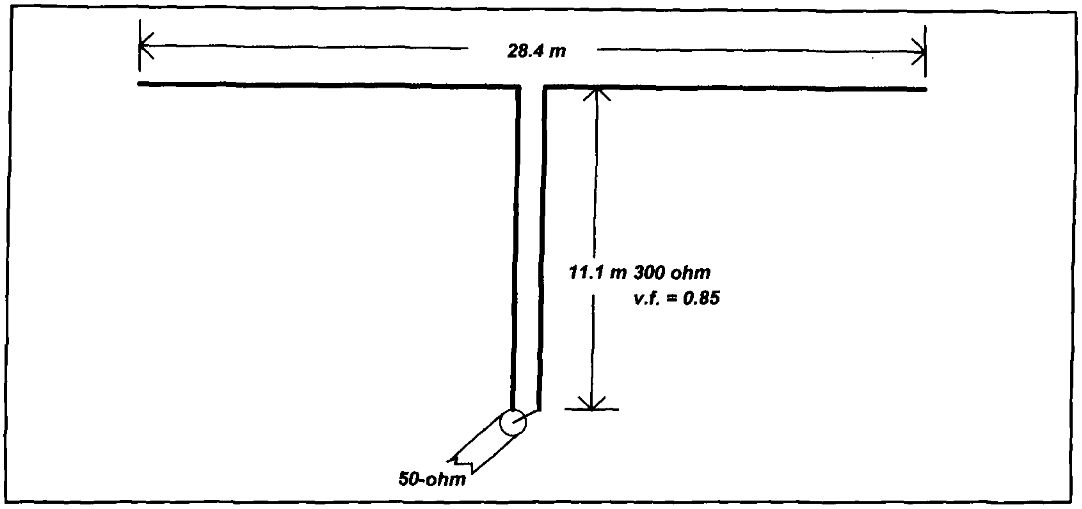

Figure 3. Improved G5RV antenna.

physics of the Half-Square antenna rather than blindly follow the advice of others.

According to transmission-line basics, a half-wavelength transmission line transfers a load from the one end of the line to the other with only a 180-degree change in phase. In other words, the far end verticals' impedance is transferred to the feedpoint with only a phase difference. Keeping this in mind, the Half Square antenna can be simplified to a common dipole antenna to aid matching the antenna.

From this, one can deduce that each vertical should be 0.95 of a quarter of a wavelength long, or a fraction shorter to compensate for ground effects. The horizontal line between the two verticals must then be exactly a half wave-

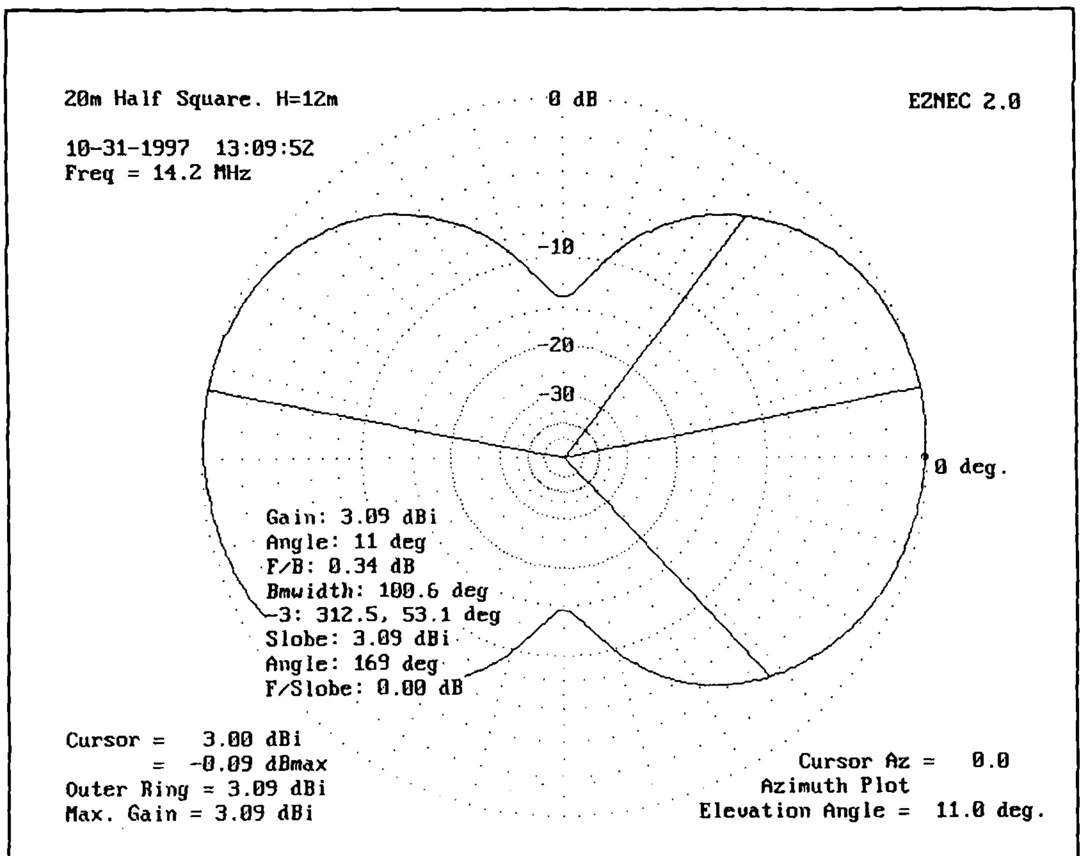

Figure 4. The Half-Square antenna simulated on 20 meters.

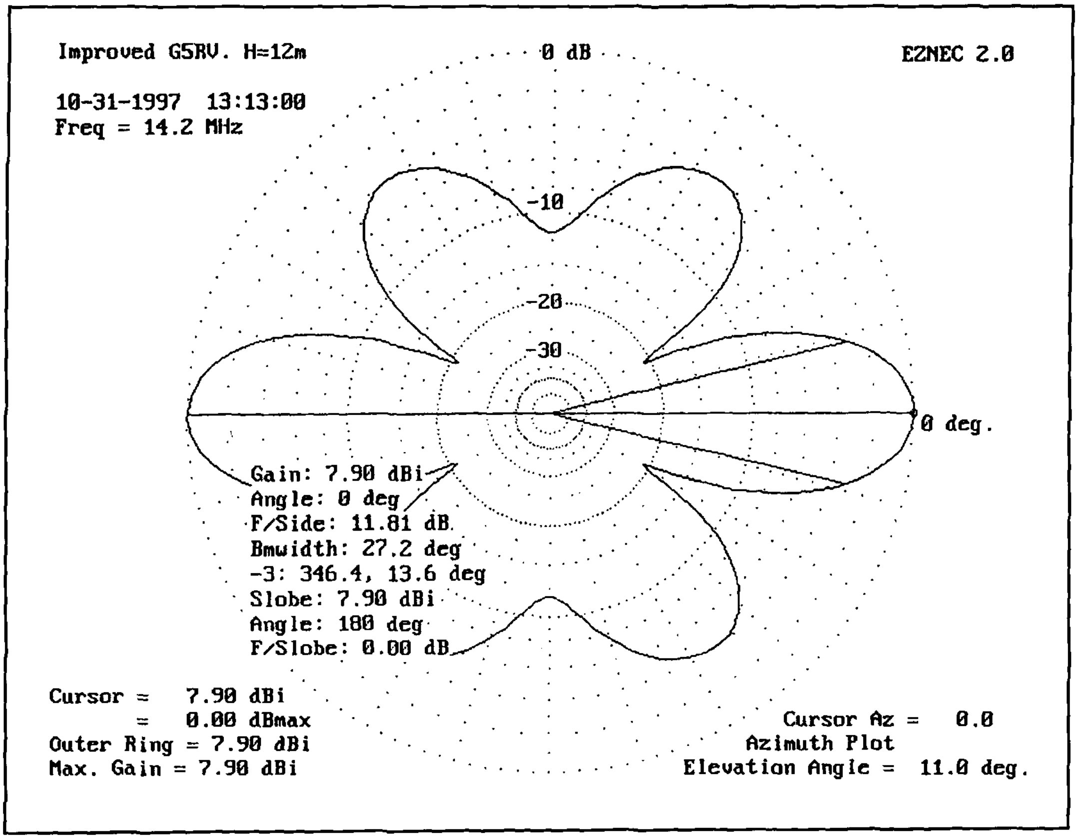

Figure 5. The improved G5RV simulated on 20 meters.

length long. I adjusted all the lengths to comply with the above deduction, and it resulted in an antenna with a very acceptable match.

When a voltage feed is used, as is normally the case for the Half-Square antenna, any reactive load presented by the antenna is resonated out by the parallel resonant circuit used for transforming the 50-ohm feedline impedance of the antenna. This enables an antenna with slightly different dimensions to present an acceptable match, although the antenna might not radiate exactly as intended.

Practical Results

As a reference antenna, I put up a version of the G5RV multiband dipole, improved by ZS6BKW (**Figure 3**)[3] at a height of 12 meters. This antenna presents an acceptable match to solid-state power amplifiers (SWR < 2:1) without the help of an ATU. It resonates on 3.6, 7, 14, 18.1, 24.9, 28.5, and, as a bonus, on 51.2 MHz.

I put up the improved G5RV in a nearly 30-degree south of east direction. As a result, the main lobe on 20 meters was aimed toward Siberia.

When the G5RV consistently outperformed the 20-meter Half-Square antenna by a considerable margin, I was very disappointed. Even lifting the Half-Square to 9 meters did little to improve matters. After many comparative tests, I had to accept defeat. The Half-Square antenna had been thoroughly beaten by a multiband dipole. I had to find the reason why!

I decided to call in the help of an antenna simulation program. Danie Brynard, ZS6AWK, had a copy of EZNEC2* by W7EL that explained things a bit.

Performance Capabilities

We simulated both antennas over average ground at a height of 12 meters (**Figures 4** and **5**). The bottom of the verticals of the Half-Square antenna were at 7 meters above the ground. I decided that a radiation angle (wave angle) of 11 degrees above the horizon was realistic for my QTH, and calculated the radiation patterns of the antennas for this elevation. The results from the computer simulations were, to say the least, enlightening.

The Half-Square antenna delivers 3 dBi of gain per main lobe. This is fairly realistic

*EZNEC2 by Roy Lewallen, W7EL, P.O. Box 6658, Beaverton, Oregon 97007.

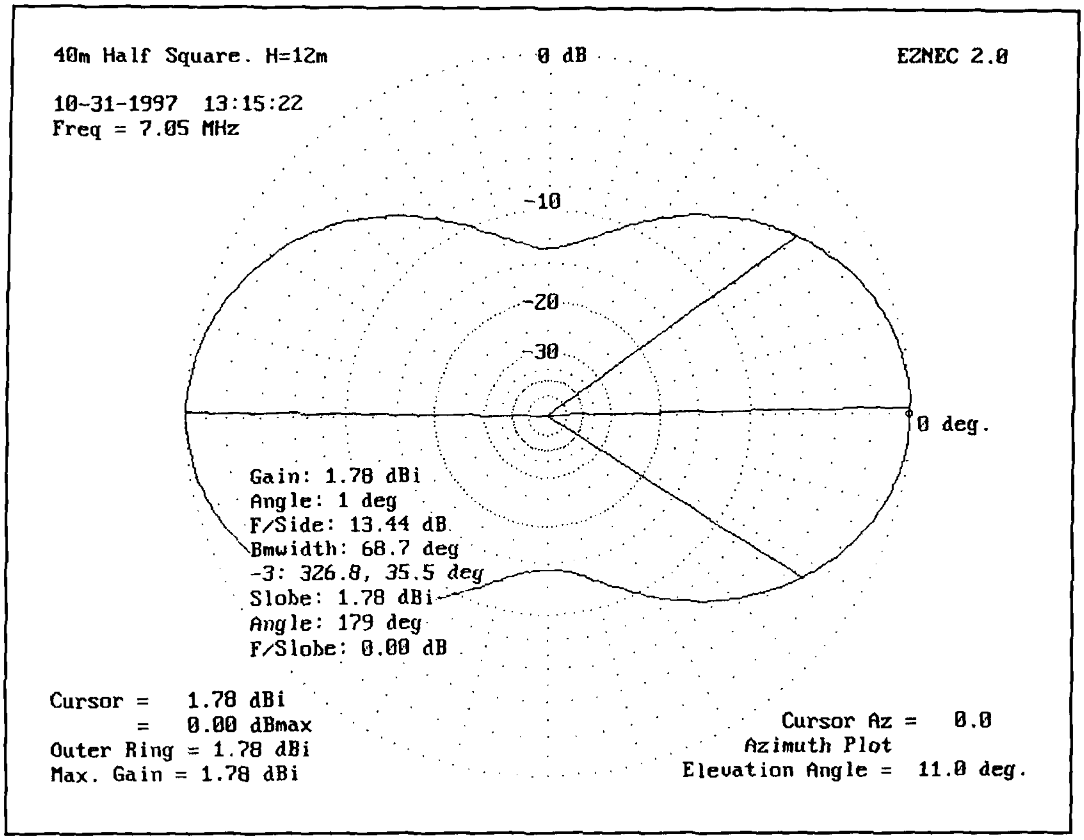

Figure 6. Simulated pattern of the 40-meter Half-Square antenna.

for two phased verticals spaced a half wavelength apart. The improved G5RV's gain came to 7 dBi in the main lobe. That explains the results of the on-the-air tests. The reason for this higher gain can, to an extent, be found in the fact that the legs of the multiband dipole are considerably longer than those of a 14-MHz half-wave dipole. Results on higher frequencies produced even more respectable gains. This antenna is definitely going to spend a lot of time on the higher bands once the sunspots decide to become active again!

Forty-meter Performance

The Half-Square antenna was originally intended for use on 40 meters, but I thought it might be possible to salvage something on the lower frequencies. Once again, the improved G5RV and the Half-Square battled it out on the computer for supremacy at a wave angle of 11 degrees above the horizon (**Figures 6** and **7**).

The Half-Square antenna delivers a bidirectional pattern with a simulated gain of 1.78 dBi. The nulls in the direction of the antenna are nearly 13 dB deep. All in all, it delivers very useful performance.

In comparison, the updated G5RV delivers a semi figure 8 pattern with a maximum gain of 1 - 1.16 dBi. This is fairly realistic for a dipole at close to a quarter-wave length above ground.

The gain difference between the updated G5RV and the Half-Square antenna is nearly 5 dBs in favor of the Half-Square. With a weak signal, this can make the difference between a station worked or a contact lost. Although not as deep as that of the G5RV, the nulls in the Half-Square's pattern can help to reduce off-axes QRM and improve the received S/N ratio under certain conditions. For me, the higher gain tilted the scale in the favor of the Half-Square antenna.

The next step was to be able to change the radiating direction of the antenna to make optimum use of band openings with the current lull in sunspot activity.

Changing the Direction of Transmission

In W8HXR's article, it's claimed that the antenna can be changed from a broadside firing array to an end-fire array with the aid of a quarter-wavelength transmission line. The transmission line is shorted at one end to accomplish an end-fire pattern or left open for the original broadside pattern. The idea is to add an additional 180-degree phase shift

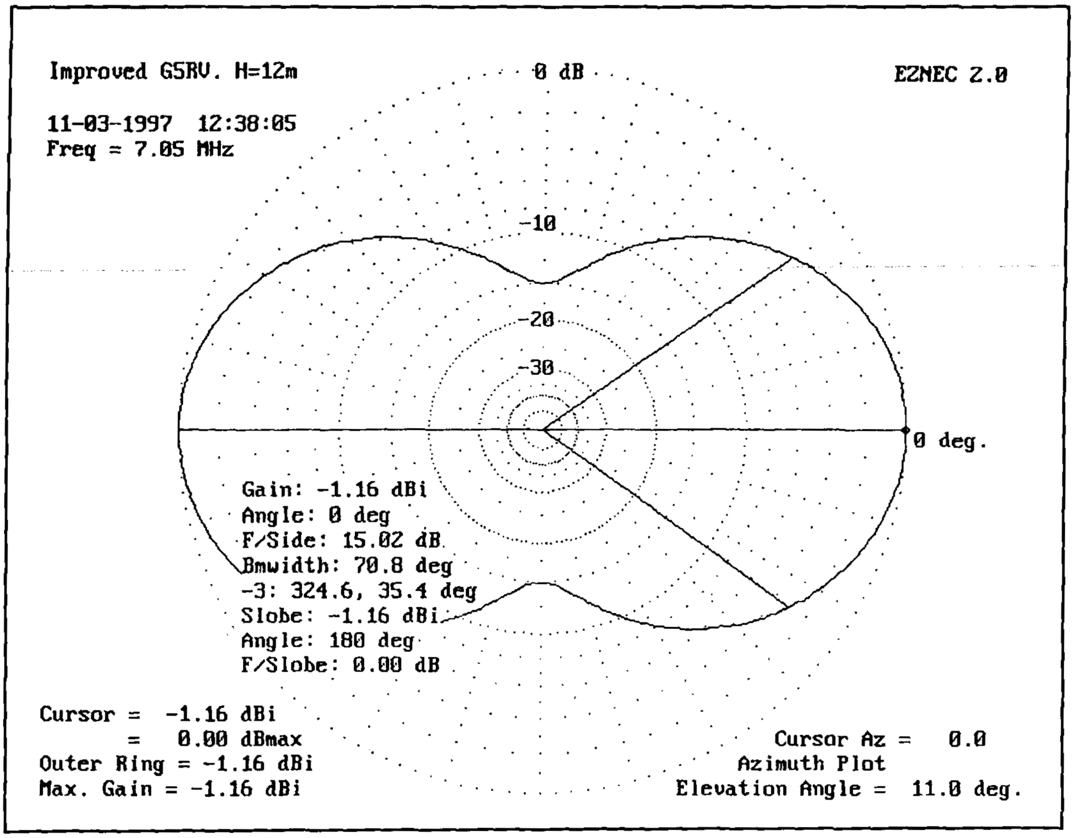

Figure 7. G5RV simulated at a height of 12 meters on 40 meters.

between the two verticals that can be switched in or out as needed.

Little red warning lights should start to flash the moment you look at the antenna shown in **Figure 8**. With the phasing line at a distance of a quarter wavelength between the vertical radiators, and also in the vertical plane, some serious interaction between the phasing line and the antenna is guaranteed. The phasing line might even start to think it's an extra element.

I tried the antenna on 20 meters with a quarter-wave phasing line made out of 300-ohm parallel transmission line. Results were very disappointing, even when the phasing line was placed in the horizontal plane.

Simulations on EZNEC showed that the horizontal line between the two vertical radiators also acts as an antenna, not only as a feedline. This gives the quarter-wave phasing line something more to interact with.

The quarter-wave phasing line is also placed at a high impedance point, and it may be that

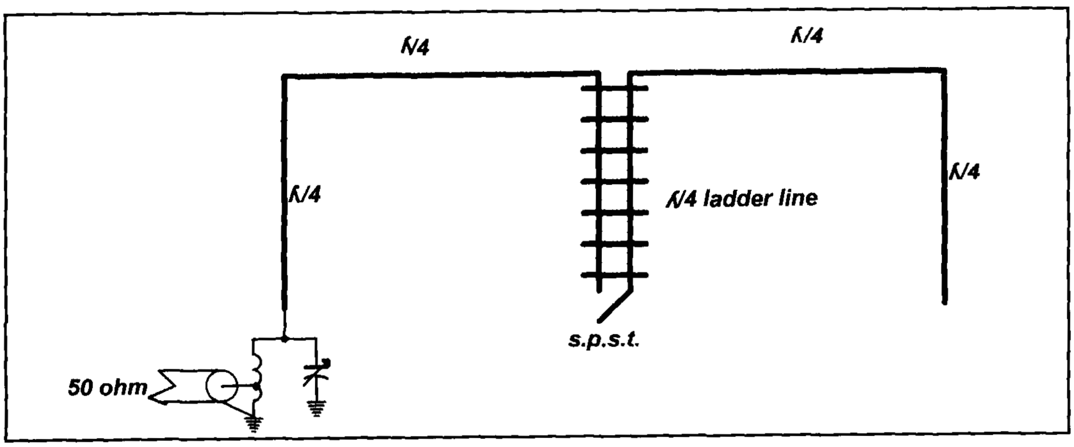

Figure 8. Changing the direction of transmission according to W8HXR.

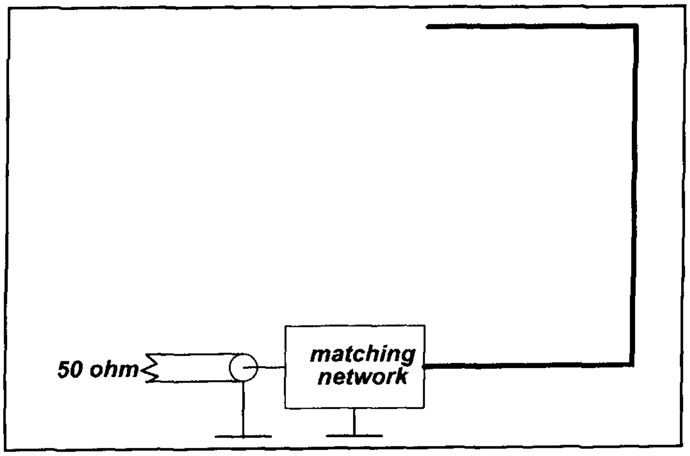

Figure 9. Lazy U antenna according to N4UH.

the 300-ohm line didn't present an acceptable match to the system. I'm not 100 percent sure about the exact reason for the problem, but the up-to-date version of EZNEC also agrees that the idea is definitely not sound.

Another Option

After going through all of the above, I felt there was definitely room for improvement. Being unable to change the radiation direction of the Half-Square antenna was a big drawback. I also wasn't very happy with the depth of the off-axes nulls. Although 13-dB suppression of an unwanted signal is definitely better than nothing, an addition 10-odd dB would be very nice to have.

It was time to engage the brain a bit before I switched the soldering iron on for the next round of experimentation.

Radiation by horizontal line is probably the cause of the lack of depth in the off-axes nulls. If this horizontal radiation can be reduced, the radiation pattern will definitely improve.

In the Winter 1992 issue of *Communications Quarterly*, Henry Elwell, N4UH described a short, vertically polarized antenna in which the horizontal radiation was to a big extent canceled out. The total length of the antenna is a half wavelength. He called his baby the Lazy U antenna (**Figure 9**).[4]

Phased Lazy U's

I figured that if two of these antennas were spaced a half wavelength apart, it might just provide a solution to my problem (**Figure 10**). "Conventional" means could be used to feed

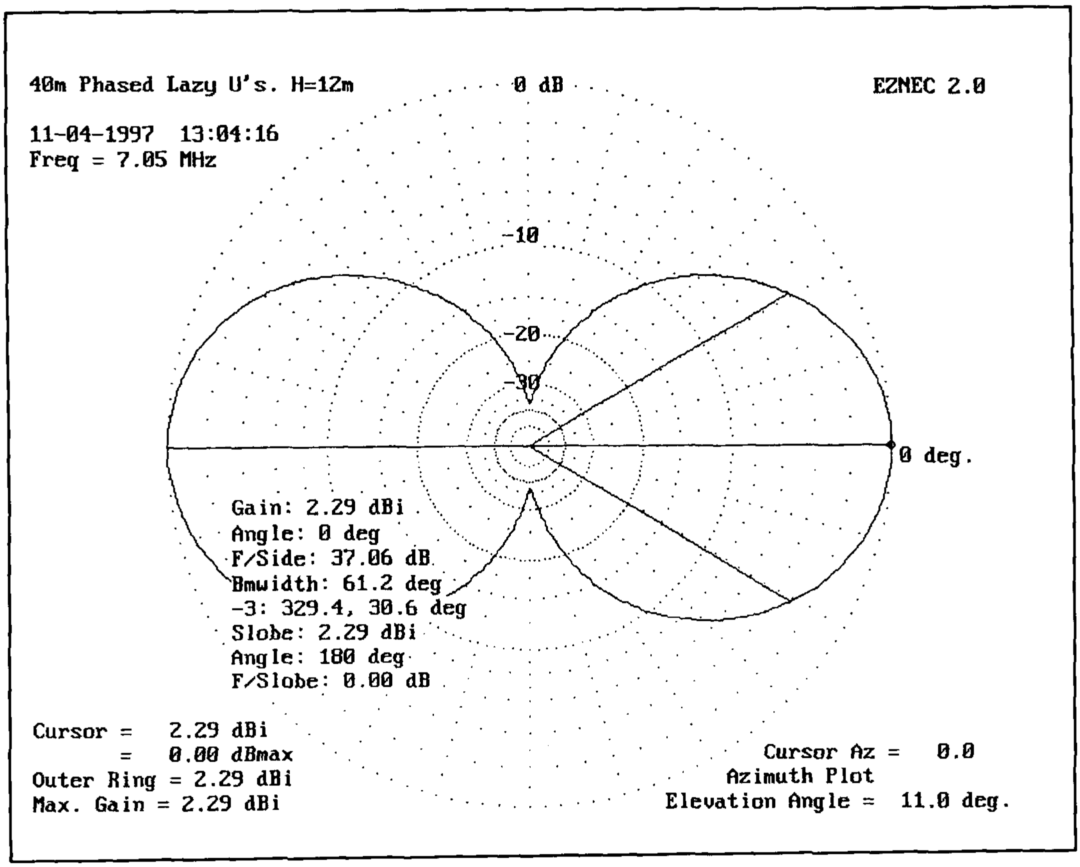

Figure 10. Phased Lazy U antennas.

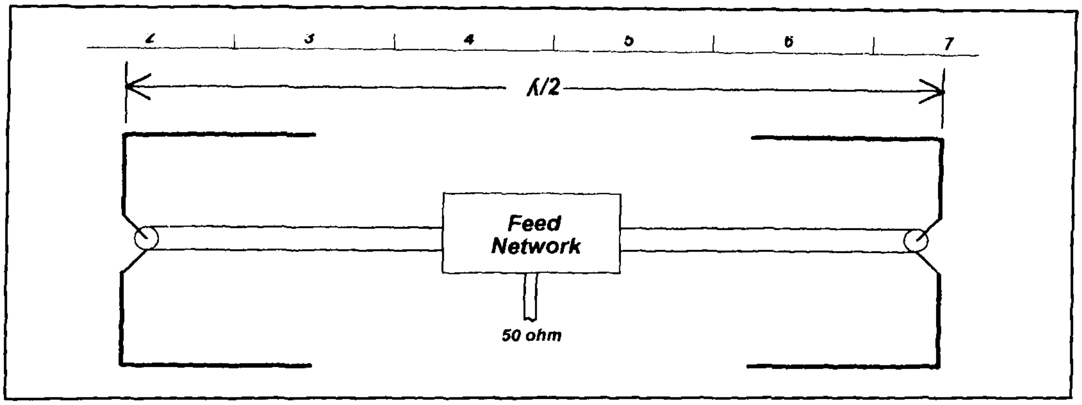

Figure 11. Simulated radiation pattern of the 40-meter Phased Lazy U's.

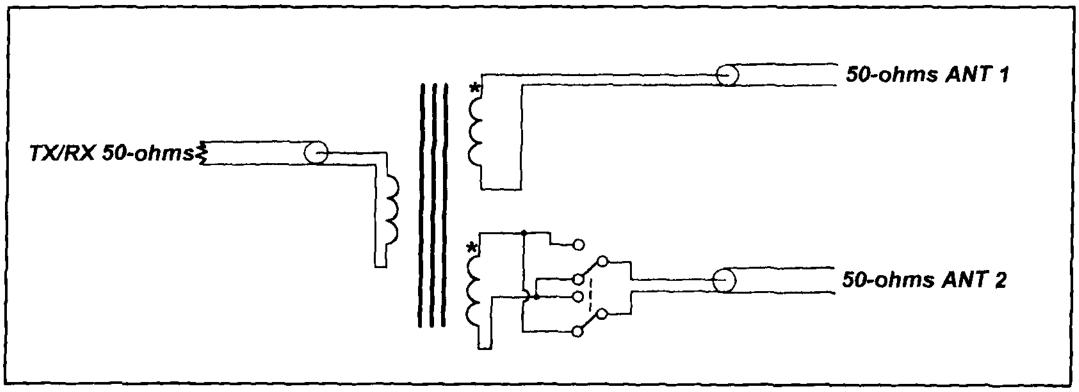

Figure 12. Details of the Phased Lazy U's feed system.

them, which would enable the radiation direction to be easily changed.

To fit on the 12-meter masts, and for operation on 40 meters, the vertical section of each Lazy U is 10 meters long with the lower ends 2 meters above the ground. The horizontal sections are each 5.2 meters long. The antennas are current-fed at the centers of the vertical elements. (This is the same method by which a dipole is "normally" fed.) Little time was lost in feeding this idea to EZNEC.

From **Figure 11**, you can clearly see the improvement in the nulls. As a bonus, the gain improved a little when compared to the Half-Square antenna of **Figure 6**.

Feeding the Array

The impedance of a single Lazy U is close enough to 50 ohms to keep any transmitter happy. Ensure that each antenna presents a proper match before connecting them in an array.

Equal lengths of 50-ohm coax are used between the two Lazy U's and the phasing transformer. The power to the two Lazy U's is equally divided by the two bifilar windings of the RF transformer (**Figure 12**). Ferrite toroids, such as those normally used as balun cores, can be used for the transformer. The winding that connects the feedline from the transceiver is also used to match the 25 ohms presented by the parallel connected Lazy U's to 50 ohms by means of the 1.414:1 turns ratio.

The radiation direction is rotated 90 degrees by changing the phase of the feed of one of the Lazy U's by 180 degrees.

Proof of the Pudding

Unfortunately, my work load has increased to such proportions that it will be some time before I will be able to put up Phased Lazy U's and perform some serious on-the-air evaluations. However, the computer simulations are so promising that I felt the idea had to be shared with other enthusiasts. Hopefully, things will improve soon enough so this antenna won't stay a computer simulation for too long.

Operation on Other Bands

According to the computer simulations, the Phased Lazy U's performance as an efficient DX antenna on 80 meters, or even 160 meters, should be hard to beat—if you've got the real estate to fit it in!

Last Thoughts

It will be interesting to make use of four Lazy U's in a four-square array. The high radiation efficiency of the individual radiators coupled to the selectable radiation direction should prove to be a winner on the low bands.

For low-band DXing, an efficient transmitting antenna system (Phased Lazy U's) represents 50 percent of the requirement for success. The other 50 percent is made up of operator skill and the use of enough transmitting power to ensure an adequate signal-to-noise ratio at the receiving station. In general, running barefoot isn't good enough for serious low-band SSB DXing.

Conclusion

Despite all the claims in the amateur press over the years, the Half-Square antenna is not the ultimate solution to all your communications needs. At 14-MHz and higher, a tribander at the same height definitely outperforms the Half-Square antenna by a fair margin.

On 7 MHz and lower, the Half-Square antenna has a distinct advantage over a small beam or dipole used at less than a third of a wavelength above ground. The directivity and off-axes nulls also count in its favor. The antenna is also simple to construct.

Phased Lazy U's are not as simple to erect as the Half-Square antenna, but the ability to change the radiation direction by simple means, as well as the deeper off-axes nulls and marginally higher gain, ensures better performance from this DX antenna when compared to the Half-Square antenna or a low dipole.

The fact that none of the above-mentioned antennas requires an extensive ground system counts for a lot of points in my book. ■

REFERENCES
1. Jerrold A. Swank, W8HXR, "Rotate the Bobtail Curtain," *73*, May 1985, pages 48, 49.
2. F.C. Smith, GW2DDX, "Variations on the Vertical," *Practical Wireless*, July 1987, page 26.
3. Brian Austin, ZS6BKW, "An Updated Version of G5RV Multiband Dipole," *Radio ZS*, June 1985, page 58, 59.
4. Henry Elwell, N4UH, "The 160-meter Semi Vertical: A Case History," *Communications Quarterly*, Winter 1992, pages 81–93.

PRODUCT INFORMATION

SDS Offers New On-Chip Debugging Environment

SDS, Inc., supports Hewlett Packard's (HP) new Emulation Tools strategy. SingleStep Emulation Solutions for HP's Emulation Probe family integrate the SingleStep graphical on-chip debugging technology with HP's latest logic analyzer technology. Complex RISC-based processors now have a real-time debug solution that meets the needs of both hardware and software development teams.

SDS' SingleStep Emulation Solutions and HP's Emulation Probe work together to deliver debugging and diagnostic capabilities, such as real-time trace functionality, advanced run-control, high-speed code downloading and programming of target system Flash memories. In addition, SingleStep Emulation Solutions handle unpredictable integration problems, such as those caused by hidden real-time dependencies with infrequent interactions. In such cases, the ability to trigger on a very small section of executable code often establishes the context for finding the cause of a timing problem in a hardware subsystem.

SingleStep Emulation Solutions can be used by design teams to build a comprehensive toolset with full cross-correlation capabilities and cross-domain triggering. The HP Emulation Probe can be integrated with a variety of HP real-time measurement equipment, including their latest logic analyzer systems, to extend functionality for a complete system debug environment.

Flash support is provided for developing products which ship before final standards are defined or when products must meet different regional or national specifications. SingleStep Emulation Solutions offer an easy to use GUI front end for programming Flash memory. This user interface supports a high-level command structure including program, erase, upload and verify, to mask the underlying complexities of controlling Flash devices.

SingleStep Solutions include compilers, simulators and debuggers for both ANSI C and C++. All tools support the ELF/DWARF standards and the M·CORE and PowerPC binary applications interface to provide complete interoperability across a wide variety of embedded software tools from a number of 3rd party suppliers. SingleStep Emulations also include integrated support for more than a dozen commercial real-time operating systems (RTOS) including pSOSsystem and VxWorks.

The SingleStep Emulation Solutions are available now and include both SDS software and HP hardware. Pricing starts at $5,495 for Windows and $7,395 for UNIX versions.

For more information, contact SDS, Inc., 815 Commerce Drive, Oak Brook, IL 60523; Phone: (630) 368-0400; Fax: (630) 990-4641; E-mail: <sales@sdsi.com>.

Dean W. Battishill, *W5LAJ*
7 Crest Way
Silver City, New Mexico 88061

THE CARE AND FEEDING OF THE 4CX1600B

Notes on specifications and usage

As we enter a new sunspot cycle, Dean's 4CX1600B amplifier should pique the interest of most DX and contest station operators. But, please note, this is a conceptual piece,not a construction article. While experienced amplifier builders would likely ferret out the missing details, we caution novice builders not to use this material as a first attempt at amplifier construction. For example, in the power supply, several voltage divider resistor values are given, but are lacking the wattage data. These values would have to be calculated with some margin for safety. Many of the smaller supplies for the filament, bias, screen, and relay voltages were originally shown as 120-volt AC designs, using the 220 neutral as a common return. Since this raises some safety issues, the editors have taken the liberty to redo the design using 220-volt components throughout. Meter shunts may require adjustment depending on the meters you select, and likewise the components associtaed with the RY2 relay time-delay circuit may also require some tweaking.

—Editor

Photo A. The Svetlana 4CX1600B high-performance tetrode.

The Svetlana 4CX1600B tetrode, now available in the United States, provides an ideal vehicle for the design of new, state-of-the-art tetrode power amplifiers.* The tube has exceptionally high power gain and a transconductance of 50000 micromhos. As such, the 4CX1600B requires care to obtain the expected performance. It is relatively rugged; there are only two areas that require watching. They are the two grids: screen and control. That isn't to say that they are particularly frail; they aren't. However, these grids are practically the only areas where a "heavy-handed" builder can challenge the tube design.

Although the circuit diagram of a highly successful amplifier built around the tube is included here (see **Figures 1** and **2**), most of its design details are not. This article was written

*Tube data sheets are available from Svetlana Electron Devices, 3000 Alpine Road, Portola Valley, California 94028.

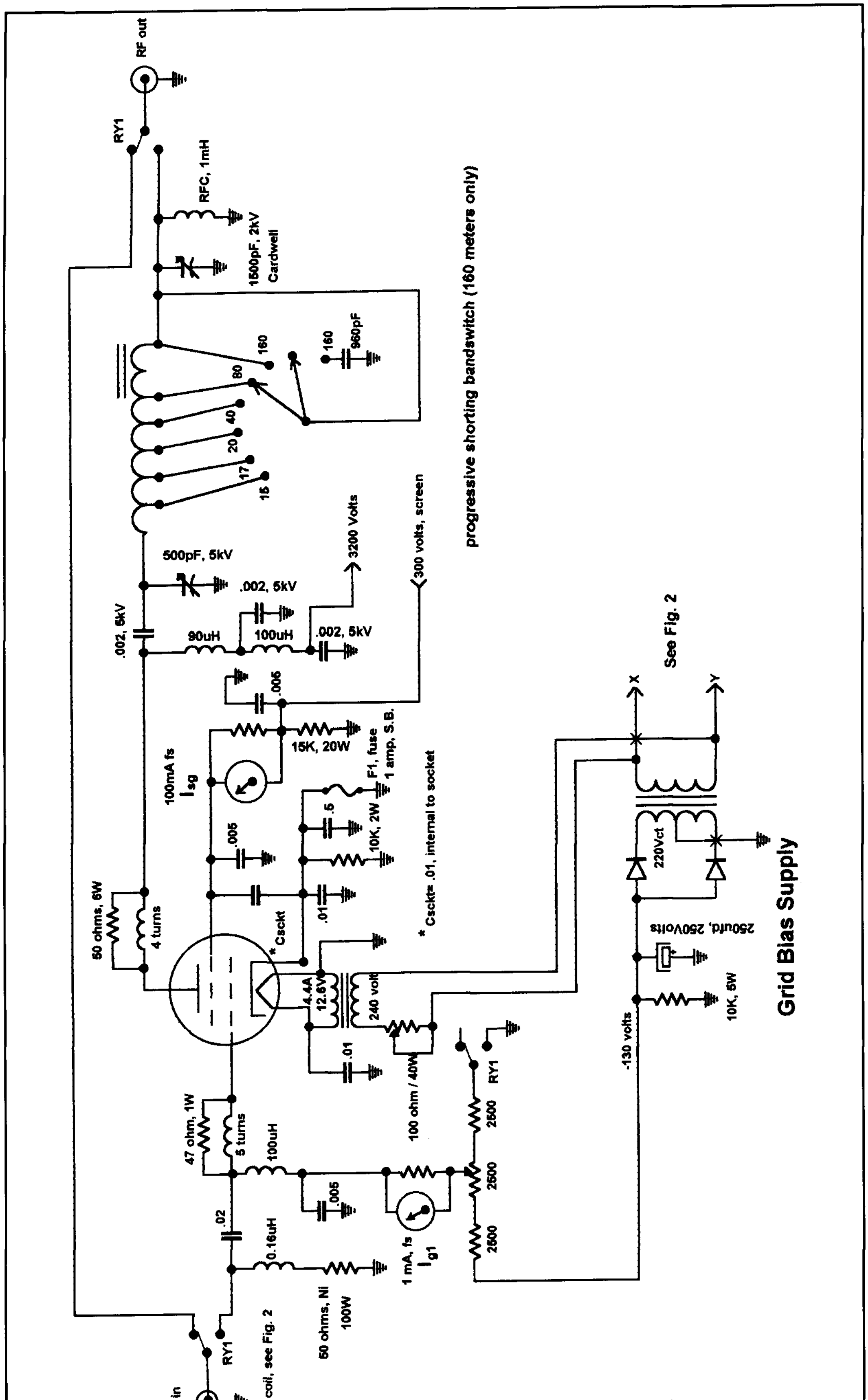

Figure 1. Amplifier schematic.

Table 1. Design Numbers from the Data Sheets

Cathode:	Oxide-coated
Voltage	12.6 ±0.6 V
Current, at 12.6 V	4.4 ±0.3 A
Voltage, cathode-heater	±100 V
Warm-up time	2.5 minutes (allow 4 or 5)
Direct interelectrode capacitance (gk)	86 pF
Cooling	Forced air
Recommended socket	Svetlana SK3A
Anode connector	Svetlana AC-2
RF Linear amplifier maximum ratings:	
DC plate voltage	3.3 kV
DC screen voltage	350 V
DC grid voltage	-150 V
DC plate current	1.4 A
Plate dissipation	1.6 kW
Screen dissipation	20 W
Grid dissipation	2 W

with the intent to describe good engineering practice *with respect to the '1600*, not as a "how to" article. However, there are some sophisticated design features which will be discussed in principle.

The tube

Photo A shows the 4CX1600B. The most important tetrode element (which influences the very high efficiency of the tube) is the anode and its interior. It is machined to present four annular cavities facing the center of the tube. They are numbered 27 (one number for four cavities). Their function represents the most important difference between the '1600 and other external anode tetrodes.

All tetrodes share a disadvantage. At the point where the instantaneous plate voltage drops near or below the screen potential, the screen attracts more of the cathode current. The cathode current is then reflected in a higher screen current reading. At this same point, the plate current is at maximum and more secondary electrons are produced. These electrons are attracted to the screen. If there is no design provision to circumvent or decrease the effects of secondary emission, the instantaneous low plate voltage *always* will produce heavier screen current.

That is where the design of the 4CX1600B shines. The aforementioned annular recesses in the anode are deep enough so that the bulk of the secondary electrons kicked out of the plate cannot escape the recess (the "trap") and are forced back into the plate. Those electrons normally would have to buck the incoming current, which may be on the order of one ampere. The cathode current stream carries with it a large negative charge commensurate with that current; hence it provides the field gradient (within the trap) to return the secondaries to the plate. Thus, it is possible for the plate voltage to dip *below* the screen voltage without producing inordinately high screen current. The most important benefit of this behavior is that the coincidental increase in *plate voltage swing* will produce both higher efficiency and higher power output. Actual confirming performance data will be presented at the conclusion of this article.

With a transconductance of 50,000 micromhos, the tube cannot be operated with a tuned-grid circuit without careful neutralization. It is designed for operation with a swamping resistor shunted directly between the grid and ground. The driver power is therefore dependent on the drive voltage (peak) and that depends upon the grid bias, also a function of the plate supply voltage. So the drive power for the tube usually is between, say, 30 and 50 watts, all of which is dissipated in the resistor. The recommended value for the shunt resistor is typically 50 ohms, non-inductive. It should be sized for the maximum *continuous* drive power, with some reserve power capability, say, 60 watts or so. It should be in the cooling air flow path; easy to do, because it will be near the base of the socket.

Table 2. 4CX1600 Air-Flow Requirements

(Air Inlet Temperature, 25°C)

Altitude	Plate Diss.,	Air Flow, cfm Watts	ΔP, Inches WG
Sea level	1000	22	0.20
	1600	36	0.40
6,000 feet	1000	27	0.25
	1600	44	0.50

(Air Inlet Temperature, 50°C)

Altitude	Plate Diss.,	Air Flow, cfm Watts	ΔP, Inches WG
Sea level	1000	27	0.33
	1600	47	0.76
6,000 feet	1000	33	0.40
	1600	58	0.95

The input capacitance of the '1600B is about 86 pF. That shouldn't be a problem on the lower bands, although a conscientious designer would certainly compensate for it. The amplifier shown here (**Figures 1** and **2**) uses a series compensating inductance, calculated to have equal and opposite reactance at 21 MHz. It was compensated only at 15 meters, and that seemed to be adequate. The main advantage seems to be in presenting a resistive load to the exciter. It would be slightly more serious at VHF; however, it proved to be no problem at 160 to 15 meters with the proper parasitic circuit and the compensated load reactance. The

Photo B. The front panel of the W5LAJ linear. Note unused input bandswitch in the lower right-hand corner. See explanation in the text.

inductance to compensate at 15 meters is 0.162 μH. The precision of an ordinary grid-dipper to evaluate the inductance is adequate. The maximum full-power rating is 250 MHz, so 15-meter operation presents no problems at all.

Svetlana recommends using the tube as a class AB_1 amplifier. This recommendation proves to be correct, and it operates very well with the no-grid current characteristic of AB_1. This particular tube wouldn't quite deliver 1500 watts at 3250 (loaded) plate volts (unloaded Ep is 3550). Because one objective was to deliver the full 1500 watts, it was decided to "push" it a little (very little) into class AB_2.

No one will notice the difference in transmitter power (at the receiving end) between, say, 1450 and 1500 watts. The exercise was performed just to see if it was possible, and to gain some additional experience. I don't recommend that anyone duplicate it. It's better to raise the screen voltage a little. The justification rests largely on the published maximum grid power dissipation. It is *2 watts, maximum*. Svetlana recommends limiting operating grid dissipation to 0.1 watt.

Let's re-emphasize that it is possible to push the tube in class AB_2, if you are comfortable with this type of work and if you can measure grid current with the necessary sensitivity and precision. The amplifier shown here has a "multimeter" type switch—with a difference. The grid current is measured on a scale position that is *1 miliampere full scale*. The necessary grid current to produce the desired 1500 watts is nominally ***110 microamperes***. Except for a small ego-trip, the increase in power and the delicateness with which it should be approached make such an adjustment not worth the trouble. Even so, the grid dissipation is quite adequate for this small excursion into class AB_2.

Important data

Some of the design numbers of use are listed in **Table 1**. More in-depth information is provided in the manufacturer's data sheet, which is available from Svetlana (address given in footnote). However, **Table 1** lists most of the necessary factors emphasized in the design of the W5LAJ amplifier. Though the absolute maximum grid dissipation is listed as 2 watts, Svetlana recommends no more than 0.1 watt as a matter of practice.

Cooling

This amplifier was constructed and operated at an elevation of 6,000 feet above sea level. **Table 2**, copied from the Svetlana '1600 data sheet, reveals that in order to operate at full plate dissipation ratings at the elevation of Silver City, New Mexico, and at an inlet air temperature of 25 degrees centigrade, 0.25-inch ΔP (w.g.) is required across the tube. The air flow is listed as 44 cfm.

A suitable blower, obtained either at a ham flea market or a supply house, may or may not

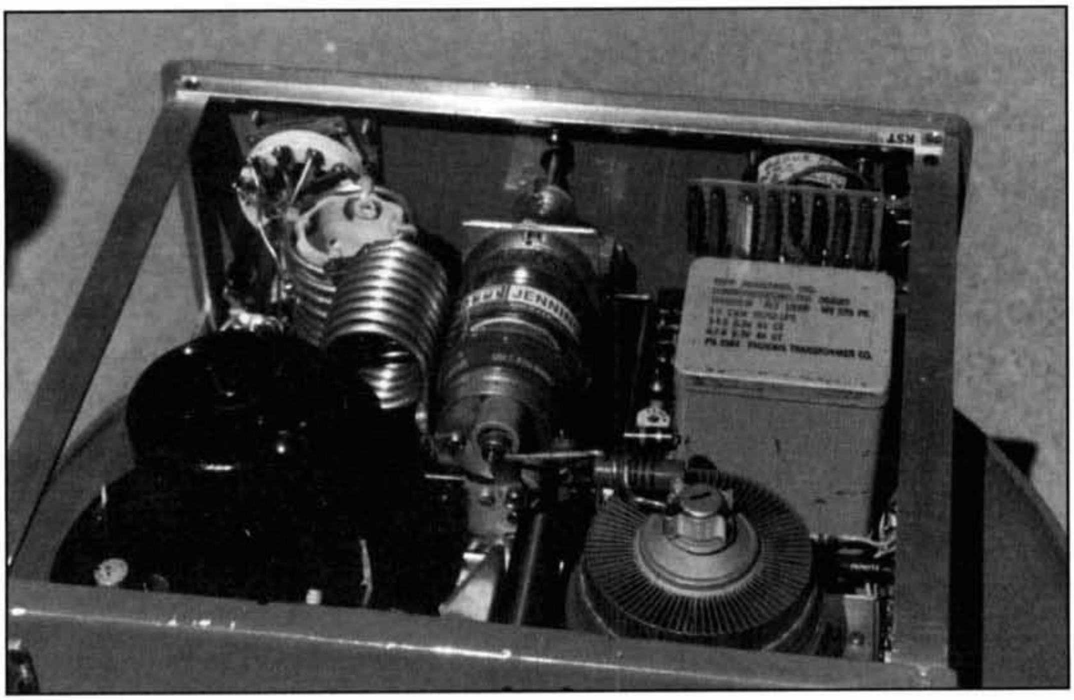

Photo C. Interior of the Svetlana 4CX1600B high-power linear.

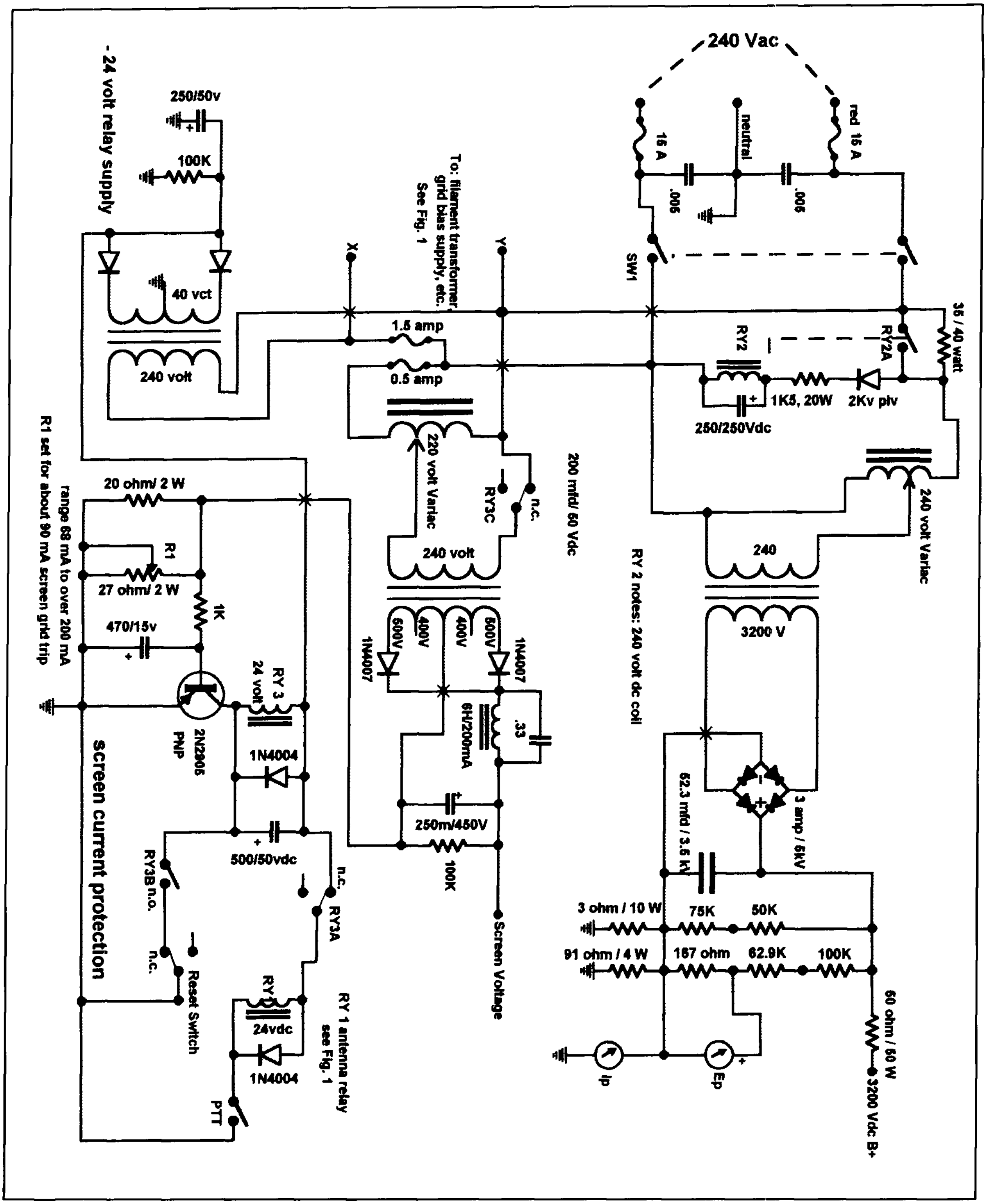

Figure 2. Power supply and protective circuits schematic.

provide successful results. The information on the nameplate may not be sufficiently accurate. Flow characteristics depend on the restrictions in the flow-path, which, for example, include even elbows and the like. It's always better to *measure it yourself*. Very few hams can measure flow, say in cfm, on their own. They *can* measure ΔP, the pressure drop around the tube anode. It can be done by improvising a temporary manometer of TYGON™ tubing and

Table 3. Amplifier Characteristics

Eg1	=	-54 V
Eg2	=	300 V
Ip (idle)	=	150 mA
Ebb (idle)	=	3550 V
Ip (loaded)	=	650 mA
Eb (loaded)	=	3250 V
Power out	=	1500 W
P drive	=	35 W
Ig1	=	110 μA
Isc	=	20 mA
[U.C. ETA] (efficiency)	=	70 percent

water. Pressure drops around the air paths will be different, and the blowers also will no doubt have different flow rates, for example. Air cooled tubes universally require centrifugal blowers; blade fans are high-volume, low-pressure drop devices. Always use the centrifugal blowers. The worst enemy of most electronic devices usually is heat, so these considerations are well worthwhile.

Screen voltage

The screen current may reverse occasionally; this is true of most tetrodes. The screen supply should be designed with this in mind. Svetlana recommends that a screen-to-cathode current path must be provided, and the source impedance of the supply should not exceed 3000 ohms. Linear operation requires a steady screen supply. This amplifier uses an unregulated supply, loaded so that an occasional "blip" of negative current can be absorbed by the bleed current. The screen supply source impedance should be at least 50 ohms in order to protect the screen in case of an arc. On the occasion of incidental or accidental removal of plate load or bias voltage, the screen voltage should be removed—the quicker the better. A screen protective circuit is designed into this amplifier.

Plate operation

The large current emitting surface of the cathode can supply *amperes*. The tube and associated circuits should be protected by including a series current-limiting resistor of 25 ohms or more. It should be capable of withstanding the high surge-current of an arc or short, and should not be used as a fuse. Svetlana recommends that you test your protection circuit by *shorting* the plate supply source to ground through a 0.09-mm diameter copper wire, at least 50-mm in length. The copper wire must remain intact.

The tube in operation

This amplifier operates very well (its efficiency is 70 percent). Other characteristics are listed in **Table 3**. The amplifier is unequivocally stable and has no bad characteristics. It is also very linear. No spurious radiation was detected, nor was any parasitic problem found. **Photos B** and **C** show the front panel of the W5LAJ Svetlana linear and its interior, respectively.

A working amplifier

Full schematics of the amplifier, power supplies, and protective circuits appear in **Figures 1** and **2**. I want to call out certain provisions (also specified by Svetlana) to accommodate the tube requirements. The cathode protective fuse is shown in **Figure 1**, as are some of the *auxiliary circuits* (PTT, etc.). The changeover relay (T/R) is shown as constructed. Should two relays be used, the output changeover relay should be the faster of the two. Ideally, the output relay should be a vacuum type, because its operation times are in the millisecond range.

The screen supply is somewhat special; it calls on techniques that have long since lost popularity. It operates as choke-input supply (not uncommon), which uses a resonating capacitor (uncommon) across the choke. This has the effect of stiffening the supply. It's an excellent application of a method that was used in the past for high-voltage plate supplies, except *this* one is for a screen supply. Linear amplifiers do require steady screen voltages.

All in all, the 4CX1600B is a very good tube, especially for this service and for other classes, too. It is linear, stable, easily tamed from parasitics, and is trouble-free. It is a delight to operate.

Acknowledgments

I want to thank Dick Linari, WØYXM, for his careful explanations of the vagaries of amplifier design. He is one of the most knowledgeable engineers I've ever encountered. His frequent sessions have been of inestimable value not only to me, but to many silent listeners as well. I would not have been able to use this tube to its full potential, or even understand fully how it works, without his help. ■

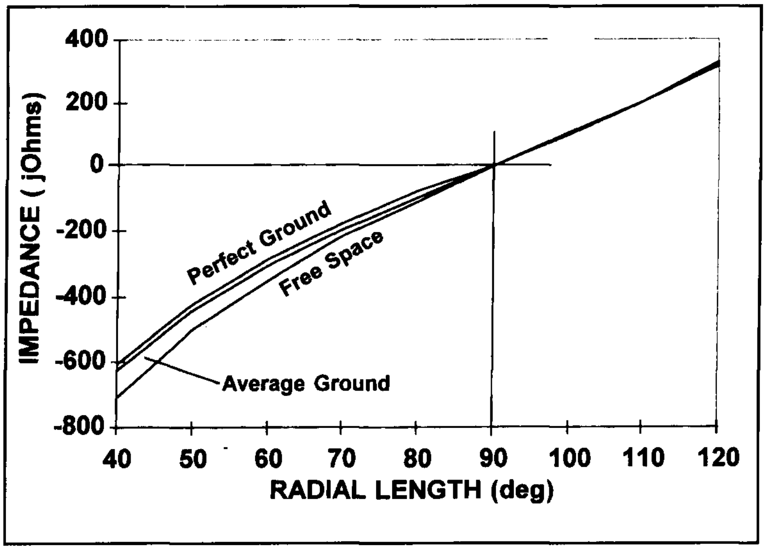

Figure 7. Impedance of a single radial, 10 feet above average and perfect ground.

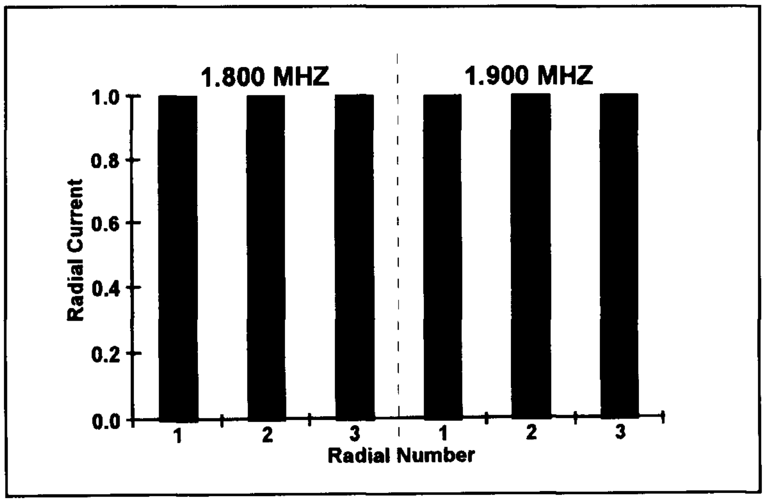

Figure 8. KE7BT's radial currents with 154-foot long elevated radials.

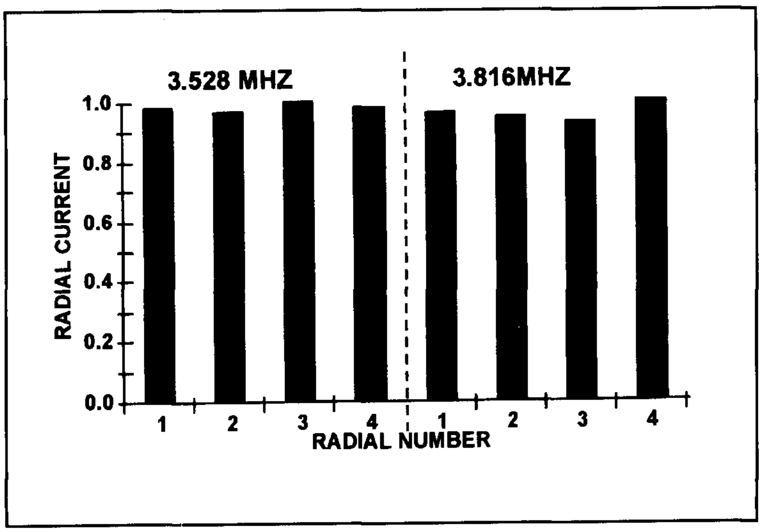

Figure 9. K5IU's radial currents with shortened radials (approximately 45 degrees).

avoid. These are the lengths that, if used for a radial system, will have the greatest sensitivity to minor radial impedance variations.

It is interesting to note that W7XU's radial currents shown in **Figure 2B** after making his 160-meter radials 127 feet long are still quite unequal. These radials are 15 feet high at the tower end, sloping down to about 5 feet. **Figure 11** shows that a radial length of 128 feet for 15-foot high radials and 125 feet for 5-foot high radials are 90 degrees long. Since W7XU's radials slope, the physical length to produce 90 degrees is between 128 and 125 feet. W7XU did exactly what Belrose advocates. The radials were made very close to a length of 90 degrees electrical and the resulting radial currents are highly unequal.

W7XU's original radial lengths that produced the currents shown in **Figure 2A** were as follows: SW radial was 126 feet,10 inches, NW radial was 129 feet, 1/2 inch, NE radial was 128 feet, 8 inches, and the SE radial was 129 feet, 3 inches. The SW radial probably has a length closest to 90 degrees electrical, while the remaining three are between 1.3 and 1.6 degrees longer. Here the SW radial had all the current, while those with several more ohms reactance had none. It is impossible to know for sure if the SW radial was exactly 90 degrees. But we do know there are several ohms differences in radial reactances. This data shows that minor length differences can contribute to radial currents being unequal. This data also conflicts with Belrose's position. Minor length differences can be the cause of unequal radial currents especially when the lengths are near 90 degrees. Minor length differences force the radial impedances to be different. The effect is greatest when the nominal radial length is targeted to be 90 degrees.

Figure 11 also helps explain the unequal radial currents shown in **Figure 3** for KE7BT's vertical and shown in **Figure 4** for KA2CDJ's system. KE7BT's radials were 15 feet high at the tower end, sloping down to 6 feet at the ends. Each were 130 feet long. Assuming average ground under this system, a 130-foot radial is about 92 degrees long. With these lengths, several ohms reactance difference among the radials would not have the same impact as if one of the radials was essentially at 90 degrees with an impedance of 0.0 + j0.0 ohms. At KA2CDJ, the radials used for the measurements shown in **Figure 4** were 133 feet long and 7 feet high. Again, assuming this system is over average ground, 133-foot radials have an electrical length of about 95 degrees. With these radial lengths, impedance variations of several ohms would be quite small compared to the nominal impedance. This accounts for the minor current imbalances measured at KA2CDJ.

In Belrose's article, he states that resonant quarter-wavelength radials can be used to simulate "connection" to ground for numerical modeling programs such as NEC2, which does not allow a wire to touch a lossy ground. I would like to discuss this. For a method to reasonably simulate a connection to ground, two requirements must be met. First, the method must simulate losses due to return currents flowing in the ground since the ground is what you're connected to. With elevated radials, currents flow as displacement currents in essentially lossless wires while minimal current flows in the ground as return currents which couple to the elevated radials. Elevated radials improve efficiency by minimizing the current that flows in the ground as return currents. With a real-world ground connection, all currents from the ground side of the antenna return to the feedpoint through the lossy ground. Clearly, ground losses are not accounted for when elevated radials are used to simulate a connection to ground.

Second, the method used to simulate connection to ground should not introduce extraneous radiated energy. Belrose provides an example on page 37 in his article. Here he shows the predicted radial currents for my 80-meter elevated radial antenna when near a tower. He shows the radial currents are not equal. Because the radial currents are unequal, there will be horizontally polarized energy radiated. This energy does not exist when connection is made to a real ground. Belrose's idea of using 90-degree radials as a method to simulate connection to ground has two flaws: this method does not capture real ground losses, and it can introduce extraneous radiated energy.

Modeling I did of my installation using a more accurate system geometry and 90-degree radials predicted unequal currents as shown in **Figure 13**. Here, too, 90-degree elevated radial currents are not equal. This is similar to what Belrose shows. As a result, horizontally polarized energy is radiated. When my model was changed to use 45-degree radials, the currents shown in **Figure 14** were predicted. With 45-degree radials, the model predicted almost equal radial currents. Based on the data in **Figure 14**, and the measured radial currents using 45-degree radials as shown in **Figure 9**, I suggest that 45-degree radials should be considered as a potential method to simulate a connection to ground. Using 45-degree radials essentially eliminates unequal radial currents and produces no extraneous energy. The only remaining issue is to replicate ground losses. Perhaps someone can work out a means to do this. Maybe highly resistive wire could be used for the model's elevated radial conductors. This would probably require a range of conductor sizes and companion resistivities to replicate a range of lossy grounds.

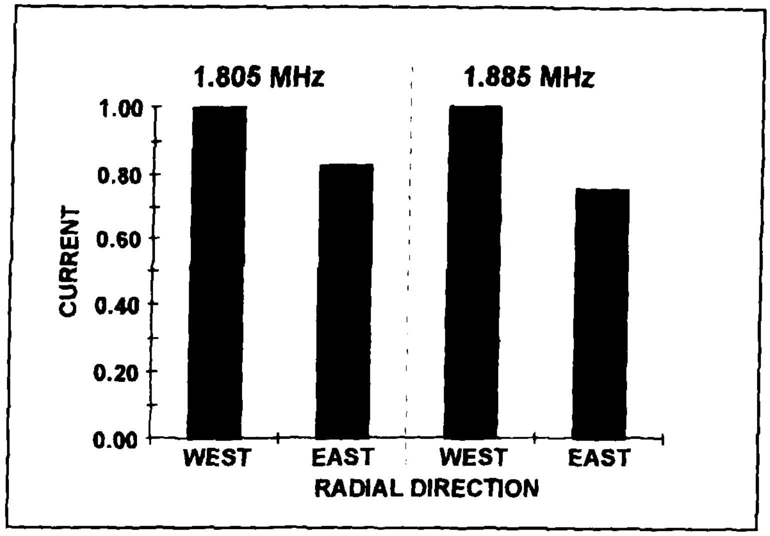

Figure 10. WXØB's antenna #1 with shortened radials.

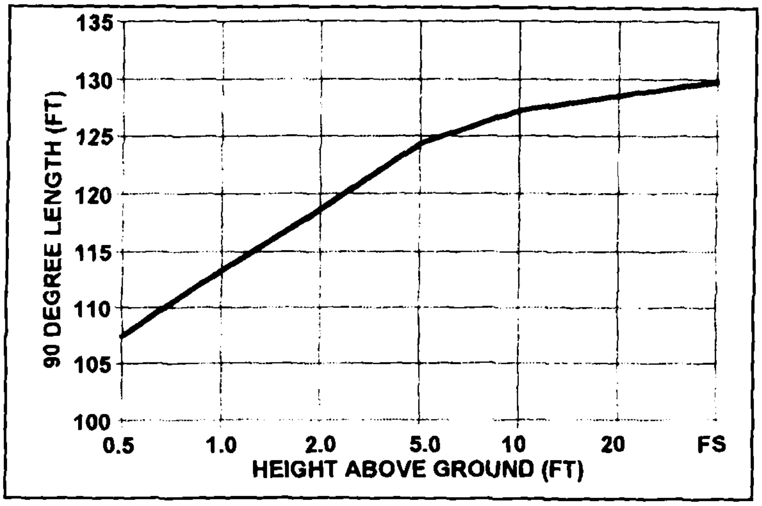

Figure 11. Length of 90-degree line over average ground at 1.85 MHz.

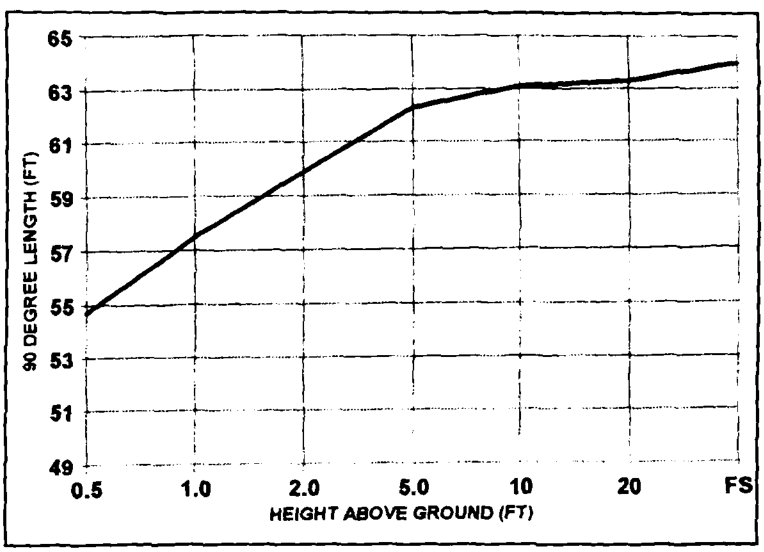

Figure 12. Length of 90-degree line over average ground at 3.75 MHz.

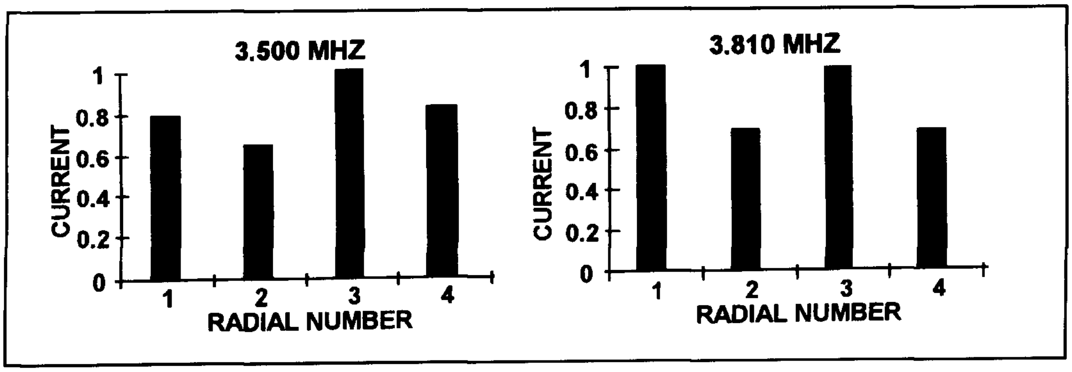

Figure 13. Predicted quarter-wavelength radial currents, near tower.

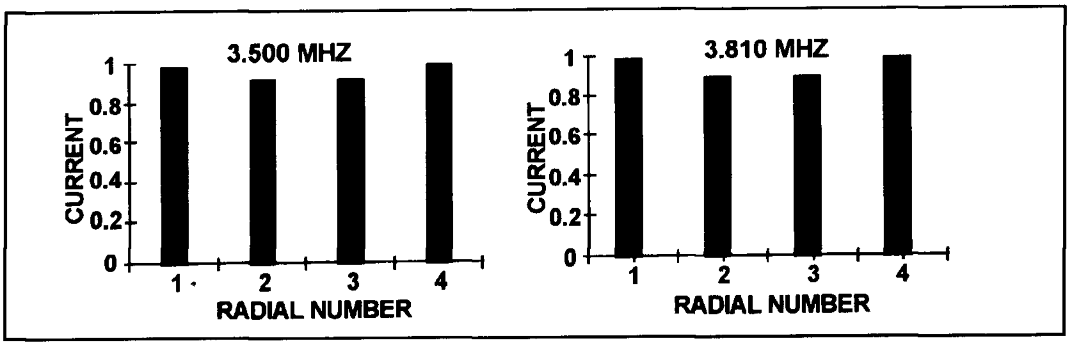

Figure 14. Predicted 45-degree radial currents near tower.

After reviewing measured radial current data taken with five different elevated radial vertical antenna systems, and studying Belrose's and my predictions for elevated radials in the near proximity of a tower, it is hard to find anything positive to say about 90-degree elevated radials. However, we can say we know which lengths to avoid when building practical elevated radial verticals or when attempting to simulate a ground connection.

Dick Weber, K5IU
Prosper, Texas

REFERENCES

1. John S. Belrose, VE2CV, "Elevated Radial Wire Systems for Vertically Polarized Ground-Plane Type Antennas," *Communications Quarterly*, Winter 1998, page 29.
2. Dick Weber, K5IU, "Optimal Elevated Radial Vertical Antennas," *Communications Quarterly*, Spring 1997, page 20.
3. Dick Weber, K5IU, "Optimal Elevated Radial Vertical Antennas," *Communications Quarterly*, Spring 1997, page 17.
4. Mr. Duane Walker, KE7BT, personal correspondence, January 1998.
5. Mr. Steve Hanzlik, KA2CDJ, personal correspondence, September 1997.
6. Dick Weber, K5IU, "Optimal Elevated Radial Vertical Antennas," *Communications Quarterly*, Spring 1997, page 16.
7. Dick Weber, K5IU, "Optimal Elevated Radial Vertical Antennas," *Communications Quarterly*, Spring 1997, page 13.
8. Dick Weber, K5IU, "Optimal Elevated Radial Vertical Antennas," *Communications Quarterly*, Spring, 1997, pages 9–27.
9. Dick Weber, K5IU, "Optimal Elevated Radial Vertical Antennas," *Communications Quarterly*, Spring 1997, pages 17–19, 23, 24.
10. Dick Weber, K5IU, "Optimal Elevated Radial Vertical Antennas," *Communications Quarterly*, Spring 1997, page 16.
11. John S. Belrose, VE2CV, "Elevated Radial Wire Systems for Vertically Polarized Ground-Plane Type Antennas," *Communications Quarterly*, Winter, 1998, page 35.
12. John S. Belrose, VE2CV, "Elevated Radial Wire Systems for Vertically Polarized Ground-Plane Type Antennas," *Communications Quarterly*, Winter 1998, page 37.

The Saga Continues

Dear Editor:

Our paper on the source impedance of tuned RF power amplifiers and the conjugate match (Fall 1997 issue) has certainly stimulated an immediate response. (This is evidenced by "Technical Conversations," Winter 1998 issue, and correspondence received by the authors.)

Letters that contain disparaging comments (directed toward editor and authors) of our attempt to clarify misconceptions and misunderstandings are unwarranted in a technical debate and are not helpful if the writer offers no technical reason why they believe that our opinion is unacceptable, other than that the arguments made are circular. In our opinion, our arguments are not circular, and we suggest a review of portions thought to be circular, along with a dash of introspection as motivation to ultimately perceive our arguments to be quite logical.

Clearly authors of such letters have read, but (as best we can judge) not understood our position. We wonder if they have read Warren Bruene, W5OLY's, publications on the subject, so that both sides of the debate can be put in perspective? We also wonder if they realize that statements appearing in Bruene's publications run counter to universal knowledge on the concept of the conjugate match that have been with us for more than 60 years?

Perhaps the problem is because we have not written in a manner which can be understood by the amateur in radio; or because we have attacked the problem on too many fronts in our attempt to convince the reader, who, as a result, does not see the forest but becomes lost amongst the trees. Or, finally, perhaps the reader is a follower of the concept that power amplifiers are **not** tuned for a conjugate match to their load, and in any case that the concern about conjugate match is for the most purposes unnecessary. Naturally, we disagree with these two latter positions.

Of a few letter responses, only one was published (the one by Bill Carver, W7AAZ), that complimented the authors on the clarity of their presentation, and for the excellent job of setting the record straight, confirmed by our various measurement techniques. However, it is apparent that some of our respondents don't understand that the debate concerning the conjugate match originated with Bruene's insistence to the ARRL that Maxwell's use of the conjugate match in his *QST* articles of the 1970s, his writings on the Z_0 match in the ARRL *Handbooks*, and in his ARRL book *Reflections—Transmission Lines and Antennas* is incorrect and should be expunged from all ARRL publications, because he (Bruene) claims the conjugate match cannot exist where RF power amplifiers are involved. (See **Reference 9** of our Fall 1997 article.)

Ignoring and refuting the opinions and publication approval of the late George Grammer and Doug DeMaw (the earlier managers of the ARRL technical department), the League editors acquiesced to Bruene's demands and deleted Maxwell's writings from their publications. This despite personal congratulations to him from both Grammer and DeMaw for what they considered an excellent and novel way of explaining and using the conjugate match with RF power amplifiers.

William Sabin, WØIYH's, correspondence ("Technical Conversations," Winter 1998) requires a more detailed response. While Sabin's technical discussion is interesting, he is concerned with **untuned** Class-A amplifiers, whereas we are concerned with **tuned** Class B and C amplifiers. *It is essential to understand that the fly-wheeling tank circuit is fundamental to Class B and C operations and analysis.* Note: we have read Sabin's views before; in our paper, we referenced his *QEX* September 1995 article (see **Reference 8**), and we have used the method he suggested to determine the output impedance of an operating amplifier (see below). Sabin's letter makes a number of points that need further discussion or comment.

1. Since for SSB amplifiers the power output with speech modulation varies from zero to full power, the amplifier's source impedance or output impedance must also vary, but by how much, see below;

2. Sabin's letter, in our view, still confuses resistance (e.g., plate resistance) and output impedance (which is a non-dissipative resistance, Re = V/I = Z_{out}, since $Z_{out} = R + j0$ when the amplifier is properly tuned);

3. When we say that the amplifier is loaded to maximum (design) output power, we mean loaded to achieve **rated** power. We do not imply loading to "maximum possible output power," such that the "tube(s) are driven and loaded to their extremes," in which case nonlinearities are involved;

4. We are perplexed by Sabin's view in "Technical Conversations" that the experimental setup devised by Bruene, which provided a means to "look back" into an operating amplifier, does *not measure* the dynamic output impedance of the amplifier. Bruene's measurements, which he felt supported his view, appear in a chapter of a book for which Sabin is a principal editor (see **Reference 14** in our paper); and

5. We are also perplexed by Sabin's view that concern about conjugate matching is unnecessary. Consider first a generator adjusted to deliver all its available power into a transmission line of impedance of Z_0. Next, consider the Z_0 mismatch appearing at the junction of a transmission line and the input terminals of an antenna. Here the reflected power reaching the generator reduces its delivery of power by the amount of the power reflected, unless some sort of impedance matching device is inserted somewhere in the line to restore the generator output to the power it would deliver had there been no z_0 mismatch (its available power). As we know, with an antenna tuner inserted at the input of the transmission line, and adjusted to obtain an input impedance equal to Z_0, the generator will again deliver all of its available power. To achieve this return to the delivery of *all available* power, the antenna tuner has provided a **conjugate match** *in the entire system*, which overrides the Z_0 mismatch at the line-antenna junction, permitting the antenna to *absorb all of the available power*. And, it is universally known that, if there is a conjugate match anywhere in the system, there is a conjugate match **everywhere** in the system, *including the RF power amplifier*. Consequently, concern about conjugate matching **is important** because conjugate matching exists in every transmission system that includes impedance and matching devices that achieve the delivery of all available power from the source to the load. And this means the inclusion of the pi-network as the impedance matching device that matches the output impedance, Z_{out}, of the source (the RF power amplifier) to the line impedance, Z_0. One of the tenets of the conjugate match is that, if the generator is delivering

all its available power to the load, **there is a conjugate match**. (See "Microwave Mismatch Analysis," *Hewlett-Packard Application Note 56*, by R.W. Beatty of the NTIA, formerly the National Bureau of Statistics.)

Let us look in some detail at the first point. Sabin presents results for an SB-400 amplifier, based on his resistance variation method, a method which we refer to as Sabin's method, that in his view (and also in our view) measures the output impedance of the amplifier. In our paper, and see below, we measure quite different values for the output impedance of a Kenwood TS-830S (which like the SB-400 amplifier uses a pair of 6146s). Sabin's measurements of output impedance indicate 147 ohms at 100 watts, 460 ohms at 50 watts, and 325 ohms at 25 watts. His measurements appear to be widely scattered compared with ours, and with no apparent proportional relationship between power and output impedance.

Our measurements, taken to obtain the results which we describe below, were performed using the Sabin method to determine the output impedance Z_{out} of an operating RF power amplifier, in which $Z_{out} = \Delta E/\Delta I$. ΔE and ΔI represent the corresponding changes in load voltage and load current, respectively, with change in the load impedance Z_{load}. In our experiments, all values Z_{load} (Z_1 and Z_2) are pure resistances, $R + j0$.

The amplifier for our experiments (a Kenwood TS-830S, as noted earlier) is initially terminated with Z_1, then tuned and loaded to a specific output power with a given level of drive, with the loading adjusted to deliver maximum available power at the given drive level. The load voltage, E_1, is then measured with load Z_1. Subsequently, we measure E_2 after changing the load to Z_2. The load currents I_1 and I_2 are determined by calculation of $I = E/R$, using the measured values of R_Z and E. Finally, as stated above, $Z_{out} = \Delta E/\Delta I$. Load impedances Z_1 and Z_2 were measured using a Hewlett-Packard RF Vector Impedance meter HP-4815 with digital readout. Load voltages E_1 and E_2 were measured using a Hewlett-Packard Vector Voltmeter HP-8405, also with digital readout. **Digital precision is absolutely essential in reading the small variations in load impedances and load voltages to obtain the necessary degree of accuracy for meaning values of Z_{out}.** We wonder if the scattering of Sabin's values could be the result of reading only from the analog scale of his Boontoon 92A RF voltmeter.

In our first experiment, we adjusted for an initial power out of 120 watts, initial load Z_1 = 51.2 ohms. No further changes were made after adjusting loading control and plate tuning for maximum available power at the present drive level. At this power level, we measured Z_{out} by the Sabin load-change method. Repeating the experiment five times, Z_{out} was measured equal to 49.4 ohms, 51.7 ohms, 52.5 ohms, 53 ohms, and 58.5 ohms, for a mean value of 53 ohms (see **Note 1**). Also note the small scatter compared to Sabin's.

The power was then decreased by reducing the drive, leaving the loading and plate tuning controls unchanged. When the power was reduced to 50 watts, Z_{out} = 33.3 ohms; and when the power was cut back to 25 watts, Z_{out} = 37.3 ohms.

In our second experiment, the amplifier drive level was set with loading and plate tuning adjusted for maximum available power at two different power levels: first for a power level of 50 watts, and then for 25 watts, Z_{out} was measured equal to 33.3 ohms and 37 ohms, respectively. These are identically the same values measured at these power levels (the first experiment) for the case where the initial adjustment was for a full power output (120 watts) and no further adjustments of loading and plate tuning were made where the power output was reduced by reducing the drive level.

In conclusion, when the amplifier is tuned and matched to deliver its full (design) power, **it is found by our measurements to be conjugately matched**; i.e., $Z_{out} = Z_{load}$ (also see **Note 2**). While our measured values for the output impedance apparently decrease when the amplifier's power output decreases by a decrease in drive power (which occurs when the amplifier is modulated by a SSB voice signal), the output impedance does not vary substantially and discontinuously with PEP. And finally, the amplifier **does not** have to be driven so hard that nonlinearities are involved in order that its source impedance is equal to the typical load impedance of 50 ohms. The amplifier is conjugately matched when delivering rated power.

Walter Maxwell, W2DU
DeLand, Florida
John S. Belrose, VE2CV
Aylmer, QC

Notes

1. To appreciate the small magnitude of the changes to be measured to determine Z_{out} by Sabin's resistance change experiment, one set of measured results is presented below:

Power output = 120 watts

Z_1 = 51.2 ohms	E_1 = 75.9 volts	I_1 = 1.482 amps	
Z_2 =44.6 ohms	E_2 = 70.6 volts	I_2 = 1.583 amps	
SWR = 1.15	ΔE = 5.3 volts	ΔI = 0.10 amps	Z_{out} = 53.0 ohms

Clearly digital read-out instrumentation ***must*** be used to measure these small changes.

2. In our paper in the Fall 1997 issue (see page 33), it was noted that there is nothing special about tuning for a match to 50 ohms, since the pi-network tank circuit of the PA could be tuned to deliver maximum available (design) power into a 25 or 100-ohm load, or any other load of reasonable value. This is obviously true, but in the follow on, we infer that in these cases Z_{out} would equal 25 or 100 ohms. However, we did not measure Z_{out} for inclusion in the Fall article. We have now performed the experiment in which we tuned the pi-network tank circuit of the PA for a load different from 50 ohms, and we have measured Z_{out} (by the Sabin resistance change experiment). For a Z_{load} (or Z_1 in the experiments described above) equal to 25.7 ohms and 16.7 ohms, we measure Z_{out} equal to 33.7 and 13.7 ohms, respectively.

I'm not convinced

Dear Editor:

I have only recently (in the past year or so) been a subscriber to *Communications Quarterly*, but look forward to each issue. Obviously, some article/issues appeal to my interests more than others, but each issue has something interesting. I applaud your efforts to provide both sides of a controversy, as you have done with the article on conjugate matching; but I hope that you don't devote large portions of each issue to the matter.

I have to admit that I didn't finish the article; after about eight pages, I decided that I had more important things to do, and only skimmed the last seven or eight pages. In this case, the authors did not convince me. What I read was a little too much like pseudo-science: a conclusion was formed, then tests were performed, and evidence was found to support the preordained conclusion.

While the authors went to a great deal of effort to measure actual output impedances, I am not completely comfortable with their technique. Source impedance is most directly measured by varying the load and observing the changes in voltage and current. I would like to see their measurements confirmed with techniques more like those of William E. Sabin, WØIYH, in the Winter 1998 issue.

While the conjugate match theorem is most certainly true, the converse is not necessarily true. Just because a load has been adjusted for maximum power doesn't mean that the source impedance is the conjugate match of the load. Other factors and circuit limitations can affect the power. Nor is it necessary to always match the source—certainly most people do not try to match the source impedance of the local power utility when they use the AC line. State-of-the-art DC power converters offer another good example; efficiencies of 80 to 90 percent are not obtained by matching the source impedance.

I also have problems with the long discussion of "non-dissipative" real impedance. I don't buy any of it! The real part of impedance (unless negative) is a dissipative impedance: the only question is where the dissipation occurs. In the case of a transmission line, the dissipation is in the load; but that doesn't make it any less real. That dissipative element is reflected in the impedance measured at various points along the transmission line—the transmission line, in effect, being a transformer.

I would like to point out what I consider an obvious error in the discussion and use of the "compensation theorem" on page 26. I have to admit, I don't remember any such theorem, nor could I find any reference to it in any of my text books; but no matter, it is self-evident. However, it fails to state that it assumes, and only applies, for a fixed network that is not changed or modified.

Near the bottom of page 26, the authors say "the tube can be replaced by a generator of zero impedance, whose generated voltage at every instant of time is equal to the instantaneous potential that exists across the load impedance R_L) due to the current flowing through it." That is okay, as far as it goes. Then they go on to claim that since they know the voltage across, and the current through the load; and since the same voltage and current come from the same source, that therefore, the source impedance must equal the load impedance.

I'm sorry, I don't know how to say it politely, but that is just plain nonsense. By their own definition, the source impedance is ZERO! The voltage and current do, in fact, define the load impedance; but they say nothing at all about the source, as they have just proved. The only way to determine source impedance is to vary the load and observe the resulting change in voltage and current. With a fixed load, there is no way to know what the source impedance is.

But, and here is the assumption that the authors ignore, the whole compensation theorem is only valid when you do not change the network or its values. That makes this theorem useless for determining source impedance.

A simple example: A 100-volt source with a 99-ohm source impedance drives a 1-ohm load. It is quite easy to calculate that the voltage across the load is going to be 1 volt; so, replace the 100-volt/99-ohm source with a 1-volt/0-ohm source and the 1-ohm load can't tell the difference. That is what the theorem says. But now change the 1-ohm load to 1/2 ohm, and you can easily see that the real 100-volt/99-ohm source will give an output voltage of about 1/2 volt, while the 1-volt/0-ohm source will still provide 1 volt out.

I certainly have no problem with an RF amplifier being designed to drive a conjugately matched load, but it isn't necessary, nor does it really matter. In fact, I could probably make a couple of million dollars if I could provide an RF amplifier with zero source impedance.

Controversy can certainly increase the level of interest and excitement; but a little goes a long way.

Jay Wicklund, KI7RH
halcyon.com

The classic cube problem

Dear Editor:

Still using Kirchoff's Laws, the problem of the cube of resistors can be much simplified if one invokes the principle of symmetry. If the cube is divided down a plane of symmetry then R_3 and R_5 are split down the middle and become R_3' and R_3'' and R_5' and R_5'', respectively, each component having twice the value of the mother resistance, namely two ohms. Having performed this operation, we have two identical parallel networks which connected together form the original cube. One of these half networks is shown in **Figure 1** where it will be seen that it comprises only three meshes.

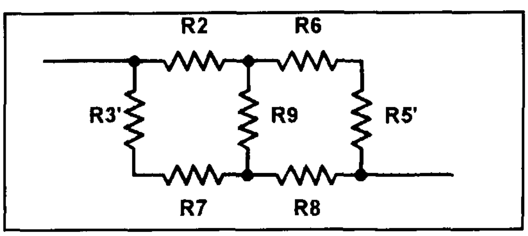

Figure 1. $R_2 = R_6 = R_7 = R_8 = 1$ **ohm;** $R_3'=R_5'= 2$ **ohms.**

Assuming, as does WV8R, that 10 volts is applied across the circuit, we can set up the three mesh equations.

$$10 = 2I_3 + I_7 + I_8$$
$$10 = I_2 + I_6 + 2I_5$$
$$10 = I_2 + I_9 + I_8$$

Adding these together, we obtain:

$$30 = 2I_2 + 2I_3 + 2I_5 + 2I_8 + I_9 + I_6 + I_7$$

But $I_9 + I_6 = I_2$ and $I_7 = I_3$

Therefore:

$$30 = 3I_2 + 3I_3 + 2I_5 + 2I_8$$

But $I_2 + I_3 = I_5 + I_8 = I$ input

Therefore:

$30 = 5I$ and $I = 6$ amperes.

Thus, the total current into the two circuits when connected in parallel will be 12 amperes and the resistance between the terminals will be 0.83 ohms.

There is another way of solving the problem without using Kirchoff's Laws. Again using the half circuit, if the central "T" comprising R_2,R_9,R_6, is transformed to its equivalent pi cir-

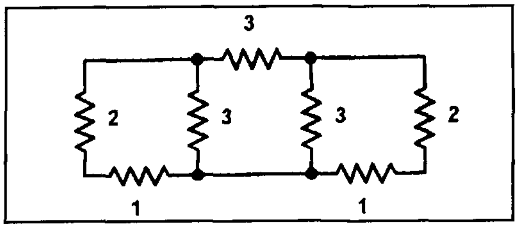

Figure 2. Changing R_2,R_6,R_9 to their equivalent pi circuit, we have the circuit shown here (values in ohms).

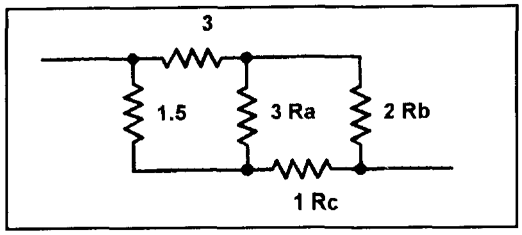

Figure 3. Combining resistors provides this circuit (values in ohms).

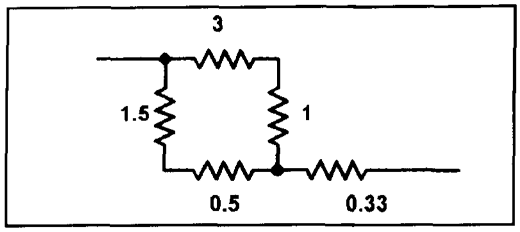

Figure 4. R_a,R_b,R_c are converted to their equivalent T circuit giving the circuit shown.

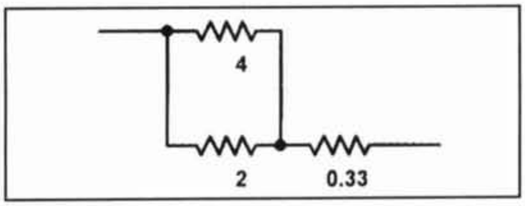

Figure 5. Once again combining resistors, gives the circuit here. The result in shown in Figure 6.

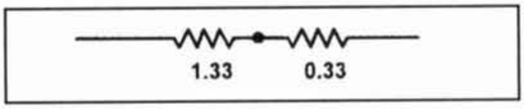

Figure 6. Adding these two resistors gives a resistance of 1.66 ohms across the half circuit, which when the two halves are paralleled, gives 0.83 ohms across the whole.

cuit it will replaced by a symmetrical circuit with each element being of three ohms resistance (**Figure 2**). Where possible these can be combined with original adjacent resistors resulting in **Figure 3**. The pi circuit comprising the resistors labeled R_a,R_b,R_c can then be transformed to their equivalent "T" circuit as shown in **Figure 4** and once again we can combine resistors which results in the values of **Figure 5**. A further combining gives a total resistance for the half circuit of 1.66 ohms and across the full cube of 0.83 ohms.

In short, there is often more than one way of killing a cat (metaphorically speaking)!

S.F. Brown, G4LU
Shropshire, UK

Appendix

The following relationships exist between the pi (**Figure 7**) and T (**Figure 8**) circuits.

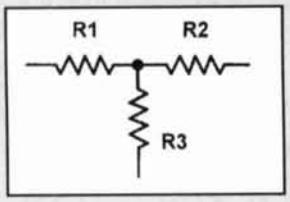

Figure 7.

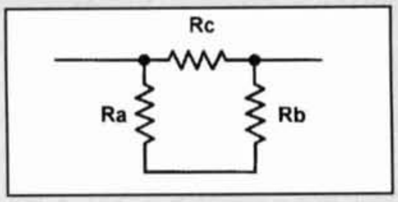

Figure 8.

$$R1 = \frac{Ra.Rc}{Ra + Rb + Rc}$$

$$R2 = \frac{Rb.Rc}{Ra + Rb + Rc}$$

$$R3 = \frac{Ra.Rb}{Ra + Rb + Rc}$$

$$Rc = \frac{R1.R2 + R1.R2 + R2.R3}{R3}$$

$$Rb = \frac{R1.R2 + R1.R3 + R2.R3}{R1}$$

$$Ra = \frac{R1.R2 + R1.R3 + R2.R3}{R2}$$

PRODUCT INFORMATION

ANALOG DEVICES PUBLISHES "ANALOG DIALOGUE" VOLUME 31-3

Analog Devices, Inc. has published Volume 31, Number 3 of Analog Dialogue. The cover feature is an article on Analog Devices' hybrid fiber coaxial cable modem chipset, the AD9853/AD8320. Other features include:

- "Selecting Mixed-Signal Components for Digital Communications System" (final installment of a tutorial series)
- "DSP 101" (part three of a tutorial)
- "Powerful Design Tools for Motion Control Applications", describing the ADMC300 and ADMC330 single-chip motor controllers
- Wideband amplifiers, TX and serial DACs. low-cost SHARC DSPs, and the new low-voltage XFET™ voltage references are among 24 products discussed in "New Product Briefs"
- "Ask the Applications Engineer" answers questions about the application of CMOS switches and multiplexers

"Editors Notes" discusses Analog Devices' new and improved Web site.

Copies of Analog Dialogue are available by calling the Analog Dialogue Literature Center at 1(800) ANALOGD. The publication can also be seen on Analog Devices' Web site: <www.analog.com/publications/magazines/Dialogue/dialog.html>.

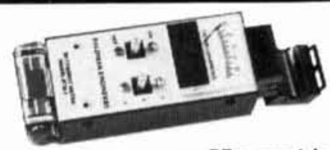

ADVERTISER'S INDEX

.... POWER ON WITH ASTRON
SWITCHING POWER SUPPLIES ....

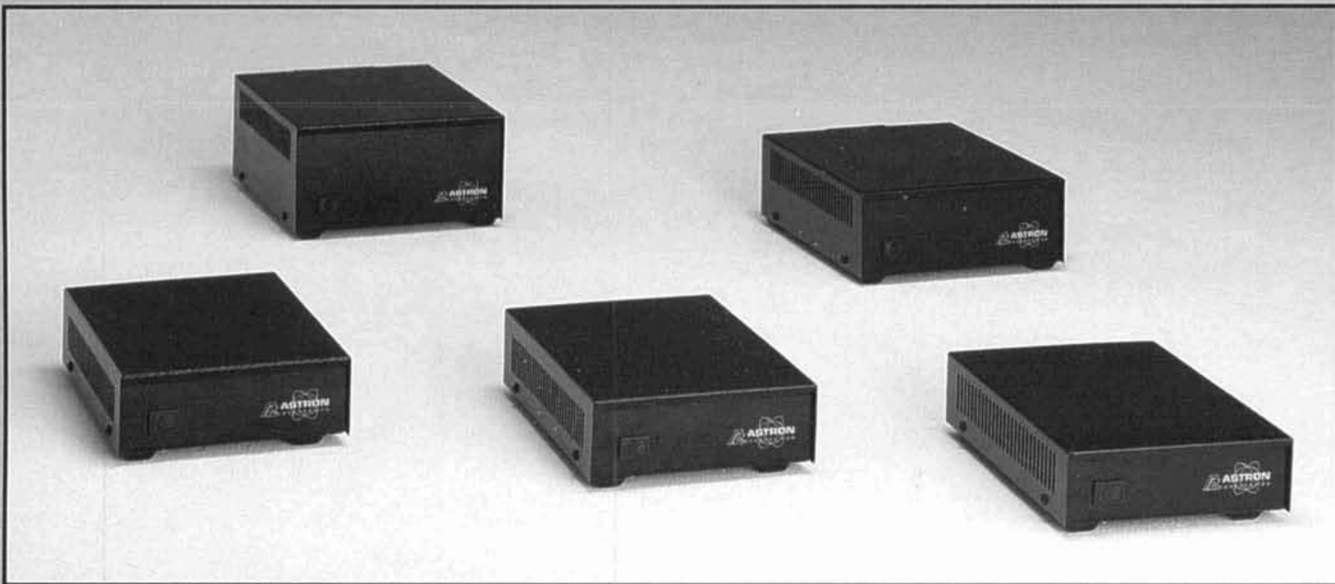

SPECIAL FEATURES:

- HIGH EFFICIENCY SWITCHING TECHNOLOGY SPECIFICALLY FILTERED FOR USE WITH COMMUNICATIONS EQUIPMENT, FOR ALL FREQUENCIES INCLUDING **HF**.
- HEAVY DUTY DESIGN
- LOW PROFILE, LIGHT WEIGHT PACKAGE.
- EMI FILTER
- MEETS FCC CLASS B

PROTECTION FEATURES:

- CURRENT LIMITING
- OVERVOLTAGE PROTECTION
- FUSE PROTECTION
- OVER TEMPERATURE SHUTDOWN

SPECIFICATIONS:

INPUT VOLTAGE: 90-132 VAC 50/60Hz OR 180-264 VAC 50/60Hz SWITCH SELECTABLE

OUTPUT VOLTAGE: 13.8 VDC

MODEL	CONT. AMP	ICS	SIZE	WT.(LBS)
SS-10	7	10	1 1/8 x 6 x 9	3.2
SS-12	10	12	1 3/8 x 6 x 9	3.4
SS-18	15	18	1 3/8 x 6 x 9	3.6
SS-25	20	25	2 7/8 x 7 x 9 3/8	4.2
SS-30	25	30	3 3/4 x 7 x 9 5/8	5

ASTRON CORPORATION

9 AUTRY, IRVINE, CALIFORNIA 92618
714-458-7277 FAX 714-458-0826
www.astroncorp.com